Universitat Autònoma de Barcelona

Implicación de los genes de la familia RAV en el desarrollo floral

Andrea Aguilar Jaramillo

Universidad Autónoma de Barcelona

Facultad de Biociencias

Departamento de Biología Animal, Biología Vegetal y Ecología

TESIS DOCTORAL

Implicación de los genes de la familia *RAV* en el desarrollo floral

Memoria presentada por Andrea Elizabeth Aguilar Jaramillo para optar al grado de Doctor en Biología y Biotecnología Vegetal por la Universidad Autónoma de Barcelona

Trabajo realizado en el Programa de desarrollo y transducción de señales del Centre de Recerca en Agrigenòmica (CRAG), Campus UAB Bellaterra, bajo la dirección de las Doctoras Soraya Pelaz Herrero y Paula Suárez López

Directoras **Tutor**

Dra. Soraya Pelaz Herrero **Dra. Paula Suárez López** **Dr. Juan Barceló Coll**

Doctoranda

Andrea Aguilar Jaramillo

BARCELONA, 2016

ÍNDICE GENERAL

ABREVIATURAS Y SIGLAS

°C	Grados centígrados
AP1	APETALA1
AP2	APETALA 2
CAL	CAULIFLOWER
cDNA	Ácido desoxirribonucleico complementario
ChIP	Inmunoprecipitación de cromatina
ChIP-qPCR	Inmunoprecipitación de cromatina seguida de PCR cuantitativa en tiempo real
CK	Citoquininas
CO	CONSTANS
Col – 0	*Arabidopsis thaliana* ecotipo silvestre Columbia-0.
DNA	Ácido desoxirribonucleico
dNTP	desoxinucleótido trifosfato
DS	desviación estándar
EGL3	ENHACER OF GLABRA3
EtBr	bromuro de etidio
EtOH	Etanol
FD	FLOWERING LOCUS D
FLC	FLOWERING LOCUS C
FLM	FLOWERING LOCUS M
FT	FLOWERING LOCUS T
g	Gramos
GA	Giberelina
GA_3	Giberelina 3
GA3OX	Giberelina 3-beta-dioxygenasa
GFP	Proteína fluorescente verde

GIS	GLABROUS INFLORESCENCE STEMS
GIS2	GLABROUS INFLORESCENCE STEMS2
GL1	GLABROUS1
GL2	GLABROUS2
GL3	GLABRA3
GUS	Beta –glucuronidasa
Kb	Kilobases
LD	Día largo (*long day*, 16 horas de luz)
LFY	LEAFY
M	Molar
mg	Miligramos
min	Minutos
miRNA	MicroRNA
ml	Militro
mM	Milimolar
mRNA	Ácido ribonucleico mensajero
MS	Medio de cultivo Murashige-Skoog
NHC	Número de hojas caulinares
NHR	Número de hojas de roseta
nm	Nanómetro
nt	Nucleótidos
NTH	Número total de hojas
pb	par de bases
PCR	reacción en cadena de la polimerasa
RB	Réplica biológica
RNA	Ácido Ribonucleico
RNAi	RNA de interferencia

rpm	revoluciones por minuto
RT-PCR	Transcripción Reversa-seguida de PCR
RT-qPCR	Transcripción reversa seguida de PCR cuantitativa en tiempo real
SAM	Meristemo apical del tallo
SD	día corto (*short day*, 8 horas de luz)
SMZ	SCHLAFMÜTZE
SNZ	SCHNARCHZAPFEN
SOC1	SUPPRESSOR OF OVEREXPRESSION OF CO1
SPL	SQUAMOSA PROMOTER BINDING PROTEIN-LIKE
SVP	SHORT VEGETATIVE PHASE
T- DNA	DNA de transferencia
Taq	*Thermus aquaticus*
TEM	TEMPRANILLO
Tm	Temperatura de fusión
TOE	TARGET OF EAT
TSF	TWIN SISTER OF FT
TTG1	TRANSPARENT TESTA GLABRA1
µg	Microgramo
µl	Microlitro
UBQ10	UBIQUITINA 10
UTR	Región no traducida
vol/vol	volumen/volumen
w/v	Peso / Volumen
WT	Tipo Silvestre (*wild type*)
ZFP8	ZINC FINGER PROTEIN8
ZT	Zeitgeber time

ABSTRACT

Flowering is probably the most important process in plant development since the perpetuation of the species depends on it. In *Arabidopsis thaliana*, floral induction is controlled by several genetic pathways that respond to environmental and endogenous stimuli. In our laboratory we have identified the *TEMPRANILLO* (*TEM*) genes as flowering repressors under both inductive long-day (LD, 16 hours of light) and non-inductive short-day (SD, 8 hours of light) conditions. The TEM proteins belong to a family of transcription factors called RAV, characterized by the presence of two DNA binding domains, the APETALA2 (AP2) and B3 domains. In *Arabidopsis* this family is composed of 6 genes. Under LD the photoperiod pathway induces flowering mainly through activation of *FLOWERING LOCUS T* (*FT*), while under SD flowering depends mainly on the accumulation of gibberellins (GAs). TEM1 and TEM2 delay flowering under both conditions by directly repressing the expression of the *FT*, *GA 3-OXIDASE 1* (*GA3OX1*) and *GA3OX2* genes, the latter two genes being responsible for the biosynthesis of bioactive GA_4. Therefore, *TEM1* and *TEM2* control flowering time through at least two of the genetic pathways that control floral induction: the photoperiod (Castillejo & Pelaz, 2008) and the GA pathway (Osnato et al, 2012).

In this PhD thesis we aimed to deepen the role of *TEM* genes in other genetic pathways controlling flowering and other developmental processes in *Arabidopsis thaliana*.

There is a genetic pathway that responds to the age of the plant and prevents flowering at the juvenile phase. First there is a transition from the juvenile to the adult vegetative stage and then floral induction occurs. The microRNAs miR156 and miR172 are involved in the regulation of these phase transitions of plant development (Huijser & Schmid, 2011). MiR156 maintains the juvenile phase and delays the floral transition (Wu & Poeting, 2006; Wu et al, 2009), while miR156-target *SQUAMOSA PROMOTER BINDING PROTEIN-LIKE* (*SPL*) genes and miR172 promote the transition to adulthood and floral induction. Our results show that *TEM* genes are involved in regulating various stages of the age-dependent pathway as they positively regulate miR156 and negatively regulate several *SPL* genes and miR172, thus delaying flowering. Therefore, *TEM* genes play a key role in responding to the age of the plant (Chapter 1, Aguilar-Jaramillo et al., manuscript in preparation).

On the other hand, when *Arabidopsis* plants grow under LD at low ambient temperatures of 16°C, flowering is delayed relative to 22°C. Our results show that *TEM* genes act as repressors of *FT* and *TWIN SISTER OF FT* (*TSF*) at 16°C. A gene that plays a key role in the response to low ambient temperatures is *SHORT VEGETATIVE PHASE* (*SVP*). *svp* mutants are insensitive to temperature changes and flower early both under warm and cool temperatures. We have found that SVP positively regulates *TEM2* expression at 16 °C under LD conditions, controlling flowering through *TEM2* but also independently of *TEM2* by directly repressing *FT* at low temperatures (Chapter 2; Marín-González et al, 2015).

In addition, we have discovered the involvement of TEM in another developmental process, the initiation of trichomes. Trichomes are epidermal protrusions that protect the plant from water loss, insects and ultraviolet radiation. We show that *TEM* genes control the initiation of trichomes by directly repressing the epidermal genes that promote trichome initiation and, more interestingly, by controlling the accumulation and distribution of GAs in the mesophyll. This function of *TEM* genes reveals a key role of a cell layer, the mesophyll, in trichome differentiation in the outer adjacent cell layer, the epidermis (Chapter 3; Matías-Hernández et al, 2016).

RESUMEN

La floración es probablemente el proceso más importante en el desarrollo de la planta, ya que la perpetuación de las especies vegetales depende de ella. En *Arabidopsis thaliana*, la inducción floral está controlada por varias rutas genéticas que responden a estímulos ambientales y endógenos. En nuestro laboratorio se han identificado los genes *TEMPRANILLO* (*TEM*) como represores de la floración tanto en condiciones inductivas de día largo (LD, 16 horas de luz) como no inductivas de día corto (SD, 8 horas de luz). Las proteínas TEM pertenecen a una familia de factores de transcripción llamada RAV, que se caracterizan por contener dos dominios de unión al DNA, que son los dominios APETALA2 (AP2) y B3. En *Arabidopsis* esta familia está compuesta por 6 genes. En LD, la ruta del fotoperiodo induce la floración principalmente a través de la activación del gen *FLOWERING LOCUS T* (*FT*), mientras que en SD la floración depende principalmente de la acumulación de giberelinas (GAs). TEM1 y TEM2 retrasan la floración en ambas condiciones al reprimir directamente la expresión de los genes *FT*, *GA3OXIDASE 1* (*GA3OX1*) y *GA3OX2*, siendo los dos últimos genes responsables de la biosíntesis de la GA bioactiva GA_4. Por tanto, *TEM1* y *TEM2* controlan el tiempo de floración a través de al menos dos de las rutas genéticas que controlan la inducción floral: la del fotoperíodo (Castillejo & Pelaz, 2008) y la de las GAs (Osnato et al, 2012).

El objetivo de este trabajo ha sido profundizar en el papel de los genes *TEM* en otras rutas genéticas implicadas en el control de la floración y en otros procesos de desarrollo en *Arabidopsis thaliana*.

Existe una ruta genética que responde a la edad de la planta y que evita que ésta florezca en su etapa juvenil. Primero se produce la transición de la etapa vegetativa juvenil a la adulta y después la inducción floral. Los microRNAs miR156 y miR172 están implicados en la regulación de estas transiciones entre las fases del desarrollo de la planta (Huijser & Schmid, 2011). miR156 mantiene la fase juvenil y retrasa la transición floral (Wu & Poeting, 2006; Wu et al, 2009), mientras que los genes diana de miR156 *SQUAMOSA PROMOTER BINDING PROTEIN-LIKE* (*SPL*) y miR172 promueven la transición a la fase adulta y la inducción floral. Nuestros resultados muestran que los genes *TEM* están involucrados en varias etapas de la ruta de la edad, ya que regulan positivamente a miR156 y negativamente a varios genes *SPL* y miR172, retrasando así la floración. Por tanto, los genes *TEM* desempeñan un papel clave en la

respuesta a la edad de la planta (Capítulo 1; Aguilar-Jaramillo et al., manuscrito en preparación).

Por otro lado, cuando las plantas crecen en LD a bajas temperaturas ambientales de 16ºC, la floración se retrasa respecto a 22°C. Nuestros resultados muestran que los genes *TEM* actúan como represores de *FT* y *TWIN SISTER OF FT (TSF*) a 16°C. Un gen que juega un papel clave en la respuesta a las bajas temperaturas ambientales es *SHORT VEGETATIVE PHASE* (*SVP*), cuyos mutantes son insensibles a los cambios de temperatura y florecen pronto tanto a temperaturas cálidas como frescas. Hemos descubierto que SVP regula positivamente la expresión de *TEM2* a 16ºC en condiciones de LD y controla la floración a través de TEM2, pero también de manera independiente mediante la represión directa de *FT* a bajas temperaturas ambientales (Capítulo 2; Marín-González et al, 2015).

Además, hemos descubierto la participación de TEM en otro proceso del desarrollo, la iniciación de los tricomas. Los tricomas son protrusiones epidérmicas que protegen a la planta de la pérdida de agua, de insectos y de las radiaciones ultravioletas. Hemos descubierto que los genes *TEM* controlan la iniciación de los tricomas mediante la represión directa de los genes epidérmicos que promueven su iniciación y, lo que es más interesante, a través del control de la acumulación y distribución de las GAs en el mesófilo. Esta función de los genes *TEM* desvela el papel clave de una capa celular, el mesófilo, en la diferenciación celular de los tricomas en la capa exterior adyacente, la epidermis (Capítulo 3; Matías-Hernández et al, 2016).

INTRODUCCIÓN

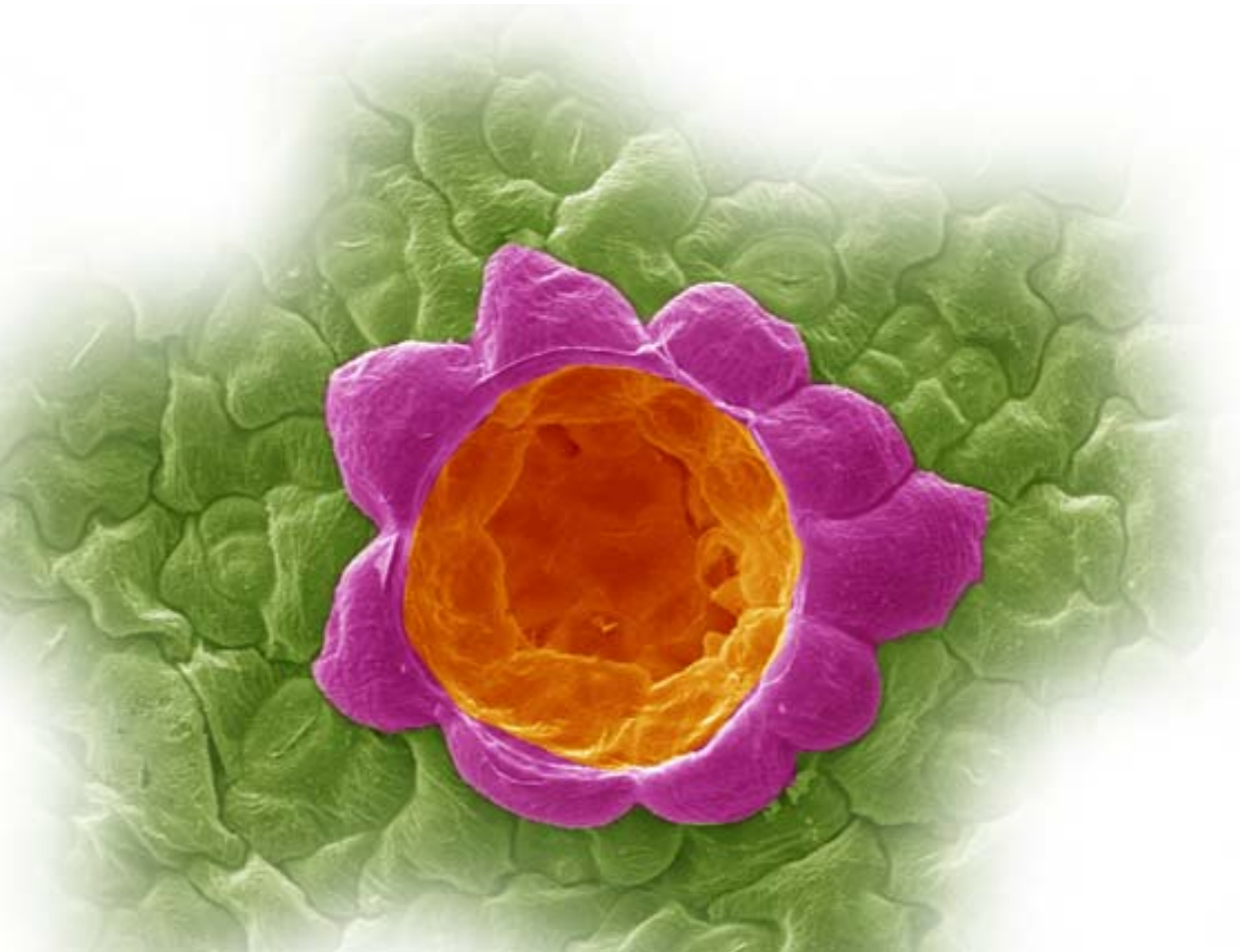

INTRODUCCIÓN GENERAL

1. *Arabidopsis thaliana,* UN MODELO DE ESTUDIO DEL DESARROLLO VEGETAL

Arabidopsis thaliana es una especie utilizada como planta modelo ya que presenta características óptimas para su manejo en el laboratorio, como son su pequeño tamaño y su corto ciclo de vida que oscila alrededor de 6 semanas (Laibach F 1943, Page & Grossniklaus, 2002). Además, el tamaño de su genoma es pequeño, de 125 Mb, y fue completamente secuenciado en el año 2000 (The *Arabidopsis* Genome Initiative, 2000). Todas estas características han permitido realizar un análisis eficiente de la función de los genes de la planta (Srikanth & Schmid, 2011).

Arabidopsis thaliana es una especie anual facultativa de día largo (LD), es decir, que florece más rápidamente en LD que en día corto (SD) (He, 2012, Bratzel &Turck 2015).

2. TRANSICIONES ENTRE LAS ETAPAS DEL DESARROLLO DE UNA PLANTA

Las plantas tienen la capacidad de percibir varias señales ambientales y adaptarse rápidamente a los cambios en el medio donde se desarrollan (Srikanth & Schmid, 2011). Las plantas pasan por una serie de etapas de desarrollo a lo largo de su vida. La primera etapa es la germinación de la semilla, que da origen a una plántula juvenil, etapa en la que sería incapaz de reproducirse incluso en condiciones ambientales favorables. Sin embargo, cuando *Arabidopsis* pasa a la fase vegetativa adulta desarrolla varios rasgos morfológicos nuevos como son el tamaño y forma de la hoja, así como la distribución y tamaño de los tricomas abaxiales (Huijser & Schmid, 2011). Todos estos rasgos son utilizados comúnmente como marcadores para determinar el cambio de la fase juvenil a la adulta (Huijser & Schmid, 2011). Cuando ocurre la transición de la fase juvenil a la fase adulta, la planta adquiere la competencia para responder al estímulo floral (Poethig, 1990). Durante la fase adulta, la planta pasa por un proceso de crecimiento vegetativo para luego dar paso a la fase reproductiva. Cuando se produce la transición a la floración, la planta deja de formar hojas de roseta y se produce el crecimiento de la inflorescencia, donde se inician las flores (Figura 1).

El paso de la fase vegetativa adulta a la fase reproductiva es denominado transición floral (Poethig, 1990). Esta transición es uno de los procesos más importantes

de las plantas y está controlada por distintas rutas genéticas que responden a distintos estímulos ambientales y endógenos. Que este proceso se realice en las condiciones óptimas determinará el éxito reproductivo de las plantas (Amasino, 2010). Los factores externos que controlan la floración son, entre otros, los cambios estacionales en la duración del día (fotoperiodo) o en la temperatura (vernalización) y los cambios diarios de la temperatura ambiental. Por otro lado, los factores endógenos que controlan la inducción floral son la acumulación de hormonas, fundamentalmente las GAs, o la edad de la planta, y además existe una ruta genética autónoma.

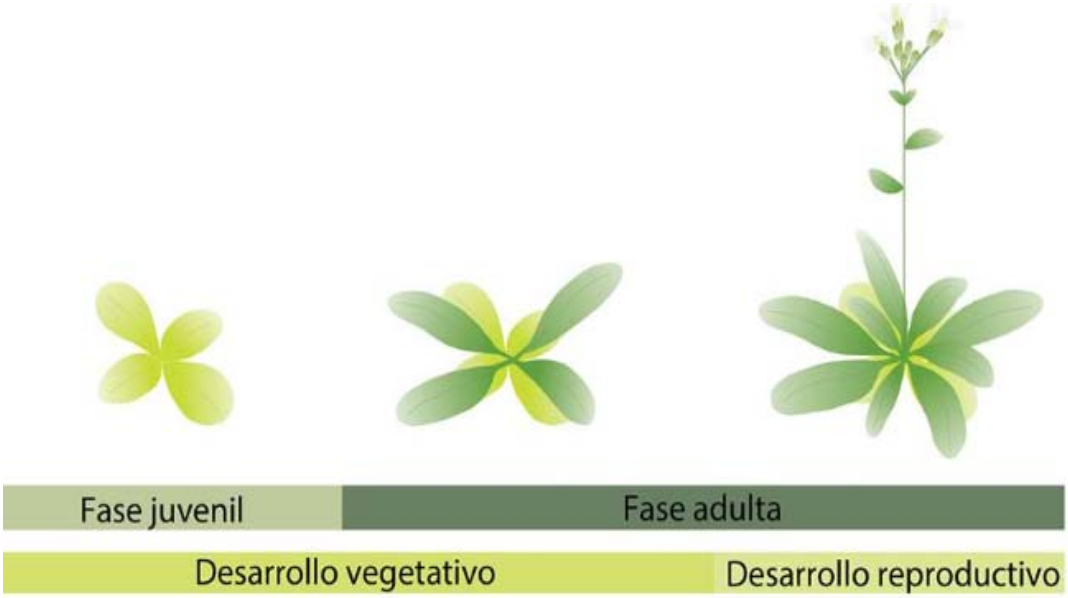

Figura 1. Esquema de las transiciones entre las fases de desarrollo en ***Arabidopsis thaliana.*** Se muestra a la izquierda una plántula en fase juvenil de desarrollo vegetativo. En el centro se representa una planta adulta en fase vegetativa, y a la derecha una planta adulta en etapa reproductiva. Es en esta última etapa en la que la planta deja de formar hojas de roseta y comienza a producir flores.

2.1 La transición de la fase juvenil a la adulta

Los microRNAs (miRNAs) son pequeñas moléculas de RNA endógeno que no codifican proteínas y actúan como moléculas reguladoras de la expresión génica. Su longitud es de 17 a 25 nucleótidos (nt), teniendo la mayoría de ellos un tamaño aproximado de 21 nt. Los miRNAs se describieron inicialmente en *Caenorhabditis elegans* (Lee et al., 1993); estos autores descubrieron un gen esencial para el control del desarrollo larvario que no codifica proteínas, sino que produce dos RNAs pequeños de diferente longitud (22 y 61 nt). El más grande podía adoptar una estructura en bucle y

así ser el precursor del más corto. A partir de este descubrimiento se han identificado muchos miRNAs en diferentes especies, incluidas las plantas (Lee, 1993; Bartel, 2004). Los miRNAs actúan induciendo la degradación de los mRNAs con los que tienen complementariedad o inhibiendo su traducción.

En *Arabidopsis thaliana*, la ruta genética que responde a la edad de la planta y que controla la transición de la fase juvenil a la adulta está regulada por miRNAs. En el año 2002 fueron identificados los primeros miRNAs en *Arabidopsis,* siendo descrito por primera vez el miR156 (Reinhart et al., 2002). En *Arabidopsis* existen 8 genes *MIR156* (*MIR156A-H*), y se descubrió que los miRNAs miR156 y miR172 juegan un papel muy importante en la transición a la fase adulta (Poethig et al., 2009). En *Arabidopsis* el nivel de expresión de miR156 es alto durante las primeras etapas de desarrollo de la planta y después decae a medida que la planta avanza hacia la etapa adulta (Wu & Poethig, 2006). Actualmente se sabe que miR156 reprime la actividad de 11 de los 17 miembros de la familia génica *SQUAMOSA PROMOTER BINDING PROTEIN-LIKE* (*SPL*): *SPL2*, *SPL3*, *SPL4*, *SPL5*, *SPL6*, *SPL9*, *SPL10*, *SPL11*, *SPL13A*, *SPL13B* y *SPL15* (Schwab et al., 2005; Wu & Poething, 2006; Gandikota et al., 2007), que son activos sólo cuando miR156 decae en la fase adulta. miR156 retrasa la transición juvenil-adulto, mientras que los SPLs la aceleran. Los SPLs activan al miR172, que confiere la transición a la fase adulta (Wu & Poethig et al., 2006). Se han descrito 5 genes, *MIR172A-E,* que dan lugar a 3 miR172 maduros distintos (Aukerman & Sakai, 2003; Chen, 2004). miR172 incrementa sus niveles de expresión durante el desarrollo de manera opuesta al decrecimiento de miR156 (Aukerman & Sakai, 2003; Jung et al., 2007; Wu et al., 2009) y similar al aumento de los *SPLs*.

2.2 La floración está controlada por diferentes rutas genéticas

La inducción floral conduce a la formación de las estructuras reproductivas. La floración debe ocurrir en el momento más propicio del año para así asegurar la perpetuación de las especies. Como ya se ha mencionado previamente, en *Arabidopsis* la inducción floral está controlada por diferentes rutas genéticas que perciben y responden a estímulos ambientales (Bernier & Périlleux, 2005; Ausin et al., 2005) y endógenos de la planta (Fornara et al., 2010).

Uno de los factores ambientales más estudiados es el fotoperiodo. Existe una ruta genética que promueve la transición floral en respuesta a la duración del día y la calidad de la luz percibida (Srikanth & Schmid, 2011, Andrés & Coupland, 2012). Otra

ruta genética es la de la vernalización, que responde a la exposición prolongada a las bajas temperaturas del invierno. Algunas especies de plantas requieren la vernalización para acelerar la floración (Andrés & Coupland, 2012). Por otro lado, otra cascada génica responde a cambios moderados de la temperatura ambiental. Además, la floración está controlada por características intrínsecas de la planta, tales como la acumulación de las giberelinas (GAs) y la edad de la planta (Mutasa-Göttgens & Hedden, 2009; Huijser & Schmid, 2011; Porri et al., 2012). Todas estas cascadas génicas convergen en la activación de unos pocos genes responsables últimos de la inducción floral, *FLOWERING LOCUS T* (*FT*) y *SUPPRESSOR OF OVEREXPRESSION OF CONSTANS 1* (*SOC1*). FT fue identificado como un componente del florígeno que viaja desde las hojas hasta el ápice del tallo para inducir la floración (Corbesier et al., 1996; Jaeger and Wigge, 2007; Mathieu et al., 2007; Lin et al., 2007). Una vez en el ápice del tallo interacciona con FLOWERING LOCUS D (FD) para activar, entre otros, a *SOC1* (Abe et al., 2005; Wigge et al., 2005).

A continuación se detallarán sólo las rutas relevantes en las que hemos trabajado a lo largo de esta tesis.

2.2.1 Ruta dependiente de la edad de la planta

Como ya se ha mencionado, la ruta genética que responde a la edad de la planta está controlada por el miR156, varios SPLs y el miR172. La reducción de la expresión de miR156 en las plantas adultas permite la actividad de los SPL, que son inductores de la floración. Por un lado, los SPL promueven la expresión del miR172 que silencia a los represores de la floración *APETALA2* (*AP2*) y *AP2-like,* como son *TARGET OF EAT 1* (*TOE1*), *TOE2* y *TOE3*, *SCHLAFMÜTZE* (*SMZ*) y *SCHNARCHZAPFEN* (*SNZ*) (Aukerman & Sakai, 2003; Chen, 2004; Jung et al., 2007; Mathieu et al., 2009; Wu et al., 2009).

Por otro lado, los factores de transcripción SPLs son reguladores positivos de *FT* en las células acompañantes del floema en la hoja (Wang et al., 2009; Kim et al.,2012), y de otros inductores de la floración, como *SOC1* y *LEAFY* (*LFY*), y de los genes de identidad del meristemo floral *APETALA1* (*AP1*) y *FRUITFULL* (*FUL)* (Wang et al, 2009; Wu et al., 2009; Yamaguchi et al, 2009; Fornara et al., 2010; Bratzel & Turck, 2015).

2.2.2 Ruta genética que responde al incremento de la longitud del día o fotoperiodo

Existen varias especies vegetales que usan la información sobre los cambios en la duración del día (fotoperiodo) que ocurren a lo largo de las estaciones para determinar el momento óptimo para que ocurra la floración (Searle & Coupland, 2004; Song et al, 2015). En esta ruta genética los fotorreceptores perciben la cantidad y la calidad de la luz, y miden la duración del día mediante el reloj circadiano.

En la ruta genética que responde al fotoperiodo, se han identificado y caracterizado varios mutantes que tienen afectado el tiempo de floración (Rédei, 1962; Koornneef et al, 1991). Existen dos clases de mutantes, los que florecen más tarde que las plantas silvestres en condiciones de LD pero no están afectados en SD, y los que tienen una floración temprana en condiciones de SD (Searle & Coupland, 2004; Searle et al., 2006). *CONSTANS* (*CO)*, que desempeña un papel clave en esta ruta genética, está regulado por las señales lumínicas y el reloj circadiano, de manera que la proteína CO solo está activa en condiciones inductoras de fotoperiodo, es decir, LD (Suárez-López et al., 2001; Valverde et al., 2004). El estudio de la función molecular de los genes implicados en la ruta de respuesta al fotoperiodo ha demostrado que CO es un activador transcripcional del gen *FT* y su homólogo *TSF*, que funcionan como integradores de las distintas cascadas génicas que controlan la inducción floral (Jarrillo & Piñero 2011). Además, la respuesta al fotoperiodo ocurre en el tejido vascular de las hojas a través del factor de transcripción CO (An et al, 2004; Ayre & Turgeon, 2004), cuya expresión oscila según los ritmos circadianos (Suárez-López et al., 2001). La percepción de la duración del día en la hoja sugirió que una señal sistémica, llamada estímulo floral o florígeno, se activa en la hoja en respuesta al fotoperiodo (Wigge, 2011). Posteriormente se ha demostrado que FT es parte del florígeno que se induce en las hojas como consecuencia de la activación de CO. La proteína FT viaja a través del floema desde la hoja hasta el meristemo apical del tallo (Corbesier et al., 1996; Jaeger and Wigge, 2007; Mathieu et al., 2007) para cumplir con su función a través de su interacción con la proteína FD, que es un factor de transcripción de tipo bZIP (*basic region and leucine zipper motif*). FT y FD activan la expresión de los genes de identidad de meristemo floral *AP1* y *SOC1*, dando lugar a la iniciación floral (Abe et al, 2005; Wigge et al, 2005; Figura 2).

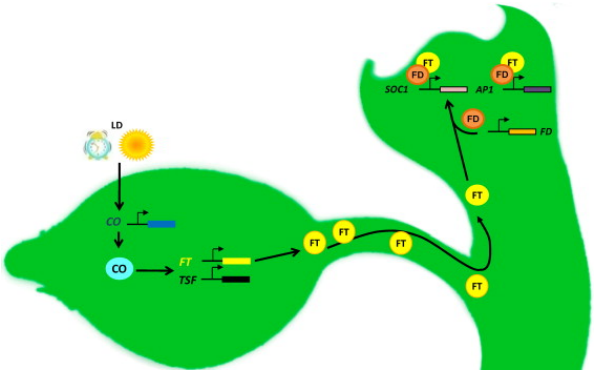

Fig.2. Modelo representativo de la floración inducida por la ruta génica que responde al fotoperiodo en ***Arabidopsis thaliana*.**
La proteína CO es el principal activador de la floración en condiciones inductivas de LD, que activa a *FT* y *TSF* en la hoja. FT se mueve por el floema desde la hoja hasta el meristemo apical del tallo donde se une a FD. El complejo proteico formado por FT y FD activa a los genes encargados de inducir la formación de las flores (extraído de Jarillo & Piñeiro, 2011).

CO y FT son los elementos clave que intervienen en el efecto de la duración del día sobre la floración. En LD, tanto *CO* como *FT* tienen niveles muy bajos de expresión durante casi todo el período de luz. CO sólo se activa al final del período de luz en LD e induce la expresión de *FT* en este momento (Suárez-López et al., 2001; Searle & Coupland., 2004 Andrés & Coupland., 2012; Figura 3).

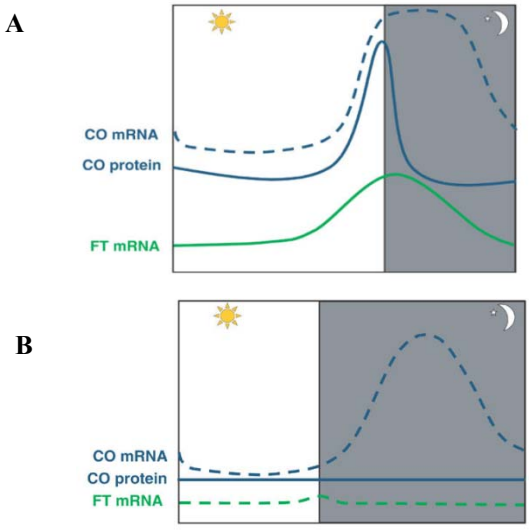

Fig. 3. (A) Niveles de expresión de CO y FT en condiciones inductivas de LD. El pico de expresión de CO coincide con la parte final del período de luz, activando así la expresión de *FT* e iniciando la floración.
(B) En condiciones no inductivas de SD la proteína CO no se acumula y, por tanto, *FT* no se expresa, retrasando así la floración (extraído de Searle & Coupland., 2004).

Por lo tanto, se requiere un mecanismo capaz de percibir la luz, de cuantificar su calidad e intensidad, y un oscilador endógeno (reloj circadiano) que mida la longitud del día. Posteriormente, los genes encargados de trasmitir la señal inductora de la floración activan a los genes de identidad del meristemo floral para así iniciar la formación de las flores.

2.2.3 Ruta genética que responde a cambios en la temperatura ambiental

La temperatura ambiental es una de las señales que regulan la floración. Para una reproducción exitosa las plantas deben percibir y responder rápidamente a los cambios en la temperatura ambiental (Lee et al., 2007). Las plantas de *Arabidopsis* que se cultivan a temperaturas moderadas bajas (16 °C) florecen más tarde que las que se cultivan a temperaturas medias (23 °C) o moderadamente altas (27° C) (Blázquez et al., 2003; Balasubramanian et al, 2006). A 16 °C las plantas florecen más tarde que a 22 °C, porque hay un retraso en la acumulación de *FT* y de *TSF* (Balasubramanian et al, 2006). A 22 °C *FT* se expresa a niveles más altos que *TSF*, mientras que a 16 °C *TSF* presenta unos niveles de expresión más altos que los de *FT* (Blázquez, et al., 2003, Lee et at., 2012, 2013). Como resultado de esta expresión diferencial, *TSF* juega un papel redundante con *FT*, secundario a 22-23°C, pero más importante a 16 °C.

Entre los genes que responden a cambios en la temperatura ambiental se encuentran varios genes de la familia MADS box, entre ellos, *SVP*, *FLOWERING LOCUS C* (*FLC*) y *FLOWERING LOCUS M* (*FLM*) (Balasubramanian et al., 2006; Lee et al., 2007; Li et al., 2008).

SVP juega un papel clave en la represión floral a bajas temperaturas ambientales. La floración temprana de los mutantes *svp* es insensible a las variaciones de temperatura (Lee et al., 2007, 2013; Fornara et al., 2010), produciendo el mismo número de hojas a 16 ºC o 23 ºC (Lee et al., 2007). Los niveles de expresión de los genes *FT* y *SOC1* en estos mutantes son más altos que en las plantas silvestres, lo que provoca una floración precoz. Por el contrario, en las plantas *35S::SVP* se suprime la expresión de estos genes (Li et al., 2008), lo que resulta en una floración muy tardía. SVP se une los sitios CArG ($CC(A/T)_6$ GG) de los promotores de *FT* y *SOC1* (Hartmann et al., 2000; Lee et al., 2007; revisado Srikanth & Schmid., 2011). Así, SVP reprime a *FT* y *TSF* en el tejido vascular de las hojas y a *SOC1* en el meristemo apical (Li et al., 2008; Jang et al., 2009).

Se ha descrito que SVP se une a sus secuencias diana en forma de homodímeros y de heterodímeros con FLC y FLM (Lee et al., 2007; Li et al., 2008, Posé et al., 2013). Por un lado, a 16 ºC hay una expresión mayor de SVP y de FLC, lo que permite la formación de un número mayor de homo- y heterodímeros represores (Balasubramanian et al., 2006; Lee et al., 2007). Por otro lado, FLM sufre un procesamiento del mRNA diferencial a distintas temperaturas. A 16 ºC el transcrito mayoritario es el *FLM-β*, que produce una proteína que interacciona con SVP generando un dímero capaz de reprimir la expresión de *FT*. Por el contrario a 22 ºC, el transcrito mayoritario es el *FLM-δ*, por lo que se genera el complejo SVP-FLM-δ que no es capaz unirse a DNA y no puede reprimir a *FT* (Posé et al., 2013).

2.2.4 Relación entre las rutas de señalización molecular

La regulación de la transición floral viene determinada por las múltiples interacciones entre la compleja red de rutas de señalización. Las rutas genéticas convergen en la regulación de los principales integradores de las cascadas genéticas inductoras de la floración, fundamentalmente *FT*, su homólogo *TSF*, *SOC1 y LFY* (Srikanth & Schmid., 2011). Estos activan la expresión de los genes que están involucrados en la identidad del meristemo floral, incluidos *AP1*, *CAULIFLOWER* (*CAL*), *FUL* y *LFY* (Simpson & Dean 2002; Figura 4).

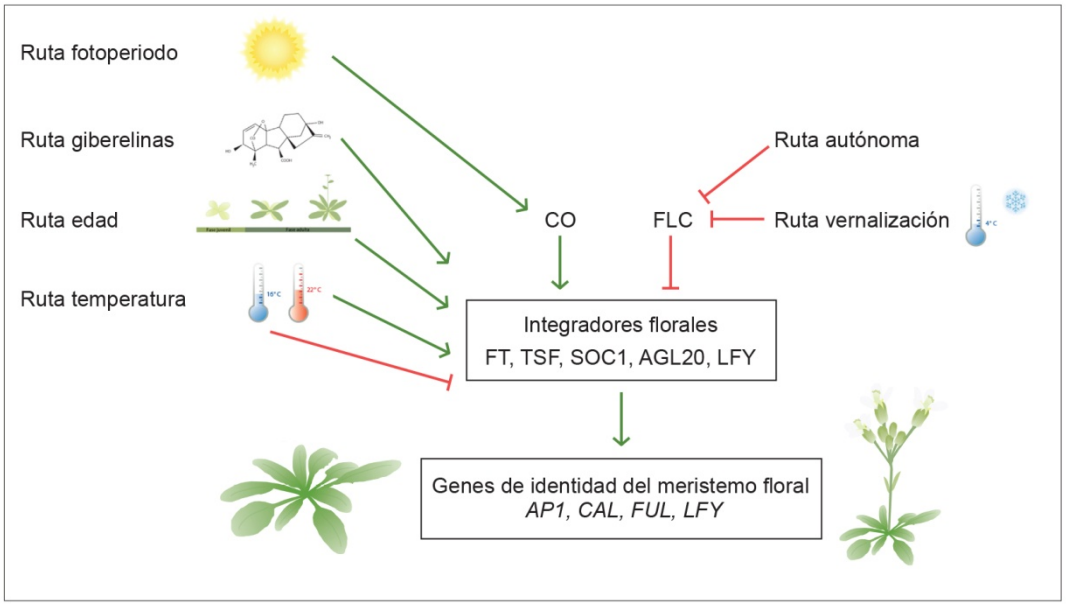

Fig. 4. Esquema de las rutas reguladoras de la floración.

3. LA FAMILIA RAV DE FACTORES DE TRANSCRIPCIÓN

3.1 Genes *TEMPRANILLO*: *TEM1* y *TEM2*

Los genes *TEMPRANILLO* (*TEM*) pertenecen a la familia *RAV*, que consta de 6 genes: *RAV1*, *RAV1-like* (*RAV1L*), *RAV2* (*TEM2*), *RAV2L* (*TEM1*), *RAV3* y *RAV3L* (Riechmann et al., 2000; Yamasaki et al., 2004, Matías-Hernández et al., 2014). Codifican factores de transcripción que poseen dos dominios de unión a DNA, AP2/ERF y B3 (Riechmann & Meyerowitz, 1998). El dominio de unión B3 está en el extremo C-terminal y reconoce la secuencia consenso CACCTG, mientras que el dominio AP2 está en la parte N-terminal y reconoce la secuencia consenso CAACA (Kagaya et al., 1999). En conjunto la secuencia diana de los RAVs engloba ambas secuencias consenso separadas por un máximo de 8 nucleótidos, esto es C(A/C/G)ACA $(N)_{2-8}$(C/A/T)ACCTG (Kagaya et al., 1999). Durante los últimos años se han caracterizado en nuestro laboratorio los genes *TEM1* y *TEM2* como represores de la floración, que reprimen directamente a *FT* (Castillejo & Pelaz., 2008), y a dos genes encargados de la biosíntesis de las GAs, *GA3OXIDASE1* (*GA3OX1*) y *GA3OX2* (Osnato et al., 2012).

En LD los mutantes *tem1-1* y *tem2-2* tienen un fenotipo de floración temprana y el doble mutante *tem1-1 tem2-2* presenta un fenotipo de floración aún más temprana, lo que indica redundancia funcional (Castillejo & Pelaz, 2008; Osnato et al., 2012). Sin embargo, las plantas que sobrexpresan *TEM1* o *TEM2* (*35S::TEM1* y *35S::TEM2*) muestran una floración tardía (Castillejo & Pelaz, 2008). Estos efectos sobre el tiempo de floración se correlacionan con cambios en los niveles de *FT* (Castillejo & Pelaz., 2008; Osnato et al., 2012). Además, se ha demostrado, mediante ChIP-qPCR (Imunoprecipitación de Cromatina seguida por PCR cuantitativa), que TEM1 se une a la región 5´UTR del gen *FT*. Los genes *TEM1* y *TEM2*, por tanto, reprimen directamente a *FT* y reprimen así la floración (Castillejo & Pelaz., 2008).

Los niveles de expresión de *TEM1 y TEM2* son elevados cuando las plantas están en sus primeras etapas de desarrollo y van decayendo con la edad. Lógicamente este patrón de expresión es opuesto al de *FT* debido a que es necesario que la cantidad de represor disminuya para que la expresión de *FT* aumente en respuesta a la actividad de CO. Además, análisis moleculares y genéticos indicaron que un equilibrio cuantitativo entre el activador CO y los represores TEM determina los niveles de *FT*,

probablemente debido a impedimentos estéricos, ya que ambos tienen sus secuencias diana muy próximas en la zona 5'UTR de *FT* (Castillejo & Pelaz., 2008).

Por otro lado, en SD CO está inactivo debido a la degradación de la proteína en la oscuridad (Valverde et al., 2004), por lo que *FT* tampoco se activa. En estas condiciones de luz la floración depende fundamentalmente de la acumulación de GAs (Wilson et al., 1992). Se observó que la expresión constitutiva de *TEM1* y de *TEM2* da lugar a plantas con características de mutantes deficientes en GAs, como son floración tardía, pérdida de dominancia apical o enanismo. Además, la aplicación exógena de GAs a estas plantas provoca el rescate del tiempo de floración y de la dominancia apical, lo que indica que el efecto de los TEM en la floración está mediado al menos en parte por las GAs (Osnato et al., 2012).

Adicionalmente, mediante ChIP-qPCR se demostró que TEM1 se une al primer exón de los genes *GA3OX1* y *GA3OX2* (Osnato et al., 2012). Por lo tanto, los genes *TEM* parecen vincular la ruta de respuesta al fotoperiodo y la ruta de respuesta a la acumulación de GAs, controlando la transición floral en condiciones de fotoperiodo inductivo y no inductivo mediante la regulación de la acumulación de FT y GAs (Osnato et al., 2012), ambas sustancias móviles que se originan en la hoja e inducen la floración en el meristemo apical del tallo (Figura 5).

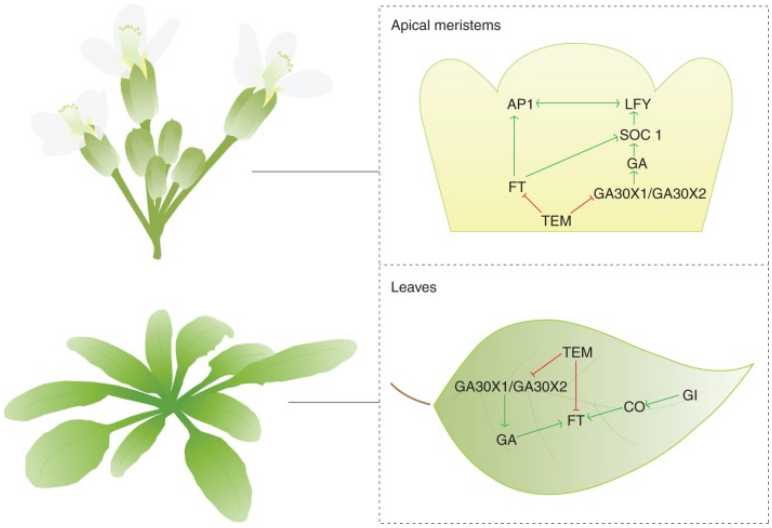

Fig. 5. Representación esquemática de la transición floral de *Arabidopsis thaliana*. Los genes *TEMPRANILLO* (*TEM1* y *TEM2*) actúan como represores de la floración en la ruta del fotoperiodo y la ruta de las giberelinas en condiciones inductivas y no inductivas, respectivamente (Matías-Hernández et al, 2014).

Estudios recientes han identificado la interacción entre *SVP* y los genes *TEM1* y *TEM2* en condiciones inductivas de LD a 22ºC (Tao et al., 2012). Estos autores identificaron la unión de SVP a secuencias CArG en los genes *TEM1* y *TEM2*. Además, los niveles de expresión de los genes *TEM1* y *TEM2* están reducidos en las plantas mutantes *svp*, que presentan floración temprana, y aumentados en plantas de floración tardía que sobrexpresan *SVP* (*35S::SVP)*, lo que indica que SVP activa directamente a los genes *TEM*, siendo más alta la activación de *TEM2* (Tao et al., 2012).

4. TRICOMAS

Como se ha descrito anteriormente, los factores de transcripción TEM1 y TEM2 actúan como represores de la biosíntesis de GAs durante la inducción floral (Osnato et al., 2012). Las GAs no sólo afectan a la floración de la planta, sino que además están implicadas en otros aspectos biológicos, tales como la promoción del crecimiento, la inducción de la germinación (interrumpen la dormición), la estimulación del crecimiento de los tallos (elongación) e hipocótilos o la iniciación de los tricomas, entre otros. Como veremos en los resultados, durante los estudios de juvenilidad en los que usamos como marcador de hojas adultas la aparición de tricomas abaxiales, observamos que el número de tricomas en general está afectado en los mutantes y sobreexpresantes de *TEM*.

4.1 Importancia de los tricomas y beneficios comerciales

Los tricomas son protuberancias pequeñas de células epidérmicas que se encuentran en la superficie de la hoja y en otros órganos de la planta (Olsson et al., 2009). En *Arabidopsis* los tricomas se forman en tallos, sépalos y hojas. En las hojas de roseta aparecen primero en el lado adaxial (cara superior, haz) y posteriormente en el lado abaxial (cara inferior, envés) (Larkin et al., 1994; Hülskamp et al., 1994). Los tricomas tienen como función proteger a las plantas de los insectos herbívoros y de factores externos como el exceso de luz UV y la pérdida de agua (Johnson., 1975; Traw and Bergelson, 2003; Olsson et al., 2009). Además, la plasticidad de las plantas permite que puedan responder al ataque de los insectos mediante el aumento del número y la densidad de los tricomas en las hojas nuevas (Agrawal., 2000; Traw & Bergelson., 2003). Dependiendo de la especie, los tricomas pueden ser glandulares o no glandulares (Olsson et al., 2009). Existen varias especies de plantas con estructuras glandulares multicelulares que sintetizan, almacenan y secretan muchos metabolitos (Schilmiller et

al., 2008) con valor comercial como productos farmacéuticos, fragancias, aditivos alimenticios y pesticidas naturales (Olsson et al., 2009). Sin embargo, en el caso de *Arabidopsis* los tricomas son estructuras unicelulares no glandulares.

4.2 Complejo de proteínas encargado de la formación de los tricomas

En las últimas décadas, se han identificado genética y molecularmente muchos reguladores de los tricomas. Uno de los últimos pasos de la cascada génica encargada de promover la formación de tricomas se lleva a cabo a través de la formación en la epidermis de un complejo proteico formado por tres clases de reguladores: una proteína MYB del tipo R2R3, GLABRA1 (GL1) (Oppenheimer et al., 1991), dos proteínas redundantes bHLH, GLABRA3 (GL3) y ENHACER OF GLABRA3 (EGL3) (Payne et al., 2000; Zhang et al., 2003) y una proteína WD40, TRANSPARENT TESTA GLABRA1 (TTG1) (Walker et al., 1999). En *Arabidopsis*, las mutaciones en todos estos genes provocan una pérdida significativa de tricomas (Payne et al., 2000; Zhou et al., 2011). Este complejo tiene una función importante en la iniciación de los tricomas, pero también está involucrado en el desarrollo del tricoma en etapas posteriores, ya que las mutaciones en dichos genes dan lugar a tricomas más pequeños y menos ramificados (Payne et al., 2000).

4.3 Las hormonas en la iniciación de los tricomas

Las GAs y citoquininas (CKs) están implicadas en la regulación de diferentes procesos de desarrollo de la planta. La red de reguladores transcripcionales que afectan a la proliferación de los tricomas está afectada por ambas hormonas (Matías-Hernández., et al 2015). En *Arabidopsis* la iniciación del desarrollo de los tricomas en las hojas de roseta, tallo e inflorescencias depende de la GAs. Así, los mutantes afectados en la biosíntesis de GAs, como *ga1* o *ga3ox*, tienen reducido el número de tricomas, y la aplicación de GAs estimula la iniciación de tricomas en dichos mutantes (Chien & Sussex., 1996; Telfer et al., 1997; Perazza et al., 1998). Por otro lado, las CKs intervienen, sobre todo, en la iniciación de los tricomas en las hojas caulinares, los tallos y los sépalos (Gan et al., 2007). Las GAs actúan a través de GLABROUS INFLORESCENCE STEM (GIS), que activa a los genes cuyas proteínas forman el complejo multimérico GL1/TTG1/GL3-EGL3 (Payne et al., 2000; Zhao et al., 2008). En cambio, las CKs se requieren para la activación en la epidermis de dos genes que codifican factores de transcripción C2H2, GLABROUS INFLORESCENCE STEM2 (GIS2) y ZINC FINGER PROTEIN8 (ZFP8) (Gan et al., 2007).

Estas dos rutas génicas que responden a la acumulación de GAs y CKs convergen en la activación de *GLABROUS2* (*GL2*), promotor universal de la iniciación de los tricomas (Szymanski et al., 1998; Lin & Aoyama, 2012; Figura 6).

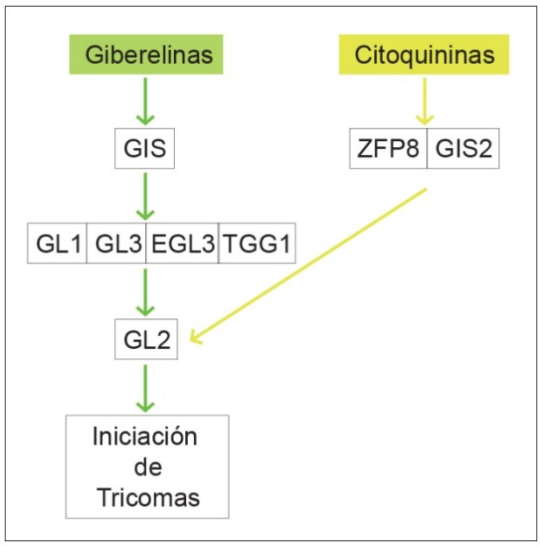

Fig. 6. Regulación genética de la iniciación de tricomas en *Arabidopsis thaliana*

BIBLIOGRAFÍA INTRODUCCIÓN

Abe, M., Kobayashi, Y., Yamamoto, S., Daimon, Y., Yamaguchi, A., Ikeda, Y., Ichinoki, H., Notaguchi, M., Goto, K., and Araki, T. (2005). FD, a bZIP protein mediating signals from the floral pathway integrator FT at the shoot apex. *Science* 309, 1052–1056

Agrawal, A. A. (2000). Communication between plants: this time it's real. *Trends in Ecology & Evolution* 15, 444-446.

Amasino, R. (2010) Seasonal and developmental timing of flowering. *Plant J* 61, 1001-1013.

An, H., Roussot, C., Suárez-López, P., Corbesier,L., Vincent, C., Piñeiro, M., …Coupland,G. (2004). CONSTANS acts in the phloem to regulate a systemic signal that induces photoperiodic flowering of Arabidopsis. *Development*, 131 (15), 3615-3626.

Andres, F., & Coupland G. (2012). The genetic basis of flowering responses to seasonal cues. *Nature Review Genetics* 13, 627-639

Aukerman, M. J., & Sakai, H. (2003). Regulation of flowering time and floral organ identity by a MicroRNA and its APETALA2-like target genes. *Plant Cell*. 15(11), 2730-2741.

Ausín, I., Alonso-Blanco, C., & Martínez-Zapater, J.M. (2005). Environmental regulation of flowering. *Int J Dev Biol*. 49(5-6), 689-705.

Ayre, B., & Turgeon, R. (2004). Graft transmission of a floral stimulant derived from CONSTANS. *Plant Physiology*, 135(4), 2271-2278.

Balasubramanian, S., & Weigel D. (2006). Temperature Induced Flowering in Arabidopsis thaliana. *Plant Signal Behav*. 1(5), 227-8.

Balasubramanian, S., Sureshkumar S., Lempe J., & Weigel D. (2006). Potent induction of Arabidopsis thaliana flowering by elevated growth temperature. *PLoS Genet*. 2(7), e106

Bartel, D. P. (2004). MicroRNAs: genomics, biogenesis, mechanism, and function. *Cell, 116*, 281-297.

Bernier, G., Périlleux, C. (2005). A physiological overview of the genetics of flowering time control. *Plant Biotechnol J*. 3(1), 3-16.

Blázquez, M. A., & Weigel, D. (2000). Integration of floral inductive signals in Arabidopsis. *Nature* 404(6780), 889-892.

Blázquez, M. A., Ahn J. H., & Weigel D. (2003). A thermosensory pathway controlling flowering time in Arabidopsis thaliana. *Nat Genet* 33, 168-171.

Bratzel., & Turck. (2015). Molecular memories in the regulation of seasonal flowering: from competence to cessation. *Genoma Biology*. 16,192.

Castillejo, C., & Pelaz S. (2008). The balance between CONSTANS and TEMPRANILLO activities determines FT expression to trigger flowering. *Curr Biol*. 18, 1338-1343.

Chen, X. (2004). A microRNA as a translational repressor of *APETALA2* in Arabidopsis flower development. *Science* 303 (5666), 2022-2025.

Chien, J. C., & Sussex, I. M. (1996). Differential regulation of trichome formation on the adaxial and abaxial leaf surfaces by gibberellins and photoperiod in Arabidopsis thaliana (L.) Heynh. *Plant Physiology* 111, 1321-1328.

Corbesier, L., Gadisseur, I., Silvestre, G., Jacqmard, A., Bernier, G. (1996). Design in Arabidopsis thaliana of a synchronous system of floral induction by one long day. *The Plant Journal* 9, 947–952.

Fornara, F., de Montaigu, A., & Coupland, G. (2010). SnapShot: Control of flowering in Arabidopsis. *Cell*.141, 550e1-2.

Gan, Y., Liu, C., Yu, H., Broun, P. (2007). Integration of cytokinin and gibberellin signalling by Arabidopsis transcription factors GIS, ZFP8 and GIS2 in the regulation of epidermal cell fate. *Development* 134, 2073–2081

Gandikota, M., Birkenbihl, R. P., Hohmann, S., Cardon, G. H., Saedler, H., et al. (2007). The miRNA156/157 recognition element in the 3' UTR of the Arabidopsis SBP box gene *SPL3* prevents early flowering by translational inhibition in seedlings. *Plant J* 49, 683-693.

Hartmann, U., Höhmann, S., Nettesheim, K., Wisman, E., Saedler, H., Huijser, P. (2000). Molecular cloning of SVP: a negative regulator of the floral transition in Arabidopsis. *Plant J* 21, 351–360

He, Y. (2012). Chromatin regulation of flowering. *Trends Plant Sci*. (9),556-62.

Huijser, P., & Schmid, M. (2011). The control of developmental phase transitions in plants. *Development* 138, 4117–4129.

Hülskamp, M., Miséra, S., & Jürgens, G. (1994). Genetic dissection of trichome cell development in Arabidopsis. *Cell* 76, 555-566.

Jaeger, & Wigge. (2007). FT protein acts as a long-range signal in Arabidopsis. *Curr Biol*.17 (12),1050-1054.

Jang, S., Torti, S., & Coupland, G. (2009). Genetic and spatial interactions between FT, TSF and SVP during the early stages of floral induction in Arabidopsis. *Plant J*. 60(4), 614-625.

Jarillo, J. A., & Piñeiro, M. (2011). Timing is everything in plant development. The central role of floral repressors, *Plant Sci*. 181, 364–378.

Johnson, H. B. (1975). Plant pubescence: an ecological perspective. *Bot. Rev*. 41, 233–258

Jung, J. H., Seo, Y. H., Seo, P. J., Reyes, J. L., Yun, J., Chua, N. H., y Park, C. M. (2007). The *GIGANTEA* regulated microRNA172 mediates photoperiodic flowering independent of *CONSTANS* in Arabidopsis. *Plant Cell* 19, 2736-2748.

Kagaya, Y., Ohmiya, K., & Hattori, T. (1999). RAV1, a novel DNA-binding protein, binds to bipartite recognition sequence through two distinct DNA-binding domains uniquely found in higher plants. *Nucleic Acids Res*. 27, 470–478.

Kim, J. J., Lee, J. H., Kim, W., Jung, H.S., Huijser, P., & Ahn, J. H. (2012). The microRNA 156- SQUAMOSA PROMOTER BINDING PROTEIN-LIKE3 module regulates ambient temperature-reponsive flowering via FLOWERING LOCUS T in Arabidopsis. *Plant Physiology*, 159 (1), 461-478.

Koornneef, M., Hanhart, C. J., & Van Der Veen J.H. (1991). A genetic and physiological analysis of late flowering mutants in Arabidopsis thaliana. *Mol Gen Genet*. 229, 57–66.

Laibach, F. (1943). *Arabidopsis thaliana* (L.) Heynh. als Objekt für genestiche und kentwicklungsphysiologische. *Bot Archiv*.44, 265-455.

Larkin, J. C., Oppenheimer, D. G., Lloyd, A., Paparozzi, E. T., Marks, M. D. (1994). Roles of the GLABROUS1 and TRANSPARENT TESTA GLABRA genes in arabidopsis trichome development. *Plant Cell* 6, 1065–1076.

Lee, J. H., Ryu, H. S., Chung, K. S., Posé, D., Kim, S., Schmid, M., Ahn, J. H. (2013). Regulation of temperature-responsive flowering by MADS-box transcription factor repressors. *Science*. 342 (6158), 628-632.

Lee, J. H., Yoo, S.J., Park, S.H., Hwang, I., Lee, J.S., & Ahn, J.H. (2007). Role of SVP in the control of flowering time by ambient temperature in Arabidopsis. *Genes Dev* 21, 397-402.

Lee, J. H., Kim, J. J., Kim, S. H., Cho, H. J., Kim, J., & Ahn, J. H. (2012) The E3 ubiquitin ligase HOS1 Regulates Low Ambient Temperature-Responsive Flowering in Arabidopsis thaliana. *Plant Cell Physiol*. 53(10), 1802-1814.

Lee, R. C., Feinbaum, R. L., Ambros, V. (1993). The C. elegans heterochronic gene lin-4 encodes small RNAs with antisense complementarity to lin-14. *Cell*. 75, 843-854.

Li, D., Liu, C., Shen, L., Wu, Y., Chen, H., Robertson, M., Helliwell, C. A., Ito, T., Meyerowitz, E., & Yu, H. (2008). A repressor complex governs the integration of flowering signals in Arabidopsis. *Dev Cell* 15, 110-120.

Lin, Q., Aoyama, T. (2012). Pathways for epidermal cell differentiation via the homeobox gene GLABRA2: update on the roles of the classic regulator. *J Integr Plant Biol* 54, 729–737.

Lin, M. K., Belanger, H., Lee, Y.J., Varkonyi-Gasic, E., Taoka, K., Miura, E., Xoconostle-Cazares, B., Gendler, K., Jorgensen, R.A., Phinney, B., et al. (2007). FLOWERING LOCUS T protein may act as the long distance florigenic signal in the cucurbits. *Plant Cell* 19, 1488–1506.

Marín-González, E., Matías-Hernández, L., Aguilar-Jaramillo, A. E., Lee, J. H., Ahn, J. H, et al. (2015). SHORT VEGETATIVE PHASE up-regulates *TEMPRANILLO2* floral repressor at low ambient temperatures. *Plant Physiol* 169, 1214-1224.

Mathieu, J., Warthmann, N., Küttner, F., Schmid, M. (2007). Export of FT protein from phloem companion cells is sufficient for floral induction in Arabidopsis. *Current Biology* 17, 1055–1060.

Mathieu, J., Yant, L. J., Mürdter, F., Küttner, F., & Schmid, M. (2009). Repression of flowering by the miR172 target *SMZ*. *PLoS Biol*. 7(7), e1000148

Matías-Hernández, L., Aguilar-Jaramillo, A. E., Marín-González, E., Suárez-López, P., Pelaz, S. (2014) *RAV* genes: regulation of floral induction and beyond. *Ann Bot* 114, 1459-1470.

Matías-Hernández, L., Aguilar-Jaramillo, A.E., Aiese Cigliano, R., Sanseverino, W., Pelaz, S. (2016). Flowering and trichomes development share hormonal and transcription factor regulation. *J Exp Bot*.67 (5), 1209-1219.

Matías-Hernández, L., Aguilar-Jaramillo, A.E., Osnato, M., Weinstain, R., Shani, E., Suárez-López, P., Pelaz, S. (2016) TEMPRANILLO reveals the mesophyll as crucial for epidermal trichome formation. Plant Physiol. 170 (3), 1624-1639.

Moon, J., Suh, S.S., Lee, H., Choi, K.R., Hong, C.B., Paek, N.C., Kim, S.G. & Lee, I. (2003). The *SOC1* MADS-box gene integrates vernalization and gibberellin signals for flowering in Arabidopsis. *Plant J*. 35(5), 613-623.

Mutasa - Göttgens, & Hedden. (2009). Gibberellin as a factor in floral regulatory networks. *J Exp Bot*. 60(7), 1979-1989.

Olsson, M.E., Olofsson, L. M., Lindahl, A. L., Lundgren, A., Brodelius, M., Brodelius, P. E. (2009). Localization of enzymes of artemisinin biosynthesis to the apical cells of glandular secretory trichomes of Artemisia annua L. *Phytochemistry* 70, 1123–1128.

Oppenheimer, D. G., Herman, P. L., Esch, J., Sivakumaran, S., & Marks, M. D. (1991). A myb-related gene required for leaf trichome differentiation in Arabidopsis is expressed in stipules. *Cell* 67, 483-493.

Osnato, M., Castillejo, C., Matías-Hernández, L., Pelaz, S. (2012). TEMPRANILLO genes link photoperiod and gibberellin pathways to control flowering in Arabidopsis. *Nat Commun*. 3(808) 1-8.

Page, D. R., & Grossniklaus, U. (2002). The art and design of genetic screens: *Arabidopsis thaliana*. *Nat. Rev. Genet*. 3, 124-136.

Payne, C. T., Zhang, F., Lloyd, A. M. (2000). GL3 encodes a bHLH protein that regulates trichome development in arabidopsis through interaction with GL1 and TTG1.*Genetics* 156, 1349–1362.

Perazza, D., Vachon, G., Herzog, M. (1998). Gibberellins promote trichome formation by Up-regulating GLABROUS1 in Arabidopsis. *Plant Physiology* 117, 375–383.

Poethig, R. S. (2009). Small RNAs and developmental timing in plants. *Curr.Opin. Genet. Dev*. 19, 374–378.

Poethig, R. S. (1990). Phase change and the regulation of shoot morphogenesis in plants. *Science* 250, 923-930.

Porri, A., Torti, S., Romera-Branchat, M., & Coupland, G. (2012). Spatially distinct regulatory roles for gibberellins in the promotion of flowering of Arabidopsis under long photoperiods. *Development* 139, 2198-2209.

Pose, D, Verhage, L, Ott, F., Yant, L., Mathieu, J., Angenent, G. C., Immink, R. G. H., Schmid, M. (2013). Temperature-dependent regulation of flowering by antagonistic FLM variants. *Nature* 503, 414–417.

Redei, G. P. (1962). Supervital mutants of Arabidopsis. *Genetics* 47, 443–460.

Reinhart, B. J., Weinstein, E.G., Rhoades, M.W., Bartel, B., & Bartel, D.P (2002). MicroRNAs in plants MicroRNAs in plants. *Genes & Development,* 16, 1616-1626.

Riechmann, J. L., & Meyerowitz, E. M. (1998). The AP2/EREBP family of plant transcription factors. *Biological Chemistry* 379, 633–646.

Riechmann, J. L., Heard, J., Martin, G., et al. (2000). Arabidopsis transcription factors: genome-wide comparative analysis among eukaryotes. *Science* 290, 2105–2110.

Schilmiller, A. L., Last, R.L., Pichersky, E (2008) Harnessing plant trichome biochemistry for the production of useful compounds. *Plant J* 54, 702–711.

Schwab, R., Palatnik, J. F., Riester, M., Schommer, C., Schmid, M, et al. (2005). Specific effects of microRNAs on the plant transcriptome. *Dev Cell* 8, 517-527.

Searle, I., & Coupland, G. (2004). Induction of flowering by seasonal changes in photoperiod. *EMBO J* 23, 1217-1222.

Searle, I., He, Y., Turck, F., Vincent, C., Fornara, F., Krober, S., Amasino, R. A., & Coupland G. (2006). The transcription factor FLC confers a flowering response to vernalization by repressing meristem competence and systemic signaling in Arabidopsis. *Genes Dev* 20, 898-912.

Simpson, G. G., & Dean, C. (2002). Arabidopsis, the Rosetta stone of flowering time?. *Science*. 296 (5566), 285-289.

Song, Y.H., Shim, J.S., Kinmonth- Schultz, H.A., Imaizumi, T. (2015). Photoperiodic flowering: time measurement mechanisms in leaves. *Annu Rev Plant Biol*. 66, 441-464.

Srikanth, A. & Schmid, M. (2011). Regulation of flowering time: all roads lead to Rome. *Cell. Mol. Life Sci*.68, 2013–2037.

Suárez-López, P., Wheatley, K., Robson, F., Onouchi, H., Valverde, F. & Coupland, G. (2001). *CONSTANS* mediates between the circadian clock and the control of flowering in Arabidopsis. *Nature* 10 (6832), 1116-1120.

Szymanski, D. B, Jilk, R. A., Pollock, S. M., Marks, M. D. (1998). Control of GL2 expression in Arabidopsis leaves and trichomes. *Development* 125: 1161–1171.

Tao, Z., Shen, L., Liu, C., Liu, L., Yan, Y., Yu, H. (2012). Genome-wide identification of SOC1 and SVP targets during the floral transition in Arabidopsis. *The Plant Journal* 70, 549–561.

Telfer, A., Bollman, K., & Poethig, S. R. (1997). Phase change and the regulation of trichome distribution in Arabidopsis thaliana. *Development* 124, 645-654.

The *Arabidopsis* Genome Initiative. (2000). Analysis of the genome sequence of the flowering plant *Arabidopsis thaliana*. *Nature* 408, 796-815.

Traw, M. B., & Bergelson, J. (2003). Interactive effects of jasmonic acid, salicylic acid, and gibberellin on induction of trichomes in Arabidopsis. *Plant Physiol* 133, 1367-1375.

Valverde, F., Mouradov, A., Soppe, W., Ravenscroft, D., Samach, A. & Coupland, G. (2004). Photoreceptor regulation of CONSTANS protein in photoperiodic flowering. *Science*. 303, 1003–1006.

Walker, A. R., Davison, P. A., Bolognesi-Winfield, A. C., James, C. M., Srinivasan, N., et al. (1999). The *Transparent Testa Glabra1* locus, which regulates trichome differentiation and anthocyanin biosynthesis in Arabidopsis, encodes a WD40 repeat protein. *Plant Cell* 11,1337–1349.

Wang, J. W., Czech, B., & Weigel, D. (2009). miR156-regulated SPL transcription factors define an endogenous flowering pathway in Arabidopsis thaliana. *Cell* 138, 738-749.

Wigge, P. A., Kim, M. C., Jaeger, K.E., Busch, W., Schmid, M., Lohmann, J. U., & Weigel, D. (2005). Integration of spatial and temporal information during floral induction in Arabidopsis. *Science*. 309, 1056–1059.

Wigge, P.A. (2011). FT, a mobile developmental signal in plants. *Curr Biol*; 21(9), R374-378.

Wilson, R. N., Heckman, J. W., Somerville, C. R. (1992). Gibberellin is required for flowering in *Arabidopsis thaliana* under short days. *Plant Physiology* 100, 403-408.

Wu, G., & Poethig, R. S. (2006). Temporal regulation of shoot development in Arabidopsis thaliana by miR156 and its target SPL3. *Development* 133, 3539-3547.

Wu, G., Park, M. Y., Conway, S. R., Wang, J. W., Weigel, D. & Poethig R. S. (2009). The sequential action of miR156 and miR172 regulates developmental timing in Arabidopsis. *Cell*. 138(4), 750-759.

Yamaguchi A., Wu M. F., Yang L., Wu G., Poethig R. S., y Wagner D. (2009). The microRNA-regulated SBP-Box transcription factor SPL3 is a direct upstream activator of *LEAFY*, *FRUITFULL*, and *APETALA1*.*Dev Cell* 17, 268-278.

Yamasaki, K., Kigawa, T., Inoue, M, et al. (2004). Solution structure of the B3DNA binding domain of the Arabidopsis cold-responsive transcription factor RAV1. *The Plant Cell* 16, 3448–3459.

Zhang, F ., Gonzalez, A., Zhao, M., Payne, C. T., Lloyd, A. (2003) A network of redundant bHLH proteins functions in all TTG1-dependent pathways of Arabidopsis. *Development* 130, 4859–4869.

Zhao, M., Morohashi, K., Hatlestad, G., Grotewold, E., Lloyd, A. (2008). The TTG1-bHLH-MYB complex controls trichome cell fate and patterning through direct targeting of regulatory loci. *Development* 135, 1991-1999.

Zhou, Z., An, L., Sun, L., Zhu, S., Xi, W., Broun, P., Yu, H., Gan, Y. (2011). Zinc finger protein5 is required for the control of trichome initiation by acting upstream of zinc finger protein8 in Arabidopsis. *Plant Physiology* 157, 673-682.

OBJETIVOS

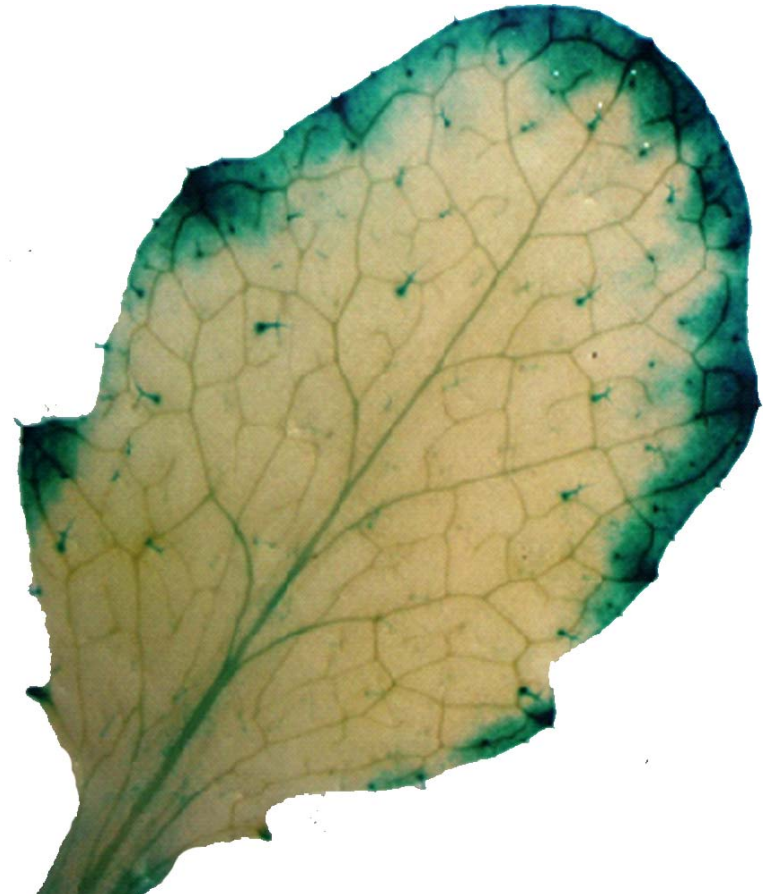

OBJETIVOS GENERALES

El objetivo general de esta tesis doctoral ha sido profundizar en el papel de los genes *TEM1 y TEM2* en el desarrollo vegetal.

A continuación se describen los objetivos que se han planteado para esta investigación:

1. Analizar el papel de los genes *TEM* en la ruta genética que controla la floración en respuesta a la edad de la planta y la función que pueden tener en la regulación de la transición de la fase juvenil a la adulta.

2. Estudiar la implicación de los genes *TEM* en la inducción floral a temperaturas ambientales bajas (16 ºC).

3. Analizar si los genes *TEM* están implicados en la iniciación del desarrollo de los tricomas en *Arabidopsis thaliana*.

CAPÍTULO I: Regulation of Developmental Timming by TEMPRANILLO through miR156 and *SPL* genes.

Regulation of Plant Developmental Timing by TEMPRANILLO through miR156 and *SPL* genes

Andrea E. Aguilar-Jaramillo[1], Esther Marín-González[1], Luis Matías-Hernández[1], Soraya Pelaz[1,2*] and Paula Suárez-López[1*]

[1] Plant Development and Signal Transduction Program, Centre for Research in Agricultural Genomics, CSIC-IRTA-UAB-UB, Bellaterra (Cerdanyola del Vallès), 08193 Barcelona, Spain

[2] Institució Catalana de Recerca i Estudis Avançats, 08010 Barcelona, Spain

* Authors for correspondence:

soraya.pelaz@cragenomica.es, Tel: 34-93-5636600, ext. 3109

paula.suarez@cragenomica.es, Tel: 34-93-5636600, ext. 3110

Summary

• The microRNA 156 (miR156) controls the timing of developmental transitions by negatively regulating several *SPL* genes, which promote the juvenile-to-adult and floral transitions in part through up-regulation of miR172. TEMPRANILLO1 (TEM1) and TEM2 delay flowering in *Arabidopsis thaliana*. *TEM* mRNA and miR156 levels decrease gradually, allowing progression through developmental phases. Given these similarities, we hypothesized that TEMs and miR156 could act through a common genetic pathway.

• We analyzed the effect of TEMs on miR156, *SPL* and miR172 levels, we tested binding of TEMs to these genes using chromatin immunoprecipitation and we analyzed the genetic interactions between *TEMs* and miR156.

• The miR156/SPL module affected mostly the juvenile-to-adult transition, whereas TEMs played a stronger role in the floral than in the juvenile-to-adult transition. TEMs induced miR156 and repressed *SPL* and miR172 expression. TEM1 bound *in vivo* to *MIR156A*, *SPL9* and *MIR172C* sequences, suggesting direct regulation of these genes. Genetic analyses indicated that TEMs affect the juvenile-to-adult and floral transitions through miR156-dependent and independent pathways, which is consistent with miR156-dependent and independent regulation of *SPLs* and miR172 by TEMs.

• Our results indicate that the regulation of developmental timing by TEMs involves at least three steps of the age-dependent pathway.

Keywords: Arabidopsis, flowering, juvenile-to-adult transition, miR156, miR172, SPL, TEMPRANILLO, vegetative phase change.

Introduction

During their life cycle, plants undergo several developmental transitions. The timing of these transitions is essential for proper development and adjustment of growth to environmental conditions. After germination, plants undergo a juvenile phase of vegetative growth, in which they are unable to flower, even under optimal environmental conditions. Following the juvenile period, there is a juvenile-to-adult transition, also termed vegetative phase change, leading to an adult phase in which plants become competent to flower (Huijser & Schmid, 2011). The juvenile-to-adult transition is associated with diverse morphological changes, and the appearance of trichomes on the abaxial side of rosette leaves is a good marker of this transition in *Arabidopsis thaliana* (Telfer *et al.*, 1997; Huijser & Schmid, 2011). In response to environmental and endogenous signals, adult plants experience a vegetative-to-reproductive or floral transition.

Flowering is an energy-consuming process and therefore plants need to accumulate enough reserves before inducing the floral transition. To ensure that flowering occurs under favorable conditions, flowering is regulated by a complex genetic network that responds to environmental and endogenous cues (Amasino, 2010; Andrés & Coupland, 2012). Arabidopsis flowers earlier under long day (LD) than short day (SD) conditions. We have previously shown that *TEMPRANILLO 1* (*TEM1*) and *TEM2* (also known as *RAV2*) inhibit flowering at early developmental stages under LDs and SDs. TEMs belong to the RAV subfamily of transcription factors (Matías-Hernández *et al.*, 2014), which bind DNA at the consensus sequence C(A/C/G)ACA$(N)_{2-8}$(C/A/T)ACCTG (Kagaya *et al.*, 1999). TEMs delay flowering through direct transcriptional repression of the florigen component FLOWERING LOCUS T (FT), its paralog TWIN SISTER OF FT (TSF), and the gibberellin (GA) biosynthesis genes *GIBBERELLIN 3-OXIDASE 1* (*GA3OX1*) and *GA3OX2* (Castillejo & Pelaz, 2008; Osnato *et al.*, 2012; Marín-González *et al.*, 2015). Thus, in Arabidopsis, RAV proteins have been shown to act as transcriptional repressors (Castillejo & Pelaz, 2008; Ikeda & Ohme-Takagi, 2009; Causier *et al.*, 2012; Osnato *et al.*, 2012; Feng *et al.*, 2014; Marín-González *et al.*, 2015). Recently, a role for TEMs in the control of juvenility in Arabidopsis has been reported (Sgamma *et al.*, 2014). Therefore, TEMs play a role in two aspects of developmental timing, the juvenile-to-adult and the floral transitions.

Among the small RNAs involved in the regulation of plant developmental timing, the microRNAs (miRNAs) miR156 and miR172 play a very prominent role (Poethig, 2009; Rubio-Somoza & Weigel, 2011). In Arabidopsis, maize and rice, miR156 delays vegetative phase change and flowering through downregulation of several *SQUAMOSA PROMOTER BINDING PROTEIN-LIKE* (*SPL*) genes (Schwab *et al.*, 2005; Wu & Poethig, 2006; Xie *et al.*, 2006; Chuck *et al.*, 2007; Schwarz *et al.*, 2008; Wu *et al.*, 2009). In Arabidopsis, these genes include *SPL3*, *SPL4*, *SPL5*, *SPL9*, *SPL10* and *SPL15* (Wu & Poethig, 2006; Gandikota *et al.*, 2007; Schwarz *et al.*, 2008; Wu *et al.*, 2009). Plants overexpressing miR156 (*35S::miR156*) show a delayed juvenile-to-adult transition, flower late and have reduced *SPL* mRNA levels (Schwab *et al.*, 2005; Wu & Poethig, 2006; Gandikota *et al.*, 2007; Wang *et al.*, 2009; Wu *et al.*, 2009). Conversely, plants in which miR156 function is reduced (*35S::MIM156* plants) lack the juvenile phase, flower early and have increased *SPL* mRNA levels (Franco-Zorrilla *et al.*, 2007; Wang *et al.*, 2009; Wu *et al.*, 2009).

Although single mutants of the miR156-targeted *SPL* genes show very weak or no obvious phenotypes, double *spl9 spl15* mutants show delayed juvenile-to-adult and floral transitions, revealing functional redundancy within the *SPL* family (Wu & Poethig, 2006; Schwarz *et al.*, 2008; Wang *et al.*, 2008). The function of the miR156/SPL module has also been investigated using miR156-resistant versions of *SPL* genes (*rSPL*). Plants overexpressing *rSPL3*, *rSPL4* or *rSPL5* show early vegetative phase change and early flowering and plants expressing *rSPL9* under the control of the *SPL9* promoter (*pSPL9::rSPL9*) show an even stronger phenotype and lack the juvenile phase (Wu & Poethig, 2006; Gandikota *et al.*, 2007; Wu *et al.*, 2009).

miR156 and miR172 show opposite temporal expression patterns, such that miR156 decreases and miR172 increases with age (Aukerman & Sakai, 2003; Wu & Poethig, 2006; Jung *et al.*, 2007; Wang *et al.*, 2009; Wu *et al.*, 2009). miR156 represses miR172 expression via down-regulation of SPL9, which directly promotes miR172 expression (Wu *et al.*, 2009). In turn, miR172 promotes the juvenile-to-adult and the floral transitions (Aukerman & Sakai, 2003; Chen, 2004; Wu *et al.*, 2009). Therefore, miR156, SPLs and miR172 constitute an age-dependent developmental pathway, in

which complex feedback regulations have been reported (Schwab *et al.*, 2005; Mathieu *et al.*, 2009; Wu *et al.*, 2009; Yant *et al.*, 2010; Jung *et al.*, 2011).

Similar to miR156, *TEM1* and *TEM2* mRNA levels decline with age (Castillejo & Pelaz, 2008). Given the similar expression patterns and similar phenotypic effects on vegetative phase change and flowering, we hypothesized that TEMs and miR156 may act through a common genetic pathway. We show here that TEMs positively regulate miR156 levels and negatively regulate *SPL* and miR172 levels. Binding of TEM1 to *MIR156A, SPL9* and *MIR172C* chromatin strongly suggests that TEM1 can directly regulate the expression of these genes. In addition, the effect of TEMs on vegetative phase change, flowering, *SPL* and miR172 expression is partly mediated by miR156. Therefore, we conclude that TEMs regulate developmental timing in part through the age-dependent pathway.

Materials and methods

Plant material and growth conditions

Arabidopsis thaliana Columbia-0 (Col-0) was used as the wild type for all the experiments. *tem1-1*, *tem2-2*, *tem1-1 tem2-2*, *35S::TEM1*, *35S::TEM2*, *pTEM1::GUS*, *35S::miR156*, *35S::MIM156* and *pSPL9::rSPL9* plants have been previously described (Schwab *et al.*, 2005; Franco-Zorrilla *et al.*, 2007; Castillejo & Pelaz, 2008; Wang *et al.*, 2008; Todesco *et al.*, 2010; Osnato *et al.*, 2012). Seeds were stratified on wet filter paper in the dark at 4°C for 3-4 d and then sown on soil and grown in controlled environment chambers at 22°C under LDs (16 h light : 8 h dark) or SDs (8 h light : 16 h dark) at a light intensity of 80-90 μmol m^{-2} s^{-1}.

Phenotypic analyses

To determine the juvenile-to-adult transition we counted the rosette leaves without and with abaxial trichomes (juvenile and adult leaves, respectively). For flowering time experiments, the shoot apex was carefully checked for visible signs of flowering every two days. Flowering time was measured as the number of days from sowing to the appearance of the floral bud and as the total number of rosette and cauline leaves produced on the main stem. At least 14 plants per genotype were used in each experiment.

Analyses of miRNA and transcript levels

For miRNA analyses, total RNA was extracted from pools of at least 10 plants using the Real ARNzol Spin kit (+PVP; Durviz) or using Trizol (Ambion) following manufacturer's instructions. RNAs were treated with DNase using the DNA-free kit (Ambion) and precipitated with sodium acetate. Stem-loop reverse transcription followed by quantitative real time PCR (stem-loop RT-qPCR) and RNA blots were performed as previously described (Martin *et al.*, 2009). Primer and probe sequences are shown in Table S8.

For analyses of transcript levels by RT-qPCR, total RNA was extracted from pools of at least 10 plants with the Real ARNzol Spin kit (+PVP; Durviz), the PureLink RNA Mini kit (Ambion) or Trizol (Ambion) and treated with DNase using the DNA-free kit (Ambion). Reverse transcription was performed with 1-2 µg of RNA using Superscript III reverse transcriptase (Invitrogen), following manufacturer's instructions. qPCR was performed on a LightCycler® 480 Real-Time PCR System (Roche Diagnostics Ltd) with gene-specific primer pairs. The reactions, performed in triplicate in a volume of 14 µl, contained 0.2 µl of cDNA, 1X Light Cycler 480 SYBR Green I Master mix (Roche), 0.3 µM forward primer and 0.3 µM reverse primer, and were incubated at 95°C for 10 min, followed by 45 cycles of 95°C for 15 s and 60°C for 1 min. The specificity of PCR was checked with dissociation curves and quantification was standardized to *UBIQUITIN10* (*UBQ10*) mRNA levels. Data from RT-qPCR were analyzed using the $2^{-\Delta\Delta C}{}_T$ method (Livak & Schmittgen, 2001). Primer sequences are listed in Table S8.

Identification of putative RAV binding sites

To find putative RAV binding sites, sequences of interest were searched for the pattern C[ACG][ACG]CAN(2,9)[ACT]NNCTG using Fuzznuc (http://emboss.bioinformatics.nl/cgi-bin/emboss/fuzznuc) or DNA Pattern Find (http://www.bioinformatics.org/sms2/dna_pattern.html).

Chromatin immunoprecipitation analyses

Chromatin immunoprecipitation (ChIP) experiments were performed using a modified version of a previously reported protocol (Matias-Hernandez *et al.*, 2010). Direct binding of TEM1 and TEM2 to the regulatory regions of putative targets was assayed

using the *35S:TEM1-HA* and *35S:TEM2-HA* lines previously described (Castillejo & Pelaz, 2008). Wild-type plants were used as negative controls. The crosslinked DNA was immunoprecipitated with an anti-HA antibody (Sigma) and purified using Protein A-Agarose resin (Millipore). Enrichment of the target regions was determined by qPCR using different primer sets specific for putative direct targets, as listed in Table S8.

The qPCR assay was conducted in triplicate using a SYBR Green Assay (SYBR Green Supermix, Roche) and was performed in a Roche LightCycler® 480 System. Relative enrichment was calculated normalizing the amount of immunoprecipitated DNA against total input DNA. For the binding of TEM1 and TEM2 to the selected genomic regions, the affinity of the purified sample obtained in the *35S:TEM1-HA* and *35S:TEM2-HA* lines was compared with the affinity-purified sample obtained in the wild-type background, which was used as negative control. Fold enrichment was calculated using the following formulas, where Ct.tg is target gene mean value, Ct.i is input DNA mean value, and Ct.nc is wild type (negative control) mean value: ΔCT.tg = CT.i - CT.tg and ΔCT.nc = CT.i - CT.nc. The propagated error values of these CTs were calculated: ΔSD. tg = $\sqrt{((SD.i)^2 + (SD.tg)^2)}/\sqrt{(n)}$ and ΔSD.nc = $\sqrt{((SD.i)^2 + (SD.nc)^2)}/\sqrt{(n)}$, where n = number of replicates per sample. Fold-change over negative control (wild-type plants) was calculated from the $\Delta\Delta$CT of the target region as follows: $\Delta\Delta$CT = ΔCT.tg - ΔCT.nc and $\Delta\Delta$SD = $\sqrt{((\Delta SD.tg)^2 + (\Delta SD.nc)^2)}$. The transformation to linear fold-change values is obtained as follows: $FC = 2^{\Delta\Delta CT}$ and FC.error = ln(2)*$\Delta\Delta$SD*FC.

Genetic crosses

F_2 plants were genotyped by checking resistance to kanamycin or Basta, by checking GFP fluorescence in seeds (*35S::TEM1* crosses) or by PCR using specific primers, listed in Table S8. Genomic DNA was isolated as previously described (Edwards *et al.*, 1991) with an additional chloroform extraction. Unless otherwise specified, F_3 homozygous plants were used for all the experiments.

GUS staining

Histochemical analyses of GUS expression were performed as previously described (Blázquez *et al.*, 1997).

Statistical analyses

Statistical analyses were performed with GraphPad Prism 6 software (GraphPad Software, Inc). Data were analyzed using one-way ANOVA followed by Tukey's multiple comparisons tests.

Results

Comparison of phenotypes caused by alterations in TEM1/TEM2 and the age-dependent pathway

Given that miR156 and TEM1/TEM2 follow similar temporal expression patterns and are involved in similar developmental processes, we compared the phenotypes of plants with altered TEM levels with those of plants affected in the age-dependent pathway. We determined the length of the juvenile and adult phases by counting the leaves without and with abaxial trichomes, respectively. Under SDs the length of the juvenile phase of *tem1* and *tem2* mutants was not altered (Table 1). Although the difference was not statistically significant, *tem1 tem2* always displayed a slightly shorter juvenile phase than the wild type under SDs. *tem1*, *tem2* and *tem1 tem2* mutants had a significantly shorter adult phase than wild-type plants (Table 1). Consistent with a shortened adult phase and with previous reports (Castillejo & Pelaz, 2008; Osnato *et al.*, 2012), early flowering was observed in *tem1*, *tem2* and, more markedly, in *tem1 tem2* (Table 2). Plants overexpressing TEM1 (*35S::TEM1*) had a dramatically extended juvenile phase, with no detectable adult phase under SDs (Table 1), and did not flower for at least 4 months (Table 2). Plants in which miR156 activity was inhibited (*35S::MIM156*) and plants expressing a miR156-resistant form of SPL9 (*pSLP9::rSPL9*) lacked the juvenile phase, in agreement with a previous report (Wu *et al.*, 2009), and had an adult phase similar to that of wild-type plants under SDs (Table 1). Therefore, *35S::MIM156* and *pSLP9::rSPL9* plants flowered with fewer leaves than wild-type plants (Table 2) due to the absence of the juvenile phase. Plants overexpressing miR156 (*35S::miR156*) showed a dramatically extended juvenile phase, consistent with the results of Wu et al (2009) (Wu *et al.*, 2009), and a shortened adult phase (Table 1), resulting in late flowering compared with wild-type plants (Table 2). Similar results were obtained under LDs (Tables 1, 2), with two exceptions: the shortening of the juvenile phase of *tem1 tem2* was statistically significant and the length of the adult phase of *35S::miR156* was extended. We can conclude that TEMs and the miR156/SPL module affect the juvenile-

to-adult and the floral transitions to different extents, with the miR156/SPL module having a more dramatic effect on the juvenile phase and TEMs affecting mainly the floral transition, with a relatively minor role in the regulation of vegetative phase change. Therefore, the miR156/SPL module and TEM1/TEM2 play partially overlapping but distinct roles in the regulation of phase transitions.

TEMs up-regulate miR156 levels

As miR156 and TEM1/TEM2 have partially overlapping phenotypic effects, we tested whether miR156 regulates *TEM1*/*TEM2* levels or vice versa. *35S::miR156* and *35S::MIM156* plants did not show significant alterations in *TEM1* and *TEM2* mRNA levels that could correlate with their flowering phenotypes under LD and SD conditions (Fig. S1). TEMs and miR156 affect the juvenile-to-adult and the floral transitions under both LD and SD (Tables 1, 2; Schwab *et al.*, 2005; Wu & Poethig, 2006; Franco-Zorrilla *et al.*, 2007; Castillejo & Pelaz, 2008; Wu *et al.*, 2009; Osnato *et al.*, 2012). We therefore used LD conditions for subsequent experiments. For the analysis of the effect of TEMs on miR156, we collected samples at two time points, one during the light period (ZT8), when *TEM* mRNA levels are low (Castillejo & Pelaz, 2008; Osnato *et al.*, 2012) and the miR156-targeted *SPL9* mRNA peaks (Fig. S2), and one during the night (ZT18), when *TEM* mRNAs peak (Castillejo & Pelaz, 2008; Osnato *et al.*, 2012). RNA blots showed that *tem1 tem2* mutants exhibited slightly reduced mature miR156 abundance at ZT8 (Fig. 1a), a result also observed in RT-qPCR experiments (Fig. S3). *35S::miR156* plants used as controls showed increased miR156 levels, as expected (Fig. 1a). The down-regulation of mature miR156 in *tem1 tem2* suggested that TEM1 and/or TEM2 positively regulate miR156. To confirm this, we tested miR156 accumulation in *35S::TEM1* plants. Indeed, *35S::TEM1* plants exhibited higher mature miR156 levels than wild-type plants at ZT8 and ZT18 (Figs. 1b, S3). To determine whether these changes in mature miR156 are due to transcriptional regulation, we analyzed primary miR156 (pri-miR156) levels in *tem1 tem2* and *35S::TEM1* plants. Levels of pri-miR156a and pri-miR156c, the two most highly expressed miR156 primary transcripts, were reduced in *tem1 tem2* and increased in *35S::TEM1* relative to wild-type plants (Fig. 1c), consistent with the changes in mature miR156. Therefore TEMs positively regulate mature miR156 levels most probably through transcriptional regulation of at least the *MIR156A* and *MIR156C* genes, suggesting that miR156 acts downstream of TEM in controlling vegetative phase change and flowering time.

Given that TEMs have been shown to act as transcriptional repressors but positively regulate miR156 expression, we examined whether the regulation of miR156 is direct. We found several putative RAV binding sites in the *MIR156A* gene (Table S3). We performed chromatin immunoprecipitation (ChIP) experiments to test whether TEM1 and TEM2 bind *in vivo* to these putative RAV binding sites. We used *35S::TEM1* and *35S::TEM2* plants, which carry an HA tag fused to the TEM1 and TEM2 protein, respectively (Castillejo & Pelaz, 2008). An anti-HA antibody was used to immunoprecipitate chromatin from these plants. A DNA fragment containing a putative RAV binding site 426 nt upstream of the *MIR156A* transcription start site (-426 fragment) was considerably enriched in *35S::TEM1* plants (Fig. 1d), strongly suggesting that TEM1 regulates miR156 expression through binding to the *MIR156A* promoter. This indicates that TEM1 can act either as a transcriptional repressor or as a transcriptional activator. We did not detect binding of TEM1 to the fragment containing the other putative RAV binding site examined (+588 fragment) and TEM2 did not bind to any of the two fragments (Fig. 1d).

TEMs down-regulate *SPL* genes and TEM1 binds to *SPL9* chromatin

miR156 represses vegetative phase change and flowering by negatively regulating *SPL3*, *SPL9* and other *SPL* genes (Wu & Poethig, 2006; Schwarz *et al.*, 2008; Wang *et al.*, 2009; Wu *et al.*, 2009). The effect of TEMs on miR156 suggested that *SPL* mRNA levels might be altered in *tem1 tem2* mutants and *35S::TEM1* plants. We found that *SPL3* and to a lower extent *SPL9* and *SPL15* transcript abundance was slightly increased in *tem1 tem2* and substantially reduced in *35S::TEM1* plants compared with the wild type (Fig. 2a), indicating that TEMs negatively regulate *SPL3*, *SPL9* and *SPL15*, consistent with the positive regulation of miR156.

A computational analysis of the *SPL9* gene revealed the presence of three putative RAV binding sites (Table S4). To test whether TEM1 and TEM2 bind to these putative RAV binding sites we performed ChIP experiments. In the chromatin from *35S::TEM1* plants immunoprecipitated with an anti-HA antibody, a fragment containing the three putative RAV binding sites was considerably enriched compared with the controls (Fig. 2b), indicating that TEM1 binds *in vivo* to *SPL9* chromatin. TEM2, however, did not bind to this fragment, a result that reminded the lack of binding of TEM2 to *MIR156A*

chromatin. Together with the effect of TEMs on miR156, these results strongly suggest that TEMs negatively regulate *SPL9* transcriptionally through binding to *SPL9* sequences and post-transcriptionally through miR156-mediated degradation.

TEMs down-regulate miR172 and bind to *MIR172C* chromatin

TEMs down-regulate *SPL9*, which in turn promotes the transcription of miR172 (Wu *et al.*, 2009). Therefore we expected that TEMs down-regulate miR172. Consistent with this hypothesis, we found increased miR172 abundance in *tem1 tem2* and reduced abundance in *35S::TEM1* plants (Fig. 3a,b). Similar results were obtained by RNA blot (Fig. 3a,b) and RT-qPCR (Fig. S4). The increase observed in *tem1 tem2* was similar to that in *pSPL9::rSPL9* plants, which had been previously reported (Wu *et al.*, 2009), consistent with the effect of TEMs on miR172 being mediated by SPL9. *35S::miR156* plants used as control showed slightly reduced miR172 levels (Fig. 3a), as expected (Wu *et al.*, 2009).

Similar to *MIR156A* and *SPL9*, we found putative RAV binding sites in four *MIR172* genes (Table S5). Because *MIR172C* has several putative RAV binding sites, we tested binding of TEM1 and TEM2 to *MIR172C* by ChIP. TEM1 clearly bound to a fragment containing two putative RAV binding sites and TEM2 also bound to some extent (Fig. 3c). This strongly suggests that TEMs repress miR172 expression through direct binding to *MIR172C* chromatin. In addition, as TEMs also regulate *SPL9* levels, TEMs probably regulate miR172 indirectly through their effect on *SPL9*.

TEMs act through miR156-dependent and independent pathways to control vegetative phase change and flowering

If the early vegetative phase change and early flowering of *tem1 tem2* plants is due to reduced miR156 abundance, overexpression of miR156 should suppress the vegetative phase change and flowering phenotypes of *tem1 tem2*. We generated *tem1 35S::miR156*, *tem2 35S::miR156* and *tem1 tem2 35S::miR156* plants, but the *35S::miR156* transgene was partially silenced in *tem1 35S::miR156* (Fig. S5) and *tem1 tem2 35S::miR156*. Silencing of transgenes by T-DNA insertion mutations has already been reported (e.g. Daxinger *et al.*, 2008; Wu *et al.*, 2009). Therefore, to analyze the genetic interaction between *TEM1* and miR156 we crossed *35S::MIM156* with *35S::TEM1*. If miR156 acts downstream of TEM1 to control vegetative phase change

and flowering, we would expect that inactivation of miR156 would suppress the phenotypes of *35S::TEM1* plants. In agreement with a previous report (Wu *et al.*, 2009), *35S::MIM156* plants essentially lacked a juvenile phase and flowered after producing fewer leaves than WT plants, whereas *35S::TEM1* plants had a very extended juvenile phase and flowered later than the WT (Tables 3, 4; Fig. S6). *35S::TEM1 35S::MIM156* plants had a similar juvenile phase to that of WT plants, much shorter than that of *35S::TEM1* plants (Table 3). *35S::TEM1 35S::MIM156* plants also flowered considerably earlier than *35S::TEM1* both in terms of days and leaves and after producing the same leaves as WT plants (Table 4; Fig. S6). These results indicate that *35S::MIM156* suppresses the late juvenile-to-adult transition and the late flowering of *35S::TEM1*. Together with the effect of TEMs on miR156 levels, this indicates that miR156 acts downstream of TEM1 in the regulation of vegetative phase change and flowering. In agreement with this, *35S::TEM1 35S::miR156* plants flowered at a similar time and with a similar leaf number to *35S::miR156* plants (Table 4). Note that the flowering of *35S::TEM1 35S::miR156* was analyzed in the F_1 generation because these plants were sterile. However, *35S::TEM1 35S::MIM156* had a longer juvenile phase and flowered after producing more leaves than *35S::MIM156* (Tables 3, 4), indicating that TEM1 can still repress the juvenile-to-adult transition and flowering in the absence of miR156 function. Altogether these observations indicate that TEM1 represses vegetative phase change and flowering through a miR156-dependent pathway, but also through miR156-independent pathway(s).

We also analyzed the genetic interaction between *TEM2* and miR156. We observed that *tem2 35S::miR156* plants had a longer juvenile phase (Table 3) and flowered with more leaves (Table 4; Fig. S6) than *tem2* and wild-type plants, indicating that *35S:miR156* suppresses the early flowering phenotype of *tem2*, consistent with miR156 acting downstream of TEM2. However, *tem2 35S::miR156* had a shorter juvenile phase (Table 3) and flowered with fewer leaves (Table 4; Fig. S6) than *35S::miR156*, indicating that when there is an excess of miR156, TEM2 can delay vegetative phase change and flowering. This reveals an effect of TEM2 on vegetative phase change that is not obvious in *tem2* mutants. The adult phase of *tem2 35S::miR156* was not significantly different from that of *tem2* plants, given that *35S::miR156* did not significantly affect the length of this phase (Table 3). Taking also into account the effect of TEMs on miR156 levels, we conclude that TEM2 regulates phase transitions through miR156-

dependent and independent pathways. This is further supported by the phenotypes of *tem2 35S::MIM156* plants, which showed an intermediate flowering phenotype between *tem2* and *35S::MIM156* plants (Table 4; Fig. S6). Like in previous experiments, *tem2* mutants did not show an alteration of the juvenile phase, as they produced the same number of leaves without abaxial trichomes as wild-type plants (Table 3). Consistent with this, *tem2 35S::MIM156* behaved like *35S::MIM156* plants and did not have a juvenile phase. Again, we could not use *tem1 35S::MIM156* plants because the *35S::MIM156* transgene was partially silenced in these plants (Fig. S7).

TEMs regulate *SPL* and miR172 levels through miR156-dependent and independent pathways

Our results suggested that TEMs regulate *SPL* and miR172 levels through direct binding, but also through the effect on miR156. To determine whether miR156 mediates the effect of TEMs on *SPLs* and miR172, we analyzed *SPL* mRNA and miR172 levels in different genetic backgrounds. As expected, *SPL3*, *SPL9* and *SPL15* were dramatically upregulated in *35S::MIM156* compared with WT plants (Fig. 4a). The reduction of *SPL3*, *SPL9* and *SPL15* mRNA levels observed in *35S::TEM1* was suppressed in *35S::TEM1 35S::MIM156*, which showed higher *SPL3*, *SPL9* and *SPL15* mRNA abundance than WT plants (Fig. 4a). This confirms that miR156 acts downstream of TEM1 and indicates that the effect of miR156 on vegetative phase change and flowering downstream of TEM1 is at least partly mediated by SPL transcription factors. Since the levels of *SPL3*, *SPL9* and *SPL15* in *35S::TEM1 35S::MIM156* are not as high as in *35S::MIM156*, *35S::TEM1* is able to down-regulate *SPLs* even in the absence of miR156 function. This indicates that TEM1 can also act through miR156-independent pathways, which include direct repression of *SPL9*, as shown in Fig. 2.

We found very similar or slightly higher levels of *SPL3*, *SPL9* and *SPL15* mRNA in *tem2 35S::MIM156* than in *35S::MIM156* plants (Fig. 4b), which showed much higher levels than *tem2* plants, indicating that *tem2* and *35S::MIM156* have only a slightly additive effect. Therefore TEM2 regulates *SPL* levels in a partially miR156-independent manner.

Similar conclusions can be drawn for the effect of TEMs on miR172. *35S::MIM156* suppresses the reduction of miR172 levels observed in *35S::TEM1*, but *35S::TEM1 35S::MIM156* shows lower miR172 levels than *35S::MIM156* (Fig. 4c), indicating that TEM1 regulates miR172 levels through miR156-dependent and independent pathways. In addition, *tem2 35S::MIM156* plants exhibited higher miR172 levels than *tem2* and *35S::MIM156* plants (Fig. 4d), suggesting that at least part of the effect of TEM2 on miR172 is miR156-independent. Our ChIP results (Figs. 2b, 3c) strongly suggest that the miR156-independent pathways include direct regulation of the expression of *SPL9* and miR172.

Discussion

We had previously shown that TEM1 and TEM2 play a role in the timing of the floral transition in Arabidopsis (Castillejo & Pelaz, 2008; Osnato *et al.*, 2012). We show here that they also affect the timing of vegetative phase change, measured by the appearance of trichomes on the abaxial surface of rosette leaves. *tem1 tem2* double mutants, but not *tem1* and *tem2* single mutants, show a shortened juvenile phase under LDs (Table 1), indicating that TEM1 and TEM2 redundantly delay vegetative phase change. A role of TEM2 in this developmental transition is also revealed in *tem2 35S::miR156* plants (Table 3). Our results are consistent with recent work showing that TEMs affect the length of the juvenile phase measured by the response of flowering to inductive photoperiods in plants transferred from long to short days (Sgamma *et al.*, 2014). In the work of Sgamma *et al.* (2014), the effect of TEMs on the juvenile phase was more dramatic than in our work. This may be explained because we used different methods to determine the length of the juvenile phase: Sgamma *et al.* (2014) measured the juvenile phase as days from germination, whereas we measured the number of leaves without abaxial trichomes. In addition, we cannot rule out that the difference can be due to the use of different growth conditions.

We show here that the effect of the miR156/SPL module on vegetative phase change, which has previously been shown under short days (Wu *et al.*, 2009), also occurs under long days. Our results indicate that TEM1/TEM2 and the miR156/SPL module have different relative importance in the control of vegetative phase change and the floral transition. Since plants with altered levels of miR156 and SPL9 show defects mainly in

the juvenile phase, with little or no effect on the length of the adult phase (Table 1), the effect of the miR156/SPL module on flowering time is mostly an indirect consequence of the effect on vegetative phase change, rather than a specific effect on the floral transition. On the contrary, TEMs play a relatively minor role in vegetative phase change and a more important role in delaying the floral transition and extending the length of the adult phase. However, when TEM1 is overexpressed, instead of an extension of the adult phase, we observed a dramatic lengthening of the juvenile phase, together with an extreme shortening or even suppression of the adult phase (Tables 1, 3). This indicates that a vegetative adult phase is not absolutely required for flowering. Taking into account that TEMs induce miR156 expression (Fig. 1), our interpretation of this result is that high miR156 levels suppress the adult phase in *35S::TEM1* plants because they extend the juvenile phase until flowering is induced through a different pathway. That *35S::TEM1 35S::MIM156* plants have juvenile and adult phases similar to those in wild-type plants supports this interpretation. We propose that the decline of *TEM* levels through development (Castillejo & Pelaz, 2008) is necessary for the juvenile-to-adult transition in part because it contributes to reducing miR156 levels.

Several factors are known to regulate miR156 levels, such as sugars, the flowering-time regulators AGAMOUS-LIKE 15, AGAMOUS-LIKE 18 and SOC1, the transcription factor FUSCA3, and the histone-modifying factors AtBMI1 (Tao *et al.*, 2012; Wahl *et al.*, 2013; Wang & Perry, 2013; Yang *et al.*, 2013; Yu *et al.*, 2013; Picó *et al.*, 2015; Serivichyaswat *et al.*, 2015). Our work establishes that TEMs are new miR156 regulators. Further work is required to understand if there are interactions among these factors and how they contribute to establish the temporal and spatial pattern of miR156 expression.

TEM1 and TEM2 had been described as transcriptional repressors that directly down-regulate *FT*, *TSF*, *GA3ox1* and *GA3ox2* (Castillejo & Pelaz, 2008; Osnato *et al.*, 2012; Marín-González *et al.*, 2015). We show here that TEMs also repress *SPL* and miR172 expression, that TEM1 directly binds to *SPL9* chromatin and that TEM1 and to a lesser extent TEM2 bind to *MIR172C* chromatin (Figs. 2, 3). Our work also shows, however, that TEMs positively regulate the expression of *MIR156* genes and that TEM1 binds to the *MIR156A* promoter (Fig. 1), strongly suggesting direct regulation of miR156 expression by TEM1. In addition, recent work has shown that TEM2, interacting with

the transcription factor GT-4, positively regulates the expression of the salt-responsive gene *COLD-REGULATED 15A* (Wang *et al.*, 2014). Therefore, TEMs seem to act as transcriptional repressors or activators depending on the target gene.

Whereas TEM1 directly binds to *MIR156A* and *SPL9* sequences, TEM2 does not seem to bind directly (Figs. 1d, 2b). However, the phenotypes of the *tem1 tem2* double mutants are stronger than those of the single *tem1* and *tem2* mutants (Tables 1, 2; Castillejo & Pelaz, 2008; Osnato *et al.*, 2012), indicating that both TEM1 and TEM2 are required for delaying the juvenile-to-adult transition and flowering. That TEM2 is required for the repression of *SPL9* is shown by the increase of *SPL9* mRNA levels in the single *tem2* mutant (Fig. 4b). We hypothesize that TEM2 may regulate miR156 and *SPL9* expression through direct interaction with TEM1 or, alternatively, that TEM1 and TEM2 may interact with common proteins in a multiprotein complex, such that TEM1 would indirectly recruit TEM2. A common interacting protein might be the transcriptional corepressor TOPLESS, which has been suggested to interact with TEM1 and TEM2 (Causier *et al.*, 2012).

TEMs act as upstream regulators of three consecutive steps - miR156, *SPLs* and miR172 - of the age-dependent pathway regulating vegetative phase change. TEMs induce miR156 and this miRNA is required for *SPL* and miR172 downregulation and for the delay of the juvenile-to-adult transition by TEMs. Our work also shows that TEMs regulate vegetative phase change and flowering in a miR156-independent manner, which includes direct repression of *SPL9* and *MIR172C* (Figs. 2, 3), as well as regulation of other flowering-time factors, such as *FT*, *TSF* and gibberellin (Castillejo & Pelaz, 2008; Osnato *et al.*, 2012; Marín-González *et al.*, 2015).

SPL3, *SPL9* and *SPL15* are transcriptionally regulated by TEMs (Fig. 2) and post-transcriptionally regulated by miR156 (Schwab *et al.*, 2005; Gandikota *et al.*, 2007). Therefore, it can be expected that the effects of TEMs and miR156 on *SPL* mRNA levels are to some extent additive. Consistent with this, *SPL3, SPL9* and *SPL15* transcript levels in *35S::TEM1 35S::MIM156* plants are intermediate between those of *35S::TEM1* and *35S::MIM156* plants (Fig. 4a), in agreement with the *35S::TEM1 35S::MIM156* phenotypes (Tables 3, 4). Also, *tem2 35S::MIM156* plants showed slightly higher *SPL3*, *SPL9* and *SPL15* mRNA levels than *tem2* and *35S::MIM156*.

Nevertheless, our results also indicate that part of the effect of TEMs on *SPL* genes, the juvenile-to-adult transition and flowering is mediated by miR156. The regulation of the juvenile-to-adult transition by miR156 downstream of TEM1 is a direct consequence of the effect of miR156 on the length of the juvenile phase. However, the effect of miR156 on flowering downstream of TEM1 is probably an indirect consequence of the effect of miR156 on the length of the juvenile phase, given that miR156 has little direct effect on the floral transition. In other words, miR156 is required for the delay of the juvenile-to-adult transition by TEMs, but is only indirectly required for delaying the floral transition.

When Arabidopsis plants are transferred from short to long days, miR156 levels do not change, but *SPL3* and *SPL9* mRNA levels increase rapidly (Schmid *et al.*, 2003; Wang *et al.*, 2009). Given that *TEM*s are down-regulated upon transfer from SD to LD (Osnato *et al.*, 2012), and that TEMs repress *SPL3* and *SPL9* (Fig. 2), we propose that the increase in *SPL3* and *SPL9* after transfer to LD results in part from the release of repression by TEMs. The up-regulation of *FT* upon transfer from SD to LD (Osnato *et al.*, 2012) probably contributes to the up-regulation of *SPL3*, because FT is a positive regulator of several *SPL* genes (Yamaguchi *et al.*, 2009; Jung *et al.*, 2012).

Our work and that of other groups indicate that TEMs repress SPL expression and function through at least four different mechanisms: direct transcriptional repression by binding to the *SPL9* promoter (Fig. 2); indirect transcriptional regulation through the repression of *FT* expression and GA biosynthesis (Castillejo & Pelaz, 2008; Osnato *et al.*, 2012), given that FT and GAs are positive regulators of several *SPL* genes (Yamaguchi *et al.*, 2009; Galvão *et al.*, 2012; Jung *et al.*, 2012; Park *et al.*, 2013) ; post-transcriptional regulation via miR156 (Figs. 1, 4; Schwab *et al.*, 2005; Gandikota *et al.*, 2007); and post-translational regulation through the repression of GA biosynthesis (Osnato *et al.*, 2012), given that DELLAs interfere with SPL transcriptional activity through direct interaction, and GA releases this interaction (Yu *et al.*, 2012). All this would ensure that SPL9 does not promote precocious juvenile-to-adult transition and flowering.

There is extensive crosstalk among the different genes acting in the flowering time network (Bouché *et al.*, 2016). By revealing the role of TEMs in the age-dependent

flowering pathway, our work suggests that TEMs link this pathway to the photoperiod, GA and ambient temperature pathways, in which TEMs are also involved (Castillejo & Pelaz, 2008; Osnato *et al.*, 2012; Marín-González *et al.*, 2015), pointing to additional crosstalk within the flowering network.

Acknowledgements

We thank Detlef Weigel and Scott Poethig for seeds; Mauricio Soto for advice with miRNA blots; Rossana Henriques for primers and discussion; Laura Ossorio, Manel Giménez, Cristina Valdivieso and CRAG greenhouse staff for technical assistance; Ángel Sánchez for pictures; and Michela Osnato and Rossana Henriques for critical reading of the manuscript. This work was supported by the Spanish Ministry of Economy and Competitiveness/European Regional Development Fund (grant no. BFU2012-33746 and CSD2007-00036), the Investigator Training Program of the Catalonian Government (PhD fellowship to A.E.A.-J.), the Spanish Government (FPI fellowship to E.M.-G.) and the Catalonian Government (Consolidated Research Group no. 2014 SGR 1406). A.E.A.-J. performed this work within the frame of a Ph.D. Program of the Universitat Autònoma de Barcelona.

Author contributions

P.S.-L., S.P. and E.M.-G. conceived and designed the experiments. A.E.A.-J., E.M.-G., L.M.-H. and P. S.-L. performed the experiments. A.E.A.-J., E.M.-G., L.M.-H., S.P. and P. S.-L. analyzed the data. P.S.-L. and S.P. wrote the manuscript, with comments from all other authors.

References

Amasino R. 2010. Seasonal and developmental timing of flowering. *The Plant Journal* **61**: 1001-1013.

Andrés F, Coupland G. 2012. The genetic basis of flowering responses to seasonal cues. *Nature Reviews Genetics* **13**: 627-639.

Aukerman MJ, Sakai H. 2003. Regulation of flowering time and floral organ identity by a microRNA and its *APETALA2*-like target genes. *The Plant Cell* **15**: 2730-2741.

Blázquez MA, Soowal LN, Lee I, Weigel D. 1997. *LEAFY* expression and flower initiation in *Arabidopsis*. *Development* **124**: 3835-3844.

Bouché F, Lobet G, Tocquin P, Périlleux C. 2016. FLOR-ID: an interactive database of flowering-time gene networks in Arabidopsis thaliana. *Nucleic Acids Research* **44**: D1167-D1171.

Castillejo C, Pelaz S. 2008. The balance between CONSTANS and TEMPRANILLO activities determines FT expression to trigger flowering. *Current Biology* **18**: 1338-1343.

Causier B, Ashworth M, Guo W, Davies B. 2012. The TOPLESS Interactome: A Framework for Gene Repression in Arabidopsis. *Plant Physiology* **158**: 423-438.

Chen X. 2004. A microRNA as a translational repressor of *APETALA2* in *Arabidopsis* flower development. *Science* **303**: 2022-2025.

Chuck G, Cigan AM, Saeteurn K, Hake S. 2007. The heterochronic maize mutant *Corngrass1* results from overexpression of a tandem microRNA. *Nature Genetics* **39**: 544-549.

Daxinger L, Hunter B, Sheikh M, Jauvion V, Gasciolli V, Vaucheret H, Matzke M, Furner I. 2008. Unexpected silencing effects from T-DNA tags in Arabidopsis. *Trends In Plant Science* **13**: 4-6.

Edwards K, Johnstone C, Thompson C. 1991. A simple and rapid method for the preparation of plant genomic DNA for PCR analysis. *Nucleic Acids Research* **19**: 1349.

Feng C-Z, Chen Y, Wang C, Kong Y-H, Wu W-H, Chen Y-F. 2014. Arabidopsis RAV1 transcription factor, phosphorylated by SnRK2 kinases, regulates the expression of ABI3, ABI4, and ABI5 during seed germination and early seedling development. *The Plant Journal* **80**: 654-668.

Franco-Zorrilla JM, Valli A, Todesco M, Mateos I, Puga MI, Rubio-Somoza I, Leyva A, Weigel D, García JA, Paz-Ares J. 2007. Target mimicry provides a new mechanism for regulation of microRNA activity. *Nature Genetics* **39**: 1033-1037.

Galvão VC, Horrer D, Küttner F, Schmid M. 2012. Spatial control of flowering by DELLA proteins in *Arabidopsis thaliana*. *Development* **139**: 4072-4082.

Gandikota M, Birkenbihl RP, Hohmann S, Cardon GH, Saedler H, Huijser P. 2007. The miRNA156/157 recognition element in the 3' UTR of the Arabidopsis SBP box gene *SPL3* prevents early flowering by translational inhibition in seedlings. *The Plant Journal* **49**: 683-693.

Huijser P, Schmid M. 2011. The control of developmental phase transitions in plants. *Development* **138**: 4117-4129.

Ikeda M, Ohme-Takagi M. 2009. A Novel Group of Transcriptional Repressors in Arabidopsis. *Plant and Cell Physiology* **50**: 970-975.

Jung J-H, Ju Y, Seo PJ, Lee J-H, Park C-M. 2012. The SOC1-SPL module integrates photoperiod and gibberellic acid signals to control flowering time in Arabidopsis. *The Plant Journal* **69**: 577–588.

Jung J-H, Seo P, Kang S, Park C-M. 2011. miR172 signals are incorporated into the miR156 signaling pathway at the SPL3/4/5 genes in Arabidopsis developmental transitions. *Plant Molecular Biology* **76**: 35-45.

Jung J-H, Seo Y-H, Seo PJ, Reyes JL, Yun J, Chua N-H, Park C-M. 2007. The *GIGANTEA*-regulated microRNA172 mediates photoperiodic flowering independent of *CONSTANS* in *Arabidopsis*. *The Plant Cell* **19**: 2736-2748.

Kagaya Y, Ohmiya K, Hattori T. 1999. RAV1, a novel DNA-binding protein, binds to bipartite recognition sequence through two distinct DNA-binding domains uniquely found in higher plants. *Nucleic Acids Research* **27**: 470-478.

Livak KJ, Schmittgen TD. 2001. Analysis of relative gene expression data using real-time quantitative PCR and the $2^{-\Delta\Delta CT}$ Method. *Methods* **25**: 402-408.

Marín-González E, Matías-Hernández L, Aguilar-Jaramillo AE, Lee JH, Ahn JH, Suárez-López P, Pelaz S. 2015. SHORT VEGETATIVE PHASE up-regulates *TEMPRANILLO2* floral repressor at low ambient temperatures. *Plant Physiology* **169**: 1214-1224.

Martin A, Adam H, Díaz-Mendoza M, Żurczak M, González-Schain ND, Suárez-López P. 2009. Graft-transmissible induction of potato tuberization by the microRNA *miR172*. *Development* **136**: 2873-2881.

Mathieu J, Yant LJ, Mürdter F, Küttner F, Schmid M. 2009. Repression of Flowering by the miR172 Target SMZ. *PLoS Biology* **7**: e1000148.

Matías-Hernández L, Aguilar-Jaramillo AE, Marín-González E, Suárez-López P, Pelaz S. 2014. *RAV* genes: regulation of floral induction and beyond. *Annals of Botany* **114**: 1459-1470.

Matias-Hernandez L, Battaglia R, Galbiati F, Rubes M, Eichenberger C, Grossniklaus U, Kater MM, Colombo L. 2010. *VERDANDI* is a direct target of the MADS domain ovule identity complex and affects embryo sac differentiation in *Arabidopsis*. *The Plant Cell* **22**: 1702-1715.

Osnato M, Castillejo C, Matías-Hernández L, Pelaz S. 2012. *TEMPRANILLO* genes link photoperiod and gibberellin pathways to control flowering in *Arabidopsis*. *Nature Communications* **3**: 808.

Park J, Nguyen KT, Park E, Jeon J-S, Choi G. 2013. DELLA Proteins and Their Interacting RING Finger Proteins Repress Gibberellin Responses by Binding to the Promoters of a Subset of Gibberellin-Responsive Genes in *Arabidopsis*. *The Plant Cell* **25**: 927–943.

Picó S, Ortiz-Marchena MI, Merini W, Calonje M. 2015. Deciphering the role of Polycomb Repressive Complex 1 (PRC1) variants in regulating the acquisition of flowering competence in Arabidopsis. *Plant Physiology* **168**: 1286-1297.

Poethig RS. 2009. Small RNAs and developmental timing in plants. *Current Opinion in Genetics & Development* **19**: 374-378.

Rubio-Somoza I, Weigel D. 2011. MicroRNA networks and developmental plasticity in plants. *Trends In Plant Science* **16**: 258-264.

Schmid M, Uhlenhaut NH, Godard F, Demar M, Bressan R, Weigel D, Lohmann JU. 2003. Dissection of floral induction pathways using global expression analysis. *Development* **130**: 6001-6012.

Schwab R, Palatnik JF, Riester M, Schommer C, Schmid M, Weigel D. 2005. Specific effects of microRNAs on the plant transcriptome. *Developmental Cell* **8**: 517-527.

Schwarz S, Grande AV, Bujdoso N, Saedler H, Huijser P. 2008. The microRNA regulated SBP-box genes *SPL9* and *SPL15* control shoot maturation in Arabidopsis. *Plant Molecular Biology* **67**: 183-895.

Serivichyaswat P, Ryu H-S, Kim W, Kim S, Chung KS, Kim JJ, Ahn JH. 2015. Expression of the Floral Repressor miRNA156 is Positively Regulated by the AGAMOUS-like Proteins AGL15 and AGL18. *Molecules and Cells* **38**: 259-266.

Sgamma T, Jackson A, Muleo R, Thomas B, Massiah A. 2014. *TEMPRANILLO* is a regulator of juvenility in plants. *Scientific Reports* **4**: 3704.

Tao Z, Shen L, Liu C, Liu L, Yan Y, Yu H. 2012. Genome-wide identification of SOC1 and SVP targets during the floral transition in *Arabidopsis*. *The Plant Journal* **70**: 549-561.

Telfer A, Bollman KM, Poethig RS. 1997. Phase change and the regulation of trichome distribution in *Arabidopsis thaliana*. *Development* **124**: 645-654.

Todesco M, Rubio-Somoza I, Paz-Ares J, Weigel D. 2010. A collection of target mimics for comprehensive analysis of microRNA function in *Arabidopsis thaliana*. *PLoS Genetics* **6**: e1001031.

Wahl V, Ponnu J, Schlereth A, Arrivault S, Langenecker T, Franke A, Feil R, Lunn JE, Stitt M, Schmid M. 2013. Regulation of Flowering by Trehalose-6-Phosphate Signaling in *Arabidopsis thaliana*. *Science* **339**: 704-707.

Wang F, Perry SE. 2013. Identification of Direct Targets of FUSCA3, a Key Regulator of Arabidopsis Seed Development. *Plant Physiology* **161**: 1251-1264.

Wang J-W, Czech B, Weigel D. 2009. miR156-Regulated SPL Transcription Factors Define an Endogenous Flowering Pathway in *Arabidopsis thaliana*. *Cell* **138**: 738-749.

Wang J-W, Schwab R, Czech B, Mica E, Weigel D. 2008. Dual Effects of miR156-Targeted *SPL* Genes and *CYP78A5/KLUH* on Plastochron Length and Organ Size in *Arabidopsis thaliana*. *The Plant Cell* **20**: 1231-1243.

Wang X-H, Li Q-T, Chen H-W, Zhang W-K, Ma B, Chen S-Y, Zhang J-S. 2014. Trihelix transcription factor GT-4 mediates salt tolerance via interaction with TEM2 in Arabidopsis. *BMC Plant Biology* **14**: 339.

Wu G, Park MY, Conway SR, Wang J-W, Weigel D, Poethig RS. 2009. The Sequential Action of miR156 and miR172 Regulates Developmental Timing in *Arabidopsis*. *Cell* **138**: 750-759.

Wu G, Poethig RS. 2006. Temporal regulation of shoot development in Arabidopsis thaliana by miR156 and its target SPL3. *Development* **133**: 3539-3547.

Xie K, Wu C, Xiong L. 2006. Genomic organization, differential expression, and interaction of SQUAMOSA promoter-binding-like transcription factors and microRNA156 in rice. *Plant Physiology* **142**: 280-293.

Yamaguchi A, Wu M-F, Yang L, Wu G, Poethig RS, Wagner D. 2009. The MicroRNA-Regulated SBP-Box Transcription Factor SPL3 Is a Direct Upstream Activator of LEAFY, FRUITFULL, and APETALA1. *Developmental Cell* **17**: 268-278.

Yang L, Xu M, Koo Y, He J, Poethig RS. 2013. Sugar promotes vegetative phase change in Arabidopsis thaliana by repressing the expression of MIR156A and MIR156C. *eLife* **2**: e00260.

Yant L, Mathieu J, Dinh TT, Ott F, Lanz C, Wollmann H, Chen X, Schmid M. 2010. Orchestration of the Floral Transition and Floral Development in *Arabidopsis* by the Bifunctional Transcription Factor APETALA2. *The Plant Cell* **22**: 2156-2170.

Yu S, Cao L, Zhou C-M, Zhang T-Q, Lian H, Sun Y, Wu J, Huang J, Wang G, Wang J-W. 2013. Sugar is an endogenous cue for juvenile-to-adult phase transition in plants. *eLife* **2**: e00269.

Yu S, Galvão VC, Zhang Y-C, Horrer D, Zhang T-Q, Hao Y-H, Feng Y-Q, Wang S, Markus S, Wang J-W. 2012. Gibberellin Regulates the Arabidopsis Floral Transition through miR156-Targeted SQUAMOSA PROMOTER BINDING–LIKE Transcription Factors. *The Plant Cell* **24**: 3320-3332.

Figure legends

Fig. 1 TEM1 and TEM2 regulate miR156 levels. (a,b) Mature miR156 levels in *tem1 tem2* (a) and *35S::TEM1* plants (b) were determined by RNA blot in rosettes from 10-day-old plants grown under LD, collected at ZT8 and ZT18. *35S::miR156* plants were used as a positive hybridization control. Hybridization to U6 small nuclear RNA was used as a loading control. The numbers below each lane indicate the fold change relative to the miR156 level in the wild type at the corresponding ZT. (c) Pri-miR156a and pri-miR156c levels in *tem1 tem2* and *35S::TEM1* plants were determined by RT-qPCR in rosettes from 10-day-old plants grown under LD, collected at ZT8 and ZT18. *UBQ10* was used as normalization control and normalized levels in the wild type at ZT8 were set to 1. Error bars show standard deviation of three technical replicates. Three independent experiments gave similar results and one is shown as representative. (d) Binding of TEM1 to *MIR156A* chromatin by ChIP-qPCR. Chromatin from 11-day-old *35S::TEM1-HA* and *35S::TEM2-HA* plants was immunoprecipitated with an anti-HA antibody. Precipitated chromatin was used as template for qPCR using specific primers for two *MIR156A* fragments containing putative RAV binding sites 426 nt upstream (fragment -426) and 588 nt downstream (fragment +588) of the transcription start site. Data are presented as fold enrichment relative to the highest value. Error bars show

standard deviation of three technical replicates. Three independent experiments gave similar results and one is shown as representative. A schematic diagram of the *MIR156A* gene is shown above the graph. Black boxes indicate exons, an arrow indicates the transcription start site, inverted triangles indicate putative RAV binding sites and arrowheads indicate fragments amplified by qPCR.

Fig. 2 TEM1 and TEM2 regulate *SPL* mRNA levels. (a) *SPL3*, *SPL9* and *SPL15* mRNA levels in *tem1 tem2* mutants and *35S::TEM1* plants were determined by RT-qPCR in rosettes from 10-day-old plants grown under LD, collected at ZT8 and ZT18. *UBQ10* was used as normalization control and normalized levels in the wild type at ZT8 were set to 1. Error bars show standard deviation of three technical replicates. At least two independent experiments gave similar results and one is shown as representative. (b) Binding of TEM1 to *SPL9* chromatin by ChIP-qPCR. Chromatin from 11-day-old *35S::TEM1-HA* and *35S::TEM2-HA* plants was immunoprecipitated with an anti-HA antibody. Precipitated chromatin was used as template for qPCR using specific primers for a *SPL9* fragment containing three putative RAV binding sites. Data are presented as fold enrichment relative to the highest value. Error bars show standard deviation of three technical replicates. Three independent experiments gave similar results and one was chosen as representative. A schematic diagram of the *SPL9* gene is shown above the graph. Black boxes indicate exons, an arrow indicates the translation start site, inverted triangles indicate putative RAV binding sites and arrowheads indicate the fragment amplified by qPCR.

Fig. 3 TEM1 and TEM2 regulate miR172 levels. (a,b) Mature miR172 levels in *tem1 tem2* (a) and *35S::TEM1* (b) plants were determined by RNA blot in rosettes from 10-day-old plants grown under LD, collected at ZT8 and ZT18. Hybridization to U6 small nuclear RNA was used as a loading control. The numbers below each lane indicate the fold change relative to the miR172 level in the wild type at the corresponding ZT. (c) Binding of TEM1 to *MIR172C* chromatin by ChIP-qPCR. Chromatin from 11-day-old *35S::TEM1-HA* and *35S::TEM2-HA* plants was immunoprecipitated with an anti-HA antibody. Precipitated chromatin was used as template for qPCR using specific primers for a *MIR172C* fragment containing two putative RAV binding sites 109 and 186 nt downstream of the transcription start site. Data are presented as fold enrichment relative to the highest value. Error bars show standard deviation of three technical replicates.

Three independent experiments gave similar results and one was chosen as representative. A schematic diagram of the *MIR172C* gene is shown above the graph. Black boxes indicate exons, an arrow indicates the transcription start site, inverted triangles indicate putative RAV binding sites and arrowheads indicate the fragment amplified by qPCR.

Fig. 4 TEMs regulate *SPL* mRNA and miR172 levels through miR156-dependent and independent pathways. (a,b) *SPL3*, *SPL9* and *SPL15* levels were analyzed by RT-qPCR in rosettes from 10-day-old *35S::TEM1 35S::MIM156* (a) and *tem2 35S::MIM156* (b) plants, collected at ZT8 and ZT18. *UBQ10* was used as normalization control and normalized levels in the wild type at ZT8 were set to 1. Error bars show standard deviation of three technical replicates. Two or three independent experiments gave similar results and one was chosen as representative. (c,d) Mature miR172 levels in *35S::TEM1 35S::MIM156* (c) and *tem2 35S::MIM156* (d) plants were determined by RNA blot in rosettes from 10-day-old plants grown under LD, collected at ZT8 and ZT18. Hybridization to U6 small nuclear RNA was used as a loading control. The numbers below each lane indicate the fold change relative to the miR172 level in the wild type at the corresponding ZT.

Supporting information

Fig. S1 *TEM1* and *TEM2* mRNA levels in *35S::miR156* and *35S::MIM156* plants.

Fig. S2 Diurnal oscillation of *SPL9* mRNA levels.

Fig. S3 Mature miR156 levels in *tem1 tem2* and *35S::TEM1* plants.

Fig. S4 Mature miR172 levels in *tem1 tem2* and *35S::TEM1* plants.

Fig. S5 Silencing of *35S::miR156* in a *tem1* background.

Fig. S6 Flowering phenotypes of *tem2 35S::miR156*, *tem2 35S::MIM156* and *35S::TEM1 35S::MIM156* plants.

Fig. S7 Silencing of *35S::MIM156* in a *tem1* background.

Table S1 Statistical analyses of data from Table 1

Table S2 Statistical analyses of data from Table 2

Table S3 Putative RAV binding sites in *MIR156A*

Table S4 Putative RAV binding sites in *SPL9*

Table S5 Putative RAV binding sites in *MIR172* genes

Table S6 Statistical analyses of data from Table 3

Table S7 Statistical analyses of data from Table 4

Table S8 Primer sequences

Table 1 Effect of TEMs, miR156, SPL9 and miR172 on the juvenile-to-adult transition

	Juvenile leaves	**Adult leaves**	**1st leaf with abaxial trichomes**
Experiment 1 (SD)			
WT	11.7 ± 1.2	50.5 ± 2.9	12.7 ± 1.2
tem1 tem2	9.9 ± 1.2	15.6 ± 3.9***	10.9 ± 1.2
35S::TEM1	NQ	NV	NV
35S::miR156	72.7 ± 6.9***	25.6 ± 5.3***	73.7 ± 6.9***
35S::MIM156	0.0 ± 0.0***	47.9 ± 6.5	1.0 ± 0.0***
pSPL9::rSPL9	0.0 ± 0.0***	46.1 ± 1.4	1.0 ± 0.0***
Experiment 2 (SD)			
WT	12.0 ± 0.9	51.7 ± 2.5	13.0 ± 0.9
tem1	12.8 ± 1.2	42.8 ± 4.3***	13.8 ± 1.2
tem2	11.1 ± 1.5	35.8 ± 2.4***	12.1 ± 1.5
tem1 tem2	10.8 ± 0.7	22.1 ± 5.4***	11.8 ± 0.7
Experiment 3 (LD)			
WT	4.5 ± 0.5	4.2 ± 0.9	5.5 ± 0.5
tem1 tem2	3.0 ± 0.5***	2.3 ± 0.6***	4.0 ± 0.5***
35S::miR156	8.9 ± 1.0***	6.2 ± 1.5***	9.9 ± 1.0***
35S::MIM156	0.0 ± 0.0***	3.0 ± 1.0**	1.0 ± 0.0***
pSPL9::rSPL9	0.0 ± 0.0***	2.4 ± 0.5***	1.0 ± 0.0***
Experiment 4 (LD)			
WT	5.2 ± 0.6	5.3 ± 0.6	6.2 ± 0.6
tem1	5.4 ± 0.5	3.8 ± 0.6***	6.4 ± 0.5
tem2	4.8 ± 0.8	3.5 ± 0.9***	5.8 ± 0.8
tem1 tem2	3.5 ± 0.5***	2.7 ± 0.6***	4.5 ± 0.5***

NQ: not quantifiable (plants continued producing juvenile leaves for the length of the experiment). NV: not visible (plants did not produce adult leaves). Means and standard deviations are shown ($n \geq 15$). Asterisks indicate statistically significant difference relative to the WT (** $p \leq 0.01$, *** $p \leq 0.001$). A complete statistical analysis of these results is shown in Table S1.

Table 2 Effect of TEMs, miR156, SPL9 and miR172 on flowering

	Rosette leaves	**Cauline leaves**	**Total leaves**	**Days**
Experiment 1 (SD)				
WT	62.2 ± 4.1	8.7 ± 0.5	70.9 ± 3.9	66.7 ± 1.9
tem1 tem2	25.5 ± 5.1	4.1 ± 1.1	29.6 ± 6.0***	37.3 ± 2.8***
35S::TEM1	NQ	NV	NQ	NQ
35S::miR156	98.3 ± 4.1	5.0 ± 0.8	103.3 ±3.9***	84.6 ± 5.3***
35S::MIM156	47.9 ± 6.5	9.5 ± 1.6	57.4 ± 7.7***	76.2 ± 4.6***
pSPL9::rSPL9	46.1 ± 1.4	9.2 ± 0.6	55.3 ± 1.8***	78.0 ± 5.6***
Experiment 2 (SD)				
WT	63.7 ± 2.7	9.7 ± 1.0	73.4 ± 3.0	69.5 ± 2.1
tem1	55.5 ± 5.2	6.3 ± 1.6	61.8 ± 6.4***	58.1 ± 3.0***
tem2	46.9 ± 3.6	8.2 ± 1.2	55.1 ± 4.4***	52.6 ± 2.9***
tem1 tem2	32.9 ± 5.4	3.6 ± 0.5	36.5 ± 5.6***	41.7 ± 4.4***
Experiment 3 (LD)				
WT	8.7 ± 0.7	1.8 ± 0.4	11.0 ± 0.9	20.6 ± 0.5
tem1 tem2	5.3 ± 0.4	2.3 ± 0.7	7.6 ± 0.5***	16.2 ± 1.0***
35S::miR156	15.1 ± 2.1	1.0 ± 0.0	16.1 ± 2.1***	21.5 ± 2.7
35S::MIM156	3.0 ± 1.0	2.8 ± 0.6	5.8 ± 0.9***	20.8 ± 2.5
pSPL9::rSPL9	2.4 ± 0.5	2.8 ± 0.6	5.1 ± 0.6***	17.0 ± 1.0***
Experiment 4 (LD)				
WT	10.5 ± 0.6	2.3 ± 0.6	12.7 ± 0.9	19.1 ± 0.8
tem1	9.2 ± 0.4	2.2 ± 0.5	11.4 ± 0.6***	18.0 ± 0.5*
tem2	8.3 ± 0.9	3.0 ± 0.5	11.2 ± 1.0***	17.0 ± 1.0***
tem1 tem2	6.2 ± 0.5	1.9 ± 0.4	8.0 ± 0.6***	14.8 ± 0.4***

NQ: not quantifiable (plants did not flower and continued producing rosette leaves for the length of the experiment). NV: not visible (plants did not flower and did not produce cauline leaves). Means and standard deviations are shown ($n \geq 15$). Statistical analyses were performed for total leaves and days. Asterisks indicate statistically significant difference relative to the WT (* $p \leq 0.05$, *** $p \leq 0.001$). A complete statistical analysis of these results is shown in Table S2.

Table 3 Genetic interaction of TEMs with miR156: juvenile-to-adult transition

	Juvenile leaves	Adult leaves	1st leaf with abaxial trichomes
Experiment 1			
WT	4.5 ± 0.5	4.4 ± 0.5	5.5 ± 0.5
35S::TEM1	19.4 ± 3.7***	0.0 ± 0.0***	NV
35S::MIM156	0.1 ± 0.3***	4.9 ± 0.3	1.1 ± 0.3***
35S::TEM1 35S::MIM156	4.3 ± 0.5	4.3 ± 0.5	5.3 ± 0.5
Experiment 2			
WT	4.3 ± 0.5	4.8 ± 1.2	5.3 ± 0.5
tem2	4.2 ± 0.5	3.1 ± 0.6***	5.2 ± 0.5
35S::miR156	10.1 ± 0.7***	5.7 ± 1.0	11.1 ± 0.7***
tem2 35S::miR156	7.5 ± 1.2***	3.8 ± 1.3*	8.5 ± 1.2***
Experiment 3			
WT	4.5 ± 0.5	4.7 ± 0.6	5.5 ± 0.5
tem2	4.4 ± 0.6	3.2 ± 0.8***	5.4 ± 0.6
35S::MIM156	0.0 ± 0.0***	3.6 ± 0.8***	1.0 ± 0.0***
tem2 35S::MIM156	0.0 ± 0.0***	4.5 ± 0.8	1.0 ± 0.0***

NV: not visible (plants did not produce leaves with abaxial trichomes). Means and standard deviations are shown ($n \geq 14$). Asterisks indicate statistically significant difference relative to the WT (* $p \leq 0.05$, ** $p \leq 0.01$, *** $p \leq 0.001$). A complete statistical analysis of these results is shown in Table S6.

Table 4 Genetic interaction of TEMs with miR156: flowering time

	Rosette leaves	**Cauline leaves**	**Total leaves**	**Days**
Experiment 1				
WT	8.9 ± 0.9	2.3 ± 0.6	11.1 ± 0.9	16.1 ± 0.8
35S::TEM1	19.9 ± 3.7	4.5 ± 1.0	24.4 ± 4.4***	36.7 ± 4.8***
35S::MIM156	4.9 ± 1.5	3.4 ± 0.7	8.3 ± 1.6*	19.7 ± 1.4**
35S::TEM1 35S::MIM156	8.6 ± 1.1	2.4 ± 0.5	11.0 ± 1.1	20.2 ± 1.5***
Experiment 2				
WT	10.7 ± 0.9	2.6 ± 0.6	13.3 ± 1.3	16.7 ± 0.8
35S::TEM1	25.1 ± 2.1	6.4 ± 1.2	31.6 ± 2.6***	41.2 ± 2.9***
35S::miR156	14.4 ± 1.7	1.6 ± 0.6	16.0 ± 1.3***	19.0 ± 1.1**
35S::TEM1 x *35S::miR156* (F_1)	13.7 ± 1.2	1.8 ± 0.4	15.6 ± 1.4*	18.3 ± 0.8
Experiment 3				
WT	9.1 ± 1.4	2.3 ± 0.4	11.4 ± 1.1	20.1 ± 1.4
tem2	7.3 ± 1.5	2.9 ± 0.4	10.1 ± 0.9*	17.2 ± 1.5***
35S::miR156	15.8 ± 1.2	1.7 ±0.6	17.4 ± 1.5***	22.2 ± 1.2***
tem2 35S::miR156	11.3 ± 1.6	2.1 ± 0.6	13.4 ± 1.6***	18.8 ± 1.6*
Experiment 4				
WT	9.1 ± 0.3	2.2 ± 0.4	11.4 ± 0.5	21.0 ± 0.5
tem2	7.6 ± 0.6	2.6 ± 0.5	10.2 ± 0.7***	19.0 ± 0.2***
35S::MIM156	3.6 ± 0.9	2.4 ± 0.5	6.0 ± 1.0***	22.0 ± 1.0***
tem2 35S::MIM156	4.5 ± 0.8	2.2 ± 0.6	6.7 ± 0.9**	21.0 ± 0.8

Means and standard deviations are shown ($n \geq 14$). Statistical analyses were performed for total leaves and days. Asterisks indicate statistically significant difference relative to the WT (* $p \leq 0.05$, ** $p \leq 0.01$, *** $p \leq 0.001$). A complete statistical analysis of these results is shown in Table S7.

CAPÍTULO I: Regulation of Developmental Timing by TEMPRANILLO through miR156 and *SPL* genes.

Supplemental Data

Fig. S1 *TEM1* and *TEM2* mRNA levels in *35S::miR156* and *35S::MIM156* plants. (a,b) *TEM1* and *TEM2* mRNA levels were determined by RT-qPCR in rosettes from plants grown under SD (a) and LD (b). Samples were collected at ZT12 (A) or ZT18 (B) at the indicated times. *UBQ10* was used as normalization control and normalized levels in the wild type at week 1 (a) or day 6 (b) were set to 1. Error bars show standard deviation of three technical replicates. Three independent experiments gave similar results and one was chosen as representative. (c) GUS staining of *pTEM1::GUS* and *pTEM1::GUS 35S::miR156*. Plants were grown under SD for the indicated times. No obvious differences in GUS staining were observed between *pTEM1::GUS* and *pTEM1::GUS 35S::mi*R156 plants.

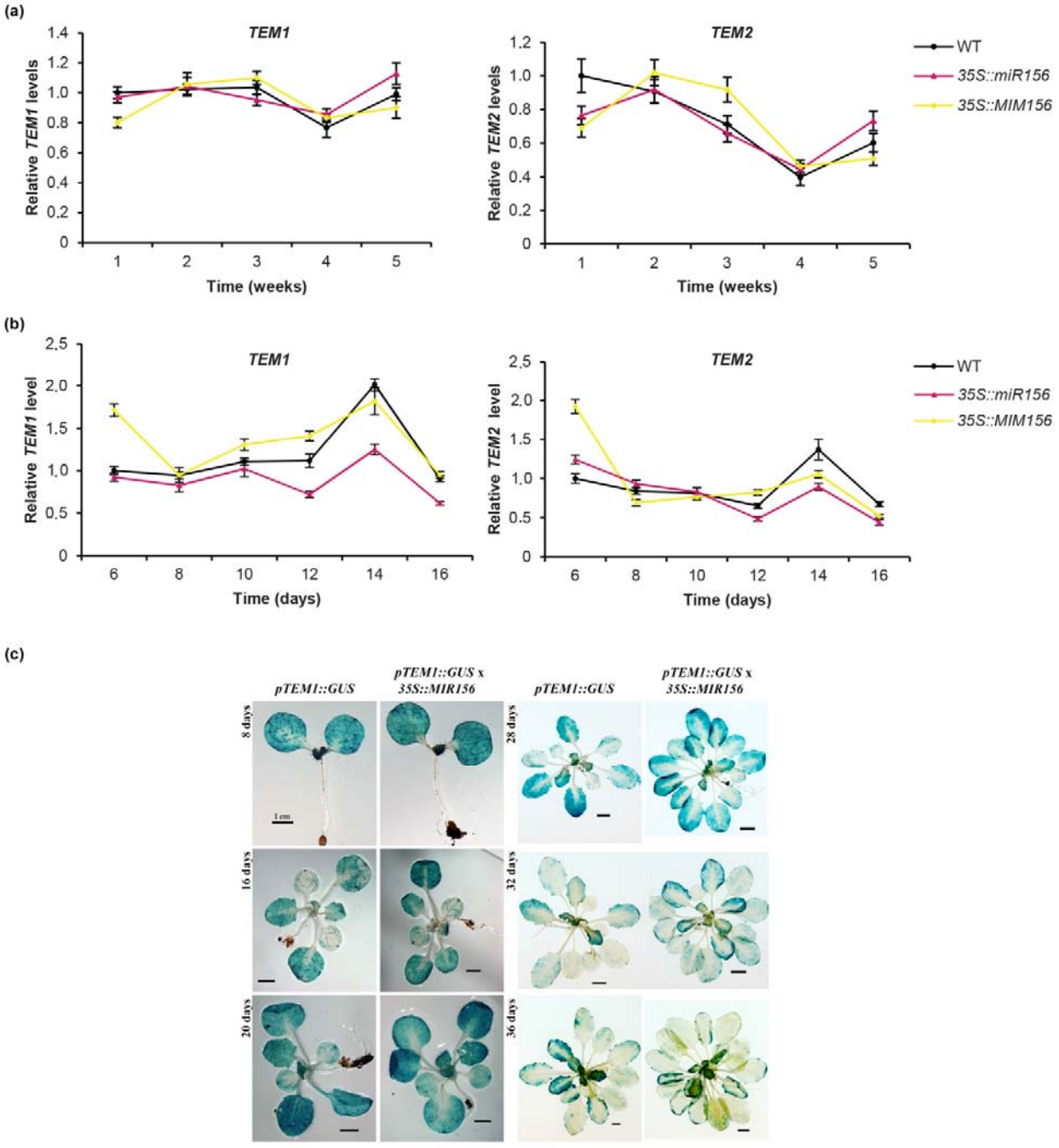
(a)
TEM1
Relative TEM1 levels
Time (weeks)
TEM2
Relative TEM2 levels
Time (weeks)
WT
35S::miR156
35S::MIM156
(b)
TEM1
Relative TEM1 level
Time (days)
TEM2
Relative TEM2 level
Time (days)
WT
35S::miR156
35S::MIM156
(c)
pTEM1::GUS
pTEM1::GUS x 35S::MIR156
pTEM1::GUS
pTEM1::GUS x 35S::MIR156
8 days
16 days
20 days
28 days
32 days
36 days
1 cm

Figure S1

Fig. S2 Diurnal oscillation of *SPL9* mRNA levels. *SPL9* mRNA levels were analyzed by RT-qPCR over a 24 h period under LD conditions. Rosettes were collected from 9-day-old wild-type seedlings every 4 h, with an additional sample at ZT18. *UBQ10* was used as normalization control and normalized levels at ZT0 were set to 1. Error bars show standard deviation of three technical replicates.

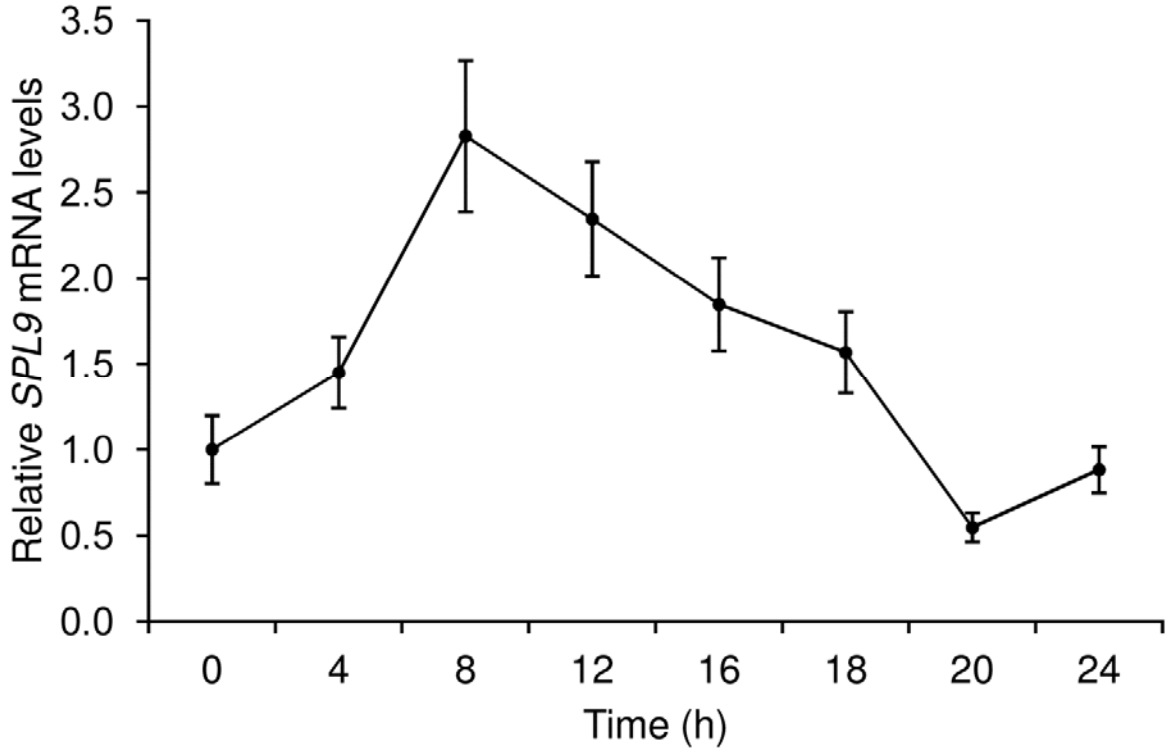

Figure S2

Fig. S3 Mature miR156 levels in *tem1 tem2* and *35S::TEM1* plants. Mature miR156 levels were determined by stem-loop RT-qPCR in rosettes from 10-day-old plants grown under LD, collected at ZT8 and ZT18. *UBQ10* was used as normalization control and normalized levels in the wild type at ZT8 were set to 1. Data represent the mean and standard deviation of three technical replicates. Three independent experiments were performed, and one is shown as representative.

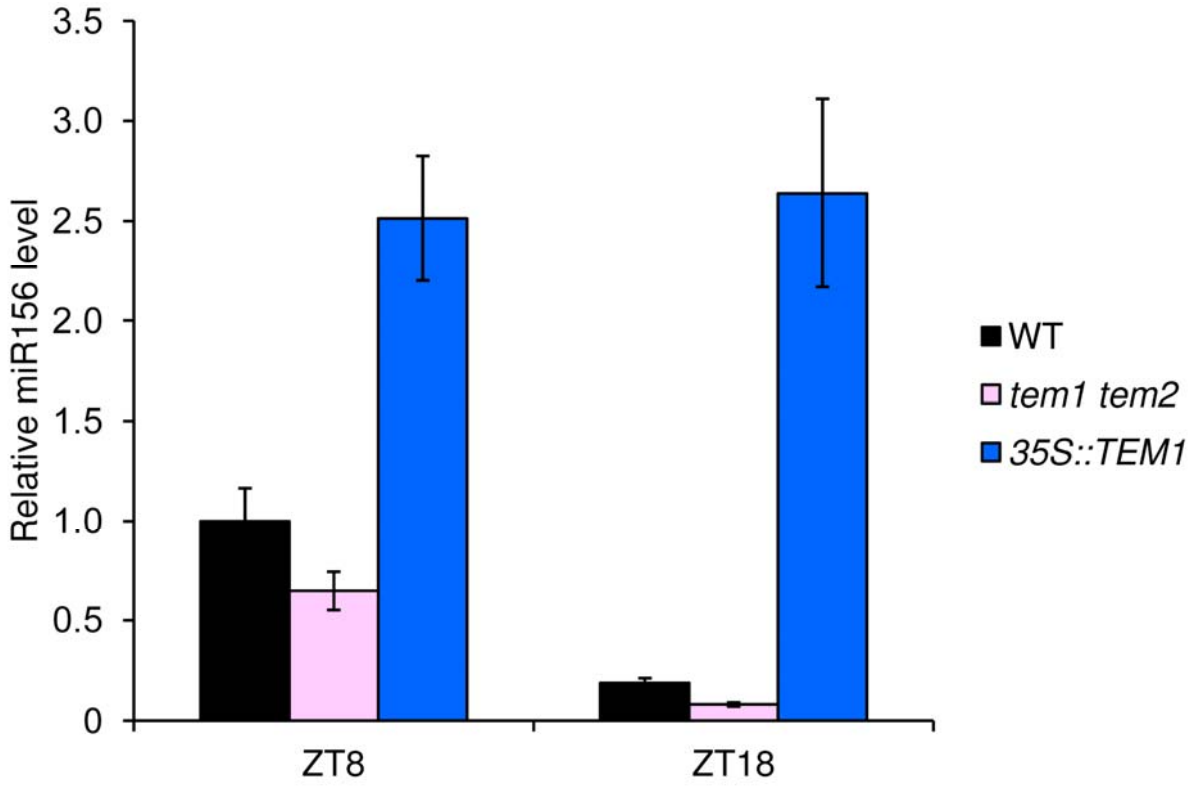

Figure S3

Fig. S4 Mature miR172 levels in *tem1 tem2* and *35S::TEM1* plants. Mature miR172 levels were determined by stem-loop RT-qPCR in rosettes from 10-day-old plants grown under LD, collected at ZT8 and ZT18. *UBQ10* was used as normalization control and normalized levels in the wild type at ZT8 were set to 1. Data represent the mean and standard deviation of three technical replicates. Three independent experiments were performed, and one is shown as representative.

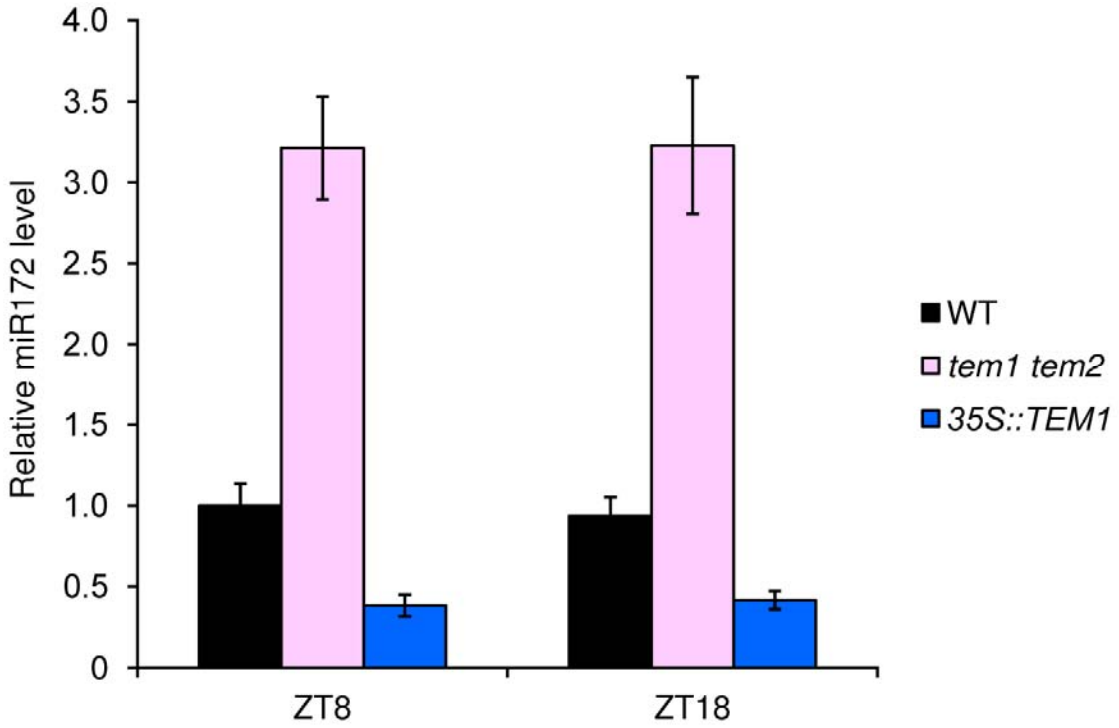

Figure S4

Fig. S5 Silencing of *35S::miR156* in a *tem1* background. Mature miR156 levels in wild-type, *tem1*, *35S::miR156* and *tem1 35S::miR156* plants were determined by RNA blot in rosettes from 10-day-old plants grown under LD, collected at ZT8. Hybridization to U6 small nuclear RNA was used as a loading control. The numbers below each lane indicate the fold change relative to the miR156 level in the wild type. All lanes come from the same blot.

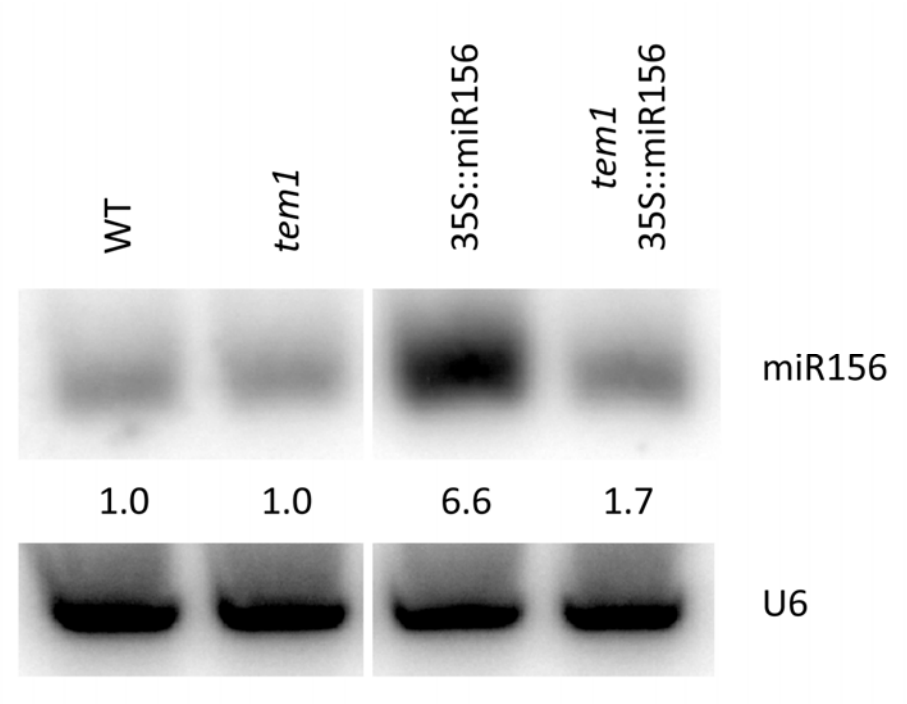

Figure S5

Fig. S6 Flowering phenotypes of *tem2 35S::miR156*, *tem2 35S::MIM156* and *35S::TEM1 35S::MIM156* plants. (a,b,c) Photographs of the indicated genotypes were taken after 27 (a), 29 (b) and 21 (c) days under LD. Scale bars: 1 cm.

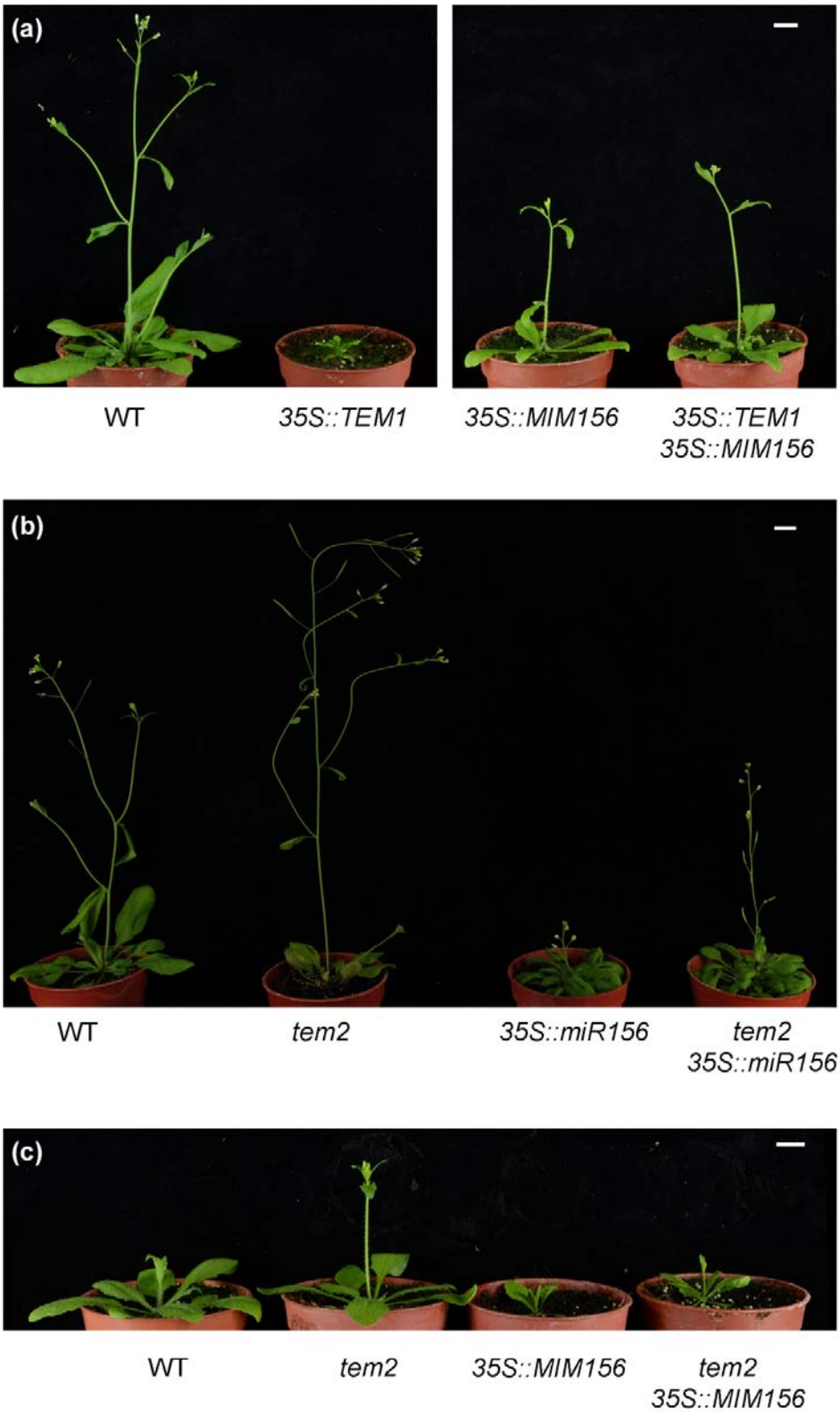
(a)
WT
35S::TEM1
35S::MIM156
35S::TEM1
35S::MIM156
(b)
WT
tem2
35S::miR156
tem2
35S::miR156
(c)
WT
tem2
35S::MIM156
tem2
35S::MIM156

Figure S6

Fig. S7 Silencing of *35S::MIM156* in a *tem1* background. Levels of *MIM156* RNA in *35S::MIM156* and *tem1 35S::MIM156* plants were determined by RT-qPCR in rosettes from 9-day-old plants grown under LD, collected at ZT8. Wild-type and *tem1* plants were used as negative controls. *UBQ10* was used as normalization control. Data represent the mean and standard deviation of three technical replicates.

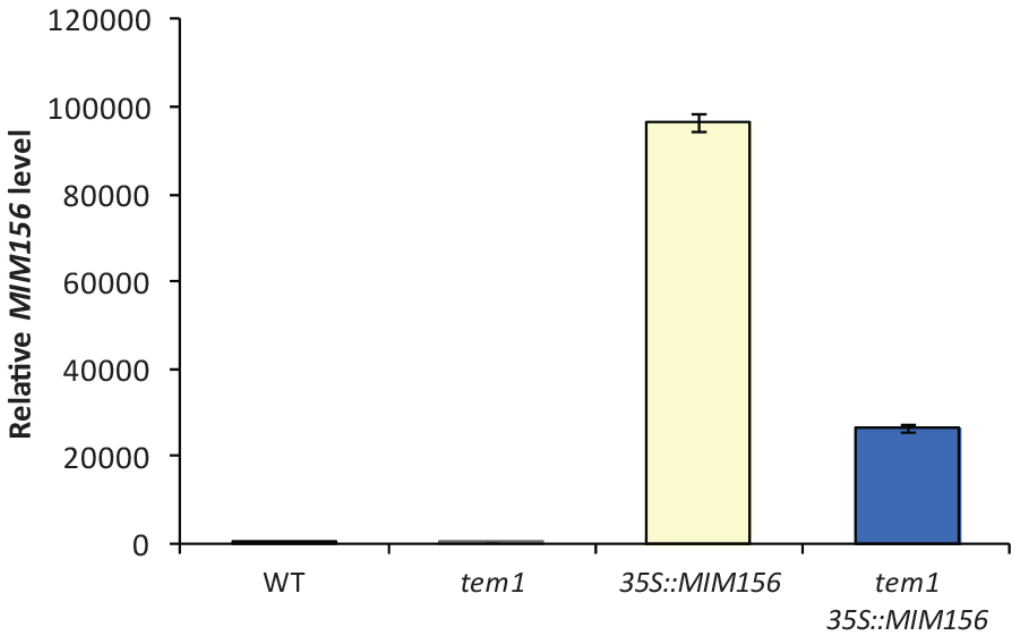

Figure S7

Table S1 Statistical analyses of data from Table 1

Comparison	Significance	*p*-value
Experiment 1: Juvenile leaves (SD)		
WT vs. *tem1 tem2*	ns	0.4078
WT vs. *35S::miR156*	***	< 0.0001
WT vs. *35S::MIM156*	***	< 0.0001
WT vs. *pSPL9::rSPL9*	***	< 0.0001
tem1 tem2 vs. *35S::miR156*	***	< 0.0001
tem1 tem2 vs. *35S::MIM156*	***	< 0.0001
tem1 tem2 vs. *pSPL9::rSPL9*	***	< 0.0001
35S::miR156 vs. *35S::MIM156*	***	< 0.0001
35S::miR156 vs. *pSPL9::rSPL9*	***	< 0.0001
35S::MIM156 vs. *pSPL9::rSPL9*	ns	> 0.9999
Experiment 1: Adult leaves (SD)		
WT vs. *tem1 tem2*	***	< 0.0001
WT vs. *35S::miR156*	***	< 0.0001
WT vs. *35S::MIM156*	ns	0.9060
WT vs. *pSPL9::rSPL9*	ns	0.3425
tem1 tem2 vs. *35S::miR156*	***	< 0.0001
tem1 tem2 vs. *35S::MIM156*	***	< 0.0001
tem1 tem2 vs. *pSPL9::rSPL9*	***	< 0.0001
35S::miR156 vs. *35S::MIM156*	***	< 0.0001
35S::miR156 vs. *pSPL9::rSPL9*	***	< 0.0001
35S::MIM156 vs. *pSPL9::rSPL9*	ns	0.9893
Experiment 2: Juvenile leaves (SD)		
WT vs. *tem1*	ns	0.3509
WT vs. *tem2*	ns	0.2014
WT vs. *tem1 tem2*	ns	0.0759
tem1 vs. *tem2*	**	0.0027
tem1 vs. *tem1 tem2*	***	0.0007
tem2 vs. *tem1 tem2*	ns	0.9516
Experiment 2: Adult leaves (SD)		
WT vs. *tem1*	***	< 0.0001
WT vs. *tem2*	***	< 0.0001
WT vs. *tem1 tem2*	***	< 0.0001
tem1 vs. *tem2*	***	0.0002
tem1 vs. *tem1 tem2*	***	< 0.0001
tem2 vs. *tem1 tem2*	***	< 0.0001

Experiment 3: Juvenile leaves (LD)		
WT vs. *tem1tem2*	***	< 0.0001
WT vs. *35S::miR156*	***	< 0.0001
WT vs. *35S::MIM156*	***	< 0.0001
WT vs. *pSPL9::rSPL9*	***	< 0.0001
tem1tem2 vs. *35S:miR156*	***	< 0.0001
tem1tem2 vs. *35S::MIM156*	***	< 0.0001
tem1tem2 vs. *pSPL9::rSPL9*	***	< 0.0001
35S:miR156 vs. *35S::MIM156*	***	< 0.0001
35S:miR156 vs. *pSPL9::rSPL9*	***	< 0,0001
35S::MIM156 vs. *pSPL9::rSPL9*	ns	0.999
Experiment 3: Adult leaves (LD)		
WT vs. *tem1tem2*	***	< 0.0001
WT vs. *35S::miR156*	***	< 0.0001
WT vs. *35S::MIM156*	**	0.004
WT vs. *pSPL9::rSPL9*	***	< 0.0001
tem1tem2 vs. *35S:miR156*	***	< 0.0001
tem1tem2 vs. *35S::MIM156*	ns	0.186
tem1tem2 vs. *pSPL9::rSPL9*	ns	0.999
35S:miR156 vs. *35S::MIM156*	***	< 0.0001
35S:miR156 vs. *pSPL9::rSPL9*	***	< 0.0001
35S::MIM156 vs. *pSPL9::rSPL9*	ns	0.331
Experiment 4: Juvenile leaves (LD)		
WT vs. *tem1*	ns	0.717
WT vs. *tem2*	ns	0.259
WT vs. *tem1 tem2*	***	< 0,0001
tem1 vs. *tem2*	*	0.024
tem1 vs. *tem1 tem2*	***	< 0.0001
tem2 vs. *tem1 tem2*	***	< 0.0001
Experiment 4: Adult leaves (LD)		
WT vs. *tem1*	***	< 0.0001
WT vs. *tem2*	***	< 0.0001
WT vs. *tem1 tem2*	***	< 0.0001
tem1 vs. *tem2*	ns	0.362
tem1 vs. *tem1 tem2*	***	< 0.0001
tem2 vs. *tem1 tem2*	**	0.004

ns: not significant. Asterisks indicate statistically significant differences (* $p \leq 0.05$, ** $p \leq 0.01$, *** $p \leq 0.001$).

Table S2 Statistical analyses of data from Table 2

Flowering time	**Significance**	***p*-value**
Experiment 1: Total leaves (SD)		
WT vs. *tem1 tem2*	***	< 0.0001
WT vs. *35S::miR156*	***	< 0.0001
WT vs. *35S::MIM156*	***	< 0.0001
WT vs. *pSPL9::rSPL9*	***	< 0.0001
tem1 tem2 vs. *35S::miR156*	***	< 0.0001
tem1 tem2 vs. *35S::MIM156*	***	< 0.0001
tem1 tem2 vs. *pSPL9::rSPL9*	***	< 0.0001
35S::miR156 vs. *35S::MIM156*	***	< 0.0001
35S::miR156 vs. *pSPL9::rSPL9*	***	< 0.0001
35S::MIM156 vs. *pSPL9::rSPL9*	ns	0.9863
Experiment 1: Days (SD)		
WT vs. *tem1 tem2*	***	< 0.0001
WT vs. *35S::miR156*	***	< 0.0001
WT vs. *35S::MIM156*	***	< 0.0001
WT vs. *pSPL9::rSPL9*	***	< 0.0001
tem1 tem2 vs. *35S::miR156*	***	< 0.0001
tem1 tem2 vs. *35S::MIM156*	***	< 0.0001
tem1 tem2 vs. *pSPL9::rSPL9*	***	< 0.0001
35S::miR156 vs. *35S::MIM156*	***	0.0005
35S::miR156 vs. *pSPL9::rSPL9*	*	0.0145
35S::MIM156 vs. *pSPL9::rSPL9*	ns	0.9746
Experiment 2: Total leaves (SD)		
WT vs. *tem1*	***	< 0.0001
WT vs. *tem2*	***	< 0.0001
WT vs. *tem1 tem2*	***	< 0.0001
tem1 vs. *tem2*	**	0.0085
tem1 vs. *tem1 tem2*	***	< 0.0001
tem2 vs. *tem1 tem2*	***	< 0.0001
Experiment 2: Days (SD)		
WT vs. *tem1*	***	< 0.0001
WT vs. *tem2*	***	< 0.0001
WT vs. *tem1 tem2*	***	< 0.0001
tem1 vs. *tem2*	***	0.0004
tem1 vs. *tem1 tem2*	***	< 0.0001
tem2 vs. *tem1 tem2*	***	< 0.0001

Experiment 3: Total leaves (LD)		
WT vs. *tem1tem2*	***	< 0.0001
WT vs. *35S::miR156*	***	< 0.0001
WT vs. *35S::MIM156*	***	< 0.0001
WT vs. *pSPL9::rSPL9*	***	< 0.0001
tem1 tem2 vs. *35S:miR156*	***	< 0.0001
tem1 tem2 vs. *35S::MIM156*	***	< 0.0001
tem1 tem2 vs. *pSPL9::rSPL9*	***	< 0.0001
35S:miR156 vs. *35S::MIM156*	***	< 0.0001
35S:miR156 vs. *pSPL9::rSPL9*	***	< 0.0001
35S::MIM156 vs. *pSPL9::rSPL9*	ns	0.48
Experiment 3: Days (LD)		
WT vs. *tem1tem2*	***	< 0.0001
WT vs. *35S::miR156*	ns	0.635
WT vs. *35S::MIM156*	ns	0.999
WT vs. *pSPL9::rSPL9*	***	< 0.0001
tem1 tem2 vs. *35S:miR156*	***	< 0.0001
tem1 tem2 vs. *35S::MIM156*	***	< 0.0001
tem1tem2 vs. *pSPL9::rSPL9*	ns	0.708
35S:miR156 vs. *35S::MIM156*	ns	0.807
35S:miR156 vs. *pSPL9::rSPL9*	***	< 0.0001
35S::MIM156 vs. *pSPL9::rSPL9*	***	< 0.0001
Experiment 4: Total leaves (LD)		
WT vs. *tem1*	***	< 0.0001
WT vs. *tem2*	***	< 0.0001
WT vs. *tem1 tem2*	***	< 0.0001
tem1 vs. *tem2*	ns	0.734
tem1 vs. *tem1 tem2*	***	< 0.0001
tem2 vs. *tem1 tem2*	***	< 0.0001
Experiment 4: Days (LD)		
WT vs. *tem1*	*	0.027
WT vs. *tem2*	***	< 0.0001
WT vs. *tem1 tem2*	***	< 0.0001
tem1 vs. *tem2*	***	< 0.0001
tem1 vs. *tem1 tem2*	***	< 0.0001
tem2 vs. *tem1 tem2*	***	< 0.0001

ns: not significant. Asterisks indicate statistically significant differences (* $p \leq 0.05$, ** $p \leq 0.01$, *** $p \leq 0.001$).

Table S3 Putative RAV binding sites in *MIR156A*

Sequence	Distance to TSS	Position	Orientation
CACCAcataATCCTG	-426	Promoter	Forward
CCACAtaATCCTG	-424	Promoter	Forward
CGCCAgaCATCTG	+82	Exon	Forward
CAGCAccggAATCTG	+588	Exon	Reverse

TSS: transcription start site. Information on the position of the TSS is from Xie *et al*. (2005). Intron positions are from Szarzynska *et al*. (2009).

Table S4 Putative RAV binding sites in *SPL9*

Sequence	Distance to ATG	Position	Orientation
CCACAtcaacCACATG	+1489	Exon	Forward
CAACAacaacaaTACATG	+1536	Exon	Forward
CAACCacCACCTG	+1597	Exon	Forward

Table S5 Putative RAV binding sites in *MIR172* genes

Gene	Sequence	Distance to TSS	Position	Orientation
MIR172A	CACCAggtcttTCTCTG	+18	Exon	Forward
MIR172A	CAACAaaacaaaGAACTG	+1214	Intron	Reverse
MIR172B	CCACActttCACCTG	-1062	Promoter	Reverse
MIR172B	CAACAagttcATACTG	-246	Promoter	Forward
MIR172C	CAGCAaaccaTTACTG	-437	Promoter	Forward
MIR172C	CACCAtttTGCTG	+109	Exon	Reverse
MIR172C	CGGCAccattTTGCTG	+109	Exon	Reverse
MIR172C	CAACAgcgaacagTAGCTG	+186	Exon	Reverse
MIR172C	CAACAcaAACCTG	+332	?	Reverse
MIR172E	CACCAaaatcatcTTGCTG	+214	Exon?	Forward

TSS: transcription start site. Information on the position of TSSs was taken from TAIR or from Xie *et al*. (2005). Annotation of *MIR172* genes in TAIR is incomplete and therefore some exon/intron positions are uncertain.

Table S6 Statistical analyses of data from Table 3

Comparison	Significance	*p*-value
Experiment 1: Juvenile leaves		
WT vs. *35S::TEM1*	***	≤ 0.0001
WT vs. *35S::MIM156*	***	≤ 0.0001
WT vs. *35S::TEM1 35S::MIM156*	ns	> 0.05
35S::TEM1 vs. *35S::MIM156*	***	≤ 0.0001
35S::TEM1 vs. *35S::TEM1 35S::MIM156*	***	≤ 0.0001
35S::MIM156 vs. *35S::TEM1 35S::MIM156*	***	≤ 0.0001
Experiment 1: Adult leaves		
WT vs. *35S::TEM1*	***	≤ 0.0001
WT vs. *35S::MIM156*	ns	> 0.05
WT vs. *35S::TEM1 35S::MIM156*	ns	> 0.05
35S::TEM1 vs. *35S::MIM156*	***	≤ 0.0001
35S::TEM1 vs. *35S::TEM1 35S::MIM156*	***	≤ 0.0001
35S::MIM156 vs. *35S::TEM1 35S::MIM156*	ns	> 0.05
Experiment 2: Juvenile leaves		
WT vs. *tem2*	ns	> 0.05
WT vs. *35S::miR156*	***	≤ 0.0001
WT vs. *tem2 35S::miR156*	***	≤ 0.0001
tem2 vs. *35S::miR156*	***	≤ 0.0001
tem2 vs. *tem2 35S::miR156*	***	≤ 0.0001
35S::miR156 vs. *tem2 35S::miR156*	***	≤ 0.0001
Experiment 2: Adult leaves		
WT vs. *tem2*	***	≤ 0.0001
WT vs. *35S::miR156*	ns	> 0.05
WT vs. *tem2 35S::miR156*	*	≤ 0.05
tem2 vs. *35S::miR156*	***	≤ 0.0001
tem2 vs. *tem2 35S::miR156*	ns	> 0.05
35S::miR156 vs. *tem2 35S::miR156*	***	≤ 0.0001
Experiment 3: Juvenile leaves		
WT vs. *tem2*	ns	> 0.05
WT vs. *35S::MIM156*	***	≤ 0.0001
WT vs. *tem2 35S::MIM156*	***	≤ 0.0001
tem2 vs. 35S::MIM156	***	≤ 0.0001
tem2 vs. *tem2 35S::MIM156*	***	≤ 0.0001
35S::MIM156 vs. *tem2 35S::MIM156*	ns	> 0.05
Experiment 3: Adult leaves		
WT vs. *tem2*	***	≤ 0.0001
WT vs. *35S::MIM156*	***	≤ 0.0001
WT vs. *tem2 35S::MIM156*	ns	> 0.05
tem2 vs. 35S::MIM156	ns	> 0.05
tem2 vs. *tem2 35S::MIM156*	***	≤ 0.0001
35S::MIM156 vs. *tem2 35S::MIM156*	***	≤ 0.0001

ns: not significant. Asterisks indicate statistically significant differences (* $p \leq 0.05$, *** $p \leq 0.001$).

Table S7 Statistical analyses of data from Table 4

Comparison	Significance	*p*-value
Experiment 1: Total leaves		
WT vs. *35S::TEM1*	***	≤ 0.0001
WT vs. *35S::MIM156*	*	≤ 0.05
WT vs. *35S::TEM1 35S::MIM156*	ns	> 0.05
35S::TEM1 vs. *35S::MIM156*	***	≤ 0.0001
35S::TEM1 vs. *35S::TEM1 35S::MIM156*	***	≤ 0.0001
35S::MIM156 vs. *35S::TEM1 35S::MIM156*	*	≤ 0.05
Experiment 1: Days		
WT vs. *35S::TEM1*	***	≤ 0.0001
WT vs. *35S::MIM156*	**	≤ 0.01
WT vs. *35S::TEM1 35S::MIM156*	***	≤ 0.001
35S::TEM1 vs. *35S::MIM156*	***	≤ 0.0001
35S::TEM1 vs. *35S::TEM1 35S::MIM156*	***	≤ 0.0001
35S::MIM156 vs. *35S::TEM1 35S::MIM156*	ns	> 0.05
Experiment 2: Total leaves		
WT vs. *35S::TEM1*	***	≤ 0.0001
WT vs. *35S::miR156*	***	≤ 0.0001
WT vs. *35S::TEM1 35S::miR156*	*	≤ 0.05
35S::TEM1 vs. *35S::miR156*	***	≤ 0.0001
35S::TEM1 vs. *35S::TEM1 35S::miR156*	***	≤ 0.0001
35S::miR156 vs. *35S::TEM1 35S::miR156*	ns	> 0.05
Experiment 2: Days		
WT vs. *35S::TEM1*	***	≤ 0.0001
WT vs. *35S::miR156*	**	≤ 0.01
WT vs. *35S::TEM1 35S::miR156*	ns	> 0.05
35S::TEM1 vs. *35S::miR156*	***	≤ 0.0001
35S::TEM1 vs. *35S::TEM1 35S::miR156*	***	≤ 0.0001
35S::miR156 vs. *35S::TEM1 35S::miR156*	ns	> 0.05
Experiment 3: Total leaves		
WT vs. *tem2*	*	≤ 0.05
WT vs. *35S::miR156*	***	≤ 0.0001
WT vs. *tem2 35S::miR156*	***	≤ 0.0001
tem2 vs. *35S::miR156*	***	≤ 0.0001
tem2 vs. *tem2 35S::miR156*	***	≤ 0.0001
35S::miR156 vs. *tem2 35S::miR156*	***	≤ 0.0001
Experiment 3: Days		
WT vs. *tem2*	***	≤ 0.0001
WT vs. *35S::miR156*	***	≤ 0.0001
WT vs. *tem2 35S::miR156*	*	≤ 0.05
tem2 vs. *35S::miR156*	***	≤ 0.0001
tem2 vs. *tem2 35S::miR156*	**	≤ 0.01
35S::miR156 vs. *tem2 35S::miR156*	***	≤ 0.0001

Experiment 4: Total leaves		
WT vs. *tem2*	***	≤ 0.001
WT vs. *35S::MIM156*	***	≤ 0.0001
WT vs. *tem2 35S::MIM156*	**	≤ 0.0001
tem2 vs. 35S::MIM156	***	≤ 0.0001
tem2 vs. *tem2 35S::MIM156*	***	≤ 0.0001
35S::MIM156 vs. *tem2 35S::MIM156*	*	≤ 0.05
Experiment 4: Days		
WT vs. *tem2*	***	≤ 0.0001
WT vs. *35S::MIM156*	***	≤ 0.0001
WT vs. *tem2 35S::MIM156*	ns	> 0.05
tem2 vs. 35S::MIM156	***	≤ 0.0001
tem2 vs. *tem2 35S::MIM156*	***	≤ 0.0001
35S::MIM156 vs. *tem2 35S::MIM156*	***	≤ 0.001

ns: not significant. Asterisks indicate statistically significant differences (* $p \leq 0.05$, ** $p \leq 0.01$, *** $p \leq 0.001$).

Table S8 Primer sequences

Primer name	Sequence (5' to 3')	Purpose
SL-RT-miR156	GTCGTATCCAGTGCAGGGTCCGAGGTATTCGCA CTGGATACGACGTGCTC	Stem loop RT
SL-RT-miR172	GTCGTATCCAGTGCAGGGTCCGAGGTATTCGCA CTGGATACGACATGCAG	Stem loop RT
SL-RT-5S	GTCGTATCCAGTGCAGGGTCCGAGGTATTCGCA CTGGATACGACAGGGAT	Stem loop RT
miR156-qFwd	CGGCGGTGACAGAAGAGAGT	Mature miRNA RT-qPCR
miR172-qFor	CGGCGGTAGAATCTTGATGATG	Mature miRNA RT-qPCR
5S For1	GGATGCGATCATACCAGCACT	Mature miRNA RT-qPCR
qRev-universal	GTGCAGGGTCCGAGGT	Mature miRNA RT-qPCR
miR156as	GTGCTCACTCTCTTCTGTCA	Probe
miR172as	ATGCAGCATCATCAAGATTCT	Probe
U6	GCAGGGGCCATGCTAATCTTCTCTGTATCGT	Probe
MIR156A-q1F	CAAGAGAAACGCAAAGAAACTGACAGA	RT-qPCR
MIR156A-q1R	AAAGAGATCAGCACCGGAATCTGAC	RT-qPCR
MIR156C-q1F	CGCATAGAAACTGACAGAAGAGAGTGAG	RT-qPCR
MIR156C-q1R	AGCCGGAATCTGACAGATAGAGCA	RT-qPCR
SPL3_RT-For	TGGAGAAACAGACAGAGACACAGAGGA	RT-qPCR
SPL3_RT-Rev	ACGCTTAGCTGGACACAACGAGAGAAG	RT-qPCR
SPL9_RT-For	CAAGGTTCAGTTGGTGGAGGA	RT-qPCR
SPL9_RT-Rev	TGAAGAAGCTCGCCATGTATTG	RT-qPCR
SPL15 RT For2	CCGTGGCAGATTAATCCAGT	RT-qPCR
SPL15 RT Rev2	TACCCAATTCATCAGCAGCA	RT-qPCR
TEM1 RT For	ATCCACTGGAAAGTCCGGTCTA	RT-qPCR
TEM1 RT Rev	GAATAGCCTAACCACAGTCTGAACC	RT-qPCR
TEM2 RT For	TGGTCCGAGAGAAAACCCG	RT-qPCR
TEM2 RT Rev	TCAACTCCGAAAAGCCGAAC	RT-qPCR
UBQ10_RT-For	AAATCTCGTCTCTGTTATGCTTAAGAAG	RT-qPCR
UBQ10_RT-Rev	TTTTACATGAAACGAAACATTGAACTT	RT-qPCR
ChIPMIR156A -426 For 1	CCACAAATAAACATGGCCTTT	ChIP-qPCR
ChIPMIR156A -426 Rev 1	TTTAAGTGAAGCGCGTTTTGG	ChIP-qPCR
ChIPMIR156A +588 For 1	CTTCTCTTGCGTGCTCACTG	ChIP-qPCR
ChIPMIR156A +588 Rev 1	AACCAAGAGAGACAGAGAAAGATTG	ChIP-qPCR
SPL9ch for 1	TACAAGGGAATTGGCGACTC	ChIP-qPCR
SPL9ch rev 1	TGGTGGTTGAGCCATTGTAA	ChIP-qPCR
MIR172C-ChIP+109fw	AAAATGGTGCCGTCTTGAGT	ChIP-qPCR
MIR172C-ChIP+109rev	CTTGATGATGCTCCAACAGC	ChIP-qPCR
LBa1	TGGTTCACGTAGTGGGCCATCG	Genotyping (*tem1-1*)
J3	GTCACAAGATGTTGATAATCGCC	Genotyping (*tem1-1* and *TEM1)*
InsTEM1	CGGGCGAAATGTCAAATGTGG	Genotyping (*TEM1)*

LB4	CGTGTGCCAGGTGCCCACGGAATAGT	Genotyping (*tem2-2*)
3Ins-rav2	GCTTCTTGGAACACCGTAACGC	Genotyping (*tem2-2* and *TEM2*)
5Ins-rav2	TTACGCCTCTACCGGATGGG	Genotyping (*TEM2*)
35S-For2	AGAACACGGGGGACGAGCT	Genotyping (35S::miR156 and 35S::MIM156)
OCS-ter Rev	CGCATATCTCATTAAAGCAGG	Genotyping (35S::miR156 and 35S::MIM156)

Supporting References

Szarzynska, B., Sobkowiak, L., Pant, B.D., Balazadeh, S., Scheible, W.-R., Mueller-Roeber, B., Jarmolowski, A. and Szweykowska-Kulinska, Z. 2009. Gene structures and processing of Arabidopsis thaliana HYL1-dependent pri-miRNAs. *Nucleic Acids Research* **37**: 3083-3093.

Xie, Z., Allen, E., Fahlgren, N., Calamar, A., Givan, S.A. and Carrington, J.C. 2005. Expression of Arabidopsis *MIRNA* Genes. *Plant Physiology* **138**: 2145-2154.

CAPÍTULO II: SHORT VEGETATIVE PHASE Up-Regulates *TEMPRANILLO2* Floral Repressor at Low Ambient Temperatures.

SHORT VEGETATIVE PHASE Up-Regulates *TEMPRANILLO2* Floral Repressor at Low Ambient Temperatures[1][OPEN]

Esther Marín-González, Luis Matías-Hernández, Andrea E. Aguilar-Jaramillo, Jeong Hwan Lee, Ji Hoon Ahn, Paula Suárez-López, and Soraya Pelaz*

Centre for Research in Agricultural Genomics, Consejo Superior de Investigaciones Científicas-Institut de Recerca i Tecnologia Agroalimentàries-Universitat Autònoma de Barcelona-Universitat de Barcelona, 08193 Barcelona, Spain (E.M.-G., L.M.-H., A.E.A.-J., P.S.-L., S.P.); Creative Research Initiatives, Department of Life Sciences, Korea University, Seoul 136–701, South Korea (J.H.L., J.H.A.); and Institució Catalana de Recerca i Estudis Avançats, 08010 Barcelona, Spain (S.P.)

ORCID IDs: 0000-0002-9158-5969 (E.M.-G.); 0000-0001-5626-9576 (L.M.-H.); 0000-0001-5748-9263 (P.S.-L.); 0000-0001-7699-9330 (S.P.).

Plants integrate day length and ambient temperature to determine the optimal timing for developmental transitions. In Arabidopsis (*Arabidopsis thaliana*), the floral integrator *FLOWERING LOCUS T* (*FT*) and its closest homolog *TWIN SISTER OF FT* promote flowering in response to their activator *CONSTANS* under long-day inductive conditions. Low ambient temperature (16°C) delays flowering, even under inductive photoperiods, through repression of *FT*, revealing the importance of floral repressors acting at low temperatures. Previously, we have reported that the floral repressors *TEMPRANILLO* (*TEM*; *TEM1* and *TEM2*) control flowering time through direct regulation of *FT* at 22°C. Here, we show that *tem* mutants are less sensitive than the wild type to changes in ambient growth temperature, indicating that *TEM* genes may play a role in floral repression at 16°C. Moreover, we have found that TEM2 directly represses the expression of *FT* and *TWIN SISTER OF FT* at 16°C. In addition, the floral repressor *SHORT VEGETATIVE PHASE* (*SVP*) directly regulates *TEM2* but not *TEM1* expression at 16°C. Flowering time analyses of *svp tem* mutants indicate that *TEM* may act in the same genetic pathway as *SVP* to repress flowering at 22°C but that SVP and TEM are partially independent at 16°C. Thus, *TEM2* partially mediates the temperature-dependent function of *SVP* at low temperatures. Taken together, our results indicate that *TEM* genes are also able to repress flowering at low ambient temperatures under inductive long-day conditions.

Plants constantly monitor environmental and endogenous signals to control their growth and adjust developmental responses to daily and seasonal cues (Penfield, 2008). During the juvenile phase, plants are not competent to flower; they are insensitive to inductive environmental factors, such as favorable conditions of day length or temperature. The transition to the adult phase permits reaching the competence to respond to those signals, which is essential to trigger flowering during the reproductive phase (Bergonzi and Albani, 2011; Huijser and Schmid, 2011). Consequently, the control of flowering time is a key determinant of reproductive success and plays an essential role in plant adaptation to seasons and geography.

Flowering time is controlled by an intricate network of interdependent genetic pathways that monitor and respond to both endogenous and environmental signals. These pathways include age, photoperiod and light quality, GA, thermosensory (ambient temperature), vernalization, and autonomous pathways (Fornara et al., 2010; Srikanth and Schmid, 2011). In Arabidopsis (*Arabidopsis thaliana*), it is well documented the noteworthy regulation of the timing of flowering by day length or photoperiod and temperature (for review, see Andrés and Coupland, 2012; Song et al., 2013; Chew et al., 2014; Romera-Branchat

[1] This work was supported by the Ministerio de Economía y Competitividad/European Regional Development Fund (grant no. BFU2012–33746), the Spanish Government (Formación de Personal Investigador fellowship to E.M.-G.), the Investigator Training Program of the Catalonian Government (predoctoral fellowship to A.E.A.-J.), and the Catalonian Government (Consolidated Research Group no. 2014 SGR 1406 to the research group of S.P.). J.H.A. and J.H.L. were supported by a National Research Foundation of Korea grant funded by the South Korean Government (Ministry of Science, ICT, and Future Planning; 2008-0061988) and Basic Science Research Program through the National Research Foundation of Korea (NRF) funded by the Ministry of Education (2015R1D1A4A0101941), respectively.

* Address correspondence to soraya.pelaz@cragenomica.es.

The author responsible for distribution of materials integral to the findings presented in this article in accordance with the policy described in the Instructions for Authors (www.plantphysiol.org) is: Soraya Pelaz (soraya.pelaz@cragenomica.es).

E.M.-G., P.S.-L., and S.P. conceived and designed the experiments; E.M.-G. is the main contributor to the experimental part of this study; L.M.-H., A.E.A.-J., J.H.L., and J.H.A. performed some of the experiments; E.M.-G., P.S.-L., and S.P. wrote the article with corrections from the rest of the authors; SHORT VEGETATIVE PHASE chromatin immunoprecipitation assays were performed at the laboratory of J.H.A.; and the rest of the work was performed in the group of S.P., who provided funding and supervised the research and the writing of the article.

[OPEN] Articles can be viewed without a subscription.

www.plantphysiol.org/cgi/doi/10.1104/pp.15.00570

et al., 2014). However, in contrast to the finely described photoperiod and light quality pathways, the nature of the primary perception of temperature and the molecular characterization of its signaling remain limited (McClung and Davis, 2010).

Lately, several studies have reported how changes in ambient temperature, defined as the physiological nonstressful temperature range of a given species, modulate many processes in plant development and in particular, how they affect flowering time (for review, see Wigge, 2013; Capovilla et al., 2015). Genetic analyses unraveled the existence of the ambient temperature pathway that mediates temperature responses in Arabidopsis (Blázquez et al., 2003; Balasubramanian et al., 2006; Lee et al., 2007; Kumar et al., 2012). It has been described that a slight decrease from 23°C to 16°C is sufficient to cause a remarkable delay in flowering, even under an inductive long-day (LD) photoperiod (Blázquez et al., 2003). Temperature-dependent differences in flowering time are controlled by multiple factors that mainly affect the expression levels of one of the key floral activators, the *FLOWERING LOCUS T* (*FT*) gene (Kardailsky et al., 1999; Kobayashi et al., 1999). Low ambient temperatures reduce the expression of *FT*, although this decrease is not caused by changes in its transcriptional activator *CONSTANS* (*CO*), which reveals the importance of floral repressors controlling flowering time under low ambient temperatures (16°C; Blázquez et al., 2003; Lee et al., 2013). However, the levels of *TWIN SISTER OF FLOWERING LOCUS T* (*TSF*), the closest homolog of *FT*, are similar at both temperatures, resulting in a higher expression of *TSF* than *FT* at 16°C (Blázquez et al., 2003; Lee et al., 2012, 2013). Although *TSF* plays a secondary but redundant role, *FT* and *TSF* act as floral pathway integrators (Kardailsky et al., 1999; Kobayashi et al., 1999; Yamaguchi et al., 2005; Jang et al., 2009), and their main function is the promotion of photoperiodic flowering (Kardailsky et al., 1999; Kobayashi et al., 1999), with *TSF* playing a secondary but redundant role. A similar relation is also observed at 16°C (Kim et al., 2013; Lee et al., 2013), and flowering of the double mutant *ft tsf* is insensitive to

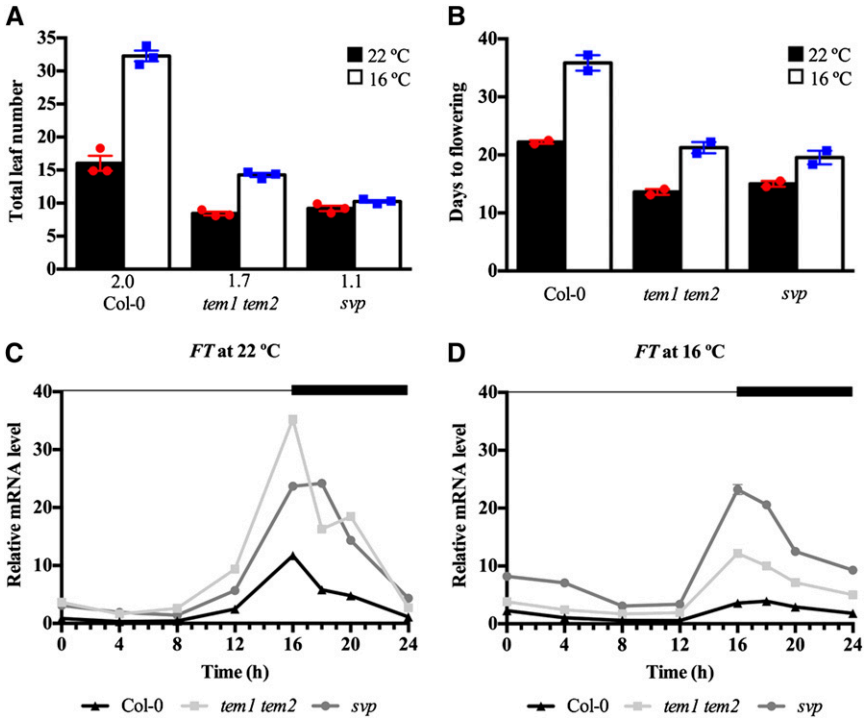

Figure 1. *tem1 tem2* mutant plants are early flowering at 16°C but still sensitive to changes in ambient growth temperature. Flowering time was measured as the number of total leaves produced at flowering (A) and the number of days to flowering (B) for wild-type (Col-0) plants and *tem1 tem2* and *svp* mutants grown under LD conditions at 22°C (black) or 16°C (white). Data are reported as mean ± SEM of three independent experiments (each dot plot represents an independent experiment; red circles indicate experiments performed at 22°C, and blue squares indicate experiments performed at 16°C). A minimum of 12 plants per genotype and experimental condition was analyzed in each independent experiment. The numbers below the bars denote the leaf number ratio (16°C/22°C). For more details, see Supplemental Table S1. C and D, Reverse transcription followed by quantitative real-time PCR (RT-qPCR) analysis of *FT* expression in wild-type (black triangles), *tem1 tem2* (gray squares), and *svp* (gray circles) plants in 9-d-old seedlings grown under LD conditions at 22°C (C) or 16°C (D). Samples were collected over a 24-h period. The dark period is denoted by the black bar. Two independent experiments gave similar results (Supplemental Fig. S1), and one was chosen as representative. RNA levels were normalized to *UBQ10*. Error bars show SD of three technical replicates.

ambient temperature changes (Kim et al., 2013), which indicates that *FT* and *TSF* play an important role in the regulation of ambient temperature-responsive flowering (Kim et al., 2013).

Previously, the *TEMPRANILLO* (*TEM*) genes were identified as main players in the control of flowering time at 22°C, and they were shown to directly repress *FT* (Castillejo and Pelaz, 2008) and the GA biosynthetic genes *GA 3-OXIDASE1* (*GA3OX1*) and *GA3OX2* (Osnato et al., 2012).

Recent genome-wide analysis has identified *TEM1* and *TEM2* as direct targets of the MCM1-AGAMOUS-DEFICIENS-SRF (MADS)-box transcription factor SHORT VEGETATIVE PHASE (SVP) under LD at 22°C (Tao et al., 2012). *TEM1* and *TEM2* are expressed at low levels in *svp-41* plants and high levels in *SVP*-overexpressing plants compared with wild-type plants, indicating a positive regulation of *TEM*s by SVP, which is more evident on *TEM2* than on *TEM1* (Tao et al., 2012). Interestingly, previous genetic studies identified *svp* mutants as insensitive to a wide range of ambient temperature changes (5°C–27°C; Lee et al., 2007, 2013). Thus, *svp* mutants show an early flowering phenotype, producing almost the same number of leaves at flowering at all temperatures (Lee et al., 2013). Similar to TEM, SVP delays flowering by direct repression of *FT* (Lee et al., 2007; Li et al., 2008). Moreover, SVP represses *TSF* in the vascular tissue of leaves and plays an antagonistic role with another MADS-box transcription factor, SUPPRESSOR OF OVEREXPRESSION OF CONSTANS1 (SOC1), in the meristem (Li et al., 2008; Jang et al., 2009).

Here, we characterized the role of *TEM* genes as repressors of flowering at moderately low ambient temperature of 16°C under LD conditions. We show that *TEM* genes act as floral repressors at 16°C under LD conditions by regulating both *FT* and *TSF* expression. Furthermore, we show that SVP specifically regulates *TEM2* at 16°C to repress flowering under LD conditions. Therefore, our results provide additional information regarding the genetic relation between *SVP* and *TEM* at low temperatures.

RESULTS

tem Mutants Are Early Flowering at 16°C But Still Sensitive to Low Temperature

To study the function of *TEM1* and *TEM2* as floral repressors at low ambient temperature, we first analyzed the flowering phenotype of the loss-of-function double mutant *tem1 tem2* at 16°C compared with 22°C under LD conditions. *tem1 tem2* showed early flowering at 22°C, in agreement with previous results (Castillejo and Pelaz, 2008; Osnato et al., 2012), but also, at 16°C and showed a bigger difference with wild-type plants at 16°C than at 22°C. However, *tem1 tem2* plants grown at 16°C produced more leaves than those grown at 22°C (Fig. 1; Supplemental Table S1), indicating that this double mutant is still thermosensitive but significantly less sensitive than wild-type plants, which produced double numbers of leaves at 16°C than at 22°C (the wild type, 16°C/22°C = 2.0; *tem1 tem2*, 16°C/22°C = 1.7; P = 0.0191). By contrast, *svp* mutants, described as insensitive to temperature (Lee et al., 2007), flowered with a similar number of leaves at both temperatures. We found that *tem1 tem2* plants flowered with slightly fewer leaves than *svp* plants at 22°C, although this difference was not statistically significant, whereas *svp* plants were clearly earlier than *tem1 tem2* at 16°C (Fig. 1A; Supplemental Table S1). *tem1 tem2* plants were also earlier than wild-type plants in terms of the number of days to flowering at both temperatures (Fig. 1B). Interestingly, *tem1 tem2* plants grown at 16°C flowered

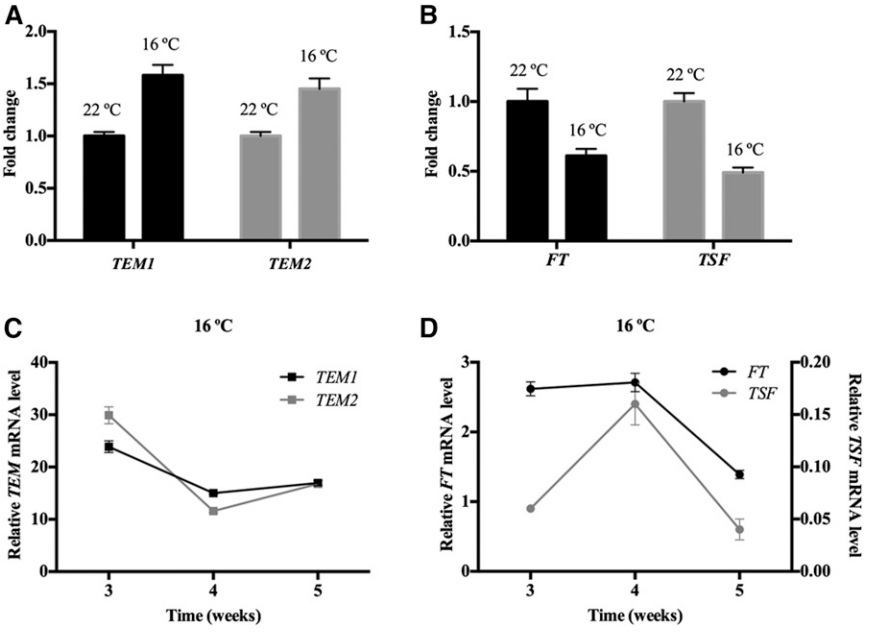

Figure 2. Opposite expression pattern of *TEM* and *FT/TSF* genes at 16°C. Expression analysis of *TEM1*, *TEM2*, *FT*, and *TSF* in 12-d-old wild-type (Col-0) plants grown at 22°C or 16°C (A and B) and wild-type plants grown at 16°C (C and D) for 5 weeks. Fold change in transcript levels at 16°C is depicted compared with 22°C. All samples were collected at ZT18. Three independent experiments gave similar results (Supplemental Fig. S5), and one was chosen as representative. Error bars show SD of three technical replicates. RNA levels were determined by RT-qPCR and normalized to *UBQ10*.

with a similar number of leaves and days to wild-type plants grown at 22°C. These flowering time data are directly correlated with the *FT* expression levels observed in wild-type, *tem1 tem2*, and *svp* mutant plants at different temperatures (Fig. 1, C and D; Supplemental Fig. S1). In *tem1 tem2* plants, *FT* expression was slightly higher than in *svp* mutants and clearly up-regulated compared with that in wild-type plants at 22°C (Fig. 1C). At 16°C, *FT* levels of *tem1 tem2* plants exhibited a clear increase compared with wild-type levels, but this increase was lower than in *svp* plants (Fig. 1D). Both results clearly correlated with the flowering time of those plants at both temperatures. Interestingly, the similar flowering time phenotype observed in wild-type plants grown at 22°C and *tem1 tem2* plants grown at 16°C was associated with similar *FT* levels.

Although GAs seem to play a minor role in flowering under LD (Reeves and Coupland, 2001), we tested if *GA3OX1* was also repressed at 22°C and 16°C, because TEM1 directly represses *GA3OX1* under short day at 22°C (Osnato et al., 2012). We found a similar derepression in *tem1 tem2* double mutants at both temperatures (Supplemental Fig. S2).

All of these results indicate that *TEM* genes have a role in the control of flowering time at low temperature.

Low Temperature Keeps High *TEM* Levels before Floral Transition

To characterize the response of *TEM1* and *TEM2* to low temperatures, we first performed diurnal analyses in 9-d-old wild-type plants grown under LD conditions at 16°C and 22°C. We harvested samples every 4 h for 24 h and added an extra point of collection at Zeitgeber time 18 (ZT18) during the peak of *TEM1* and *TEM2* expression. Our results indicate that *TEM* mRNA levels were not affected by low temperature at this stage, because *TEM* daily oscillation showed a similar pattern at both temperatures (Supplemental Fig. S3). In particular, *TEM1* exhibited a clear peak of expression at ZT18 as previously described (Osnato et al., 2012) and a small peak during the day between ZT8 and ZT12 at 22°C and also, 16°C; *TEM2* showed high levels during the night until the beginning of the day, when it was gradually reduced. Because of the importance of *TEM*s as repressors of flowering time genes along development (Castillejo and Pelaz, 2008; Osnato et al., 2012), we then analyzed *TEM* expression pattern later in development under LD conditions. As we already knew, under LD at 22°C, *TEM* genes showed high expression levels during early stages of development, which prevents a precocious activation of *FT* and a consequent early flowering (Castillejo and Pelaz, 2008). After that, there was a gradual decline of their levels until *TEM*s reached their minimum expression around day 12, when *FT* activation takes place (Supplemental Fig. S4).

To test our hypothesis of a possible thermal regulation, we compared *TEM* expression in 12-d-old wild-type plants grown at 16°C and 22°C. Our results show that plants grown at 16°C keep high *TEM1* and *TEM2* levels longer than those grown at 22°C, maintaining high levels at 16°C at a developmental phase in which they normally reached their minimum at 22°C (Fig. 2; Supplemental Fig. S4A). This indicates that a thermal regulation of *TEM* exists under LD conditions. Moreover, the increased *TEM* levels at 16°C (Fig. 2A) were correlated with a reduction of *FT* expression at low temperature (Fig. 2B). In addition to *FT*, we decided to include the analysis of *TSF* in our experiments, because it is known to play a role in the regulation of ambient temperature-responsive flowering (Kim et al., 2013). We found that *TSF* and *FT* display a similar expression pattern throughout development in wild-type plants grown at 22°C under LD conditions (Supplemental Fig. S4B), a pattern opposite to *TEM* abundance (Supplemental Fig. S4A).

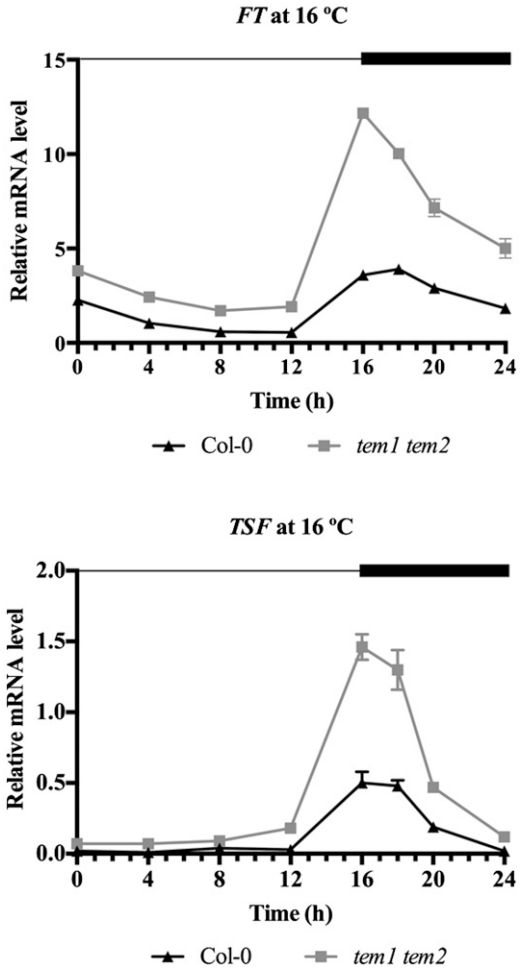

Figure 3. TEMs regulate *FT* and *TSF* levels at 16°C. Relative *FT* and *TSF* mRNA levels in *tem1 tem2* mutant compared with wild-type (Col-0) plants. Nine-day-old seedlings were sampled at 4-h intervals, except from ZT16 to ZT20, when samples were collected every 2 h. Two independent experiments gave similar results (Supplemental Fig. S6), and one was chosen as representative. Error bars show SD of three technical replicates. RNA levels were determined by RT-qPCR and normalized to *UBQ10*.

Next, to better characterize the *TEM* thermal regulation along development and determine when *TEM* abundance reaches the minimum at low temperatures, we performed time course analyses of wild-type plants grown at 16°C during 5 weeks. The relative mRNA levels of *TEM1* and *TEM2* showed the expected gradual decrease along development. In contrast to what happens at 22°C (Supplemental Fig. S4A), at low temperature, their levels dropped later (around the third to fourth week; Fig. 2C; Supplemental Fig. S5). In accordance with that, plants grown at 16°C showed a later rise of *FT* and *TSF* levels than at 22°C, and this rise occurred almost simultaneously with the descent of *TEM* expression (around the third to fourth week; Fig. 2D; Supplemental Fig. S5B). These results indicate that there is a correlation between the decrease of *TEM* abundance and the increase of *FT* and *TSF* levels at 16°C and that this happens later than at 22°C, which is in agreement with the delayed flowering at low temperatures.

TEMs Directly Repress *FT* and *TSF* at 16°C

To further confirm whether *TEM* genes regulate *FT* and/or *TSF*, we carried out expression analyses in wild-type and *tem1 tem2* mutant plants grown at 16°C. As we expected, *FT* and *TSF* were clearly up-regulated in *tem1 tem2* (Fig. 3; Supplemental Fig. S6). To understand whether the repression of *FT* and *TSF* was direct or indirect, we performed chromatin immunoprecipitation (ChIP) experiments at low-temperature conditions. TEM proteins, like other Related to ABI3/VP1 (RAV) members, recognize and bind a canonical sequence known as RAV binding site (Kagaya et al., 1999). Direct binding of TEM1 to the RAV binding site of the 5′-untranslated region of *FT* was previously reported under LD at 22°C (Castillejo and Pelaz, 2008). Here, we show that TEM2 binds in vivo specifically to both *FT* and *TSF* chromatin at 16°C. We found a significant enrichment of the 5′-untranslated region of *FT* containing the canonical RAV binding site (5′-CAACAN$_9$CACCTG-3′; Fig. 4; Supplemental Fig. S7) 43 nucleotides upstream of the ATG start codon in *35S*::*TEM2* plants, whereas only a slight enrichment was found in *35S*::*TEM1* plants. In addition, a clear significant enrichment of the *TSF* promoter was detected in *35S*::*TEM2* but not *35S*::*TEM1* plants in a region 321 nucleotides upstream of the ATG, which contains a noncanonical RAV binding site (5′-CAAGAN$_2$CAAGTG-3′; underlined nucleotides indicate those that are different from the consensus RAV binding site; Fig. 4B; Supplemental Fig. S7B). Taken together, these data show that TEM2 specifically binds to both *FT* and *TSF* and directly regulates their expression at 16°C.

SVP Positively Regulates *TEM2* at 16°C

As a result of genome-wide analyses, *TEM* genes were identified as targets of SVP under LD conditions at 23°C (Tao et al., 2012). Given that SVP is involved in the thermosensory pathway, our next question was whether SVP regulates *TEM* genes at low temperatures. To test the possibility that SVP protein regulates *TEM1* and *TEM2* expression through direct binding to the CArG motifs, where the MADS domain proteins are known to bind (West et al., 1997), present in the *TEM1* and *TEM2* genomic loci, we performed ChIP assays

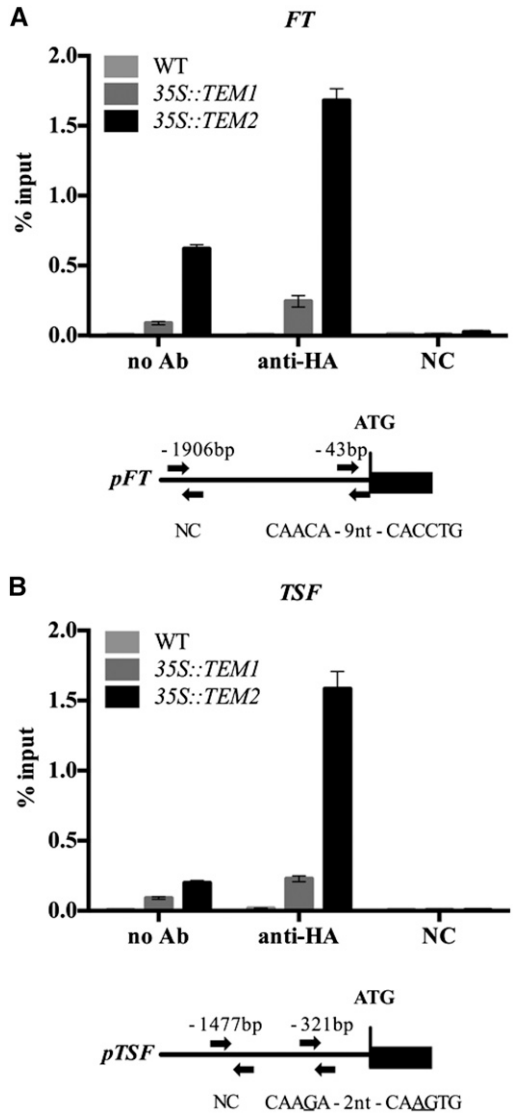

Figure 4. Binding of TEM2 protein to the *FT* and *TSF* promoters at 16°C. ChIP assay of binding of TEM1-HA and TEM2-HA proteins to the RAV motifs in the *FT* (A) and *TSF* (B) promoters. Fragments containing the canonical RAV binding site for *FT*, a putative RAV binding site for *TSF*, and noncontaining RAV binding sequences (used as negative controls [NCs]) were analyzed by ChIP using 9-d-old *35S*::*TEM1* and *35S*::*TEM2* plants carrying an HA tag. Precipitated chromatin was used as a template in qPCR. Immunoprecipitated DNA enrichment is presented as a percentage of input DNA. Two (*FT*) or three (*TSF*) independent experiments gave similar results (Supplemental Fig. S7), and one was chosen as representative. Error bars show SD of three technical replicates. Schematic diagrams of the *FT* and *TSF* promoters are shown below graphs. Arrows indicate fragments amplified by qPCR after ChIP. WT, Wild type.

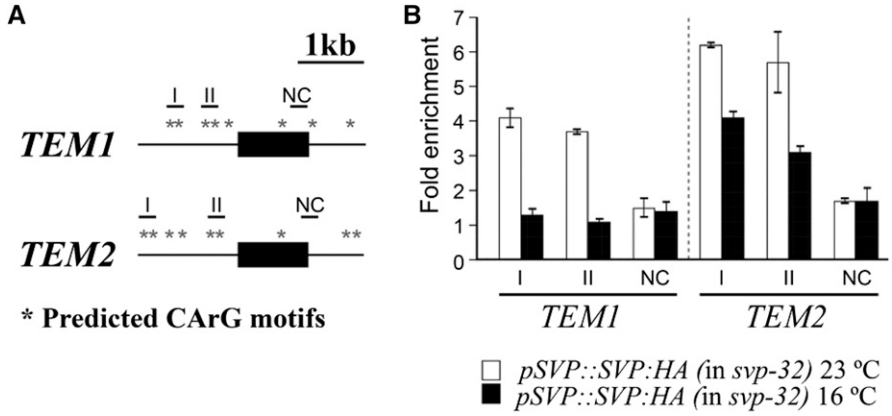

Figure 5. Binding of SVP protein to the *TEM1* and *TEM2* genomic loci. A, Schematic diagram of the *TEM1* and *TEM2* genomic regions. Black boxes and thin lines represent exons and introns, respectively. Asterisks indicate the predicted CArG and variant CArG motifs. Short horizontal lines indicate amplicons in ChIP-qPCR assays. Regions I and II, carrying CArG motifs, were selected to amplify; negative control (NC) was the amplicon used as a negative control. B, ChIP analysis of binding of SVP protein to the *TEM1* and *TEM2* genomic regions at 23˚C and 16˚C in 9-d-old *pSVP::SVP:HA svp-32* plants. An anti-HA antibody was used for immunoprecipitation. Black bars denote the amplified fragments in qPCR: region I (−1,005 to −920; relative to ATG), region II (−350 to −271), and NC (+1,011 to +1,085) for *TEM1* and region I (−1,429 to −1,385; relative to ATG), region II (−434 to −345), and NC (+1,005 to +1,065) for *TEM2*. Two independent experiments gave similar results (Supplemental Fig. S9), and one was chosen as representative. Error bars show SD of three technical replicates.

using *pSVP::SVP:hemagglutinin tag* (*HA*) *svp-32* plants (Lee et al., 2013; Supplemental Fig. S8) under the two temperature conditions (23°C and 16°C). We chose two regions containing CArG motifs (Tao et al., 2012) in the *TEM1* and *TEM2* promoter sequences (Fig. 5; Supplemental Fig. S9). A region lacking a CArG motif was used as a negative control. Strong binding of SVP protein was observed in regions I and II of *TEM1* and *TEM2* at 22°C, whereas interestingly, at 16°C, we only observed a clear binding to *TEM2* but not *TEM1* regulatory regions (Fig. 5B).

To determine if the binding of SVP to *TEM1* and *TEM2* genomic loci affects *TEM* expression, we carried out expression analysis in wild-type and *svp* mutant plants at 22°C and 16°C. A strong down-regulation of *TEM2* was observed in *svp* plants at both 22°C and 16°C, whereas a slight or no *TEM1* reduction was found in *svp* at 22°C and 16°C, respectively (Fig. 6; Supplemental Fig. S10). Taken together, these data show that SVP regulates the expression levels of *TEM* genes by direct binding to the CArG motifs in *TEM1* and *TEM2* genomic loci at 22°C but only to *TEM2* at 16°C for the regulation of ambient temperature-responsive flowering.

To test whether there could be reciprocal regulation between *TEM* and *SVP*, we examined the expression levels of *SVP* in *tem1 tem2* plants. However, we did not find changes in the expression levels of *SVP* in *tem1 tem2* compared with those in wild-type plants at either 22°C or 16°C (Supplemental Fig. S11), suggesting that TEMs do not regulate *SVP* levels.

Genetic Interactions between *svp* and *tem* Mutations at Different Temperatures

Finally, to examine the genetic relationship between *SVP* and *TEM*s in the thermosensory pathway, we measured the flowering times of *tem* single mutants, *tem1 tem2* double mutant, *svp* mutant, and the double and triple combinations of *svp* and *tem* mutations under LD conditions at 22°C and 16°C (Fig. 7; Supplemental Table S2). As shown above, at 16°C, *tem1 tem2* flowered earlier than wild-type plants, and *tem* single mutants also showed an early flowering phenotype. Despite their early flowering, we observed that *tem* double mutants flowered later than any combination with *svp* mutation. *svp*, *svp tem1*, *svp tem2*, and the triple *svp tem1 tem2* all flowered earlier at 16°C than *tem1 tem2* plants (Fig. 7). Accordingly, *FT* levels are higher in triple mutants at 16°C than in *tem1 tem2* double mutants (Supplemental Fig. S12). By contrast, at 22°C, *tem1 tem2* flowered with a similar number of leaves as mutants including *tem* and *svp* mutations, and the small differences observed were not statistically significant (Fig. 7). We found that these differences were correlated with *FT* expression levels (Supplemental Fig. S12); *tem1 tem2* double mutants showed similar *FT* levels as triple mutants. Interestingly, *tem2* single mutants flowered with a similar number of leaves to *svp* at 22°C but flowered later than *svp* at 16°C, whereas *tem2* showed a slight delay compared with *svp tem2* at 22°C, which was more evident at 16°C (Fig. 7). Taken together, these results indicate that *TEM*s regulate flowering at 22°C in an *SVP*-dependent manner and 16°C in a partially *SVP*-independent manner.

DISCUSSION

Plants have developed mechanisms to perceive and respond to environmental fluctuations by adjusting their growth as well as predict upcoming daily and

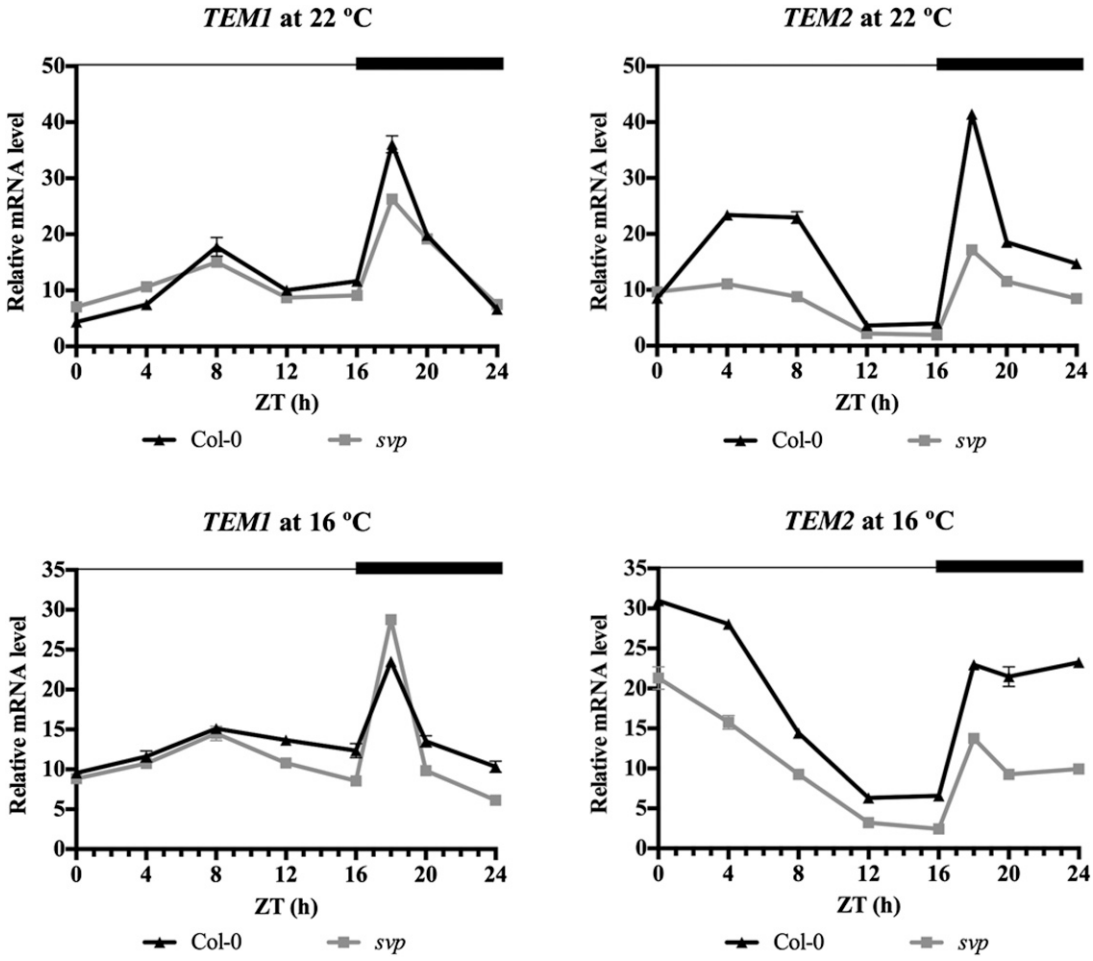

Figure 6. SVP positively regulates *TEM2* expression at 22˚C and 16˚C. Relative mRNA levels of *TEM1* and *TEM2* at 22˚C (upper) and 16˚C (lower) in *svp* mutant compared with wild-type (Col-0) plants. Nine-day-old seedlings were sampled at 4-h intervals, except from ZT16 to ZT20, when samples were collected every 2 h. Two independent experiments gave similar results (Supplemental Fig. S10), and one was chosen as representative. Error bars show SD of three technical replicates. RNA levels were determined by RT-qPCR and normalized to *UBQ10*.

seasonal cues, which result in massive developmental plasticity (Franklin, 2009). Photoperiod and ambient temperature provide relevant information for the adaptation to seasonal changes, which would allow plants to respond to a cold snap or a sudden warmup and optimize flowering time. Hence, light and temperature cues have a key role in flowering time regulation (Andrés and Coupland, 2012).

TEM Genes Repress Flowering at Low Ambient Temperatures

It has been shown that a slight decrease from 23°C to 16°C down-regulates *FT* expression, even under a favorable photoperiod (Blázquez et al., 2003; Fig. 1). This suggests that, under low ambient temperature and LD conditions, floral repressors gain a relevant role in maintaining low *FT* expression levels, despite the presence of its activator *CO*. One of the most studied repressors acting in these conditions is SVP, which interacts with other floral repressors, such as FLOWERING LOCUS M (FLM; Lee et al., 2013), FLOWERING LOCUS C (FLC; Lee et al., 2007; Li et al., 2008), and possibly, other members of the FLC clade (*MADS AFFECTING FLOWERING* genes; Gu et al., 2013) to repress *FT*, *TSF*, and *SOC1*.

The role of *TEM* genes as flowering repressors under LD at 22°C has been previously reported (Castillejo and Pelaz, 2008); however, their function at low ambient temperatures was unknown. The early flowering observed in the *tem1 tem2* mutant at both 22°C and 16°C compared with wild-type plants indicates that *TEM*s act as floral repressors as well at low ambient temperature. However, this double mutant flowered later at 16°C than at 22°C (Figs. 1A and 7). Therefore, in contrast to other genes, which have loss of function that causes insensitivity to ambient temperature, such as *SVP* or *FLM* (Balasubramanian et al., 2006; Lee et al., 2007, 2013; Posé et al., 2013), *tem* mutants are still sensitive to low ambient temperature, although their

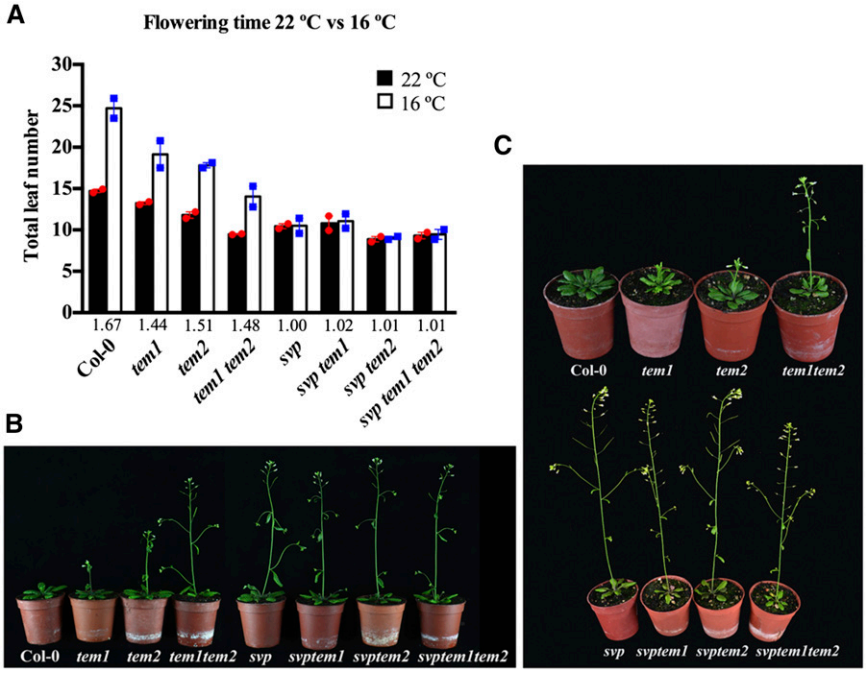

Figure 7. Genetic interaction between *tem* and *svp* mutants. A, Flowering time measured as the number of total leaves produced at flowering for the wild type (Col-0), *tem* mutants, and *svp tem* double and triple mutants grown under LD conditions at 22˚C or 16˚C. Data are reported as mean ± SEM of two independent experiments (each dot plot represents an independent experiment; red circles indicate experiments performed at 22˚C, and blue squares indicate experiments performed at 16˚C). A minimum of 10 plants per genotype and experimental condition was analyzed in each independent experiment. The numbers below the bars denote the leaf number ratio (16˚C/22˚C). For more details, see Supplemental Table S2. B and C, Photographs of plants used in flowering time analysis grown for 24 d at 22˚C (B) and 32 d at 16˚C (C).

response is reduced compared with that of wild-type plants. Thus, *TEM* genes do not seem to control the low temperature-responsive pathway but somehow, act downstream of *SVP* in transmitting the response signal. Indeed, there is a clear correlation between the flowering time of *tem1 tem2* and *svp* mutants and the *FT* relative expression at both temperatures (Fig. 1, C and D; Supplemental Fig. S1). At 22°C, the *FT* up-regulation displayed in *tem1 tem2* and *svp* plants gave rise to the same earlier flowering, probably because in both mutant plants, *FT* exceeded the expression threshold required to induce the floral transition (Fig. 1, A and C). By contrast, at 16°C, the higher level of *FT* in *svp* mutants leads to an earlier flowering than in *tem1 tem2* (Fig. 1, A and D). Therefore, the later flowering of *tem* mutants relative to *svp* at 16°C seems to be caused by the presence of active SVP, which keeps some repression on *FT* expression in *tem* mutants. In that sense, SVP directly represses *FT* expression through direct binding to the *FT* promoter (Lee et al., 2007, 2013).

Late Decay in *TEM* Gene Expressions at 16°C Delays Flowering

Like *SVP*, which shows practically the same mRNA levels at 16°C and 22°C to 23°C (Lee et al., 2007; Supplemental Fig. S11), *TEM* expression is not increased at 16°C at early stages of development, because we did not detect changes in *TEM1* or *TEM2* mRNA levels in 9-d-old wild-type seedlings at 16°C relative to 22°C (Supplemental Fig. S3). However, our results showed that, in 12-d-old seedlings, *TEM* genes are expressed at higher levels at 16°C than at 22°C, which correlated with a decrease in *FT* and *TSF* expression at 16°C (Fig. 2, A and B). These data indicate that *TEM* gene expression decays later at low ambient temperatures, a conclusion supported by the analysis of *TEM* expression throughout development at 16°C and 22°C (Fig. 2, C and D; Supplemental Fig. S4).

FT and *TSF* act as floral promoters at 22°C to 23°C and 16°C (Michaels et al., 2005; Yamaguchi et al., 2005; Jang et al., 2009; Kim et al., 2013; Lee et al., 2013), with *FT* being the main player. We previously reported that *TEM* genes are floral repressors under LD and short-day conditions at 22°C by controlling *FT* (Castillejo and Pelaz, 2008) and GA biosynthetic genes *GA3ox1/2* (Osnato et al., 2012). Here, we report that *TEM* genes also delay flowering and repress *FT* as well as *TSF* and *GA3OX1* at 16°C under LD conditions. The *FT* and *TSF* daily patterns of expression were mostly unchanged in *tem1 tem2* mutants, but their abundance was increased at both 22°C and 16°C (Figs. 1 and 3; Supplemental Figs. S1 and S6). This up-regulation of *FT* and *TSF* in *tem1 tem2* plants (Fig. 3) together with the binding of TEM to *FT* and *TSF* regulatory regions (Fig. 4) indicate that TEM and more specifically, TEM2 directly repress *FT* and *TSF* at low ambient temperatures. Thus, the later drop of *TEM* gene expression at 16°C results in a longer *FT* and *TSF* repression and therefore, a later flowering compared with plants growing at 22°C.

SVP Up-Regulates *TEM2* through Direct Binding in Response to Low Temperatures

Previous high-throughput experiments indicated that SVP positively regulates *TEM* genes at 22°C under LD conditions (Tao et al., 2012). Here, we show that the effect of low temperature on *TEM2* can be explained by the positive and direct regulation that SVP exerts over it

as well at 16°C (Figs. 5 and 6). Bioinformatic analyses detected several MADS binding sites in the promoters of *TEM1* and *TEM2* where SVP could putatively bind, and these sites were experimentally tested by ChIP assays at 23°C and 16°C. Indeed, our results confirmed the binding of SVP to *TEM1* and *TEM2* at 23°C described by Tao et al. (2012) through ChIP-chip analysis and also, provide unique data on the specific regulation of *TEM2* but not *TEM1* by SVP at 16°C (Figs. 5 and 6). At both temperatures, SVP binding on *TEM2* seemed to be stronger than that on *TEM1*, which correlated with the strong down-regulation of *TEM2* observed in *svp* mutants at 22°C and 16°C (Fig. 6). Furthermore, in *svp* mutants, *TEM2* presented practically the same relative mRNA levels at 22°C and 16°C, which were reduced in both cases compared with wild-type plants. This indicates that, although *TEM* genes are redundant in function as repressors of *FT* and *GA3ox1/2* (Castillejo and Pelaz, 2008; Osnato et al., 2012), they are differentially regulated by SVP in the ambient temperature pathway. The different binding of SVP to *TEM*s at different temperatures might be because of the interaction of SVP with FLM-β at 16°C; *TEM2* but not *TEM1* has been identified as a target of FLM-β (Posé et al., 2013). In addition, *TEM* chromatin modifications might occur at low temperatures, making them differentially accessible.

TEM Acts at Least Partially Independently of *SVP* at Low Ambient Temperatures

The analyses of *tem1*, *tem2*, and *svp* mutants in multiple combinations at 22°C indicate that *TEM1* and *TEM2* act basically on the same genetic pathway as *SVP*. However, at 16°C, the global analysis of our flowering time data indicates that a slight additive effect of *TEM* and *SVP* exists, which suggests that they may act in a partially independent manner at low ambient temperature (Fig. 7). Analyzed in detail, at 22°C, the flowering time of *tem2* and *svp* was almost the same, because the difference in the total leaves produced was not statistically significant, and we did not find a significant difference between the double *tem1 tem2* mutant and *svp* plants. However, when we compared *tem2* and *svp tem2*, we found that *svp tem2* is slightly earlier, which indicates that not all of the effect of *SVP* is through *TEM2*. These flowering time data correlate with the strong binding of SVP to *TEM2* obtained by ChIP-quantitative PCR (qPCR; Fig. 5) and the down-regulation of *TEM2* observed in *svp* mutant plants (Fig. 6). At 16°C, *svp tem1 tem2* is not much earlier than the single *svp* mutant, and the difference obtained was not statistically significant, which is in agreement with the similar *FT* levels observed (Supplemental Fig. S12). This suggests that loss of *SVP* activity masks the effect of *TEM* on flowering time at lower temperatures. Therefore, at 16°C, SVP represses flowering partly through *TEM*, specifically *TEM2*, and partly through direct binding to *FT* (Lee et al., 2007, 2013).

CONCLUSION

In conclusion, we have identified new players, *TEM* genes, in the ambient temperature pathway as well as their regulation by SVP. *SVP* and *TEM* can reinforce the temperature responses by signaling partially through distinct pathways to control common outputs, such as *FT* and *TSF*. Moreover, SVP protein accumulation is higher during the day than during the night under LD conditions (Yoshida et al., 2009), in agreement with its mRNA expression (Supplemental Fig. S11), whereas TEM1 protein, and most probably, TEM2 have the opposite pattern (Osnato et al., 2012). This could suggest that SVP and TEM could regulate *FT* and *TSF* in different moments of the day. SVP represses *FT* during the morning (for review, see Song et al., 2013), and TEM would repress *FT*, *TSF*, and *GA3ox1/2* during the night. This work and previous reports indicate that *TEM* genes are involved in several genetic pathways that regulate flowering.

MATERIALS AND METHODS

Plant Material and Growth Conditions

Arabidopsis (*Arabidopsis thaliana*) Columbia-0 (Col-0) ecotype was used as the wild-type control in all of the experiments.

All mutants and transgenic lines are in the Col-0 background. *tem1-1*, *35S::TEM1*, *35S::TEM2* (Castillejo and Pelaz, 2008), *tem2-2*, *tem1-1 tem2-2* (Osnato et al., 2012), and *svp-32* (Lee et al., 2007) have been described previously. The *svp-41* mutant (Hartmann et al., 2000) was donated by Martin Kater. The *tem1-1 svp-41*, *tem2-2 svp-41*, and *tem1-1 tem2-2 svp-41* combinations were generated by crosses. Genotypes were confirmed by PCR using published oligonucleotides (Supplemental Table S3). Seeds were stratified in darkness at 4°C for 3 d and sown on soil. All plants were grown in chambers under a controlled LD photoperiod (16-h-light/8-h-dark cycle) at 22°C to 23°C or 16°C under a mixture of cool white (TL5 54 W; 965) and warm white (TL5 54 W; 840) fluorescent lights, with a fluence rate of 80 to 90 μmol m^{-2} s^{-1}.

Generation of Transgenic Plants

To generate the *pSVP::SVP:HA* construct, the open reading frame of *SVP* was amplified by reverse transcription (RT)-PCR using RNA isolated from 8-d-old seedlings. The resulting amplicons were cloned into the pCHF3 vector harboring the approximately 2.5-kb promoter fragment of *SVP*. This construct was introduced into *svp-32* plants (Lee et al., 2007) using the floral dip method with minor modifications (Weigel and Glazebrook, 2002). Subsequently, transformants were selected for kanamycin resistance, and about 30 to 40 T1 seedlings were analyzed (Lee et al., 2013). Oligonucleotide primers used for cloning are listed in Supplemental Table S3. In *pSVP::SVP:HA svp-32* plants, the production of the SVP-HA protein was confirmed (Supplemental Fig. S8A), and the early flowering and ambient temperature-insensitive flowering phenotypes of *svp-32* mutants were rescued by *pSVP::SVP:HA* (Supplemental Fig. S8B), indicating that HA-tagged SVP protein is functional.

Phenotypic and Statistical Analyses

For flowering time measurements, plants were randomized with the respective controls and grown on soil in controlled environment growth chambers. Flowering time was determined by counting the number of cauline and rosette leaves of at least 12 individual plants. The number of days to flowering was determined when the floral bud was visible to the naked eye. Data are reported as a mean value of the total leaf number ± SD for each genotype and experimental condition used; we use the mean value of the total leaf number ± SEM to compare the mean of independent experiments. All flowering time assays were performed at least two times. Flowering time data were subjected to ANOVAs. Post hoc tests were performed using Tukey's multiple comparisons test after two-way ANOVA. Statistical analyses were performed with Prism 6 software (GraphPad Software, Inc.).

RNA Isolation and Expression Analysis

Samples consisted of pools of seedlings (12–59 individuals for each time point depending on the time of collection) sown on soil, which were quickly frozen in liquid nitrogen and powdered before RNA extraction. RNA was extracted using the PureLink Micro-to-Midi Total RNA Purification Kit (Invitrogen-Ambion) and DNAse treated using the DNA-Free Kit (Ambion). RNA integrity was checked on agarose gels, and concentration was measured using an ND-1000 Spectrophotometer (Thermo Scientific). Between 1 and 1.5 μg of DNAse-treated RNA was used for cDNA synthesis by using SuperScript III Reverse Transcriptase (Invitrogen) according to the manufacturer's instructions. The resulting cDNA was diluted before subsequent expression analyses. qPCR was performed on a LightCycler 480 (Roche) using SYBR Premix ExTaq (Takara). Three technical replicates were made per sample. The relative expression was calculated using the $2^{-\Delta\Delta Ct}$ (Livak and Schmittgen, 2001). Ubiquitin10 (*UBQ10*) was used as a reference gene. Results from biological duplicates are shown. Oligonucleotide primers used for qPCR are listed in Supplemental Table S3.

ChIP Assays

Two grams of *pSVP::SVP:HA* seedlings grown on soil under LD conditions at 23°C or 16°C were cross linked in 1% (v/v) formaldehyde on ice using vacuum infiltration. Nuclear extracts were isolated, and the immunoprecipitation assays were conducted as described previously (Kim et al., 2012). After shearing chromatin by sonication, rabbit anti-HA polyclonal antibody (about 5 μg; Santa Cruz Biotechnology) was used to immunoprecipitate genomic DNA fragments. qPCR was performed using DNA recovered from immunoprecipitation or 10% input DNA with a number of primer sets spanning the regulatory regions of *TEM1* and *TEM2* (Supplemental Table S3). The relative enrichment of each fragment was calculated by comparing samples immunoprecipitated with HA and cMyc (negative control) antibodies (Livak and Schmittgen, 2001). ChIP experiments were performed in two biological replicates (samples independently harvested on different days) with three technical replicates each with similar results.

From 1 to 1.5 g of *35S::TEM1:HA* and *35S::TEM2:HA* seedlings were grown on soil under LD conditions at 22°C and 16°C to test direct binding of TEM to *FT* and *TSF* loci. Cross linked DNA was immunoprecipitated with an anti-HA antibody (Sigma), purified using Protein A-Agarose Resin (Millipore), and tested by qPCR using specific primer sets (Supplemental Table S3) on regulatory regions of *FT* and *TSF*. ChIP experiments were performed in at least two biological replicates (samples independently harvested on different days) with three technical replicates each with similar results.

Supplemental Data

The following supplemental materials are available.

Supplemental Figure S1. Upregulation of FT in *tem1 tem2* and *svp* mutants.

Supplemental Figure S2. Upregulation of *GA3ox1* in *tem1 tem2*.

Supplemental Figure S3. Low temperature does not increase *TEM* levels early in development.

Supplemental Figure S4. Opposite expression pattern of *TEM* and *FT/TSF* at 22°C.

Supplemental Figure S5. Opposite expression pattern of *TEM* and *FT/TSF* at 16°C.

Supplemental Figure S6. TEMs regulate *FT* and *TSF* levels at 16°C.

Supplemental Figure S7. TEM2 protein binds to the *FT* and *TSF* promotors at 16°C.

Supplemental Figure S8. Characterization of *pSVP::SVP:HA svp-32* transgenic plants.

Supplemental Figure S9. Binding of SVP protein to the *TEM1* and *TEM2* genomic loci.

Supplemental Figure S10. SVP positively regulates *TEM2* expression at 22°C and 16°C.

Supplemental Figure S11. TEMs do not regulate *SVP* levels.

Supplemental Figure S12. Upregulation of *FT* in *tem1 tem2*, *svp*, and *svp tem1 tem2*.

Supplemental Table S1. Flowering time and statistical analysis of data in Figure 1.

Supplemental Table S2. Flowering time and statistical analysis of data in Figure 7.

Supplemental Table S3. Oligonucleotide sequences.

ACKNOWLEDGMENTS

We thank Martin Kater for *svp-41* seeds. A.E.A.-J. performed this work within the framework of a PhD program of the Universitat Autònoma de Barcelona.

Received April 17, 2015; accepted August 2, 2015; published August 4, 2015.

LITERATURE CITED

Andrés F, Coupland G (2012) The genetic basis of flowering responses to seasonal cues. Nat Rev Genet **13:** 627–639

Balasubramanian S, Sureshkumar S, Lempe J, Weigel D (2006) Potent induction of Arabidopsis thaliana flowering by elevated growth temperature. PLoS Genet **2:** e106

Bergonzi S, Albani MC (2011) Reproductive competence from an annual and a perennial perspective. J Exp Bot **62:** 4415–4422

Blázquez MA, Ahn JH, Weigel D (2003) A thermosensory pathway controlling flowering time in Arabidopsis thaliana. Nat Genet **33:** 168–171

Capovilla G, Schmid M, Posé D (2015) Control of flowering by ambient temperature. J Exp Bot **66:** 59–69

Castillejo C, Pelaz S (2008) The balance between CONSTANS and TEMPRANILLO activities determines FT expression to trigger flowering. Curr Biol **18:** 1338–1343

Chew YH, Smith RW, Jones HJ, Seaton DD, Grima R, Halliday KJ (2014) Mathematical models light up plant signaling. Plant Cell **26:** 5–20

Fornara F, de Montaigu A, Coupland G (2010) SnapShot: control of flowering in Arabidopsis. Cell **141:** 550e1–550.e2

Franklin KA (2009) Light and temperature signal crosstalk in plant development. Curr Opin Plant Biol **12:** 63–68

Gu X, Le C, Wang Y, Li Z, Jiang D, Wang Y, He Y (2013) Arabidopsis FLC clade members form flowering-repressor complexes coordinating responses to endogenous and environmental cues. Nat Commun **4:** 1947

Hartmann U, Höhmann S, Nettesheim K, Wisman E, Saedler H, Huijser P (2000) Molecular cloning of SVP: a negative regulator of the floral transition in Arabidopsis. Plant J **21:** 351–360

Huijser P, Schmid M (2011) The control of developmental phase transitions in plants. Development **138:** 4117–4129

Jang S, Torti S, Coupland G (2009) Genetic and spatial interactions between FT, TSF and SVP during the early stages of floral induction in Arabidopsis. Plant J **60:** 614–625

Kagaya Y, Ohmiya K, Hattori T (1999) RAV1, a novel DNA-binding protein, binds to bipartite recognition sequence through two distinct DNA-binding domains uniquely found in higher plants. Nucleic Acids Res **27:** 470–478

Kardailsky I, Shukla VK, Ahn JH, Dagenais N, Christensen SK, Nguyen JT, Chory J, Harrison MJ, Weigel D (1999) Activation tagging of the floral inducer FT. Science **286:** 1962–1965

Kim JJ, Lee JH, Kim W, Jung HS, Huijser P, Ahn JH (2012) The *microRNA156-SQUAMOSA PROMOTER BINDING PROTEIN-LIKE3* module regulates ambient temperature-responsive flowering via *FLOWERING LOCUS T* in Arabidopsis. Plant Physiol **159:** 461–478

Kim W, Park TI, Yoo SJ, Jun AR, Ahn JH (2013) Generation and analysis of a complete mutant set for the Arabidopsis FT/TFL1 family shows specific effects on thermo-sensitive flowering regulation. J Exp Bot **64:** 1715–1729

Kobayashi Y, Kaya H, Goto K, Iwabuchi M, Araki T (1999) A pair of related genes with antagonistic roles in mediating flowering signals. Science **286:** 1960–1962

Kumar SV, Lucyshyn D, Jaeger KE, Alós E, Alvey E, Harberd NP, Wigge PA (2012) Transcription factor PIF4 controls the thermosensory activation of flowering. Nature **484:** 242–245

Lee JH, Kim JJ, Kim SH, Cho HJ, Kim J, Ahn JH (2012) The E3 ubiquitin ligase HOS1 regulates low ambient temperature-responsive flowering in Arabidopsis thaliana. Plant Cell Physiol **53:** 1802–1814

Lee JH, Ryu HS, Chung KS, Posé D, Kim S, Schmid M, Ahn JH (2013) Regulation of temperature-responsive flowering by MADS-box transcription factor repressors. Science **342:** 628–632

Lee JH, Yoo SJ, Park SH, Hwang I, Lee JS, Ahn JH (2007) Role of SVP in the control of flowering time by ambient temperature in Arabidopsis. Genes Dev **21:** 397–402

Li D, Liu C, Shen L, Wu Y, Chen H, Robertson M, Helliwell CA, Ito T, Meyerowitz E, Yu H (2008) A repressor complex governs the integration of flowering signals in Arabidopsis. Dev Cell **15:** 110–120

Livak KJ, Schmittgen TD (2001) Analysis of relative gene expression data using real-time quantitative PCR and the $2^{-\Delta\Delta Ct}$ Method. Methods **25:** 402–408

McClung CR, Davis SJ (2010) Ambient thermometers in plants: from physiological outputs towards mechanisms of thermal sensing. Curr Biol **20:** R1086–R1092

Michaels SD, Himelblau E, Kim SY, Schomburg FM, Amasino RM (2005) Integration of flowering signals in winter-annual Arabidopsis. Plant Physiol **137:** 149–156

Osnato M, Castillejo C, Matías-Hernández L, Pelaz S (2012) TEMPRANILLO genes link photoperiod and gibberellin pathways to control flowering in Arabidopsis. Nat Commun **3:** 808

Penfield S (2008) Temperature perception and signal transduction in plants. New Phytol **179:** 615–628

Posé D, Verhage L, Ott F, Yant L, Mathieu J, Angenent GC, Immink RG, Schmid M (2013) Temperature-dependent regulation of flowering by antagonistic FLM variants. Nature **503:** 414–417

Reeves PH, Coupland G (2001) Analysis of flowering time control in Arabidopsis by comparison of double and triple mutants. Plant Physiol **126:** 1085–1091

Romera-Branchat M, Andrés F, Coupland G (2014) Flowering responses to seasonal cues: what's new? Curr Opin Plant Biol **21:** 120–127

Song YH, Ito S, Imaizumi T (2013) Flowering time regulation: photoperiod- and temperature-sensing in leaves. Trends Plant Sci **18:** 575–583

Srikanth A, Schmid M (2011) Regulation of flowering time: all roads lead to Rome. Cell Mol Life Sci **68:** 2013–2037

Tao Z, Shen L, Liu C, Liu L, Yan Y, Yu H (2012) Genome-wide identification of SOC1 and SVP targets during the floral transition in Arabidopsis. Plant J **70:** 549–561

Weigel D, Glazebrook J (2002) Arabidopsis: A Laboratory Manual. Cold Spring Harbor Laboratory Press, Cold Spring Harbor, New York, USA

West AG, Shore P, Sharrocks AD (1997) DNA binding by MADS-box transcription factors: a molecular mechanism for differential DNA bending. Mol Cell Biol **17:** 2876–2887

Wigge PA (2013) Ambient temperature signalling in plants. Curr Opin Plant Biol **16:** 661–666

Yamaguchi A, Kobayashi Y, Goto K, Abe M, Araki T (2005) TWIN SISTER OF FT (TSF) acts as a floral pathway integrator redundantly with FT. Plant Cell Physiol **46:** 1175–1189

Yoshida RO, Fekih R, Fujiwara S, Oda A, Miyata K, Tomozoe Y, Nakagawa M, Niinuma K, Hayashi K, Ezura H, et al (2009) Possible role of early flowering 3 (ELF3) in clock-dependent floral regulation by short vegetative phase (SVP) in Arabidopsis thaliana. New Phytol **182:** 838–850

CAPÍTULO II: SHORT VEGETATIVE PHASE Up-Regulates *TEMPRANILLO2* Floral Repressor at Low Ambient Temperatures.

Supplemental Data

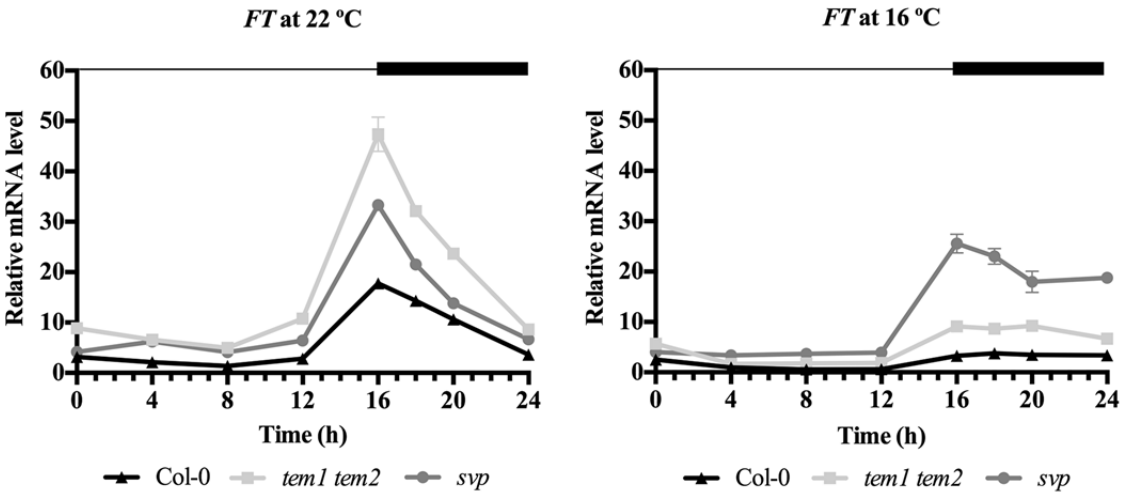

Supplemental Figure S1

Supplemental Figure S1.

Upregulation of *FT* in *tem1 tem2* and *svp* mutant plants at 22ºC and 16ºC. *FT* expression in wild-type (Col-0), *tem1 tem2* and *svp* plants grown under LD conditions at 22ºC or 16ºC. Nine-day-old plants were collected at 4-hours intervals over a 24h-period. Error bars show SD of three technical replicates. RNA levels were determined by RT-qPCR and normalized to *UBQ10*. Biological replicate of Fig. 1.

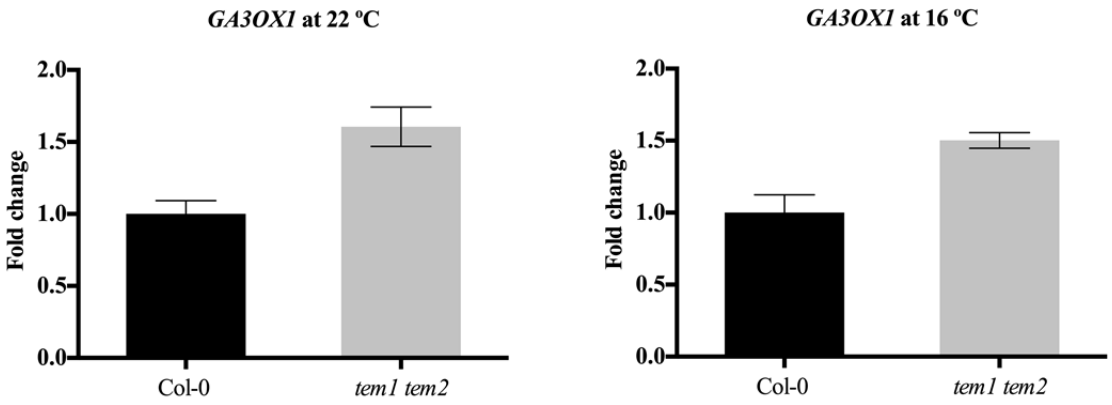

Supplemental Figure S2

Supplemental Figure S2.

Upregulation of *GA3ox1* in *tem1 tem2* at 22 ºC and 16 ºC. *GA3OX1* expression in wild-type (Col-0) and *tem1 tem2* plants grown under LD conditions at 22 ºC or 16 ºC. Nine-day-old plants were collected at ZT12. Two independent experiments gave similar results and one was chosen as representative. Error bars show SD of three technical replicates. RNA levels were determined by RT-qPCR and normalized to *UBQ10*.

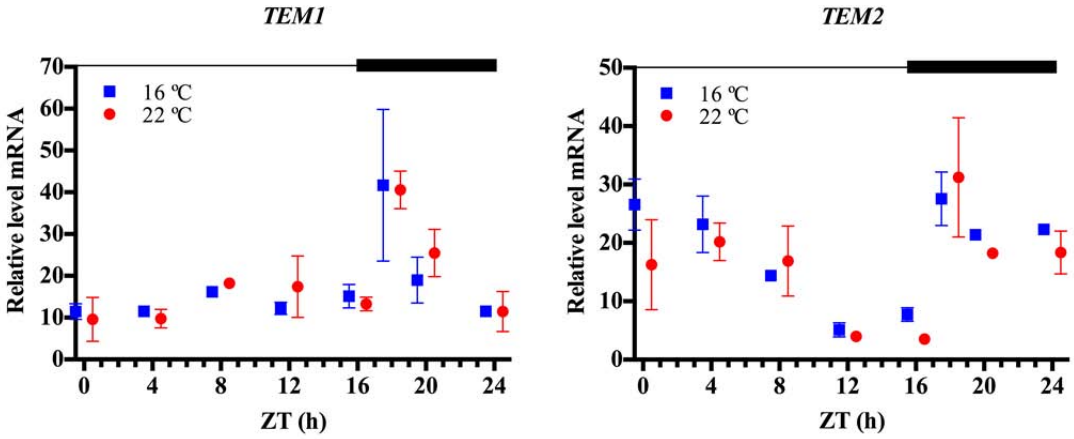

Supplemental Figure S3

Supplemental Figure S3.

Low temperature does not increase *TEM* levels early in development. Relative mRNA levels of *TEM1* (left) and *TEM2* (right) in wild-type plants at 22ºC and 16ºC. Nine-day-old seedlings were sampled at 4-h intervals, except from ZT16 to ZT20 when samples were collected every 2h (to add the ZT18 time point). Data are reported as mean ± SEM of two independent experiments represented by blue squares (16ºC) and red dots (22ºC). The dark period is denoted by the black bar. RNA levels were determined by RT-qPCR and normalized to *UBQ10*. ZT, zeitgeber time.

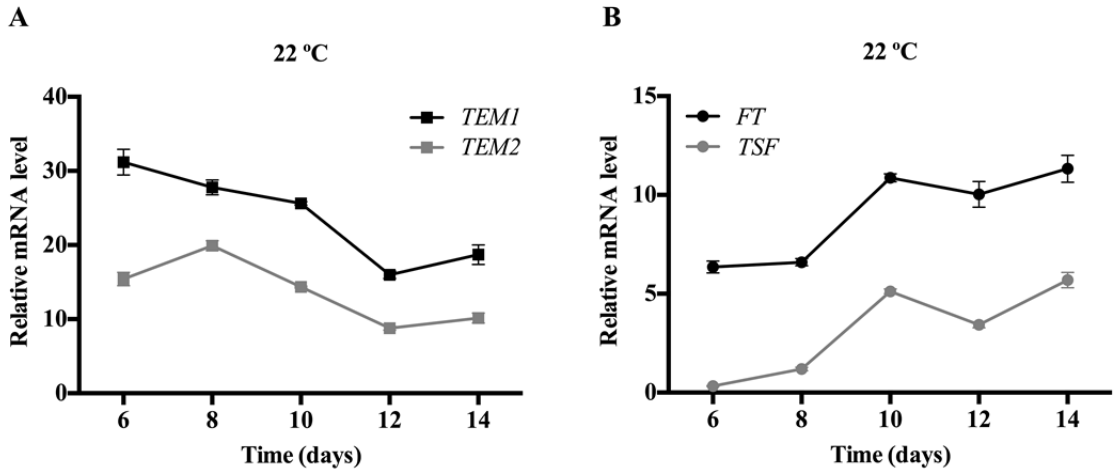

Supplemental Figure S4

Supplemental Figure S4.

Opposite expression pattern of *TEM* and *FT/TSF* genes along development at 22ºC.

(A) *TEM1* and *TEM2* expression, and (B) *FT* and *TSF* expression in wild-type plants grown under LD conditions at 22ºC during 2 weeks. Samples were collected at ZT18. Error bars show SD of three technical replicates. RNA levels were determined by RT-qPCR and normalized to *UBQ10*.

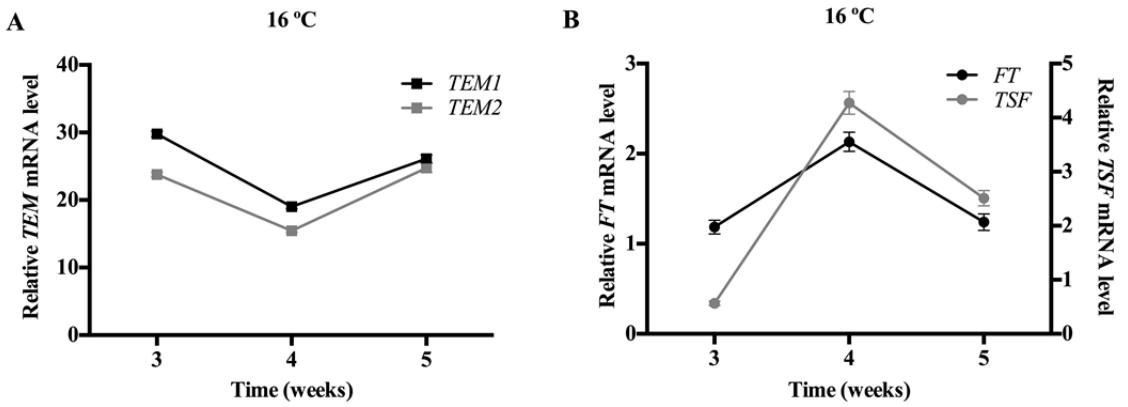

Supplemental Figure S5

Supplemental Figure S5.

Opposite expression pattern of *TEM* and *FT/TSF* genes along development at 16ºC.

(A) *TEM1* and *TEM2* expression, and (B) *FT* and *TSF* expression in wild-type plants grown under LD conditions at 16ºC during 5 weeks. Samples were collected at ZT18. Error bars show SD of three technical replicates. RNA levels were determined by RT-qPCR and normalized to *UBQ10*. Biological replicates of Fig. 2.

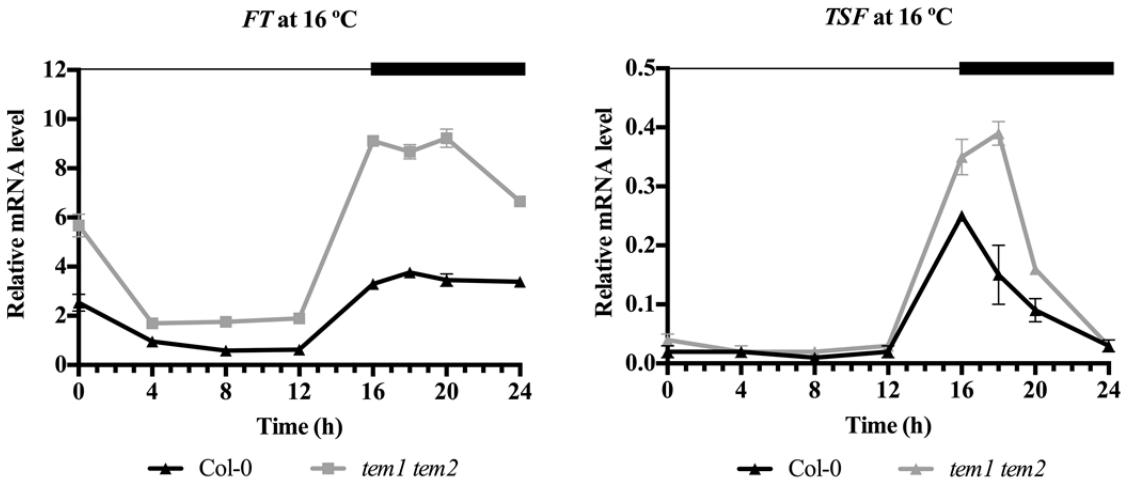

Supplemental Figure S6

Supplemental Figure S6.

TEMs regulate *FT* and *TSF* levels at 16ºC. Relative *FT* and *TSF* mRNA levels in *tem1 tem2* mutant compared to wild-type (Col-0) plants. Nine-day-old seedlings were sampled at 4-h intervals, except from ZT16 to ZT20 when samples were collected every 2h. Error bars show SD of three technical replicates. RNA levels were determined by RT-qPCR and normalized to *UBQ10*. Biological replicates of Fig. 3.

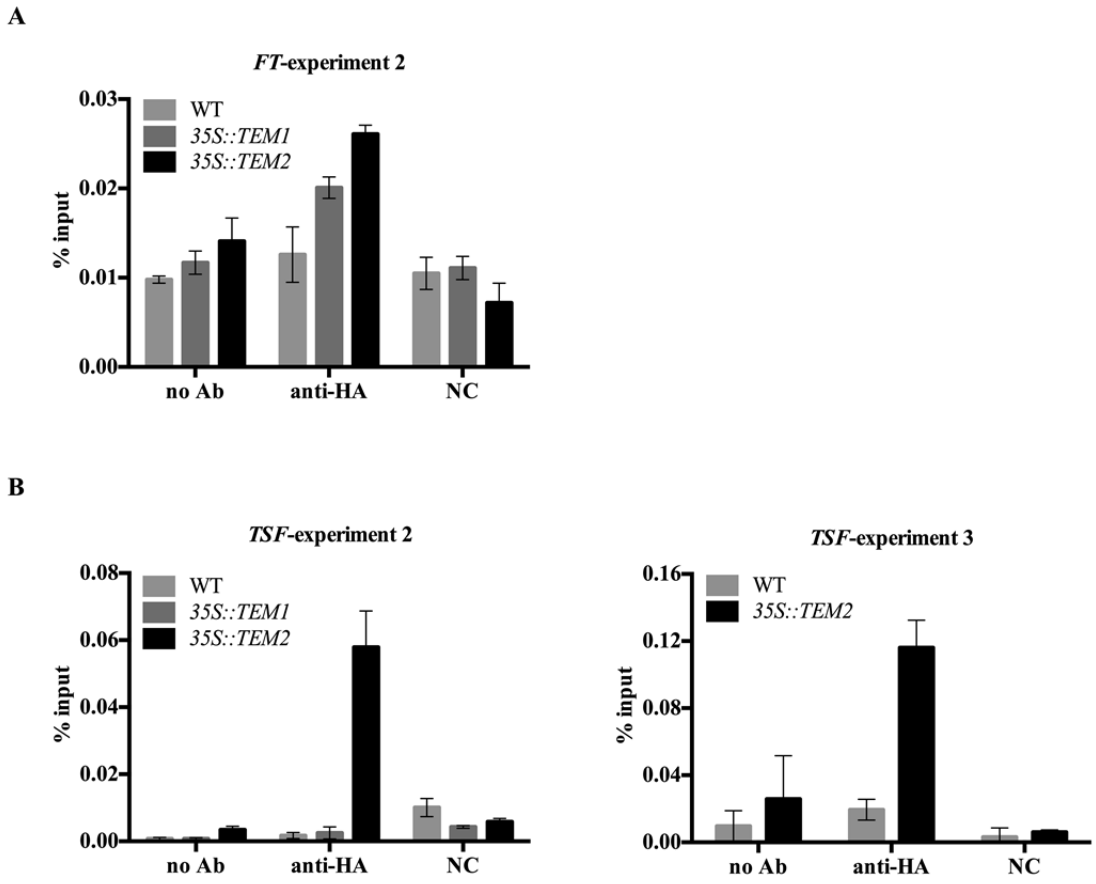

Supplemental Figure S7

Supplemental Figure S7.

TEM2 protein binds to the *FT* and *TSF* promotors at 16ºC. ChIP assay of binding of TEM1-HA and TEM2-HA proteins to the RAV motifs in the (A) *FT* and (B) *TSF* regulatory regions. DNA fragments containing the RAV binding site were analyzed by chromatin immunoprecipitation (ChIP) using 9-day-old *35S::TEM1* and *35S::TEM2* plants carrying an HA tag. Precipitated chromatin was used as a template in qPCR. Immunoprecipitated DNA enrichment is presented as percentage of input DNA. NC is a negative control. Error bars show SD of three technical replicates. Biological replicates of Fig. 4.

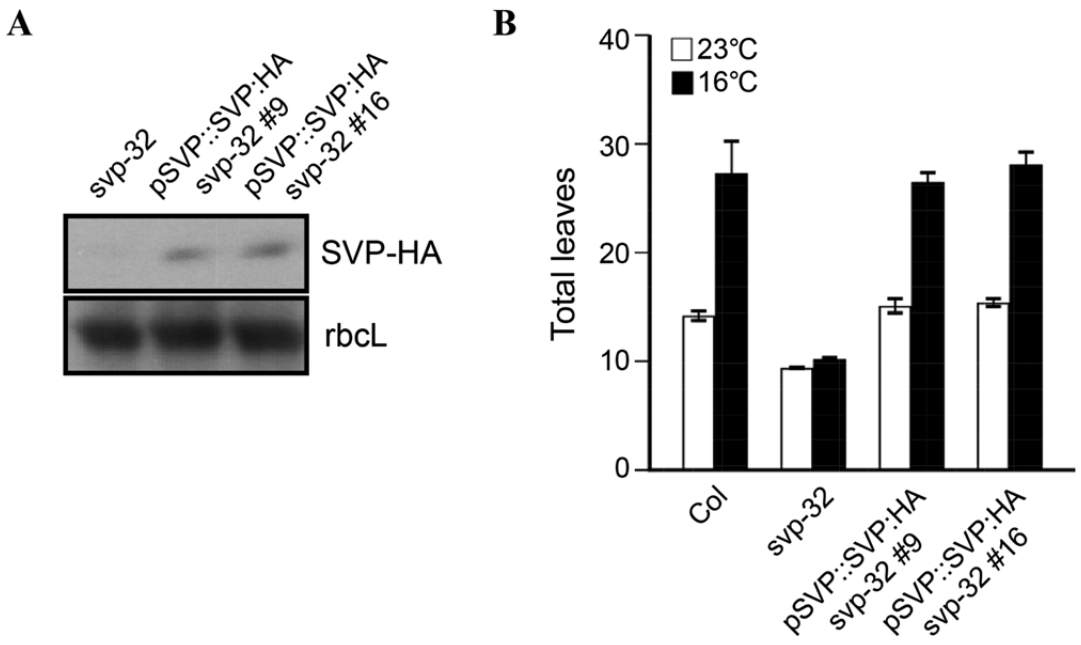

Supplemental Figure S8

Supplemental Figure S8.

Characterization of *pSVP::SVP:HA svp-32* transgenic plants. (A) SVP-HA protein expression in two independent *pSVP::SVP:HA svp-32* lines (#9 and #16) grown at 23°C under LD conditions. An anti-HA antibody was used to detect SVP-HA protein. RbcL was used as a loading control. (B) Flowering time of two independent homozygous *pSVP::SVP:HA svp-32* plants at 23°C and 16°C under LD conditions. Error bars show SD. The numbers of plants used in this analysis are as follows: wild-type, n=30; *svp-32*, n=34; *pSVP::SVP-HA svp-32* #9, n=20; *pSVP::SVP-HA* svp-32 #9, n=26.

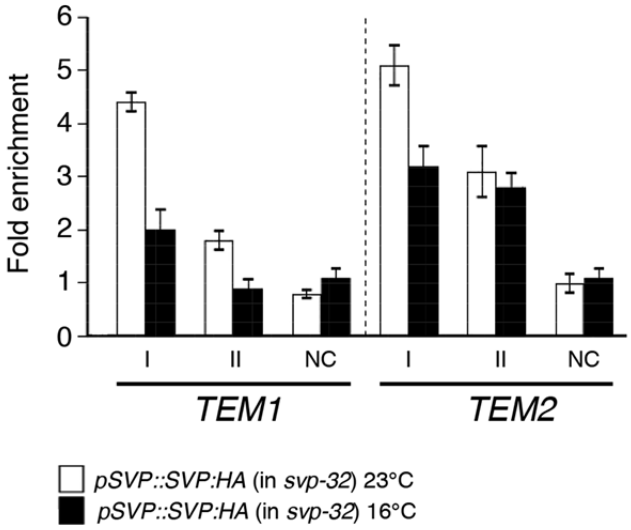

Supplemental Figure S9

Supplemental Figure S9.

Binding of SVP protein to the *TEM1* and *TEM2* genomic loci. Chromatin immunoprecipitation (ChIP) analysis of binding of SVP protein to the *TEM1* and *TEM2* genomic regions at 23°C and 16°C in 9-day old plants *pSVP::SVP:HA svp-32*. Error bars show SD of three technical replicates. Biological replicates of Fig. 5.

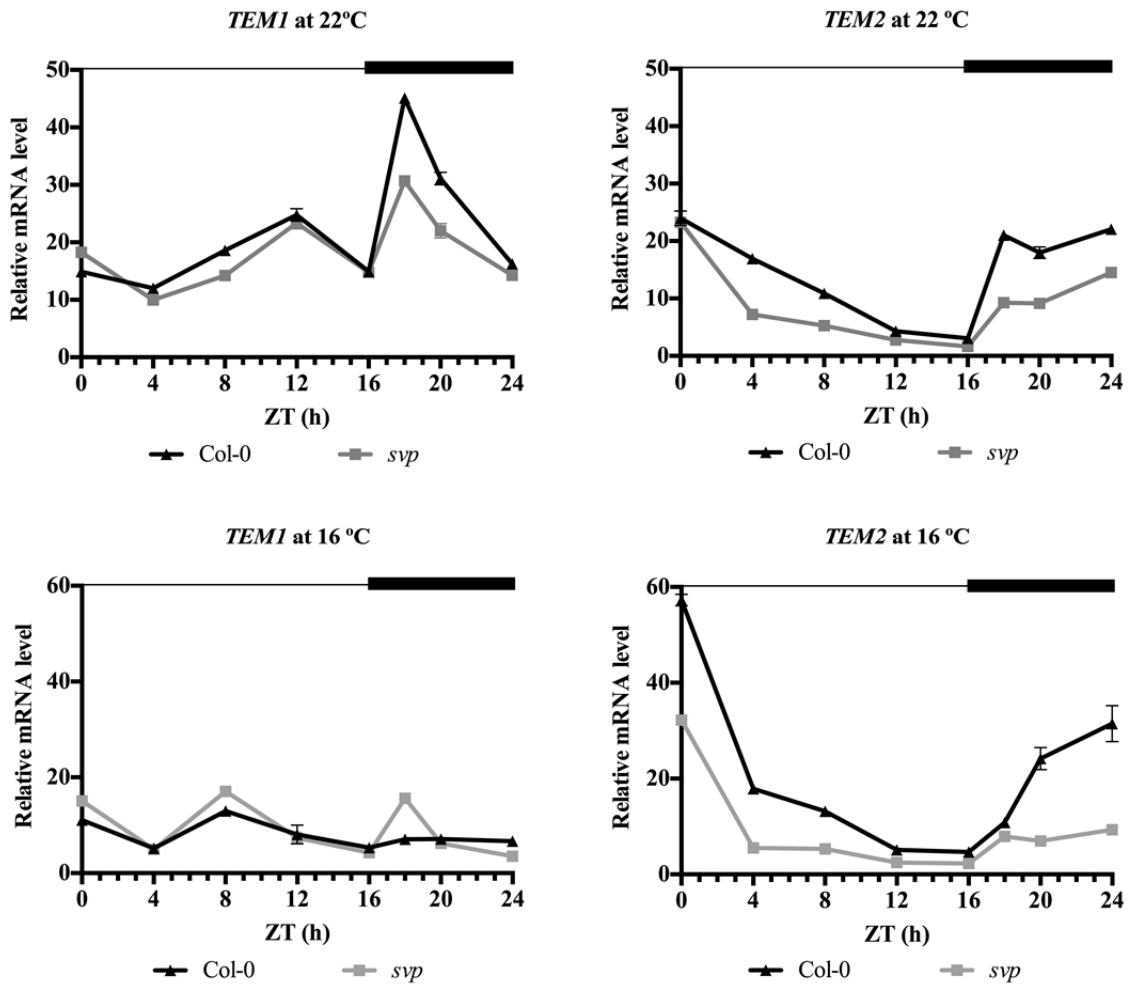

Supplemental Figure S10

Supplemental Figure S10.

SVP positively regulates *TEM2* expression at 22ºC and 16ºC. Relative mRNA levels of *TEM1* and *TEM2* in *svp* mutant compared to wild-type (Col-0) plants. Nine-day-old seedlings were sampled at 4-h intervals, except from ZT16 to ZT20 when samples were collected every 2h. Bars show SD of three technical replicates. RNA levels were determined by RT-qPCR and normalized to *UBQ10*. Biological replicate of Fig. 6.

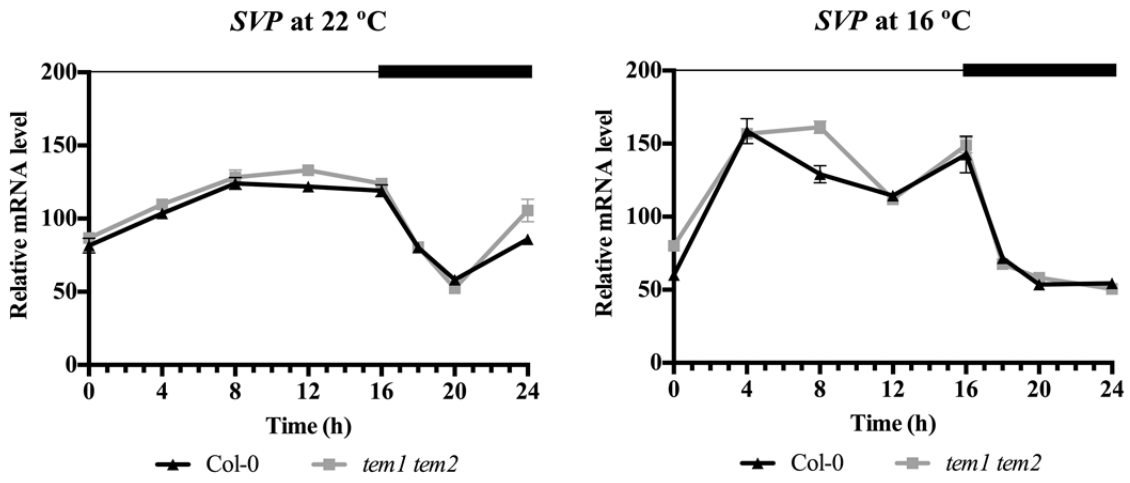

Supplemental Figure S11

Supplemental Figure S11.

TEMs do not regulate *SVP* levels. Relative *SVP* mRNA levels at 22ºC (left) and 16ºC (right) in *tem1 tem2* mutant compared to wild-type plants. 9-day-old seedlings were sampled at 4-h intervals, except from ZT16 to ZT20 when samples were collected every 2h. Two independent experiments gave similar results and one was chosen as representative. Error bars show SD of three technical replicates. RNA levels were determined by RT-qPCR and normalized to *UBQ10*.

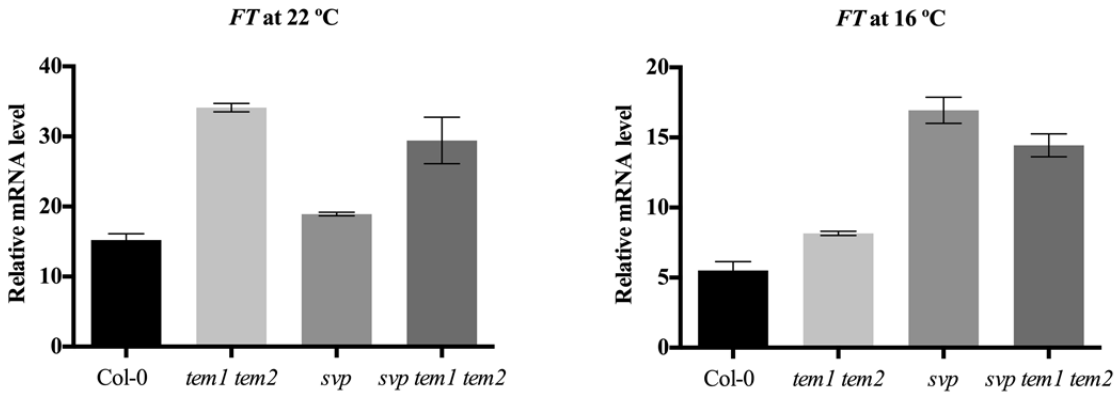

Supplemental Figure S12

Supplemental Figure S12.

Upregulation of *FT* in *tem1 tem2*, *svp* and *svp tem1 tem2* at 22 ºC and 16 ºC. Relative *FT* mRNA levels at 22 ºC (left) and 16 ºC (right) in *tem1 tem2*, *svp* and *svp tem1 tem2* mutant compared to wild-type plants. 10-day-old seedlings were sampled at ZT16. Two independent experiments gave similar results and one was chosen as representative. Error bars show SD of three technical replicates. RNA levels were determined by RT-qPCR and normalized to *UBQ10*.

Supplemental Table S1

(A) **Flowering time** (corresponding to data in Figure 1) and (B) **statistical analysis** of total leaf numbers. RL: rossete leaves; CL: cauline leaves; TL: total leaves; n: number of plants per genotype and experiment; NQ: not quantified; NS: not significant. For total leaves and days, mean ± SD are shown for each genotype and experimental condition.

A

22 ºC						**16 ºC**				
Genotype	**RL**	**CL**	**TL±SD**	**Days±SD**	**n**	**RL**	**CL**	**TL±SD**	**Days±SD**	**n**
Experiment 1						Experiment 1				
Col-0	12.2	2.7	14.9±0.7	21.9±0.9	13	26.2	5.8	32.0 ± 2.1	34.5±1.4	12
tem1 tem2	5.9	2.1	8.1±0.7	13.1±0.8	17	10.7	3.7	14.4 ± 0.9	20.3±0.5	13
svp	6.1	2.4	8.5±0.5	15.5±0.7	12	7.2	2.8	9.9 ± 0.5	18.4±0.5	12
Experiment 2						Experiment 2				
Col-0	14.5	3.8	18.3±0.7	22.5±0.5	15	28.0	5.8	33.8 ± 2.3	37.2±0.9	13
tem1 tem2	6.1	2.9	9.0±1.0	14.1±0.8	18	10.9	3.8	14.7 ± 0.8	22.2±0.4	12
svp	6.2	2.9	9.2±0.4	14.5±0.5	18	7.4	2.9	10.3 ± 1.4	20.7±1.5	13
Experiment 3						Experiment 3				
Col-0	11.9	3.0	14.9±0.7	NQ	15	23.6	7.4	31.0 ± 1.2	NQ	15
tem1 tem2	5.6	2.6	8.2±0.8	NQ	15	11.4	2.3	13.7 ± 1.4	NQ	15
svp	7.9	2.0	9.9±0.7	NQ	15	8.4	2.1	10.6 ± 1.1	NQ	15

B. Supplemental Table S1 (continued).

Multiple Comparisons of Total Leaf Number	Significance	*p*-value
22 ºC: Col-0 Exp1 vs. 16 ºC: Col-0 Exp1	****	< 0.0001
22 ºC: Col-0 Exp1 vs. 16 ºC: Col-0 Exp2	****	< 0.0001
22 ºC: Col-0 Exp1 vs. 16 ºC: Col-0 Exp3	****	< 0.0001
22 ºC: Col-0 Exp2 vs. 16 ºC: Col-0 Exp1	****	< 0.0001
22 ºC: Col-0 Exp2 vs. 16 ºC: Col-0 Exp2	****	< 0.0001
22 ºC: Col-0 Exp2 vs. 16 ºC: Col-0 Exp3	****	< 0.0001
22 ºC: Col-0 Exp3 vs. 16 ºC: Col-0 Exp1	****	< 0.0001
22 ºC: Col-0 Exp3 vs. 16 ºC: Col-0 Exp2	****	< 0.0001
22 ºC: Col-0 Exp3 vs. 16 ºC: Col-0 Exp3	****	< 0.0001
22 ºC: *tem1 tem2* Exp1 vs. 16 ºC: *tem1 tem2* Exp1	****	< 0.0001
22 ºC: *tem1 tem2* Exp1 vs. 16 ºC: *tem1 tem2* Exp2	****	< 0.0001
22 ºC: *tem1 tem2* Exp1 vs. 16 ºC: *tem1 tem2* Exp3	****	< 0.0001
22 ºC: *tem1 tem2* Exp2 vs. 16 ºC: *tem1 tem2* Exp1	****	< 0.0001
22 ºC: *tem1 tem2* Exp2 vs. 16 ºC: *tem1 tem2* Exp2	****	< 0.0001
22 ºC: *tem1 tem2* Exp2 vs. 16 ºC: *tem1 tem2* Exp3	****	< 0.0001
22 ºC: *tem1 tem2* Exp3 vs. 16 ºC: *tem1 tem2* Exp1	****	< 0.0001
22 ºC: *tem1 tem2* Exp3 vs. 16 ºC: *tem1 tem2* Exp2	****	< 0.0001
22 ºC: *tem1 tem2* Exp3 vs. 16 ºC: *tem1 tem2* Exp3	****	< 0.0001
22 ºC: *svp* Exp1 vs. 16 ºC: *svp* Exp1	NS	0.1468
22 ºC: *svp* Exp1 vs. 16 ºC: *svp* Exp2	**	0.0064
22 ºC: *svp* Exp1 vs. 16 ºC: *svp* Exp3	***	0.0002
22 ºC: *svp* Exp2 vs. 16 ºC: *svp* Exp1	NS	0.9604
22 ºC: *svp* Exp2 vs. 16 ºC: *svp* Exp2	NS	0.3381
22 ºC: *svp* Exp2 vs. 16 ºC: *svp* Exp3	*	0.00315
22 ºC: *svp* Exp3 vs. 16 ºC: *svp* Exp1	***	0.0002
22 ºC: *svp* Exp3 vs. 16 ºC: *svp* Exp2	NS	> 0.9999
22 ºC: *svp* Exp3 vs. 16 ºC: *svp* Exp3	NS	0.9525
22 ºC: Col-0 Exp1 vs. 22 ºC: *tem1 tem2* Exp1	****	< 0.0001
22 ºC: Col-0 Exp1 vs. 22 ºC: *tem1 tem2* Exp2	****	< 0.0001
22 ºC: Col-0 Exp1 vs. 22 ºC: *tem1 tem2* Exp3	****	< 0.0001
22 ºC: Col-0 Exp2 vs. 22 ºC: *tem1 tem2* Exp1	****	< 0.0001
22 ºC: Col-0 Exp2 vs. 22 ºC: *tem1 tem2* Exp2	****	< 0.0001
22 ºC: Col-0 Exp2 vs. 22 ºC: *tem1 tem2* Exp3	****	< 0.0001
22 ºC: Col-0 Exp3 vs. 22 ºC: *tem1 tem2* Exp1	****	< 0.0001
22 ºC: Col-0 Exp3 vs. 22 ºC: *tem1 tem2* Exp2	****	< 0.0001
22 ºC: Col-0 Exp3 vs. 22 ºC: *tem1 tem2* Exp3	****	< 0.0001
22 ºC: Col-0 Exp1 vs. 22 ºC: *svp* Exp1	****	< 0.0001
22 ºC: Col-0 Exp1 vs. 22 ºC: *svp* Exp2	****	< 0.0001
22 ºC: Col-0 Exp1 vs. 22 ºC: *svp* Exp3	****	< 0.0001
22 ºC: Col-0 Exp2 vs. 22 ºC: *svp* Exp1	****	< 0.0001
22 ºC: Col-0 Exp2 vs. 22 ºC: *svp* Exp2	****	< 0.0001
22 ºC: Col-0 Exp2 vs. 22 ºC: *svp* Exp3	****	< 0.0001
22 ºC: Col-0 Exp3 vs. 22 ºC: *svp* Exp1	****	< 0.0001
22 ºC: Col-0 Exp3 vs. 22 ºC: *svp* Exp2	****	< 0.0001
22 ºC: Col-0 Exp3 vs. 22 ºC: *svp* Exp3	****	< 0.0001
16 ºC: Col-0 Exp1 vs. 16 ºC: *tem1 tem2* Exp1	****	< 0.0001

16 ºC: Col-0 Exp1 vs. 16 ºC: *tem1 tem2* Exp2	****	< 0.0001
16 ºC: Col-0 Exp1 vs. 16 ºC: *tem1 tem2* Exp3	****	< 0.0001
16 ºC: Col-0 Exp2 vs. 16 ºC: *tem1 tem2* Exp1	****	< 0.0001
16 ºC: Col-0 Exp2 vs. 16 ºC: *tem1 tem2* Exp2	****	< 0.0001
16 ºC: Col-0 Exp2 vs. 16 ºC: *tem1 tem2* Exp3	****	< 0.0001
16 ºC: Col-0 Exp3 vs. 16 ºC: *tem1 tem2* Exp1	****	< 0.0001
16 ºC: Col-0 Exp3 vs. 16 ºC: *tem1 tem2* Exp2	****	< 0.0001
16 ºC: Col-0 Exp3 vs. 16 ºC: *tem1 tem2* Exp3	****	< 0.0001
16 ºC: Col-0 Exp1 vs. 16 ºC: *svp* Exp1	****	< 0.0001
16 ºC: Col-0 Exp1 vs. 16 ºC: *svp* Exp2	****	< 0.0001
16 ºC: Col-0 Exp1 vs. 16 ºC: *svp* Exp3	****	< 0.0001
16 ºC: Col-0 Exp2 vs. 16 ºC: *svp* Exp1	****	< 0.0001
16 ºC: Col-0 Exp2 vs. 16 ºC: *svp* Exp2	****	< 0.0001
16 ºC: Col-0 Exp2 vs. 16 ºC: *svp* Exp3	****	< 0.0001
16 ºC: Col-0 Exp3 vs. 16 ºC: *svp* Exp1	****	< 0.0001
16 ºC: Col-0 Exp3 vs. 16 ºC: *svp* Exp2	****	< 0.0001
16 ºC: Col-0 Exp3 vs. 16 ºC: *svp* Exp3	****	< 0.0001
22 ºC: *tem1 tem2* Exp1 vs. 22 ºC: *svp* Exp1	NS	> 0.9999
22 ºC: *tem1 tem2* Exp1 vs. 22 ºC: *svp* Exp2	NS	0.2170
22 ºC: *tem1 tem2* Exp1 vs. 22 ºC: *svp* Exp3	***	0.0007
22 ºC: *tem1 tem2* Exp2 vs. 22 ºC: *svp* Exp1	NS	0.9990
22 ºC: *tem1 tem2* Exp2 vs. 22 ºC: *svp* Exp2	NS	> 0.9999
22 ºC: *tem1 tem2* Exp2 vs. 22 ºC: *svp* Exp3	NS	0.6377
22 ºC: *tem1 tem2* Exp3 vs. 22 ºC: *svp* Exp1	NS	> 0.9999
22 ºC: *tem1 tem2* Exp3 vs. 22 ºC: *svp* Exp2	NS	0.4406
22 ºC: *tem1 tem2* Exp3 vs. 22 ºC: *svp* Exp3	**	0.0036
16 ºC: *tem1 tem2* Exp1 vs. 16 ºC: *svp* Exp1	****	<0.0001
16 ºC: *tem1 tem2* Exp1 vs. 16 ºC: *svp* Exp2	****	<0.0001
16 ºC: *tem1 tem2* Exp1 vs. 16 ºC: *svp* Exp3	****	<0.0001
16 ºC: *tem1 tem2* Exp2 vs. 16 ºC: *svp* Exp1	****	<0.0001
16 ºC: *tem1 tem2* Exp2 vs. 16 ºC: *svp* Exp2	****	<0.0001
16 ºC: *tem1 tem2* Exp2 vs. 16 ºC: *svp* Exp3	****	<0.0001
16 ºC: *tem1 tem2* Exp3 vs. 16 ºC: *svp* Exp1	****	<0.0001
16 ºC: *tem1 tem2* Exp3 vs. 16 ºC: *svp* Exp2	****	<0.0001
16 ºC: *tem1 tem2* Exp3 vs. 16 ºC: *svp* Exp3	****	<0.0001
22 ºC: Col-0 Exp1 vs. 16 ºC: *tem1 tem2* Exp1	NS	0.9995
22 ºC: Col-0 Exp1 vs. 16 ºC: *tem1 tem2* Exp2	NS	> 0.9999
22 ºC: Col-0 Exp1 vs. 16 ºC: *tem1 tem2* Exp3	NS	0.2582
22 ºC: Col-0 Exp2 vs. 16 ºC: *tem1 tem2* Exp1	****	<0.0001
22 ºC: Col-0 Exp2 vs. 16 ºC: *tem1 tem2* Exp2	****	<0.0001
22 ºC: Col-0 Exp2 vs. 16 ºC: *tem1 tem2* Exp3	****	<0.0001
22 ºC: Col-0 Exp3 vs. 16 ºC: *tem1 tem2* Exp1	NS	0.9992
22 ºC: Col-0 Exp3 vs. 16 ºC: *tem1 tem2* Exp2	NS	> 0.9999
22 ºC: Col-0 Exp3 vs. 16 ºC: *tem1 tem2* Exp3	NS	0.2020

**** $p \leq 0.0001$; *** $p \leq 0.001$; ** $p \leq 0.01$; * $p \leq 0.05$; N.S $p > 0.05$

Supplemental Table S2

(A) Flowering time (corresponding to data in Figure 7) and (B) **statistical analysis** of total leaf numbers. RL: rossete leaves; CL: cauline leaves; TL: total leaves; n: number of plants per genotype and experiment; NS: not significant. For total leaves and days, mean ± SD are shown for each genotype and experimental condition.

A

22 ºC						**16 ºC**				
Genotype	**RL**	**CL**	**TL±SD**	**Days±SD**	**n**	**RL**	**CL**	**TL±SD**	**Days±SD**	**n**
Experiment 1						Experiment 1				
Col-0	12.1	2.8	14.9±1.1	19.7±0.8	14	20.2	5.7	25.9±2.1	30.3±1.7	12
tem1	10.4	2.7	13.1±0.9	18.4±0.6	14	16.3	4.5	20.8±1.4	25.4±1.3	14
tem2	9.2	3	12.2±1.6	15.1±1.2	16	13.2	4.9	18.1±3.6	22.3±1.8	14
tem1 tem2	6.9	2.5	9.4±1.0	14.2±0.8	14	11.5	3.8	15.3±1.1	19.9±1.2	14
svp	7.1	3.1	10.2±1.0	13.5±0.5	12	8.1	3.3	11.4±1.0	17.7±0.8	12
svp tem1	7.3	2.6	9.9±0.9	15.7±0.8	15	8.3	3.6	11.9±0.6	18.7±1.5	14
svp tem2	5.9	2.6	8.5±0.5	12.9±0.6	16	6.3	2.9	9.2±0.7	17.9±0.5	14
svp tem1 tem2	6.4	2.5	8.9±0.6	8.9±0.6	14	6.9	3.2	10.1±0.9	17.9±0.5	14
Experiment 2						Experiment 2				
Col-0	12.3	2.2	14.5±1.2	17.3±0.7	10	18.6	4.9	23.5±1.4	29.0±1.6	12
tem1	10.8	2.6	13.4±1.2	15.5±0.5	13	14.4	3.1	17.5±1.7	24.6±1.8	14
tem2	8.3	3.1	11.4±1.4	13.9±1.0	12	13.3	4.2	17.5±2.6	23.3±1.8	14
tem1 tem2	7.0	2.5	9.5±1.0	12.8±0.7	13	9.9	2.9	12.8±1.7	18.5±2.1	14
svp	7.6	3.1	10.7±0.6	13.3±0.5	12	6.7	2.9	9.6±0.7	16.2±0.6	12
svp tem1	8.3	3.4	11.7±0.8	13.2±0.7	16	7.3	2.9	10.2±0.8	16.3±0.7	14
svp tem2	6.1	3.1	9.2±0.8	12.9±0.7	20	6.2	2.6	8.8±0.9	16.3±0.7	14
svp tem1 tem2	6.4	3.3	9.7±0.7	9.7±0.7	17	6.1	2.7	8.8±0.8	16.2±0.5	14

B. Supplemental Table S2 (continued).

Multiple Comparisons of Total Leaf Number	Significance	*p*-value
22 ºC: Col-0 Exp1 vs. 16 ºC: Col-0 Exp1	****	<0.0001
22 ºC: Col-0 Exp1 vs. 16 ºC: Col-0 Exp2	****	<0.0001
22 ºC: Col-0 Exp2 vs. 16 ºC: Col-0 Exp1	****	<0.0001
22 ºC: Col-0 Exp2 vs. 16 ºC: Col-0 Exp2	****	<0.0001
22 ºC: *tem1 tem2* Exp1 vs. 16 ºC: *tem1 tem2* Exp1	****	<0.0001
22 ºC: *tem1 tem2* Exp1 vs. 16 ºC: *tem1 tem2* Exp2	****	<0.0001
22 ºC: *tem1 tem2* Exp2 vs. 16 ºC: *tem1 tem2* Exp1	****	<0.0001
22 ºC: *tem1 tem2* Exp2 vs. 16 ºC: *tem1 tem2* Exp2	****	<0.0001
22 ºC: *svp* Exp1 vs. 16 ºC: *svp* Exp1	NS	0.9006
22 ºC: *svp* Exp1 vs. 16 ºC: *svp* Exp2	NS	>0.9999
22 ºC: *svp* Exp2 vs. 16 ºC: *svp* Exp1	NS	>0.9999
22 ºC: *svp* Exp2 vs. 16 ºC: *svp* Exp2	NS	0.9516
22 ºC: *svp tem1* Exp1 vs. 16 ºC: *svp tem1* Exp1	*	0.0191
22 ºC: *svp tem1* Exp1 vs. 16 ºC: *svp tem1* Exp2	NS	>0.9999
22 ºC: *svp tem1* Exp2 vs. 16 ºC: *svp tem1* Exp1	NS	>0.9999
22 ºC: *svp tem1* Exp2 vs. 16 ºC: *svp tem1* Exp2	NS	0.3666
22 ºC: *svp tem2* Exp1 vs. 16 ºC: *svp tem2* Exp1	NS	>0.9999
22 ºC: *svp tem2* Exp1 vs. 16 ºC: *svp tem2* Exp2	NS	>0.9999
22 ºC: *svp tem2* Exp2 vs. 16 ºC: *svp tem2* Exp1	NS	>0.9999
22 ºC: *svp tem2* Exp2 vs. 16 ºC: *svp tem2* Exp2	NS	>0.9999
22 ºC: *svp tem1 tem2* Exp1 vs. 16 ºC: *svp tem1 tem2* Exp1	NS	0.9148
22 ºC: *svp tem1 tem2* Exp1 vs. 16 ºC: *svp tem1 tem2* Exp2	NS	>0.9999
22 ºC: *svp tem1 tem2* Exp2 vs. 16 ºC: *svp tem1 tem2* Exp1	NS	>0.9999
22 ºC: *svp tem1 tem2* Exp2 vs. 16 ºC: *svp tem1 tem2* Exp2	NS	0.9970
22 ºC: Col-0 Exp1 vs. 22 ºC: *tem1 tem2* Exp1	****	<0.0001
22 ºC: Col-0 Exp1 vs. 22 ºC: *tem1 tem2* Exp2	****	<0.0001
22 ºC: Col-0 Exp2 vs. 22 ºC: *tem1 tem2* Exp1	****	<0.0001
22 ºC: Col-0 Exp2 vs. 22 ºC: *tem1 tem2* Exp2	****	<0.0001
22 ºC: Col-0 Exp1 vs. 22 ºC: *svp* Exp1	****	<0.0001
22 ºC: Col-0 Exp1 vs. 22 ºC: *svp* Exp2	****	<0.0001
22 ºC: Col-0 Exp2 vs. 22 ºC: *svp* Exp1	****	<0.0001
22 ºC: Col-0 Exp2 vs. 22 ºC: *svp* Exp2	****	<0.0001
22 ºC: Col-0 Exp1 vs. 22 ºC: *svp tem1* Exp1	****	<0.0001
22 ºC: Col-0 Exp1 vs. 22 ºC: *svp tem1* Exp2	****	<0.0001
22 ºC: Col-0 Exp2 vs. 22 ºC: *svp tem1* Exp1	****	<0.0001
22 ºC: Col-0 Exp2 vs. 22 ºC: *svp tem1* Exp2	****	<0.0001
22 ºC: Col-0 Exp1 vs. 22 ºC: *svp tem2* Exp1	****	<0.0001
22 ºC: Col-0 Exp1 vs. 22 ºC: *svp tem2* Exp2	****	<0.0001
22 ºC: Col-0 Exp2 vs. 22 ºC: *svp tem2* Exp1	****	<0.0001
22 ºC: Col-0 Exp2 vs. 22 ºC: *svp tem2* Exp2	****	<0.0001
22 ºC: Col-0 Exp1 vs. 22 ºC: *svp tem1 tem2* Exp1	****	<0.0001
22 ºC: Col-0 Exp1 vs. 22 ºC: *svp tem1 tem2* Exp2	****	<0.0001
22 ºC: Col-0 Exp2 vs. 22 ºC: *svp tem1 tem2* Exp1	****	<0.0001
22 ºC: Col-0 Exp2 vs. 22 ºC: *svp tem1 tem2* Exp2	****	<0.0001
22 ºC: *tem1* Exp1 vs. 22 ºC: *svp* Exp1	****	<0.0001
22 ºC: *tem1* Exp1 vs. 22 ºC: *svp* Exp2	**	0.0041

22 ºC: *tem1* Exp2 vs. 22 ºC: *svp* Exp1	****	<0.0001
22 ºC: *tem1* Exp2 vs. 22 ºC: *svp* Exp2	***	0.0003
22 ºC: *tem2* Exp1 vs. 22 ºC: *svp* Exp1	*	0.0246
22 ºC: *tem2* Exp1 vs. 22 ºC: *svp* Exp2	NS	0.5294
22 ºC: *tem2* Exp2 vs. 22 ºC: *svp* Exp1	NS	0.9006
22 ºC: *tem2* Exp2 vs. 22 ºC: *svp* Exp2	NS	> 0.9999
22 ºC: *tem2* Exp1 vs. 22 ºC: *svp tem1* Exp1	**	0.0011
22 ºC: *tem2* Exp1 vs. 22 ºC: *svp tem1* Exp2	NS	> 0.9999
22 ºC: *tem2* Exp2 vs. 22 ºC: *svp tem1* Exp1	NS	0.4822
22 ºC: *tem2* Exp2 vs. 22 ºC: *svp tem1* Exp2	NS	> 0.9999
22 ºC: *tem2* Exp1 vs. 22 ºC: *svp tem2* Exp1	****	<0.0001
22 ºC: *tem2* Exp1 vs. 22 ºC: *svp tem2* Exp2	****	<0.0001
22 ºC: *tem2* Exp2 vs. 22 ºC: *svp tem2* Exp1	****	<0.0001
22 ºC: *tem2* Exp2 vs. 22 ºC: *svp tem2* Exp2	**	0.0027
22 ºC: *tem2* Exp1 vs. 22 ºC: *svp tem1 tem2* Exp1	****	<0.0001
22 ºC: *tem2* Exp1 vs. 22 ºC: *svp tem1 tem2* Exp2	****	<0.0001
22 ºC: *tem2* Exp2 vs. 22 ºC: *svp tem1 tem2* Exp1	***	0.0010
22 ºC: *tem2* Exp2 vs. 22 ºC: *svp tem1 tem2* Exp2	NS	0.1521
22 ºC: *tem1 tem2* Exp1 vs. 22 ºC: *svp* Exp1	NS	> 0.9999
22 ºC: *tem1 tem2* Exp1 vs. 22 ºC: *svp* Exp2	NS	0.7755
22 ºC: *tem1 tem2* Exp2 vs. 22 ºC: *svp* Exp1	NS	> 0.9999
22 ºC: *tem1 tem2* Exp2 vs. 22 ºC: *svp* Exp2	NS	0.9128
22 ºC: *tem1 tem2* Exp1 vs. 22 ºC: *svp tem1* Exp1	NS	> 0.9999
22 ºC: *tem1 tem2* Exp1 vs. 22 ºC: *svp tem1* Exp2	**	0.0022
22 ºC: *tem1 tem2* Exp2 vs. 22 ºC: *svp tem1* Exp1	NS	> 0.9999
22 ºC: *tem1 tem2* Exp2 vs. 22 ºC: *svp tem1* Exp2	**	0.0063
22 ºC: *tem1 tem2* Exp1 vs. 22 ºC: *svp tem2* Exp1	NS	0.9965
22 ºC: *tem1 tem2* Exp1 vs. 22 ºC: *svp tem2* Exp2	NS	> 0.9999
22 ºC: *tem1 tem2* Exp2 vs. 22 ºC: *svp tem2* Exp1	NS	0.9843
22 ºC: *tem1 tem2* Exp2 vs. 22 ºC: *svp tem2* Exp2	NS	> 0.9999
22 ºC: *tem1 tem2* Exp1 vs. 22 ºC: *svp tem1 tem2* Exp1	NS	> 0.9999
22 ºC: *tem1 tem2* Exp1 vs. 22 ºC: *svp tem1 tem2* Exp2	NS	> 0.9999
22 ºC: *tem1 tem2* Exp2 vs. 22 ºC: *svp tem1 tem2* Exp1	NS	> 0.9999
22 ºC: *tem1 tem2* Exp2 vs. 22 ºC: *svp tem1 tem2* Exp2	NS	> 0.9999
22 ºC: *svp* Exp1 vs. 22 ºC: *svp tem1* Exp1	NS	> 0.9999
22 ºC: *svp* Exp1 vs. 22 ºC: *svp tem1* Exp2	NS	0.4027
22 ºC: *svp* Exp2 vs. 22 ºC: *svp tem1* Exp1	NS	0.9995
22 ºC: *svp* Exp2 vs. 22 ºC: *svp tem1* Exp2	NS	0.9939
22 ºC: *svp* Exp1 vs. 22 ºC: *svp tem2* Exp1	NS	0.2779
22 ºC: *svp* Exp1 vs. 22 ºC: *svp tem2* Exp2	NS	0.9861
22 ºC: *svp* Exp2 vs. 22 ºC: *svp tem2* Exp1	**	0.0067
22 ºC: *svp* Exp2 vs. 22 ºC: *svp tem2* Exp2	NS	0.2904
22 ºC: *svp* Exp1 vs. 22 ºC: *svp tem1 tem2* Exp1	NS	0.8683
22 ºC: *svp* Exp1 vs. 22 ºC: *svp tem1 tem2* Exp2	NS	> 0.9999
22 ºC: *svp* Exp2 vs. 22 ºC: *svp tem1 tem2* Exp1	NS	0.1256
22 ºC: *svp* Exp2 vs. 22 ºC: *svp tem1 tem2* Exp2	NS	0.9696
22 ºC: *svp tem1* Exp1 vs. 22 ºC: *svp tem1 tem2* Exp1	NS	0.9780
22 ºC: *svp tem1* Exp1 vs. 22 ºC: *svp tem1 tem2* Exp2	NS	> 0.9999

22 ºC: *svp tem1* Exp2 vs. 22 ºC: *svp tem1 tem2* Exp1	****	<0.0001
22 ºC: *svp tem1* Exp2 vs. 22 ºC: *svp tem1 tem2* Exp2	**	0.0079
22 ºC: *svp tem2* Exp1 vs. 22 ºC: *svp tem1 tem2* Exp1	NS	> 0.9999
22 ºC: *svp tem2* Exp1 vs. 22 ºC: *svp tem1 tem2* Exp2	NS	0.8026
22 ºC: *svp tem2* Exp2 vs. 22 ºC: *svp tem1 tem2* Exp1	NS	> 0.9999
22 ºC: *svp tem2* Exp2 vs. 22 ºC: *svp tem1 tem2* Exp2	NS	> 0.9999
16 ºC: Col-0 Exp1 vs. 16 ºC: *tem1* Exp1	****	<0.0001
16 ºC: Col-0 Exp1 vs. 16 ºC: *tem1* Exp2	****	<0.0001
16 ºC: Col-0 Exp2 vs. 16 ºC: *tem1* Exp1	****	<0.0001
16 ºC: Col-0 Exp2 vs. 16 ºC: *tem1* Exp2	****	<0.0001
16 ºC: Col-0 Exp1 vs. 16 ºC: *tem2* Exp1	****	<0.0001
16 ºC: Col-0 Exp1 vs. 16 ºC: *tem2* Exp2	****	<0.0001
16 ºC: Col-0 Exp2 vs. 16 ºC: *tem2* Exp1	****	<0.0001
16 ºC: Col-0 Exp2 vs. 16 ºC: *tem2* Exp2	****	<0.0001
16 ºC: Col-0 Exp1 vs. 16 ºC: *tem1 tem2* Exp1	****	<0.0001
16 ºC: Col-0 Exp1 vs. 16 ºC: *tem1 tem2* Exp2	****	<0.0001
16 ºC: Col-0 Exp2 vs. 16 ºC: *tem1 tem2* Exp1	****	<0.0001
16 ºC: Col-0 Exp2 vs. 16 ºC: *tem1 tem2* Exp2	****	<0.0001
16 ºC: Col-0 Exp1 vs. 16 ºC: *svp* Exp1	****	<0.0001
16 ºC: Col-0 Exp1 vs. 16 ºC: *svp* Exp2	****	<0.0001
16 ºC: Col-0 Exp2 vs. 16 ºC: *svp* Exp1	****	<0.0001
16 ºC: Col-0 Exp2 vs. 16 ºC: *svp* Exp2	****	<0.0001
16 ºC: Col-0 Exp1 vs. 16 ºC: *svp tem1* Exp1	****	<0.0001
16 ºC: Col-0 Exp1 vs. 16 ºC: *svp tem1* Exp2	****	<0.0001
16 ºC: Col-0 Exp2 vs. 16 ºC: *svp tem1* Exp1	****	<0.0001
16 ºC: Col-0 Exp2 vs. 16 ºC: *svp tem1* Exp2	****	<0.0001
16 ºC: Col-0 Exp1 vs. 16 ºC: *svp tem2* Exp1	****	<0.0001
16 ºC: Col-0 Exp1 vs. 16 ºC: *svp tem2* Exp2	****	<0.0001
16 ºC: Col-0 Exp2 vs. 16 ºC: *svp tem2* Exp1	****	<0.0001
16 ºC: Col-0 Exp2 vs. 16 ºC: *svp tem2* Exp2	****	<0.0001
16 ºC: Col-0 Exp1 vs. 16 ºC: *svp tem1 tem2* Exp1	****	<0.0001
16 ºC: Col-0 Exp1 vs. 16 ºC: *svp tem1 tem2* Exp2	****	<0.0001
16 ºC: Col-0 Exp2 vs. 16 ºC: *svp tem1 tem2* Exp1	****	<0.0001
16 ºC: Col-0 Exp2 vs. 16 ºC: *svp tem1 tem2* Exp2	****	<0.0001
16 ºC: *tem1* Exp1 vs. 16 ºC: *svp* Exp1	****	<0.0001
16 ºC: *tem1* Exp1 vs. 16 ºC: *svp* Exp2	****	<0.0001
16 ºC: *tem1* Exp2 vs. 16 ºC: *svp* Exp1	****	<0.0001
16 ºC: *tem1* Exp2 vs. 16 ºC: *svp* Exp2	****	<0.0001
16 ºC: *tem2* Exp1 vs. 16 ºC: *svp* Exp1	****	<0.0001
16 ºC: *tem2* Exp1 vs. 16 ºC: *svp* Exp2	****	<0.0001
16 ºC: *tem2* Exp2 vs. 16 ºC: *svp* Exp1	****	<0.0001
16 ºC: *tem2* Exp2 vs. 16 ºC: *svp* Exp2	****	<0.0001
16 ºC: *tem2* Exp1 vs. 16 ºC: *svp tem1* Exp1	****	<0.0001
16 ºC: *tem2* Exp1 vs. 16 ºC: *svp tem1* Exp2	****	<0.0001
16 ºC: *tem2* Exp2 vs. 16 ºC: *svp tem1* Exp1	****	<0.0001
16 ºC: *tem2* Exp2 vs. 16 ºC: *svp tem1* Exp2	****	<0.0001
16 ºC: *tem2* Exp1 vs. 16 ºC: *svp tem2* Exp1	****	<0.0001
16 ºC: *tem2* Exp1 vs. 16 ºC: *svp tem2* Exp2	****	<0.0001

16 ºC: *tem2* Exp2 vs. 16 ºC: *svp tem2* Exp1	****	<0.0001
16 ºC: *tem2* Exp2 vs. 16 ºC: *svp tem2* Exp2	****	<0.0001
16 ºC: *tem2* Exp1 vs. 16 ºC: *svp tem1 tem2* Exp1	****	<0.0001
16 ºC: *tem2* Exp1 vs. 16 ºC: *svp tem1 tem2* Exp2	****	<0.0001
16 ºC: *tem2* Exp2 vs. 16 ºC: *svp tem1 tem2* Exp1	****	<0.0001
16 ºC: *tem2* Exp2 vs. 16 ºC: *svp tem1 tem2* Exp2	****	<0.0001
16 ºC: *tem1 tem2* Exp1 vs. 16 ºC: *svp* Exp1	****	<0.0001
16 ºC: *tem1 tem2* Exp1 vs. 16 ºC: *svp* Exp2	****	<0.0001
16 ºC: *tem1 tem2* Exp2 vs. 16 ºC: *svp* Exp1	NS	0.7056
16 ºC: *tem1 tem2* Exp2 vs. 16 ºC: *svp* Exp2	****	<0.0001
16 ºC: *tem1 tem2* Exp1 vs. 16 ºC: *svp tem1* Exp1	****	<0.0001
16 ºC: *tem1 tem2* Exp1 vs. 16 ºC: *svp tem1* Exp2	****	<0.0001
16 ºC: *tem1 tem2* Exp2 vs. 16 ºC: *svp tem1* Exp1	NS	0.9983
16 ºC: *tem1 tem2* Exp2 vs. 16 ºC: *svp tem1* Exp2	***	0.0002
16 ºC: *tem1 tem2* Exp1 vs. 16 ºC: *svp tem2* Exp1	****	<0.0001
16 ºC: *tem1 tem2* Exp1 vs. 16 ºC: *svp tem2* Exp2	****	<0.0001
16 ºC: *tem1 tem2* Exp2 vs. 16 ºC: *svp tem2* Exp1	****	<0.0001
16 ºC: *tem1 tem2* Exp2 vs. 16 ºC: *svp tem2* Exp2	****	<0.0001
16 ºC: *tem1 tem2* Exp1 vs. 16 ºC: *svp tem1 tem2* Exp1	****	<0.0001
16 ºC: *tem1 tem2* Exp1 vs. 16 ºC: *svp tem1 tem2* Exp2	****	<0.0001
16 ºC: *tem1 tem2* Exp2 vs. 16 ºC: *svp tem1 tem2* Exp1	****	<0.0001
16 ºC: *tem1 tem2* Exp2 vs. 16 ºC: *svp tem1 tem2* Exp2	****	<0.0001
16 ºC: *svp* Exp1 vs. 16 ºC: *svp tem1* Exp1	NS	> 0.9999
16 ºC: *svp* Exp1 vs. 16 ºC: *svp tem1* Exp2	NS	0.8960
16 ºC: *svp* Exp2 vs. 16 ºC: *svp tem1* Exp1	**	0.0032
16 ºC: *svp* Exp2 vs. 16 ºC: *svp tem1* Exp2	NS	> 0.9999
16 ºC: *svp* Exp1 vs. 16 ºC: *svp tem2* Exp1	**	0.0096
16 ºC: *svp* Exp1 vs. 16 ºC: *svp tem2* Exp2	***	0.0005
16 ºC: *svp* Exp2 vs. 16 ºC: *svp tem2* Exp1	NS	> 0.9999
16 ºC: *svp* Exp2 vs. 16 ºC: *svp tem2* Exp2	NS	> 0.9999
16 ºC: *svp* Exp1 vs. 16 ºC: *svp tem1 tem2* Exp1	NS	0.7345
16 ºC: *svp* Exp1 vs. 16 ºC: *svp tem1 tem2* Exp2	***	0.0005
16 ºC: *svp* Exp2 vs. 16 ºC: *svp tem1 tem2* Exp1	NS	> 0.9999
16 ºC: *svp* Exp2 vs. 16 ºC: *svp tem1 tem2* Exp2	NS	> 0.9999
16 ºC: *svp tem1* Exp1 vs. 16 ºC: *svp tem1 tem2* Exp1	NS	0.0639
16 ºC: *svp tem1* Exp1 vs. 16 ºC: *svp tem1 tem2* Exp2	****	<0.0001
16 ºC: *svp tem1* Exp2 vs. 16 ºC: *svp tem1 tem2* Exp1	NS	> 0.9999
16 ºC: *svp tem1* Exp2 vs. 16 ºC: *svp tem1 tem2* Exp2	NS	0.6527
16 ºC: *svp tem2* Exp1 vs. 16 ºC: *svp tem1 tem2* Exp1	NS	0.9938
16 ºC: *svp tem2* Exp1 vs. 16 ºC: *svp tem1 tem2* Exp2	NS	> 0.9999
16 ºC: *svp tem2* Exp2 vs. 16 ºC: *svp tem1 tem2* Exp1	NS	0.8483
16 ºC: *svp tem2* Exp2 vs. 16 ºC: *svp tem1 tem2* Exp2	NS	> 0.9999

**** $p \leq 0.0001$; *** $p \leq 0.001$; ** $p \leq 0.01$; * $p \leq 0.05$; N.S $p > 0.05$

Supplemental Table S3.

Oligonucleotide sequences used for cloning, RT-qPCR and ChIP-qPCR. Lowercase letters denote synthetic oligonucleotide sites for restriction enzymes or in-fusion cloning.

Gene	Primer	Purpose	Sequence (5' to 3')*
TEM1	SP_19	Genotyping	CCGAATTCTCACAAGATGTTGATAATCGCCT
	SP_20		CGGGCGAAATGTCAAATGTGG
TEM2	SP_80	Genotyping	TTACGCCTCTACCGGATGGG
	SP_81		GCTTCTTGGAACACCGTAACGC
SVP	SP_284	Genotyping	GACCCACTAGTTATCAGCTCAG
	SP_285		AAGTTATGCCTCTCTAGGAC
	SP_286		AAGTTATGCCTCTCTAGGTT
UBQ10	SP_190	RT-qPCR	AAATCTCGTCTCTGTTATGCTTAAGAAG
	SP_191		TTTTACATGAAACGAAACATTGAACTT
TEM1	SP_27	RT-qPCR	ATCCACTGGAAAGTCCGGTCTA
	SP_28		GAATAGCCTAACCACAGTCTGAACC
TEM2	SP_29	RT-qPCR	TGGTCCGAGAGAAAACCCG
	SP_30		TCAACTCCGAAAAGCCGAAC
SVP	SP_192	RT-qPCR	GCAACTAACGGAAGAGAACGAG
	SP_193		GAGCTCTCGGAGTCAACAGG
FT	SP_60	RT-qPCR	CCATTGGTTGGTGACTGATATCC
	SP_61		TTGCCAAAGGTTGTTCCAGTT
TSF	SP_90	RT-qPCR	GAGTCCAAGCAACCCTCACCAA
	SP_91		CACAATACGATGAATTCCCGAG
SVP	JH2934	Cloning	ggatccATGGCGAGAGAAAAGATTC
	JH2935		ggatccACCACCATACGGTAAGCCG
	JH7917		tctagaggatctcgagTCGTAGAACACAAACGCAAACCA
	JH7918		ctctcgccatggatccCACAACGAACAAAAAAACCCTAGAA
FT	SP_450	ChIP-qPCR	GTTATGATTTCACCGACCCG
	SP_445		GATCCAAGCCATTAGTCACC
TSF	SP_686	ChIP-qPCR	TGGCTAGCAAGAAACAAGTGG
	SP_687		ACCAGGGTCTTTTCGTGTATAGT
FT	SP_778	ChIP-qPCR NC	GTGGCGGACAATCCATCTAT
	SP_779	ChIP-qPCR NC	AAATATTGGACAGGAGAGCTCAG
TSF	SP_776	ChIP-qPCR NC	TGCCAAGCATACGTCCATAG
	SP_777	ChIP-qPCR NC	TTTGGCAGCATGTACGATTT
TEM1	JH9425	ChIP-qPCR	TTCTACGTACAAAGAAAGTGCTTAGGG
	JH9426		TCCATATTTGGAACATGACGTG
	JH9427		ATGAAGGGACTAATTATGGCAACA
	JH9428		AAGTTTCGTGGGAAGAGTCCA
	JH9429		CGGTTCAGACTGTGGTTAGGC
	JH9430		AATCGCCTGCTTCTTGGAAC
TEM2	JH9431	ChIP-qPCR	AATTGCTTCAAAGGGGGATG
	JH9432		GGTTACATGTTCATGGTAAATGTGG
	JH9433		GAAAATGTTCTTACGCCGTTGA
	JH9434		ACGCTTTCAAGAACGGCAAA
	JH9435		TTGCGTTACGGTGTTCCAAG
	JH9436		CAACCTAGCATGAATCACAACCT
GA3OX1	SP_228	ChIP-qPCR	AGGAGAAGGAGCAGCGGAGAAGAGGAG
	SP_229		CATCCCATTCACCTCCCACACTCTCACATAC

CAPÍTULO III: TEMPRANILLO reveals the mesophyll as crucial for epidermal trichome formation.

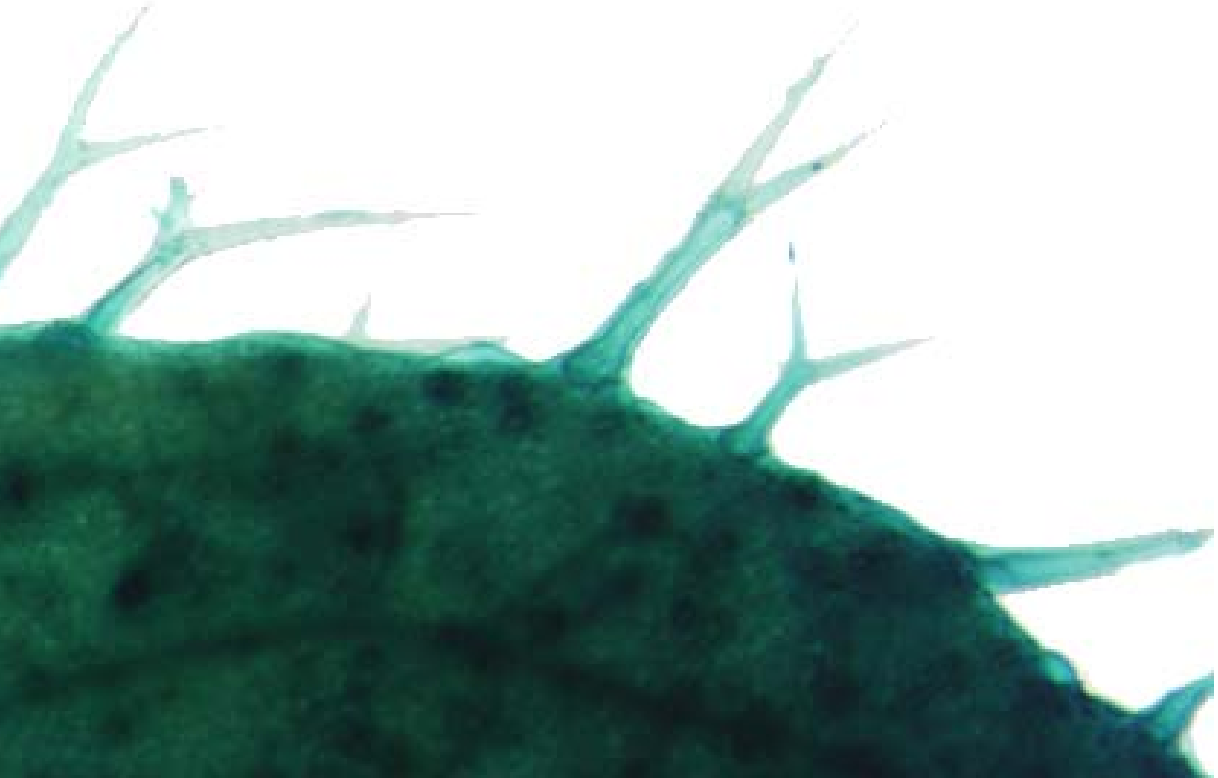

TEMPRANILLO Reveals the Mesophyll as Crucial for Epidermal Trichome Formation[1][OPEN]

Luis Matías-Hernández, Andrea E. Aguilar-Jaramillo, Michela Osnato, Roy Weinstain, Eilon Shani, Paula Suárez-López, and Soraya Pelaz*

Centre for Research in Agricultural Genomics, CSIC-IRTA-UAB-UB, Campus UAB, Bellaterra (Cerdanyola del Vallès) 08193 Barcelona, Spain (L.M.-H., A.E.A.-J., M.O., P.S.-L., S.P.); ICREA (Institució Catalana de Recerca i Estudis Avançats), Barcelona, Spain (S.P.); and Department of Molecular Biology and Ecology of Plants, Faculty of Life Sciences, Tel Aviv University, 39040, Tel Aviv, Israel (R.W., E.S.)

ORCID IDs: 0000-0001-5626-9576 (L.M.-H.); 0000-0002-1300-6802 (R.W.); 0000-0001-5748-9263 (P.S.-L.); 0000-0001-7699-9330 (S.P.).

Plant trichomes are defensive specialized epidermal cells. In all accepted models, the epidermis is the layer involved in trichome formation, a process controlled by gibberellins (GAs) in Arabidopsis rosette leaves. Indeed, GA activates a genetic cascade in the epidermis for trichome initiation. Here we report that *TEMPRANILLO* (TEM) genes negatively control trichome initiation not only from the epidermis but also from the leaf layer underneath the epidermis, the mesophyll. Plants over-expressing or reducing TEM specifically in the mesophyll, display lower or higher trichome numbers, respectively. We surprisingly found that fluorescently labeled GA_3 accumulates exclusively in the mesophyll of leaves, but not in the epidermis, and that TEM reduces its accumulation and the expression of several newly identified GA transporters. This strongly suggests that TEM plays an essential role, not only in GA biosynthesis, but also in regulating GA distribution in the mesophyll, which in turn directs epidermal trichome formation. Moreover, we show that TEM also acts as a link between GA and cytokinin signaling in the epidermis by negatively regulating downstream genes of both trichome formation pathways. Overall, these results call for a re-evaluation of the present theories of trichome formation as they reveal mesophyll essential during epidermal trichome initiation.

Trichomes are epidermal cell protrusions present in most of the vascular plants surfaces that defend the plant against insect herbivores, UV light, and water loss (Traw and Bergelson, 2003; Olsson et al., 2009). Many plant species respond to insect damage by increasing the density and/or number of trichomes on new leaves (Traw and Bergelson, 2003). In Arabidopsis, leaf trichomes are unicellular structures, whose development has been used as a model for addressing crucial questions in plant biology such as control of cell fate specification and differentiation as well as plant defense mechanisms (Traw and Bergelson, 2003; Olsson et al., 2009; Hülskamp, 2004; Gilding and Marks, 2010). Once an epidermal cell precursor is specified to enter the trichome pathway, an elaborated and well-regulated morphogenetic cell transformation occurs in order for it to become a trichome (Gilding and Marks, 2010). First, radial cell expansion occurs centered on the external face of the epidermal trichome precursor that develops into an elongated stalk (Szymanski et al., 1998). Then, cell expansion on the stalk produces branch initiation and growth. Finally, once trichome expansion is complete, the cell wall gets thicker and many papillae form on the outer surface of the trichome, resulting in a mature trichome (Gilding and Marks, 2010).

Trichome proliferation and development process involves diverse genes at different regulatory pathways (Payne et al., 2000; Bernhardt et al., 2005). These include a multimeric complex formed by the R2R3 MYB GLABROUS1 (GL1); two redundant trichome formation bHLH proteins, GLABRA3 (GL3) and ENHANCER OF GLABRA3 (EGL3); and a WD-40 repeat containing protein TRANSPARENT TESTA GLABROUS1 (TTG1) (Bernhardt et al., 2005). Mutations in GL1, TTG1, and both GL3 and EGL3, result in a significant loss of trichomes per leaf (Payne et al., 2000; Bernhardt et al., 2005). This complex has a role not only in trichome initiation but also in later stages of trichome development, because mutations lead to smaller and less-branched trichomes (Payne et al., 2000). Furthermore, hormones play an important role in trichome initiation by controlling essential

[1] This work was supported by a MINECO/FEDER grant (no. BFU2012-33746). The funder had no role in study design, data collection and analysis, decision to publish, or preparation of the manuscript.

* Address correspondence to soraya.pelaz@cragenomica.es.

The author responsible for distribution of materials integral to the findings presented in this article in accordance with the policy described in the Instructions for Authors (www.plantphysiol.org) is: Soraya Pelaz (soraya.pelaz@cragenomica.es).

L.M.-H., P.S.-L., and S.P. conceived, designed, and discussed the experiments; L.M.-H. is the main contributor to the experimental part of this manuscript; A.E.A.-J. and M.O. performed some of the experiments; R.W. and E.S. provided GA-Fl and helped with the manuscript; and L.M.-H., P.S.-L., and S.P. wrote the manuscript. The work was performed in the group of S.P., who supervised the research and the writing of the manuscript.

[OPEN] Articles can be viewed without a subscription.

www.plantphysiol.org/cgi/doi/10.1104/pp.15.01309

downstream genes (Schellmann et al., 2002; Gan et al., 2006; Zhao et al., 2008a). In particular, gibberellins (GAs) and cytokinins (CK) overlap in stimulating this process (Nemhauser et al., 2006; Gan et al., 2007; D'Aloia et al., 2011). GAs are required in the epidermis for trichome proliferation in rosette leaves, stem, and inflorescences (Chien and Sussex, 1996; Perazza et al., 1998; An et al., 2012), while CK action is limited to trichome initiation in upper inflorescence organs, including cauline leaves, stems, and sepals (Gan et al., 2007). The GA-dependent pathway acts partially through GLABROUS INFLORESCENCE STEMS (GIS), a C2H2 transcription factor, which positively regulates the trichome activation complex formed by GL1, GL3, EGL3, and TTG1 in the epidermis (Payne et al., 2000; Zhao et al., 2008a). Furthermore, within the CK-dependent pathway, trichome production control requires two C2H2 transcription factors, GLABROUS INFLORESCENCE STEMS2 (GIS2) and ZINC FINGER PROTEIN8 (ZFP8) (Gan et al., 2007). Both genes, ZFP8 and GIS2, are similarly expressed at early stages of inflorescence development but differentially expressed in inflorescence organs (Gan et al., 2007). Mutations in ZFP8 display a reduction in trichome density on the upper cauline leaves and branches, but not in vegetative organs; while mutations in GIS2 give rise to trichome reduction mainly in flowers (Gan et al., 2007). Similarly to GIS, GIS2, and ZFP8 also mediate the regulation of trichome initiation by GA; however, GIS does not play a significant role in CK response (Gan et al., 2007). Therefore, GIS, GIS2, and ZFP8 play partially redundant roles in inflorescence trichome initiation, and integration of CK and GA requires the action of all these genes.

In Arabidopsis, both epidermal GA- and CK-dependent trichome regulatory pathways converge on the activation of *GLABROUS2* (GL2), considered as the universal promoter of trichome initiation (Szymanski et al., 1998; Lin and Aoyama, 2012). GL2 is a homeodomain transcription factor required for trichome formation as well as for subsequent trichome morphogenesis phases such as cell expansion, branching, and maturation of trichome cell wall (Szymanski et al., 1998). Indeed, GL2 expression profile shows spatio-temporal variation either in leaves and trichomes. GL2 is strongly expressed in developing trichomes and surrounding cells; however, its expression persists but decreases in mature trichomes (Szymanski et al., 1998).

TEM1 and TEM2 transcription factors, two proteins belonging to the small plant-specific RELATED TO ABI3 AND VP1 (RAV) family, have been previously identified as repressors of floral induction (Castillejo and Pelaz, 2008; Osnato et al., 2012). TEM1 and TEM2 act redundantly to negatively control floral induction by controlling and integrating both the photoperiod and GA signaling pathways during long days and short days (Castillejo and Pelaz, 2008; Osnato et al., 2012). As other transcription factors, it has been suggested that these may control different biological aspects during plant development (Matías-Hernández et al., 2014). Here we report that TEM gene products play pivotal roles during the repression of another developmental process: trichome initiation. TEM1 and TEM2 directly repress trichome initiation by controlling GA accumulation and distribution in the leaf mesophyll as well as by integrating both GA- and CK-dependent regulatory pathways in the epidermis.

RESULTS

TEM1 and TEM2 Repress Trichome Initiation in Leaves and Inflorescences

TEM proteins belong to the unique RAV transcription factor family, characterized by the presence of two different DNA-binding domains, an AP2 and a B3 domain (Riechmann et al., 2000; Matías-Hernández et al., 2014). Since TEM*1* and TEM*2* are consistently expressed in diverse but specific plant tissues and at diverse moments during Arabidopsis development (Castillejo and Pelaz, 2008; Osnato et al., 2012), it has been suggested that TEM may control other plant developmental processes (Matías-Hernández et al., 2014). To investigate possible contributions of TEM toward additional biological processes, phenotypical analyses of diverse TEM loss of function and gain of function were performed. As results show, it was clearly observed that the different mutants and over-expressors analyzed were defected in trichome initiation number and density (Fig. 1, A to G, Supplemental Fig. 1, and Supplemental Table S1). Although *tem1-1* mutant did not show a clear trichome phenotype, single *tem2-2* mutants produced more trichomes in rosette leaves than wild-type plants (Fig. 1G). This effect was stronger in *tem1-1 tem2-2* and in a previously characterized RNA_i lines that partially silence both TEM genes (Castillejo and Pelaz, 2008), not only in rosette leaves, but also in inflorescences (Fig. 1, A, D, and G, and Supplemental Fig. S1). In contrast, TEM*1* and TEM*2* over-expressors (*P35S:*TEM*1*, *P35S:*TEM*2*) showed almost glabrous leaves, stems, and flowers (Fig. 1, C, F, and G, Supplemental Fig. S1, and Supplemental Table S1). Taken together, these data indicate that, similarly to the effect on floral induction, TEM1 and TEM2 act redundantly to repress trichome initiation. In addition, GUS expression analyses using *P*TEM*1:GUS* and *P*TEM*2:GUS* reporter lines were conducted. The expression of the β-glucuronidase gene driven by the promoters of TEM*1* (Castillejo and Pelaz, 2008) and TEM*2* was clearly detected in both the epidermis and the mesophyll layers of rosette leaves (Supplemental Fig. S2). As expected, GUS activity was also detected in trichomes of rosette leaves at different stages of development (Fig. 1, H and I, and Supplemental Fig. S2) consistent with the effect of TEM*1* and TEM*2* on trichome initiation.

TEM Controls Trichome Initiation by Affecting GA Biosynthesis

TEM transcription factors are known to repress GA biosynthesis during floral induction (Osnato et al.,

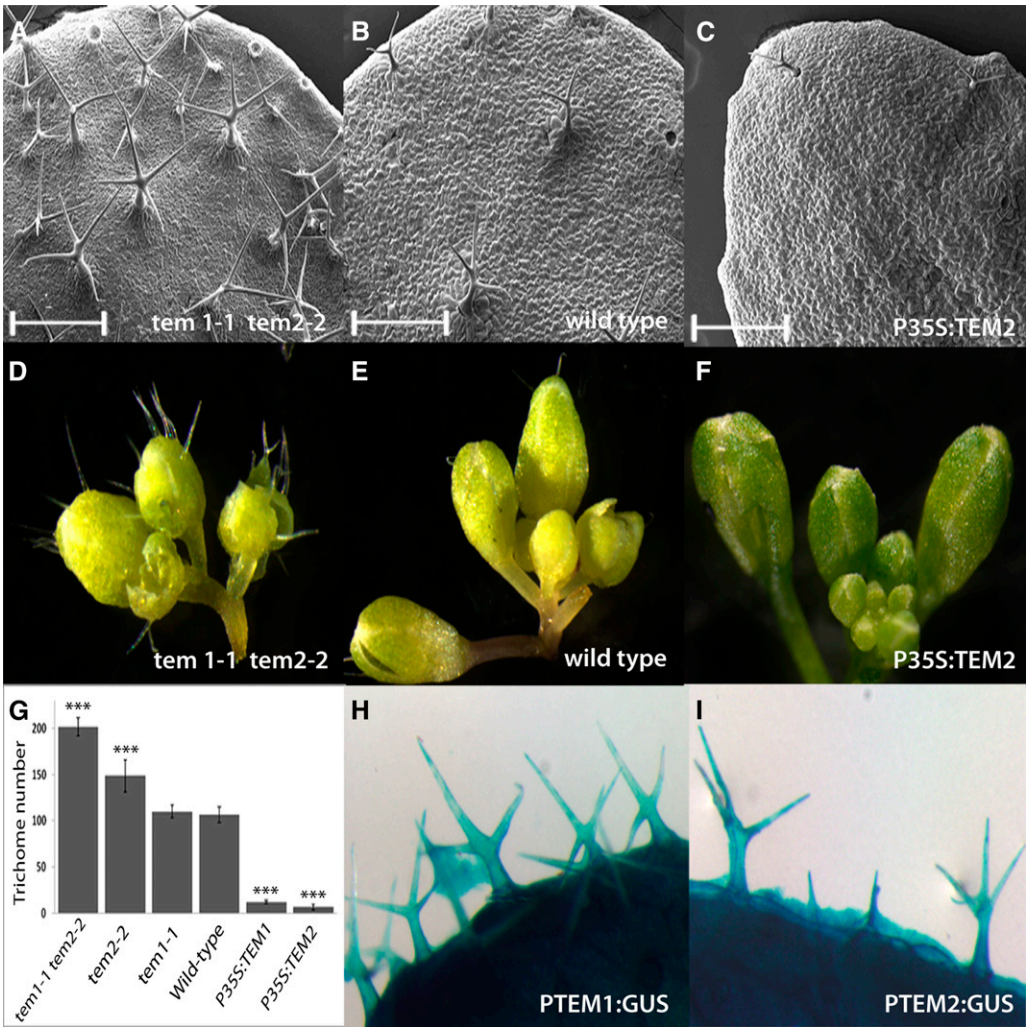

Figure 1. *TEMPRANILLO* affects trichome number. A, B, and C, SEM of *tem1-1 tem2-2* (A), wild-type (B), and *P35S:*TEM*2* rosette leaves (C). Scale bars represent 500 μm (A–C). D, E, and F, Inflorescences of the same genotypes showing sepal trichomes. *tem1-1 tem2-2* shows more trichomes (A and D) than the wild-type (B and E), whereas *P35S:*TEM*2* (C and F) are almost glabrous. G, Trichome number in the 5th-6th rosette leaves of 21 DAG plants of different genetic backgrounds, as indicated. Error bars indicate SD of the mean number of trichomes. Asterisks indicate statistically significant differences (* $P \leq 0.05$, ** $P \leq 0.01$, *** $P \leq 0.001$) obtained using Tukey's range test. H and I, GUS staining of *P*TEM*1:GUS* (H) and *P*TEM*2:GUS* (I) reveals a strong expression of both TEM genes in trichomes. Pictures were taken at same magnification (D–F, H, and I).

2012). TEM1 directly represses the expression of *GIBBERELLIN3 OXIDASE1* [GA*3ox1*) and GA*3ox2* (Osnato et al., 2012)], which encode the enzymes that transform GA_9 to bioactive GA_4 (Mitchum et al., 2006). To further explore whether TEM action affects plant GA biosynthesis, hormone measurements were conducted in Arabidopsis plants collected five days after bolting (DAB). GA_4 was significantly increased in *tem1-1 tem2-2* plants while it decreased in *P35S:*TEM2 (Fig. 2A). On the other hand, inactive GA_9 accumulated in *P35S:* TEM*2* to higher levels than in the wild type, indicating reduced conversion of GA_9 into GA_4 in plants overexpressing TEM*2* (Fig. 2A). GAs are involved in diverse biological processes and these results may suggest that TEM negative control of GA biosynthesis may affect other important processes within the plant development, including trichome proliferation in the epidermis. Indeed, it is known that *ga3ox1-3* and *ga3ox2-1* mutants produce almost undetectable levels of bioactive GA_4 (Mitchum et al., 2006). Accordingly, these mutants displayed fewer trichomes, in number and density, on the adaxial side of rosette leaves than wild-type plants (Fig. 2B and Supplemental Table S1), and when GA is exogenously added, trichome production is restored (Chien and Sussex, 1996; Traw and Bergelson, 2003). Interestingly, the reduction in trichome number was much stronger in *P35S:*TEM*1* and *P35S:*TEM*2* leaves than in *ga3ox1-3 ga3ox2-1* leaves (Fig. 2B); suggesting that TEM affects trichome formation contributing to the control not only of GA biosynthesis but also of other trichome GA-independent pathways.

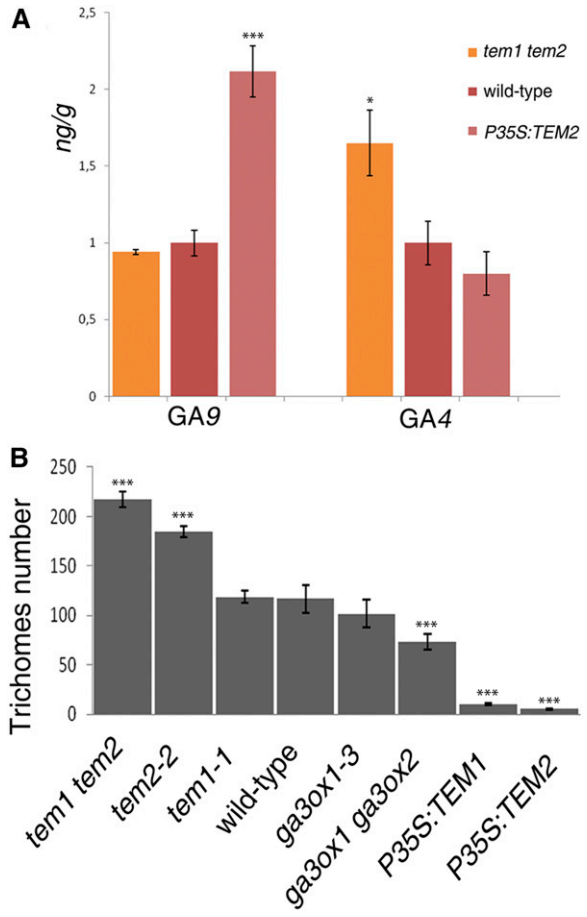

Figure 2. TEMPRANILLO regulates GA biosynthesis and trichome initiation. A, GA hormone measurements in mutants and over-expressors of TEM genes 5 DAB, shown with error bars. B, Trichome number in the 5th-6th rosette leaves in different TEM backgrounds and GA biosynthesis mutants at 21 DAG. Error bars indicate SD of the mean number of trichomes. Asterisks indicate statistically significant differences (* $P \leq 0.05$, ** $P \leq 0.01$, *** $P \leq 0.001$) obtained using Tukey's range test.

Exogenous GA_3-Fl Accumulates Exclusively in the Mesophyll and Is Controlled by TEM

Plants are able to regulate the spatial distribution of their hormones (Wolters and Jürgens, 2009). GA distribution and accumulation are active processes regulated by localized synthesis, transport, and inactivation (Yamaguchi, 2008). GA distribution has been studied in plant roots using a bioactive fluorescent-GA (GA_3-Fl), an in vivo stable fluorescent GA-surrogate that retains similar biological activity to GA_3 (Shani et al., 2013). To address the issue of GA distribution in rosette leaves, we used confocal microscopy following exogenous overnight application of this fluorescently tagged GA. Unexpectedly, results showed that exogenous GA_3-Fl accumulates exclusively in the leaf mesophyll layer (Fig. 3, A and C), distinctly recognizable from epidermal cells by their rounded shape (Deeks and Hussey, 2003; Smith, 2003). In wild-type Arabidopsis rosette leaves, GA_3-Fl accumulated in the mesophyll in a highly specific manner at different stages of development (Fig. 3G and Supplemental Fig. S3). Since GA_3-Fl was applied on top of leaves (adaxial side) as a water solution, in order for it to reach the mesophyll layer, it had to pass through the epidermis. Nevertheless, we found GA_3-Fl mostly in patches that correspond to isolated zones in the mesophyll layer but not in the epidermis (neither adaxial nor abaxial). In only one exceptional case, we observed one stained patch in the adaxial puzzle-shaped epidermal cells, just on top of a mesophyll cell group that showed strong fluorescence (Supplemental Fig. S3). This exception may be due to saturation of the underneath layer. We additionally observed several examples of accumulation in companion cells of the vascular tissue (Supplemental Fig. S3) likely reflecting GA long-distance movement.

TEM transcription factors are known to repress GA biosynthesis during floral induction (Osnato et al., 2012). Therefore, in order to test whether TEM is also capable of controlling GA's accumulation in the mesophyll layer, the distribution of GA_3-Fl in leaves was studied in different TEM mutants and over-expressors lines. In *tem1-1 tem2-2* double mutant plants, GA_3-Fl uptake increased in comparison with wild-type plants, as GA_3-Fl accumulated and was distributed through a much larger area of the leaf (Fig. 3D and Supplemental Fig. S3). The observed GA_3-Fl broader distribution throughout the leaf might be directly related to normal TEM repression of GA biosynthesis in the leaf mesophyll structure and/or due to an effect on GA transport. To further support this, we first cloned an artificial microRNA (amiRNA), previously used for partial silencing of both TEM genes (Osnato et al., 2012), under the mesophyll-specific *CHLOROPHYLL A/B BINDING PROTEIN 3* promoter (PCAB3; Endo et al., 2007; Ranjan et al., 2011). Transgenic plants expressing *amiR*TEM under the mesophyll-specific PCAB3 promoter, showed similar GA_3-Fl accumulation patterns to *tem1-1 tem2-2*. PCAB3:*amiR*TEM leaves displayed a higher GA_3-Fl uptake in the mesophyll in comparison with wild-type leaves (Fig. 3E and Supplemental Fig. S3), while plants over-expressing TEM2 in the mesophyll (PCAB3:TEM2) in *tem1-1 tem2-2* background showed a strong reduction in GA_3-Fl accumulation compared with *tem1-1 tem2-2*, reaching a similar pattern to that of wild-type leaves (Fig. 3H and Supplemental Fig. S3). On the other hand, leaves of PCAB3:TEM2 in wild-type background showed an almost complete absence of fluorescence signal compared with wild-type plants (Fig. 3I and Supplemental Fig. S3). As mentioned, TEM transcription factors are known to repress GA biosynthesis by directly repressing the expression of GA*3ox1* and GA*3ox2* enzymes (Osnato et al., 2012). Therefore, for testing whether the expression or down-regulation of TEM in the mesophyll mimics the effect of *P35S:*TEM and *tem1-1 tem2-2*, respectively; expression analyses of GA*3ox1* and GA*3ox2* in different PCAB3:*amiR*TEM and PCAB3:TEM2 plant lines were conducted. Indeed, results showed that TEM over-expression or silencing exclusively in the mesophyll is enough to affect GA

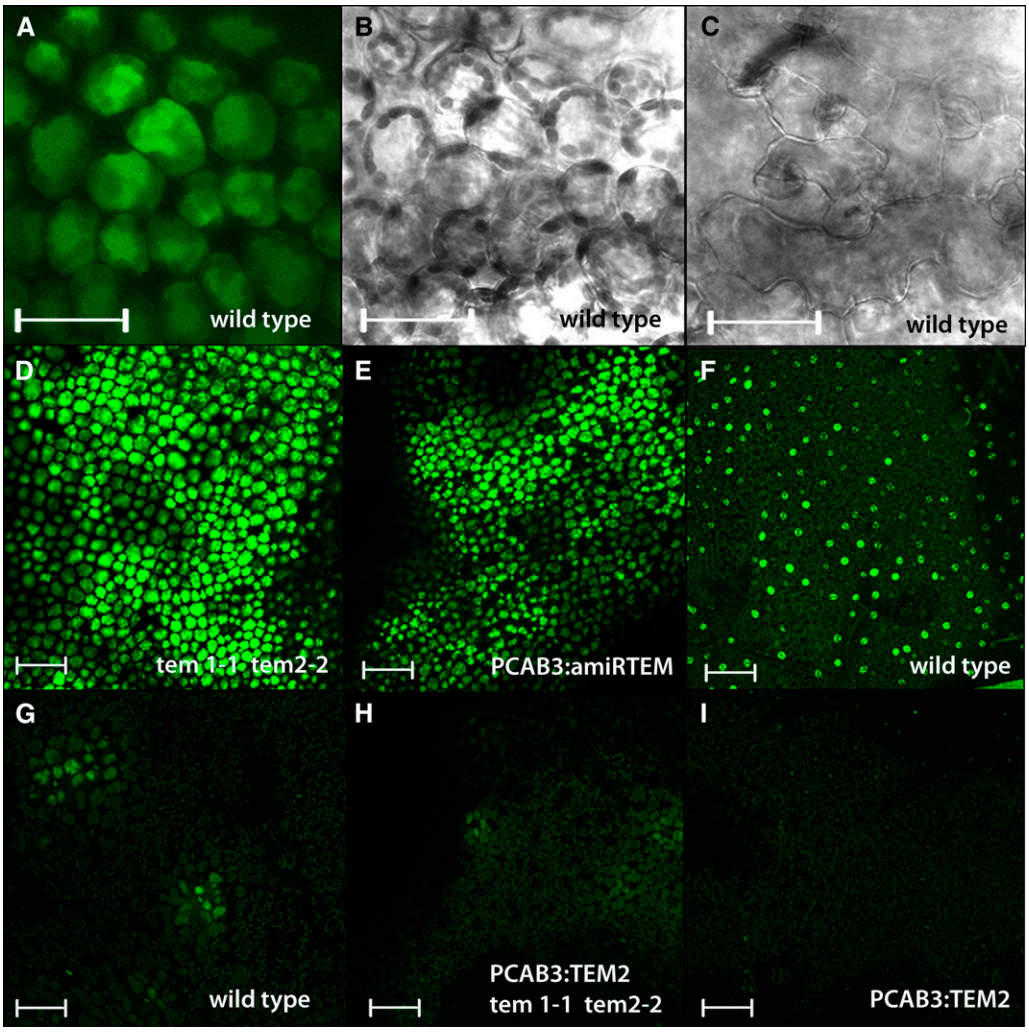

Figure 3. Exogenous GA accumulation in the mesophyll is regulated by *TEMPRANILLO*. A, B, C, D, E, F, G, H, and I, Arabidopsis rosette leaf confocal sections of the first two rosette leaves of 9 DAG plants. A, B, C, GA_3-Fl accumulates exclusively in the mesophyll (A, B) while not in the epidermis (C) of 9 DAG plants. B, C, Images taken in bright field. D, E, GA_3-Fl accumulates with a higher intensity compared with wild type (G) and it is distributed in a much bigger area in the mesophyll of *tem1-1 tem2-2* (D), and PCAB3*:amiR*TEM (E) rosette leaf of 9 DAG plants. (F) Exogenous Fl used as a negative control only accumulates in the epidermal stomas but not in the mesophyll. G, H, I, GA_3-Fl accumulation in wild type (G), PCAB3*:*TEM*2 tem1-1 tem2-2* (H), and PCAB3*:* TEM*2* (I) mesophyll of 9 DAG rosette leaves. Scale bars from (A to C) represent 50 μm and from (D to I) represent 100 μm.

biosynthesis by affecting these GA biosynthetic enzymes (Fig. 4A).

Thus, GA_3-Fl uptake in the leaf seems to be a dynamic and well-regulated process that results in specific accumulation in the mesophyll layer, similarly to its accumulation in root endodermal cells (Shani et al., 2013). This GA_3-Fl accumulation pattern may reflect the endogenous GA accumulation as it retains similar biological activities in roots (Shani et al., 2013). Thus, this unique accumulation pattern, at least partially controlled by TEM, suggests that GA can move not only over long distances but also locally among neighboring cells. Interestingly, this GA's accumulation and movement in the mesophyll layer could affect biological processes occurring at other leaf layers, including trichome proliferation in the epidermis.

TEM Affects Palisade Mesophyll Development and GA Transport in the Rosette Leaves

In order to investigate why the GA_3-Fl uptake to the mesophyll was higher in *tem* mutants and reduced in TEM over-expressors plants, we analyzed the mesophyll structure of *tem1-1 tem2-2* double mutants and TEM*2* over-expressors. Morphological analysis of the mesophyll structure was carried out in the first pair of leaves of 21-day-old Arabidopsis plants. At this stage, the leaf is fully expanded and does not exhibit any evidence of senescence. *tem1-1 tem2-2* rosette leaves displayed mesophyll cells with an apparent increased size (Fig. 4, B and E). In contrast, mesophyll cells were smaller in *P35S:*TEM*2* (Fig. 4, D and G) than in wild types (Fig. 4, C and E). Consequently, these palisade

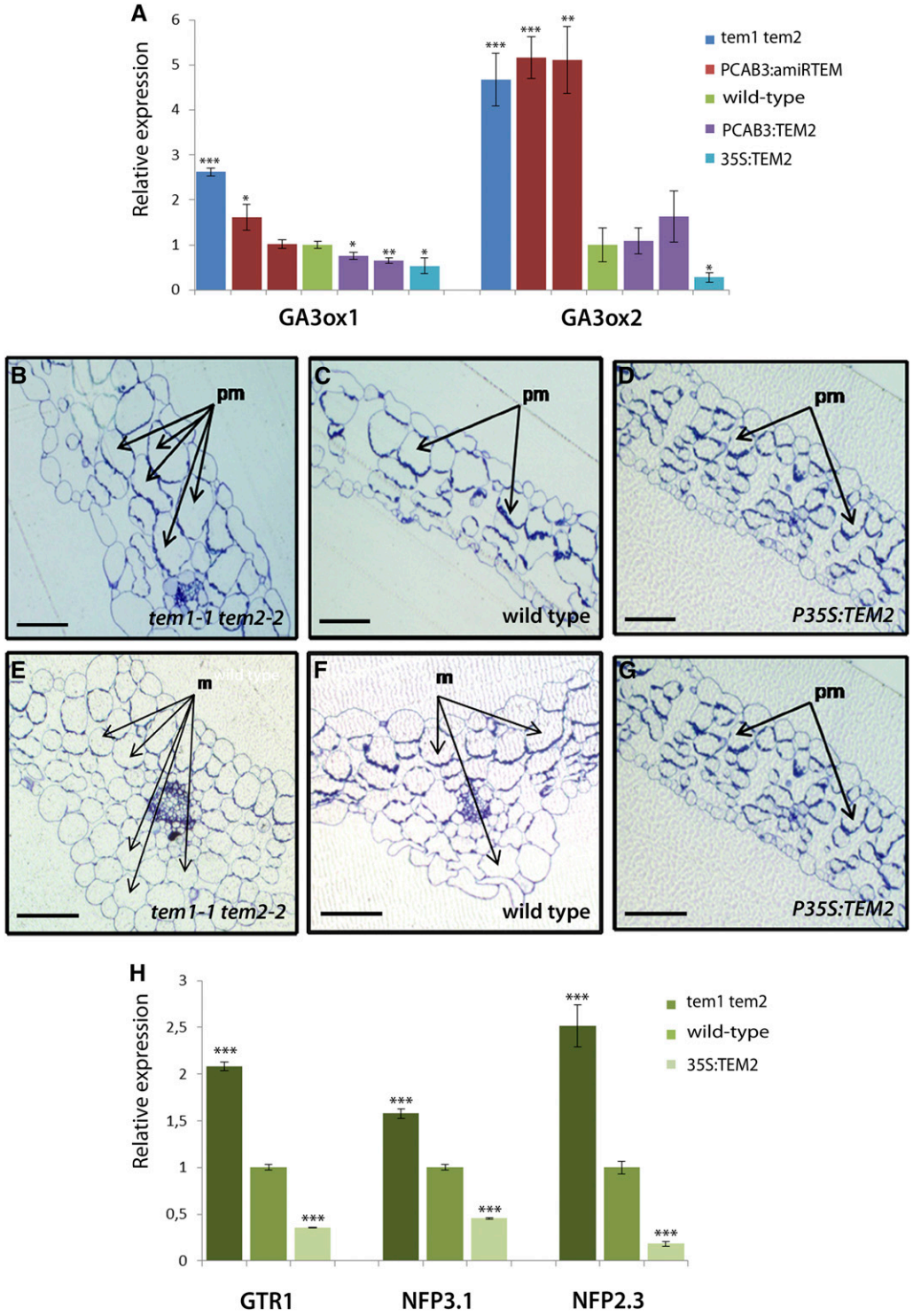

Figure 4. *TEMPRANILLO* controls leaf mesophyll morphology and GA accumulation in the mesophyll. A, Expression analysis of GA biosynthesis enzymes GA*3ox1* and *GA3ox2* in *tem1 tem2, PCAB:amiR*TEM, wild-type, *PCAB·:*TEM*2* and *P35S:*TEM*2* seedlings at 11 DAG grown under LD. Two independent lines over-expressing (PCAB3*:* TEM*2.1* and PCAB3*:* TEM*2.2*)and partially silencing TEM specifically in the mesophyll *(*PCAB3*:amiR*TEM*13.3* and PCAB3*:amiR*TEM*10.2*) were included in the expression analyses. B, C, D, E, F, and G, Arabidopsis leaf cross sections. B, C, D, Leaf cross sections of *tem1-1 tem2-2* (B), wild type (C), and *P35S:*TEM*2* (D) in 11 DAG plants. E, F, G, central leaf cross sections of *tem1-1 tem2-2* (E), wild type (F), and *P35S:*TEM*2* (G) in 11 DAG plants. Cross sections show the central area of the rosette leaf including the main vascular bundle. pm, palisade mesophyll cells; m, mesophyll cells. Scale bars represent 100 μm. (H) Relative expression of different NPF transporter genes in TEM mutants

mesophyll defects in both *tem1-1 tem2-2* and *P35S:*TEM plants may imply a primary role for TEM genes in rosette leaf development.

Not only GA biosynthesis (Osnato et al., 2012) but also GA mesophyll accumulation and distribution seem to be controlled by TEM. GA_3-Fl uptake in the mesophyll of rosette leaves in *tem1-1 tem2-2* mutants increased and it was distributed throughout a larger leaf area in comparison with wild-type plants. However, morphological analysis *tem1-1 tem2-2* of mesophyll structure showed that these mutant rosette leaves displayed mesophyll cells with an increased size. In order to exclude the possibility that the accumulation of GA_3-Fl in *tem1-1 tem2-2* mesophyll cells was higher due only to the alteration in the leaf morphology, further analyses were conducted.

Plant hormones are active in plant tissues at very low concentration; therefore the synthesis, transport and signaling of hormones are precisely controlled processes (Chiba et al., 2015). Recent studies suggest that GA movement and distribution might be regulated by a group of GA transporters (Chiba et al., 2015; Saito et al., 2015). The NITRATE TRANSPORTER 1/PEPTIDE TRANSPORTER FAMILY (NPF) is a family of proteins initially identified as nitrate or peptide transporters (Tsay et al., 2007; Léran et al., 2014), and was later found to also transport hormones such as auxin and abcisic acid (Krouk et al., 2010; Kanno et al., 2012). It was recently reported that some members of this NPF family were also efficient transporters of GA and/or Jasmonic acid (Chiba et al., 2015; Saito et al., 2015). Therefore, we investigated the expression of several NPF transporters reported to show yeast-based GA transport function (Chiba et al., 2015; Saito et al., 2015) under TEM genetic manipulation. We first applied in silico analysis to observe that the chosen NPF genes were expressed in the rosette leaf mesophyll (Arabidopsis eFP Browser 2.0). Interestingly, the expression levels of NPF*2.3*, NPF*2.10*, and NPF*3.1* were clearly down-regulated by TEM in 11-day-old plants (Fig. 4H). This data strongly suggests that TEM seems to affect GA accumulation and distribution in the mesophyll cells by modulating the expression of specific GA transporters, which at the same time would affect the GA transport toward neighboring epidermal cells.

TEM Reveals the Mesophyll as a Layer Controlling Trichome Initiation

For unraveling whether the role of TEM in controlling GA accumulation in the mesophyll layer affects epidermal trichome initiation, transgenic plants expressing TEM*1* and TEM*2* under the mesophyll-specific *CAB3* promoter were analyzed. Surprisingly, we found that plants over-expressing either TEM*1* or TEM*2* in the mesophyll (PCAB3*:*TEM), which had reduced GA_3-Fl accumulation, showed a strong reduction in trichome number and density, behaving almost as TEM over-expressors (Fig. 5A and Supplemental Table S1).

Moreover, specific TEM expression in the mesophyll of *tem1 tem2* mutants, PCAB3*:*TEM *tem1-1 tem2-2*, restored *tem1-1 tem2-2* trichome number to the wild-type level (Fig. 5B). These results led us to propose that TEM-specific mesophyll expression might be sufficient for formation of a normal trichome number. To further support this, PCAB3*:amiR*TEM lines were analyzed. As expected, PCAB3*:amiR*TEM lines showed an increased production of trichomes, resulting in hairier leaves with normal epidermal cells (Fig. 5C, Supplemental Fig. S4 and Supplemental Table S1). Therefore, these data provide robust and independent evidence that specific mesophyll over-expression or silencing of TEM genes is enough to affect trichome development, indicating that TEM mesophyll expression is necessary and sufficient for normal trichome initiation. This strongly supports that not only the epidermis but also the mesophyll layer is essential to direct epidermal trichome initiation during early stages of development, where a bigger palisade mesophyll cell would promote increased trichome production, while smaller cells would result in reduced number of trichomes.

According to this rationale, mutants that specifically affect the mesophyll layer should exhibit altered trichome numbers. Therefore, we studied the number of trichomes per leaf of two mutants, *CHLOROPHYLL A/B-BINDING PROTEIN-UNDEREXPRESSED1-1* mutant (cue1-6) and cab3-1, which display defects only in the leaf mesophyll but not in the epidermis (Li et al., 1995; Lundquist et al., 2014). We found that both mutants showed a significant reduction in the number and density of trichomes resembling pCAB3*:*TEM plants (Fig. 5D and Supplemental Table S1); strongly supporting the mesophyll as an essential layer that control epidermal trichome initiation.

TEM Integrates GA- and CK-Dependent Trichome Pathways in the Epidermis

As expected, when exogenous GA is added, trichome production of PCAB3*:*TEM*2* leaves is restored to wild-type level, yet, it was only partially restored in *P35S:* TEM*2* leaves (Fig. 6A and Supplemental Table S1), suggesting that TEM control additional epidermal GA-independent genes involved in trichome initiation. Similar results were obtained when plants were treated exogenously with GA_3-Fl at similar concentrations (Fig. 6B and Supplemental Table S1), showing that GA_3-Fl retains similar bioactivity than GA_3 for trichome induction.

Furthermore, integration of hormone signaling is essential for many processes in plant development (Gan

Figure 4. (*Continued.*)
and over-expressors 11 DAG. One representative of three biological replicates is shown with error bars of three qPCR replicates. Asterisks indicate statistically significant differences (* $P \leq 0.05$, ** $P \leq 0.01$, *** $P \leq 0.001$) obtained using Student's *t* test.

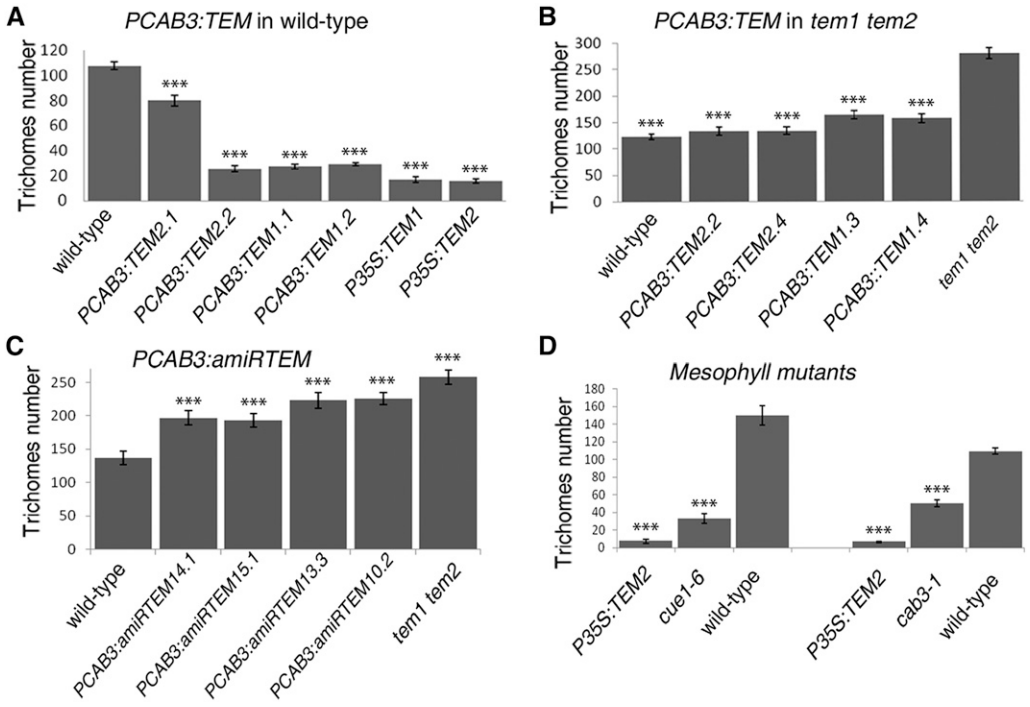

Figure 5. *TEMPRANILLO* controls trichome initiation from the mesophyll. A, B, and C, Trichome average number in the 5th-6th rosette leaves of 21 DAG plants of different independent lines over-expressing TEM specifically in the mesophyll in wild-type (A) and *tem1-1 tem2-2* (B) backgrounds, or partially silencing TEM*1* or TEM*2* (C). D, Trichome average number in cue1-1 and cab3-1 mutants that show defects only in the mesophyll. Error bars indicate SD of the mean number of trichomes. Asterisks indicate statistically significant differences (* $P \leq 0.05$, ** $P \leq 0.01$, *** $P \leq 0.001$) obtained using Tukey's range test.

et al., 2007; D'Aloia et al., 2011). GA and CK act antagonistically in leaf formation and shoot meristem maintenance (Weiss and Ori, 2007), where GAs counteract some CK effects on epidermal differentiation as the inflorescence develops (Gan et al., 2006; Nemhauser et al., 2006). However, both phytohormones overlap in stimulating trichome initiation in different plant tissues (Gan et al., 2007). CK trichome production action is limited to upper inflorescence organs (D'Aloia et al., 2011), whereas GA action affects all trichome-producing epidermal tissues (Gan et al., 2006, 2007). Interestingly, the number of trichomes in mutants and over-expressors of TEM genes was clearly affected not only in rosette leaves but also in upper inflorescence organs (Supplemental Fig. S1), where trichome formation is at least partially controlled by CK. Consequently, we hypothesized that TEM may control other hormones involved in trichome proliferation. We therefore analyzed the levels of CK, and detected higher levels of *Trans-Zeatin*, the bioactive form of CK, in *tem1-1 tem2-2* and lower levels in *P35S::*TEM2 than in wild-type plants 5 DAB (Fig. 6C). These data suggest that TEM may also regulate the CK biosynthetic pathway, which in turn affects trichome formation.

As previously described, the trichome GA-dependent pathway acts in the epidermis partially through GIS, which positively regulates GL1, GL3, EGL3, and TTG1 genes whose proteins form the trichome activation complex (Payne et al., 2000; Zhao et al., 2008a). On the other hand, the trichome CK-dependent pathway acts also in the epidermis and is controlled by GIS2 and ZFP8 (Gan et al., 2007). Mutations in all these main genes result in a significant loss of trichomes, but none of these mutants were as glabrous as TEM over-expressors. TEM is not only widely expressed in the rosette mesophyll but also in the epidermis (Supplemental Fig. S2). To investigate the molecular basis underlying the trichome suppressing effect of TEM in the epidermis, we performed gene expression analysis in TEM mutants and over-expressors 11 days after germination (DAG), when new rosette leaves with new trichomes are proliferating, i.e. before bolting, and 5 DAB. Our results indicated that GIS, GL1, GL3, and EGL3 were clearly repressed by TEM, while TTG1 and some trichome repressor genes, such as *CAPRICE* (CPC) and *SPINDLY* (SPY) (Perazza et al., 1999; Kirik et al., 2004), were not affected (Fig. 7A, Supplemental Fig. S5, and Supplemental Fig. S6). As we wondered whether the trichome suppressing effect of TEM through down-regulation of epidermal transcription factors could also take place from the mesophyll, we conducted gene expression analyses on different PCAB3*:amiR*TEM and PCAB3*:*TEM2 plant lines at the same stage of development (Supplemental Fig. S5). Results showed that exclusive mesophyll TEM over-expression or silencing clearly affect the expression of trichome GA-dependent genes (Supplemental Fig. S5). In addition, GIS2 and ZFP8 expression was also

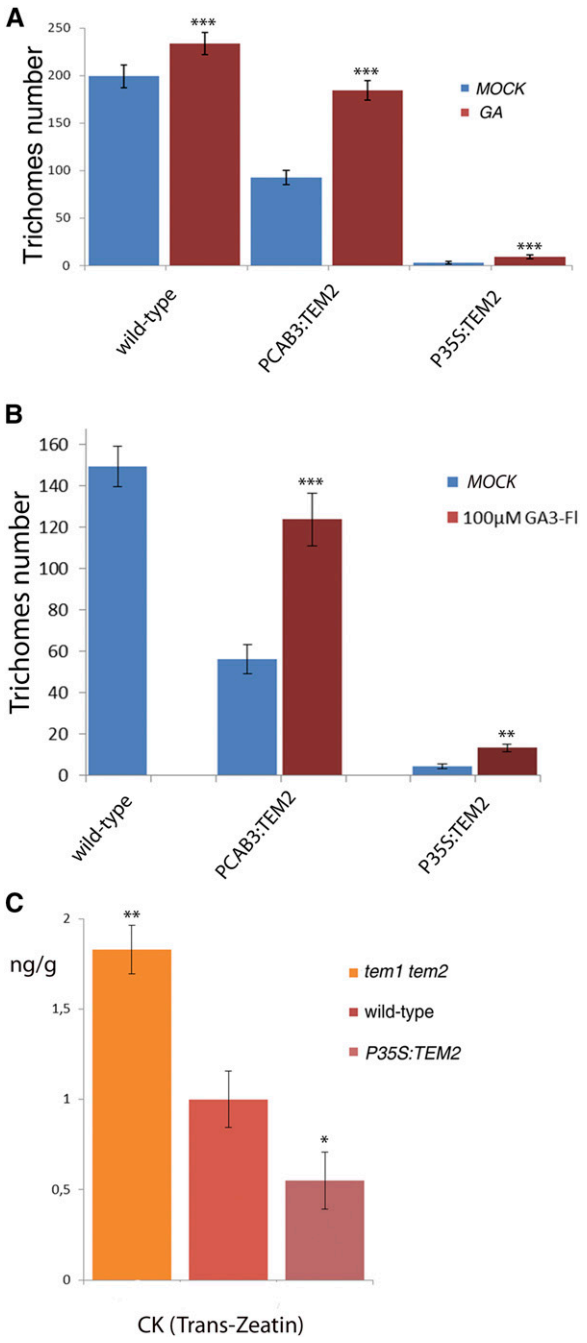

Figure 6. TEMPRANILLO also affects CK. A, Trichome number in the 7th-8th rosette leaves in different TEM backgrounds after MOCK and GA treatment at 25 DAG. Error bars indicate SD of the mean number of trichomes. B, Trichome number in the 6th-7th rosette leaves in different TEM backgrounds after MOCK and 100 μM GA_3-FI treatment (at 18 DAG). Error bars indicate SD of the mean number of trichomes. C, CK hormone measurements in mutants and over-expressors of TEM genes 5 DAB, shown with error bars. Asterisks indicate statistically significant differences (* $P \leq 0.05$, ** $P \leq 0.01$, *** $P \leq 0.001$) obtained using Student's *t* test.

significantly repressed by TEM at 5 DAB (Fig. 7A) but not so clearly at 11 DAG (Supplemental Fig. S5). At 11 DAG, plants have not yet produced any inflorescence organs, consistent with the fact that CK-dependent genes were less affected at this stage.

Integration of CK and GA signaling requires the action of all these GA- and CK-dependent genes on GL2 epidermal expression (Szymanski et al., 1998; Gan et al., 2007). GL2 is considered to be the universal activator of trichome proliferation and it is required from the earliest morphogenetic events of trichome growth (Szymanski et al., 1998; Lin and Aoyama, 2012). A highly plant-conserved mechanism that transduces GAs to promote epidermal cell elongation has been recently revealed: GL2 protein interacts with DELLA complex to affect epidermal cell elongation during trichome formation and seed germination (Rombola-Caldentey et al., 2014; Shan et al., 2014). Additionally, it is well known that GL2 acts downstream of the GA-activation complex (GL1/GL3/TTG1/EGL3) as well as the CK-dependent GIS2/ZFP8 genes during early stages of trichome development (Szymanski et al., 1998; Gan et al., 2007). Because our data showed that both GA- and CK-dependent trichome pathways were controlled by TEM, we next investigated whether GL2 expression levels were affected. As expected, GL2 expression was clearly repressed by TEM at both stages of plant development, 11 DAG and 5 DAB (Fig. 7A and Supplemental Fig. S5), suggesting that the strong trichome phenotypes found in *tem* mutants and *P35S:*TEM plants are, at least partially, caused by GL2 repression. To substantiate our findings we next investigated whether the spatial pattern of GL2 transcription was affected in *tem1-1 tem2-2* and *P35S:*TEM2 plants. For this purpose, we used *PGL2:GUS* lines containing the 2,1Kb of the 5′-untranslated promoter region of GL2 (Szymanski et al., 1998) (Supplemental Fig. S7). In wild-type plants we observed *PGL2:GUS* expression throughout trichome development including surrounding epidermal pavement cells, cells that will not enter to the trichome pathway (Szymanski et al., 1998) (Supplemental Fig. S7). By contrast, *PGL2:GUS* activity was not detected in the few *P35S:*TEM2 trichomes that develop (Supplemental Fig. S8). These data support the finding that GL2 is strongly repressed by TEM during trichome initiation and development.

To further identify the molecular mechanism underlying the trichome-suppressing effect of TEM, we next used *P35S:*TEM*1-HA* and *P35S:*TEM*2-HA* plants for chromatin immuno-precipitation (ChIP) using an anti-HA antibody followed by qPCR. These experiments revealed binding of TEM2 to the RAV binding sites of the regulatory regions of four essential trichome initiation genes: GL1, GIS2, ZFP8, and GL2 at both stages of plant development with enrichments above 2.5 fold (Fig. 7B, Supplemental Fig. S6, and Supplemental Fig. S8). Interestingly, these genes were found to be direct targets of TEM2 but not of TEM1. Altogether, our data suggest that TEM transcriptionally repress trichome initiation in the epidermis by binding in vivo to diverse downstream genes essential to both main trichome initiation pathways, which at the same time are affected by the hormones GA and CK.

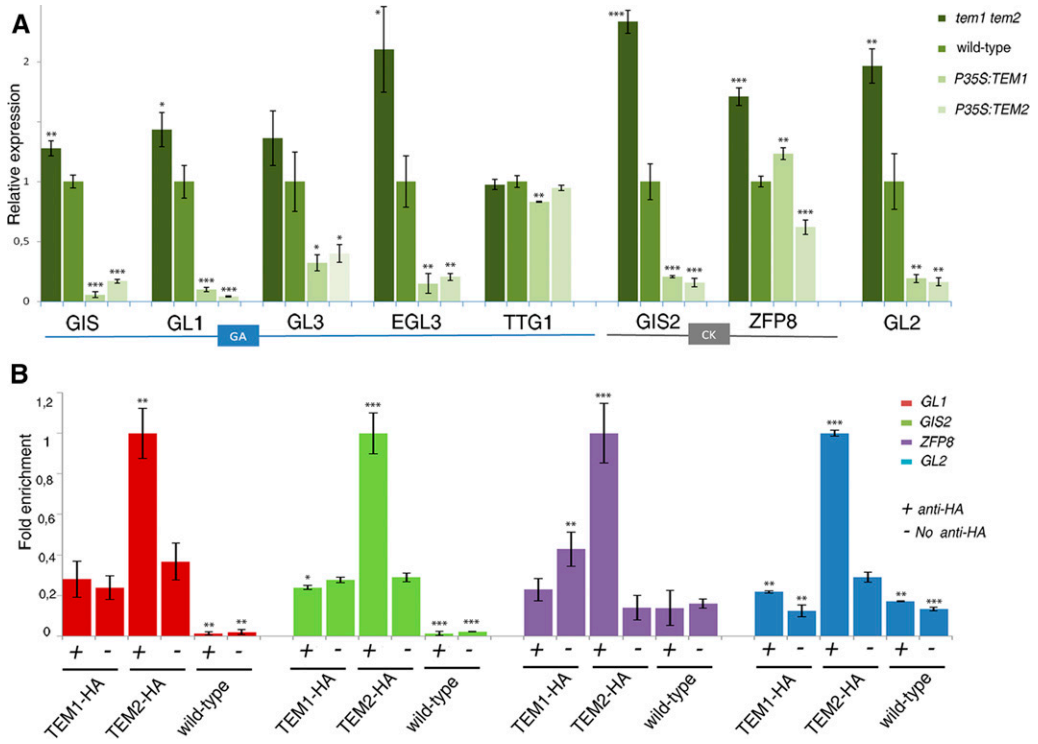

Figure 7. TEMs control expression and binds in vivo to the regulatory regions of several trichome initiation genes. A, Relative expression of GA and CK pathway genes in TEM mutants and over-expressors 5 DAB. One representative of three biological replicates is shown with error bars of three qPCR replicates. B, Relative enrichment of the regulatory regions of GL1, GIS2, ZFP8, and GL2 after immuno-precipitation of TEM1 or TEM2 followed by a qRT PCR in plant collected 5 DAB. One representative of two biological replicates shown with error bars of three qPCR replicates. Asterisks indicate statistically significant differences (* $P \leq 0.05$, ** $P \leq 0.01$, *** $P \leq 0.001$) obtained using Student's *t* test.

DISCUSSION

Trichomes are specialized epidermal protrusions on the surfaces of leaves and other aerial organs of many plants (Olsson et al., 2009), which defend plants against insect herbivores, virus, UV light, and excessive water loss (Traw and Bergelson, 2003). In addition, trichomes are able to synthesize, store, and sometimes secrete large amounts of specialized metabolites with significant commercial value as pharmaceuticals, natural pesticides, or food additives (Schilmiller et al., 2008). Consequently, a better understanding of the molecular mechanisms that control trichome formation will be important for future commercial biopharming applications as trichomes would be able to produce and store such specialized valuable metabolites (Murphy, 2007; Ahmad et al., 2012).

Here we report, to our knowledge, a novel double role for TEM genes in trichome initiation. Our data clearly indicate that, similarly to their effect on floral induction (Castillejo and Pelaz, 2008), TEM1 and TEM2 act redundantly to repress trichome initiation from two leaf tissue layers, epidermis and mesophyll. In the epidermis they directly control trichome gene expression, and in the mesophyll the accumulation and distribution of GA, that ultimately activates the epidermal trichome factors, through the repression of GA biosynthetic genes and GA transporters. The GAs could transiently move to the epidermis, as well as other proteins including TEM, to activate the trichome initiation cascade. In this way, TEMs tightly control trichome formation, acting as secure locks at different steps and locations.

TEM Negatively Affects Trichome Initiation in Arabidopsis

Transcription factors of the RAV family are unique plant-specific proteins, mainly characterized by the presence of two different DNA-binding domains, AP2 and B3 (Riechmann et al., 2000; Matías-Hernández et al., 2014). In Arabidopsis, TEM1 and TEM2, two members of this family, have been previously identified as repressors of floral induction (Castillejo and Pelaz, 2008; Osnato et al., 2012). TEM*1* and TEM*2* genes act redundantly to repress floral transition by integrating both the photoperiod and GA signaling pathways under long days and short days (Castillejo and Pelaz, 2008; Osnato et al., 2012). In addition, recent results indicated that both TEM*1* and TEM*2* are regulated by genes acting upstream in other flowering pathways, suggesting a possible role for TEM in integrating

information from diverse redundant pathways (Yant et al., 2010; Tao et al., 2012; Marín-González et al., 2015). Similarly to other transcription factor families, it has been suggested that RAV genes may control additional biological aspects during plant development (Matías-Hernández et al., 2014). Indeed, flowering is not the only process controlled by RAV proteins. RAV members have been found to be involved in other plant development aspects such as leaf senescence, pathogen infections, abiotic stresses, and growth regulation (Zhao et al., 2008b; Woo et al., 2010; Matías-Hernández et al., 2014; Fu et al., 2014; Wang et al., 2014).

*P35S:*TEM*1* and *P35S:*TEM*2* showed almost completely glabrous leaves, stems, and flowers, while *tem1-1 tem2-2* plants produced an approximately double number of trichomes than wild types. Although TEM*1* and TEM*2* seemed to play a redundant role in repressing trichome initiation, TEM*2* had a stronger effect on this negative regulation. *tem2-2* plants produced more trichomes in rosette leaves than *tem1-1* and wild-type plants. Additionally, GUS expression analyses showed that both genes are expressed in all plant trichomes: in juvenile rosette leaves, adult leaves, stems, and sepals. However at later stages of leaf development, TEM*2* but not TEM*1* expression was restricted to trichomes formed at the central part and the periphery of adult leaves.

In Arabidopsis, after initiation, trichomes develop and grow through endoreduplication, a process where cell replicates its genome but without cytokinesis (Szymanski et al., 1998). As a consequence of this endoreduplication, an Arabidopsis plant will form trichomes with three to four branches in the rosette leaves, one to two branches in the stem, and one branch in the sepals (Gilding and Marks, 2010). However, phenotypical analyses conducted in mutants and overexpressors of TEM genes exclude the possibility of TEM being involved in later processes of trichome development as the branching of *tem1-1 tem2-2*, *P35S:* TEM*1*, and *P35S:*TEM*2* trichomes resembled wild-type trichomes.

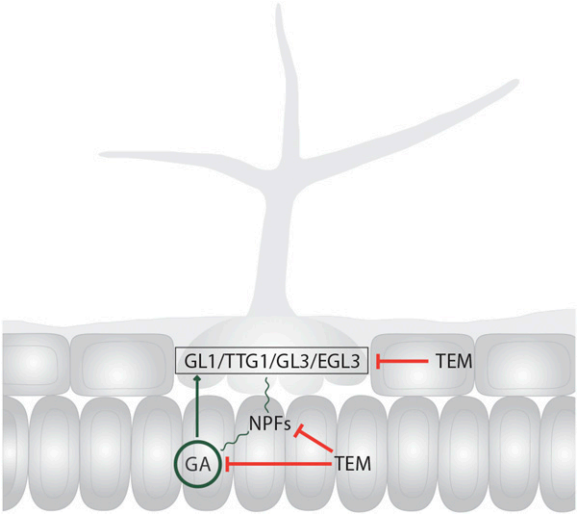

Figure 8. Mechanisms of epidermal trichome formation controlled by TEM. TEMs repress trichome initiation from two leaf tissue layers, the epidermis and the mesophyll. In the epidermis TEMs directly control trichome gene expression, and in the mesophyll the accumulation and distribution of GA, that ultimately activates the epidermal trichome factors, through the repression of GA biosynthetic genes and GA transporters.

TEM Reveals the Palisade Mesophyll as Essential for Trichome Initiation

In plants, leaf development meticulously follows a sequence of events that produce a complex organ with diverse kinds of cells types, thereby the morphological differentiation of cells and their relative position patterns are essential for ensuring the correct function of the leaf (Lin and Aoyama, 2012). The outer L1 layer of the SAM will form the leaf epidermis, while L2 and L3 cell layers will become mesophyll and vascular tissue, respectively (Langdale, 1998; Balkunde et al., 2010).

Trichomes are formed by the specification of epidermal cells. Once an epidermal precursor is specified to enter the trichome pathway, an elaborate morphogenetic cell transformation occurs in order for it to become a trichome (Langdale 1998; Kirik et al., 2004). It is widely accepted that patterns of trichome cell fate should be explained by mechanisms of lateral inhibition toward the epidermal surrounding cells that involves cell to cell communication with a spatial and temporal control (Langdale 1998; Kirik et al., 2004). In Arabidopsis, negative regulators of trichome initiation and patterning, such as CPC, and ENHANCER OF TRIPTYCHON AND CAPRICE1 (ETC1) traffic from trichome cell precursor to neighboring epidermal pavement cells in the epidermis to repress trichome formation (Balkunde et al., 2010; Zhao et al., 2008a). This is due to trichome activation factors turning on their inhibitors, which can subsequently move into neighboring epidermal cells to avoid trichome formation (Balkunde et al., 2011). Similar regulation occurs between positive regulators such as GL3 and TTG1 (Zhao et al., 2008a; Savage et al., 2008). It has been shown that TTG1 moves between epidermal cells and when artificially expressed in the subepidermis, freely moves to the epidermis to rescue *ttg1* mutant phenotype (Bouyer et al., 2008). In addition, its function as trichome promoter is mediated by a trapping mechanism and translocation to the nucleus in the trichome cells through interaction with GL3 (Balkunde et al., 2011), resulting in TTG1 depletion from nontrichome cells (Bouyer et al., 2008). Although it is widely accepted that in Arabidopsis, the competency to enter the trichome pathway is limited to epidermal cells, our results uncover, to our knowledge, a novel mesophyll-epidermis communication mechanism required to control the transition of epidermal cells into trichomes; and that, consequently, may be at odds with the dogma of trichome epidermal specificity. This mechanism would involve the NPF GA transporters that would

allow the GA-dependent epidermis genes be activated from GA specific mesophyll accumulation.

Our data indicate that intercellular signaling between the mesophyll and the epidermis might be affected by TEM, CUE, and CAB3. Although these proteins or other molecules regulated by them may move from mesophyll to epidermal cells, our results suggest that at least GA would use their NPF transports to activate the epidermal trichome initiation genes.

Here we showed that the levels of GA, a mobile hormone (King et al., 2003; Yamaguchi, 2008), are also controlled by TEM (Osnato et al., 2012). GA distribution is an active and highly regulated process (Yamaguchi, 2008; Shani et al., 2013). Our results, using a fluorescently labeled GA, clearly indicate that mesophyll cells have unique features that enable GA accumulation and distribution, suggesting that the mesophyll plays a special role in GA storage. TEM is able to negatively control, not only GA biosynthesis but also NPF-specific GA transporters. These data lead us to propose, to our knowledge, a novel plausible mechanism, where TEM may regulate mesophyll cell development and epidermal trichome initiation, in part, by affecting the GA levels and distribution in the mesophyll as well as the GA transport toward neighbored cells such as epidermal cells (Fig. 8). In the absence of GA accumulation in the mesophyll, as in Arabidopsis lines over-expressing TEM genes, there is a significant reduction in trichome number. This would explain, at least partially, how trichome proliferation is controlled from the mesophyll: the mesophyll plays an essential role in controlling GA storage, distribution, and transport, through the action of TEM, which at the end also controls trichome initiation in the epidermis.

Thus, our data unravel a unique communication channel from one cell layer (mesophyll) to another (epidermis), to inform cell differentiation processes, and that might be mediated by NPF transporters. Potentially, this novel communication channel might also be contributing to additional essential leaf developmental events.

TEM Directly Binds and Represses Genes from both GA- and CK-Dependent Trichome Pathways in the Epidermis

Hormones play an essential role in trichome initiation (D'Aloia et al., 2011; Perazza et al., 1998) and plants use various strategies to orchestrate the competing hormone signals (Nemhauser et al., 2006; Perazza et al., 1998). Among these strategies, a crucial one is the use of specialized regulators that integrate diverse genetic networks in the epidermis (Nemhauser et al., 2006). Indeed, GA and CK hormones have synergistic effects on the constitutive induction of epidermal defensive trichomes and gene regulators may be shared between these two hormonal signaling pathways (Chien and Sussex, 1996; Perazza et al., 1998). Here, we report that TEMs seem to be one of these essential regulators. TEMs affect not only the GA and CK levels within the plants but also genetically control GA- and CK-dependent trichome pathways in the epidermis, which in turn negatively affect trichome formation in all Arabidopsis trichome-producing tissues. TEM1 and TEM2 act redundantly to repress the transcription of most essential positive epidermal regulators in at least two different developmental stages, 11 DAG and 5 DAB, that is before and after bolting, respectively. Among these genes, GL2, considered to be the universal activator of trichome initiation due to the fact that both GA- and CK-dependent trichome pathways converge in its activation, was also repressed. These results suggest that the strong trichome phenotypes found in *tem* mutants and *P35S:*TEM plants were, at least partially, caused by alterations in GL2 expression. Interestingly, some of these genes were found to be in vivo direct targets of TEM2 but not of TEM1. Combined with the fact that *tem2*-2 plants produced more trichomes than *tem1-1* and wild-type plants, these suggest that TEM2 may take over TEM1 functions, playing a more important role in trichome initiation. In conclusion, our results strongly suggest that TEM genes control trichome initiation, acting differently in distinct leaf cell layers. In the mesophyll, they seem to regulate trichome formation by controlling the amounts and distribution, through NPF transporters, of GA, known to affect trichome development in the upper cell layer. In that upper layer, the epidermis, they seem to directly repress transcription of well-known transcription factors involved in trichome initiation as GL3, EGL3, or GL2 (Fig. 8). Thus, our data, including, to our knowledge, the novel finding of GA storage, transport, and distribution in the palisade mesophyll and its essentiality for epidermal trichome initiation, reinforces the developmental plasticity found in plant growth and emphasizes the vital role of TEM genes as repressors in several plant developmental programs. As such, TEM may contribute toward additional important processes affected by the GA and CK hormones, such as cell proliferation, leaf formation, or shoot meristem maintenance and formation (Gan et al., 2007; D'Aloia et al., 2011).

MATERIALS AND METHODS

Plant Material and Growth Conditions

Arabidopsis seeds were stratified for 3 d at 4°C, and plants were grown in soil under controlled conditions at 22°C and long days (16 h light/8 h dark). Col-0 was used as wild type in all the experiments. Transgenic, mutant, and control plants used for phenotypic analyses and live-imaging have Col-0 background and were grown together at the growth chamber. For minimizing the effect of environmental fluctuations, each tray was randomly positioned at the growth chambers. *tem1-1* and *tem2-2* were previously described (Castillejo and Pelaz, 2008; Osnato et al., 2012).

Cloning

For mesophyll-specific TEM expression, we first modified the pENTR-3C vector (Gateway; Invitrogen, Carlsbad, CA) by introducing the PCAB3 and the *Nos* terminator, resulting in the PCAB3-*Nos* vector. The Nos terminator was amplified by PCR and cloned in pENTR-3C as a *Kpn*I-*Eco*RV restriction fragment. The CAB3 promoter was amplified by PCR and cloned in pENTR3C-Nos terminator as a *Sal*I-*Bam*HI fragment.

For mesophyll-specific silencing, we generated PCAB3:*amiR*TEM. The previously described artificial miRNA (amiRNA) sequence targeted against TEM genes (amiR-TEM) was cloned into the PCAB3-*Nos* plasmid (Osnato et al.,

2012). The resulting plasmid was then linearized with *Nhe*I, dephosphorylated with alkaline phosphatase, and recombined by the LR Reaction into pMDC100, a Gateway-compatible binary vector (Curtis and Grossniklaus, 2003).

Similarly, PCAB3:TEM*1* and PCAB3:TEM*2* plasmids were generated by cloning the TEM*1* and TEM2cDNAS as *Bam*HI-*Not*I restriction fragments into the PCAB3-*Nos*. These vectors were later recombined by the LR reaction into pMDC99 and pMDC123, respectively.

In addition, for *P*TEM2:*GUS* plasmid construction, a 1.9 Kb promoter region of TEM2 was cloned first in pENTRD-TOPO (Gateway; Invitrogen). This plasmid was further recombined by a LR reaction into pBGWFS7, a Gateway plasmid containing *GUS* (Karimi et al., 2002).

For all PCR reactions, Col-0 genomic DNA was used as template with specific primers as listed in Supplemental Table S1 and in previous publications (Castillejo and Pelaz, 2008; Osnato et al., 2012). All PCR products were verified by sequencing. *Agrobacterium tumefaciens* (pGV2260 strain) was electroporated with plant expression vectors, and used to transform Col-0 wild-type plants by floral-dip (Clough and Bent, 1998). Between 5 and 10 T1 transgenic lines were selected for each construct on MS1 supplemented with the appropriate antibiotic.

Phenotypic Analyses

For trichome analysis, all the experiments were repeated on soil-grown plants at least twice. Trichome initiation was monitored using a model no. DP71 microscope (Olympus, Melville, NY) by counting all trichomes on the adaxial surface of individual and fully developed rosette leaves (Gan et al., 2007; Yu et al., 2010). 1st-2nd, 3rd-4th, 5th-6th, and 7th-8th rosette leaf trichomes were counted independently given that these leaves showed different trichome production. However, despite the trichome number differences, a similar tendency was observed. Trichome production on the main stem was evaluated by counting trichomes on the first, second, and third inflorescence internodes independently, starting from the bottom to the top. Trichome number was recorded when the main stem reached approximately 17–18 cm in size. Trichome numbers on the first, second, and third cauline leaves of Arabidopsis plants were measured in the whole adaxial area of each fully expanded leaf. In addition, trichome production on sepals was evaluated by counting sepal trichomes in flowers at different developmental stages in plants whose main stem reached approximately 10 cm in size, approximately 5–8 d after flowering. Unless otherwise specified, a minimum of 20 plants was used for trichome analysis for each developmental stage and genotype combination. Data are reported as mean value and SD of the number of trichomes for each genotype.

Hormone Analyses and Treatments

Hormones were measured at the hormone quantification service at the Institute for Plant Molecular and Cell Biology, Valencia, Spain. At least 200 mg of fresh independent Arabidopsis plants for each genotype collected 5 DAB were used. GA was quantified after different steps of extraction and purification including three steps of 80% MeOH-1% acetic acid and a final step using 80% MeOH-1% formic acid. CK was quantified after extraction and purification including 80% MeOH-1% acetic acid and 60% MeOH-5% NH_3. GA and CK were finally quantified using an MS-HPLC-Q-Exactive Orbitrap (Thermo Fisher Scientific, Waltham, MA; Glauser et al., 2014). Exogenous GA_3 was used for hormone treatment. As described (Gan et al., 2007), different line plants were grown on soil until the first 3–4 leaves had emerged and then plants are sprayed twice a week with MOCK and 100 μM GA_4 solutions until plants during 2–3 weeks. For measuring the effect of GA application, 7th-8th rosette leaf trichomes from 20 plants were counted for each genotype combination. Experiments were repeated on soil-grown plants at least twice.

Epidermis and Mesophyll Phenotypic Analyses

SEM was performed as previously described (Sánchez-Chardi et al., 2011). In short, samples were fixed in 2.5% (vol/vol) glutaraldehyde in 0.1 M P-buffer (pH 7.4) for 2 h at 4°C, washed 4 times for 10 min each time in 0.1 M P-buffer, postfixed in 1% (w/t) osmium tetraoxide with 0.7% ferrocyanide in P-buffer, washed in water, dehydrated in an ascending ethanol series (50, 70, 80, 90, and 95% for 10 min each and twice with 100% ethanol), and dried by critical-point drying with CO_2 (Julián et al., 2010). On the other side, ultra-thin transverse sections of the central part of rosette leaves 11 DAG were first fixed with osmium, dehydrated with acetone, embedded in Spurr resin and finally stained with toluidine blue (Sánchez-Chardi et al., 2011). For cell morphology analysis, sections of 0.5–1 μm were cut with an ultra-thin microtome using a diamond knife. All measurements and image analyses were done using an AixoPhot DP70 microscope (Olympus).

Exogenous GA_3 Bioactivity Assays

For GA_3-Fl bioactivity assays and analyses seeds from different genotype were germinated and grown in MS medium under controlled conditions at 22°C and long days (16 h light/8 h dark). Plants were treated with 10 μM GA_3-Fl liquid solution for 20 h and then 1st-2nd rosette leaves were imaged (Shani et al., 2013). GA_3-Fl bioactivity assays were performed in rosette leaves through development. For that reason, 1st-2nd rosette leaves from at least six plants for each genotype combination lines were imaged at different plant developmental stages 9, 11, 13, 16 DAG. Confocal microscopy (Leica, Wetzlar, Germany) and ImageJ (National Institutes of Health, Bethesda, MD) were used for imaging. Exogenous GA_3-Fl was used for hormone treatment. Different line plants were grown in MS medium under controlled conditions at 22°C and long days on soil until the first 2–3 leaves had emerged and then plants are sprayed twice a week with MOCK and 100 μM GA_4 solutions during 10 days. For measuring the effect of GA application, 6th-7th rosette leaf trichomes from 20 plants were counted for each genotype combination.

Identification of Putative RAV Binding Site Sequences

The genomic regions located 3 kb upstream of the ATG, 1 kb downstream of the stop codon and in the exons, and introns of the genes involved in GA- and CK-dependent trichome regulatory pathways, were analyzed to identify RAV binding sites sequences (C(A/C/G)ACA$(N)_{2-8}$(C/A/T)ACCTG). The Fuzznucbioinformatic program available at the Web site (http://www.hpa-bioinfotools.org.uk/pise/fuzznuc.html) allowed us to identify perfect RAV binding sites, and RAV binding sites sequences with one/two mismatches. To restrict the sample further, we selected genes containing at least two putative RAV binding sites sequences within a distance of 300 bp.

Expression Analyses, ChIP, and GUS Assays

Real-time analyses were designed to comply with standards of RT-qPCR (Rieu and Powers, 2009). For RT-qPCR reactions, plants were grown in soil under long days and samples collected at ZT18 at the indicated days. RNA was extracted from a pool of 20 plants 11 DAG or 10 adult plants 5 DAB with PureLink RNA Mini Kit (Ambion; Thermo Fisher Scientific), treated with RNase-free DNaseI (Ambion, Thermo Fisher Scientific) and 1 μg was retrotranscribed with oligo(dT) and SuperScript III (Invitrogen). The expression levels of genes of interest were monitored by qPCR using SYBR Green I Master Mix and Light Cycler 480 (Roche, Basel, Switzerland) with the primers listed in Supplemental Table S2 and below. Data were normalized using the *UBQ10* gene as reference. PCR efficiency was calculated and determined as previously described (Talke et al., 2006). For the GA- and CK-dependent pathways, we chose to study only those genes that are involved in the final steps of trichome initiation, which are highly expressed in trichomes, and for which mutants have already been described. Gene-specific primer sequences previously described (Gan et al., 2006, 2007; Balkunde et al., 2010) are listed in Supplemental Table S2 and here:

GIS, 5′-TTCATGAACGTCGAATCCTTCTC-3′ and 5′-ACGAATGGGTTTAGGGTTCTTATCT-3′;
GL1, 5′-CGACTCTCCACCGTCATTGTT-3′ and 5′-TTCTCGTAGATATTTTCTTGTTGATGATG-3′;
GL3, 5′-GGTACCACAGAACATATTACGGAAGA-3′ and 5′-CAAGAACGTTGTCGATGTGATAATC-3′;
EGL3, 5′-ATGGCAACCGGAGAAAACAGAACG-3′ and 5′-TCTCAAGGACTCCTCCAAGAAACG-3′;
TTG1, 5′-ATGGATAATTCAGCTCCAG-3′ and 5′-TCAAACTCTAAGGAGCTGC-3′;
GIS2, 5′-ACCGCCAACAAAACCACATT-3′ and 5′-CGCGTCGTTGATTTGAACAG-3′;
ZFP8, 5′-AAGCCGCCATTATTCGTCTCT-3′ and 5′-CTGCGGATAAGTTGTCGGAGTT-3′;
GL2, 5′-GGACGAGAAGCAAAGACAGC-3′ and 5′-TCTCTAGTTCCGCCTTGAGC-3′;
CPC, 5′-TGGGAAGCTGTGAAGATGTCAG-3′ and 5′-AAGTCTCTTCGTCTGTTGGCA-3′;

SPY, 5′-TGGAAAAGGGATATGCTTGC-3′ and 5′-CTGCCATCAATGCTTTCTG-3′;
UBQ10,5′-AAATCTCGTCTCTGTTATGCTTAAGAAG-3′ and 5′-TTTTACATGAAACGAAACATTGAACTT-3′.

ChIP experiments were performed as a modified version of a previously reported protocol (Matías-Hernández et al., 2010). The direct binding of TEM1 and TEM2 to the regulatory regions of putative targets was assayed using the *P35S:*TEM*1-HA* lines previously described (Osnato et al., 2012) and *P35S:* TEM*2-HA*. Wild-type plants were used as negative controls. The cross-linked DNA was immuno-precipitated with an anti-HA antibody (Sigma-Aldrich, St. Louis, MO), purified using Protein A-Agarose resin (Millipore, Billerica, MA), and tested by qPCR using different primer sets specific for putative direct targets, as listed in Supplemental Table S2.

Enrichment of the target region was determined using a Sybr Green Assay (SYBR Green Supermix; Roche). The quantitative real-time PCR assay was conducted in triplicate and was performed in a LightCycler480 System (Roche). Relative enrichment was calculated normalizing the amount of immunoprecipitated DNA against a UBIQUITIN (UBQ10) fragment and against total INPUT DNA. In particular, for the binding of TEM1 and TEM2 to the selected genomic regions, the affinity of the purified sample obtained in the *P35S:*TEM*1-HA* and *P35S:*TEM*2-HA* lines background was compared with the affinity-purified sample obtained in the wild-type background, which was used as negative control. Fold enrichment was calculated using the following formulas, where *Ct.tg* is target gene mean value, *Ct.i* is input DNA mean value, and *Ct.nc* is ubiquitin (negative control) mean value: *dCT.tg* = *CT.i-CT.tg* and *dCT.nc* = *CT.i-CT.nc*. The propagated error values of these CTs are calculated: *dSD.tg* = *sqrt* ((*SD.i*)^2+ (*SD.tg*^2)/*sqrt*(*n*) and *dSD.nc* = *sqrt*((*SD.i*)^2+ (*SD.nc*^2)/*sqrt*(*n*), where *n* = number of replicate per sample. Fold-change over negative control (ubiquitin and wild-type plants) was calculated finding the "delta delta CT" of the target region as follows: *ddCT* = *dCT.tg-dCT.nc* and *ddSD* = *sqrt*((*dSD.tg*)^2+ (*dSD.nc*)^2. The transformation to linear fold-change values is obtained as follows: *FC* = 2^(*ddCT*) and *FC.error* = ln(2)**ddSD**FC.

On the other side, *PGL2:GUS* seedlings were used for GUS expression analyses. *PGL2:GUS* plants were crossed with *tem1*-1 *tem2*-2 and *P35S:*TEM*2*, and three plant generations (F3) were grown in order to obtain homozygous *PGL2:GUStem1 tem2* and *PGL2:GUSP35S:*TEM*2*. All GUS staining assays were performed overnight as described previously (Blázquez et al., 1997; Liljegren et al., 2000). Samples were incubated in clearing solution, dissected, and observed using a model no. DP71 microscope equipped with DIC optics (Olympus).

In silico analyses of NPF genes for checking if they were expressed in the rosette mesophyll was done using Arabidopsis eFP Browser 2.0:
http://bar.utoronto.ca/efp2/Arabidopsis/Arabidopsis_eFPBrowser2.html.

Supplemental Data

The following supplemental materials are available.

Supplemental Figure S1. Trichome number on different upper inflorescence organs.

Supplemental Figure S2. *PTEM1:GUS* and *PTEM2:GUS* are highly expressed through trichome development.

Supplemental Figure S3. Exogenous GA accumulation in the mesophyll is regulated by *TEMPRANILLO* at different stages of development.

Supplemental Figure S4. SEM of abaxial epidermal cells.

Supplemental Figure S5. Before bolting *TEMPRANILLO* regulates GA- but not CK-dependent trichome gene expression.

Supplemental Figure S6. Regulation of other trichome genes by *TEMPRANILLO*.

Supplemental Figure S7. *TEM* affects trichome *pGL2:GUS* activity.

Supplemental Figure S8. *TEM2* binds in vivo to the main GA- and CK-dependent trichome genes in plants that have not yet flowered.

Supplemental Table S1. Trichome number and density on different TEM genetic backgrounds.

Supplemental Table S2. List of primers used for cloning and ChIP.

Supplemental Table S3. Statistical analyses of data from Figures 1, 2, 4, 5, 6, and 7.

ACKNOWLEDGMENTS

We thank Rossana Henriques and Josep Casacuberta for helpful discussions and critical reading of the manuscript; Monste Amenós and the High Resolution Imaging Facility at the Universitat Autònoma de Barcelona for help with confocal microscopy and the ultra-thin transverse sections and imaging, respectively; and Jose Luis Micol for providing cue1-*6* seeds and NASC for seeds. A.E.A.-J. performed this work within the framework of a Ph.D. Program of the Universitat Autònoma de Barcelona.

Received August 19, 2015; accepted January 21, 2016; published January 22, 2016.

LITERATURE CITED

Ahmad P, Ashraf M, Younis M, Hu X, Kumar A, Akram NA, Al-Qurainy F (2012) Role of transgenic plants in agriculture and biopharming. Biotechnol Adv **30:** 524–540

An L, Zhou Z, Su S, Yan A, Gan Y (2012) GLABROUS INFLORESCENCE STEMS (GIS) is required for trichome branching through gibberellic acid signaling in Arabidopsis. Plant Cell Physiol **53:** 457–469

Balkunde R, Bouyer D, Hülskamp M (2011) Nuclear trapping by GL3 controls intercellular transport and redistribution of TTG1 protein in Arabidopsis. Development **138:** 5039–5048

Balkunde R, Pesch M, Hülskamp M (2010) Trichome patterning in Arabidopsis thaliana from genetic to molecular models. Curr Top Dev Biol **91:** 299–321

Bernhardt C, Zhao M, Gonzalez A, Lloyd A, Schiefelbein J (2005) The bHLH genes GL3 and EGL3 participate in an intercellular regulatory circuit that controls cell patterning in the Arabidopsis root epidermis. Development **132:** 291–298

Blázquez MA, Soowal LN, Lee I, Weigel D (1997) LEAFY expression and flower initiation in Arabidopsis. Development **124:** 3835–3844

Bouyer D, Geier F, Kragler F, Schnittger A, Pesch M, Wester K, Balkunde R, Timmer J, Fleck C, Hülskamp M (2008) Two-dimensional patterning by a trapping/depletion mechanism: the role of TTG1 and GL3 in Arabidopsis trichome formation. PLoS Biol **6:** e141

Castillejo C, Pelaz S (2008) The balance between CONSTANS and TEMPRANILLO activities determines FT expression to trigger flowering. Curr Biol **18:** 1338–1343

Clough SJ, Bent AF (1998) Floral dip: a simplified method for Agrobacterium-mediated transformation of Arabidopsis thaliana. Plant J **16:** 735–743

Curtis MD, Grossniklaus U (2003) A gateway cloning vector set for high-throughput functional analysis of genes in planta. Plant Physiol **133:** 462–469

Chiba Y, Shimizu T, Miyakawa S, Kanno Y, Koshiba T, Kamiya Y, Seo M (2015) Identification of Arabidopsis thaliana NRT1/PTR FAMILY (NPF) proteins capable of transporting plant hormones. J Plant Res **128:** 679–686

Chien JC, Sussex IM (1996) Differential regulation of trichome formation on the adaxial and abaxial leaf surfaces by gibberellins and photoperiod in Arabidopsis thaliana (L.) Heynh. Plant Physiol **111:** 1321–1328

D'Aloia M, Bonhomme D, Bouché F, Tamseddak K, Ormenese S, Torti S, Coupland G, Périlleux C (2011) Cytokinin promotes flowering of Arabidopsis via transcriptional activation of the FT paralogue TSF. Plant J **65:** 972–979

Deeks MJ, Hussey PJ (2003) Arp2/3 and 'the shape of things to come'. Curr Opin Plant Biol J **6:** 561–567

Endo M, Mochizuki N, Suzuki T, Nagatani A (2007) CRYPTOCHROME2 in vascular bundles regulates flowering in Arabidopsis. Plant Cell **19:** 84–93

Fu M, Kang HK, Son SH, Kim SK, Nam KH (2014) A subset of Arabidopsis RAV transcription factors modulates drought and salt stress responses independent of ABA. Plant Cell Physiol **55:** 1892–1904

Gan Y, Kumimoto R, Liu C, Ratcliffe O, Yu H, Broun P (2006) GLABROUS INFLORESCENCE STEMS modulates the regulation by gibberellins of epidermal differentiation and shoot maturation in Arabidopsis. Plant Cell **18:** 1383–1395

Gan Y, Liu C, Yu H, Broun P (2007) Integration of cytokinin and gibberellin signalling by Arabidopsis transcription factors GIS, ZFP8 and GIS2 in the regulation of epidermal cell fate. Development **134:** 2073–2081

Gilding EK, Marks MD (2010) Analysis of purified glabra3-shapeshifter trichomes reveals a role for NOECK in regulating early trichome morphogenic events. Plant J **64:** 304–317

Glauser G, Vallat A, Balmer D (2014) Hormone profiling. Methods Mol Biol **1062:** 597–608

Hülskamp M (2004) Plant trichomes: a model for cell differentiation. Nat Rev Mol Cell Biol **5:** 471–480

Julián E, Roldán M, Sánchez-Chardi A, Astola O, Agustí G, Luquin M (2010) Microscopic cords, a virulence-related characteristic of Mycobacterium tuberculosis, are also present in nonpathogenic mycobacteria. J Bacteriol **192:** 1751–1760

Kanno Y, Hanada A, Chiba Y, Ichikawa T, Nakazawa M, Matsui M, Koshiba T, Kamiya Y, Seo M (2012) Identification of an abscisic acid transporter by functional screening using the receptor complex as a sensor. Proc Natl Acad Sci USA **109:** 9653–9658

Karimi M, Inzé D, Depicker A (2002) GATEWAY vectors for Agrobacterium-mediated plant transformation. Trends Plant Sci **7:** 193–195

King RW, Evans LT, Mander LN, Moritz T, Pharis RP, Twitchin B (2003) Synthesis of gibberellin GA6 and its role in flowering of Lolium temulentum. Phytochemistry **62:** 77–82

Kirik V, Simon M, Huelskamp M, Schiefelbein J (2004) The ENHANCER OF TRY AND CPC1 gene acts redundantly with TRIPTYCHON and CAPRICE in trichome and root hair cell patterning in Arabidopsis. Dev Biol **268:** 506–513

Krouk G, Lacombe B, Bielach A, Perrine-Walker F, Malinska K, Mounier E, Hoyerova K, Tillard P, Leon S, Ljung K, Zazimalova E, Benkova E, et al (2010) Nitrate-regulated auxin transport by NRT1.1 defines a mechanism for nutrient sensing in plants. Dev Cell **18:** 927–937

Langdale JA (1998) Cellular differentiation in the leaf. Curr Opin Cell Biol **10:** 734–738

Léran S, Varala K, Boyer JC, Chiurazzi M, Crawford N, Daniel-Vedele F, David L, Dickstein R, Fernandez E, Forde B, Gassmann W, Geiger D, et al (2014) A unified nomenclature of NITRATE TRANSPORTER 1/PEPTIDE TRANSPORTER family members in plants. Trends Plant Sci **19:** 5–9

Li H, Culligan K, Dixon RA, Chory J (1995) CUE1: a mesophyll cell-specific positive regulator of light-controlled gene expression in Arabidopsis. Plant Cell **7:** 1599–1610

Liljegren SJ, Ditta GS, Eshed Y, Savidge B, Bowman JL, Yanofsky MF (2000) SHATTERPROOF MADS-box genes control seed dispersal in Arabidopsis. Nature **404:** 766–770

Lin Q, Aoyama T (2012) Pathways for epidermal cell differentiation via the homeobox gene GLABRA2: update on the roles of the classic regulator. J Integr Plant Biol **54:** 729–737

Lundquist PK, Rosar C, Bräutigam A, Weber AP (2014) Plastid signals and the bundle sheath: mesophyll development in reticulate mutants. Mol Plant **7:** 14–29

Marín-González E, Matías-Hernández L, Aguilar-Jaramillo A-E, Lee J-H, Ahn J-H, Suárez-López P, Pelaz S (2015) SHORT VEGETATIVE PHASE up-regulates TEMPRANILLO2 floral repressor at low ambient temperatures. Plant Physiol **169:** 1214–1224

Matías-Hernández L, Aguilar-Jaramillo AE, Marín-González E, Suárez-López P, Pelaz S (2014) RAV genes: regulation of floral induction and beyond. Ann Bot (Lond) **114:** 1459–1470

Matías-Hernandez L, Battaglia R, Galbiati F, Rubes M, Eichenberger C, Grossniklaus U, Kater MM, Colombo L (2010) VERDANDI is a direct target of the MADS domain ovule identity complex and affects embryo sac differentiation in Arabidopsis. Plant Cell **22:** 1702–1715

Mitchum MG, Yamaguchi S, Hanada A, Kuwahara A, Yoshioka Y, Kato T, Tabata S, Kamiya Y, Sun TP (2006) Distinct and overlapping roles of two gibberellin 3-oxidases in Arabidopsis development. Plant J **45:** 804–818

Murphy DJ (2007) Improving containment strategies in biopharming. Plant Biotechnol J **5:** 555–569

Nemhauser JL, Hong F, Chory J (2006) Different plant hormones regulate similar processes through largely nonoverlapping transcriptional responses. Cell **126:** 467–475

Olsson ME, Olofsson LM, Lindahl AL, Lundgren A, Brodelius M, Brodelius PE (2009) Localization of enzymes of artemisinin biosynthesis to the apical cells of glandular secretory trichomes of Artemisia annua L. Phytochemistry **70:** 1123–1128

Osnato M, Castillejo C, Matías-Hernández L, Pelaz S (2012) TEMPRANILLO genes link photoperiod and gibberellin pathways to control flowering in Arabidopsis. Nat Commun **3:** 808

Payne CT, Zhang F, Lloyd AM (2000) GL3 encodes a bHLH protein that regulates trichome development in arabidopsis through interaction with GL1 and TTG1. Genetics **156:** 1349–1362

Perazza D, Herzog M, Hülskamp M, Brown S, Dorne AM, Bonneville JM (1999) Trichome cell growth in Arabidopsis thaliana can be derepressed by mutations in at least five genes. Genetics **152:** 461–476

Perazza D, Vachon G, Herzog M (1998) Gibberellins promote trichome formation by Up-regulating GLABROUS1 in arabidopsis. Plant Physiol **117:** 375–383

Ranjan A, Fiene G, Fackendahl P, Hoecker U (2011) The Arabidopsis repressor of light signaling SPA1 acts in the phloem to regulate seedling de-etiolation, leaf expansion and flowering time. Development **138:** 1851–1862

Riechmann JL, Heard J, Martin G, Reuber L, Jiang C, Keddie J, Adam L, Pineda O, Ratcliffe OJ, Samaha RR, Creelman R, Pilgrim M, et al (2000) Arabidopsis transcription factors: genome-wide comparative analysis among eukaryotes. Science **290:** 2105–2110

Rieu I, Powers SJ (2009) Real-time quantitative RT-PCR: design, calculations, and statistics. Plant Cell **21:** 1031–1033

Rombolá-Caldentey B, Rueda-Romero P, Iglesias-Fernández R, Carbonero P, Oñate-Sánchez L (2014) Arabidopsis DELLA and two HD-ZIP transcription factors regulate GA signaling in the epidermis through the L1 box cis-element. Plant Cell **26:** 2905–2919

Saito H, Oikawa T, Hamamoto S, Ishimaru Y, Kanamori-Sato M, Sasaki-Sekimoto Y, Utsumi T, Chen J, Kanno Y, Masuda S, Kamiya Y, Seo M, et al (2015) The jasmonate-responsive GTR1 transporter is required for gibberellin-mediated stamen development in Arabidopsis. Nat Commun **6:** 6095

Sánchez-Chardi A, Olivares F, Byrd TF, Julián E, Brambilla C, Luquin M (2011) Demonstration of cord formation by rough Mycobacterium abscessus variants: implications for the clinical microbiology laboratory. J Clin Microbiol **49:** 2293–2295

Savage NS, Walker T, Wieckowski Y, Schiefelbein J, Dolan L, Monk NA (2008) A mutual support mechanism through intercellular movement of CAPRICE and GLABRA3 can pattern the Arabidopsis root epidermis. PLoS Biol **6:** e235

Schellmann S, Schnittger A, Kirik V, Wada T, Okada K, Beermann A, Thumfahrt J, Jürgens G, Hülskamp M (2002) TRIPTYCHON and CAPRICE mediate lateral inhibition during trichome and root hair patterning in Arabidopsis. EMBO J **21:** 5036–5046

Schilmiller AL, Last RL, Pichersky E (2008) Harnessing plant trichome biochemistry for the production of useful compounds. Plant J **54:** 702–711

Shan CM, Shangguan XX, Zhao B, Zhang XF, Chao LM, Yang CQ, Wang LJ, Zhu HY, Zeng YD, Guo WZ, Zhou BL, Hu GJ, et al (2014) Control of cotton fibre elongation by a homeodomain transcription factor GhHOX3. Nat Commun **5:** 5519

Shani E, Weinstain R, Zhang Y, Castillejo C, Kaiserli E, Chory J, Tsien RY, Estelle M (2013) Gibberellins accumulate in the elongating endodermal cells of Arabidopsis root. Proc Natl Acad Sci USA **110:** 4834–4839

Smith LG (2003) Cytoskeletal control of plant cell shape: getting the fine points. Curr Opin Plant Biol **6:** 63–73

Szymanski DB, Jilk RA, Pollock SM, Marks MD (1998) Control of GL2 expression in Arabidopsis leaves and trichomes. Development **125:** 1161–1171

Talke IN, Hanikenne M, Krämer U (2006) Zinc-dependent global transcriptional control, transcriptional deregulation, and higher gene copy number for genes in metal homeostasis of the hyperaccumulator Arabidopsis halleri. Plant Physiol **142:** 148–167

Tao Z, Shen L, Liu C, Liu L, Yan Y, Yu H (2012) Genome-wide identification of SOC1 and SVP targets during the floral transition in Arabidopsis. Plant J **70:** 549–561

Traw MB, Bergelson J (2003) Interactive effects of jasmonic acid, salicylic acid, and gibberellin on induction of trichomes in Arabidopsis. Plant Physiol **133:** 1367–1375

Tsay YF, Chiu CC, Tsai CB, Ho CH, Hsu PK (2007) Nitrate transporters and peptide transporters. FEBS Lett **581:** 2290–2300

Wang XHLQ, Li QT, Chen HW, Zhang WK, Ma B, Chen SY, Zhang JS (2014) Trihelix transcription factor GT-4 mediates salt tolerance via interaction with TEM2 in Arabidopsis. BMC Plant Biol **14:** 339

Weiss D, Ori N (2007) Mechanisms of cross talk between gibberellin and other hormones. Plant Physiol **144:** 1240–1246

Wolters H, Jürgens G (2009) Survival of the flexible: hormonal growth control and adaptation in plant development. Nat Rev Genet **10:** 305–317

Woo HR, Kim JH, Kim J, Kim J, Lee U, Song IJ, Kim JH, Lee HY, Nam HG, Lim PO (2010) The RAV1 transcription factor positively regulates leaf senescence in Arabidopsis. J Exp Bot **61:** 3947–3957

Yamaguchi S (2008) Gibberellin metabolism and its regulation. Annu Rev Plant Biol **59:** 225–251

Yant L, Mathieu J, Dinh TT, Ott F, Lanz C, Wollmann H, Chen X, Schmid M (2010) Orchestration of the floral transition and floral development in Arabidopsis by the bifunctional transcription factor APETALA2. Plant Cell **22:** 2156–2170

Yu N, Cai WJ, Wang S, Shan CM, Wang LJ, Chen XY (2010) Temporal control of trichome distribution by microRNA156-targeted SPL genes in Arabidopsis thaliana. Plant Cell **22:** 2322–2335

Zhao L, Luo Q, Yang C, Han Y, Li W (2008b) A RAV-like transcription factor controls photosynthesis and senescence in soybean. Planta **227:** 1389–1399

Zhao M, Morohashi K, Hatlestad G, Grotewold E, Lloyd A (2008a) The TTG1-bHLH-MYB complex controls trichome cell fate and patterning through direct targeting of regulatory loci. Development **135:** 1991–1999

CAPÍTULO III: TEMPRANILLO reveals the mesophyll as crucial for epidermal trichome formation.

Supplemental Data

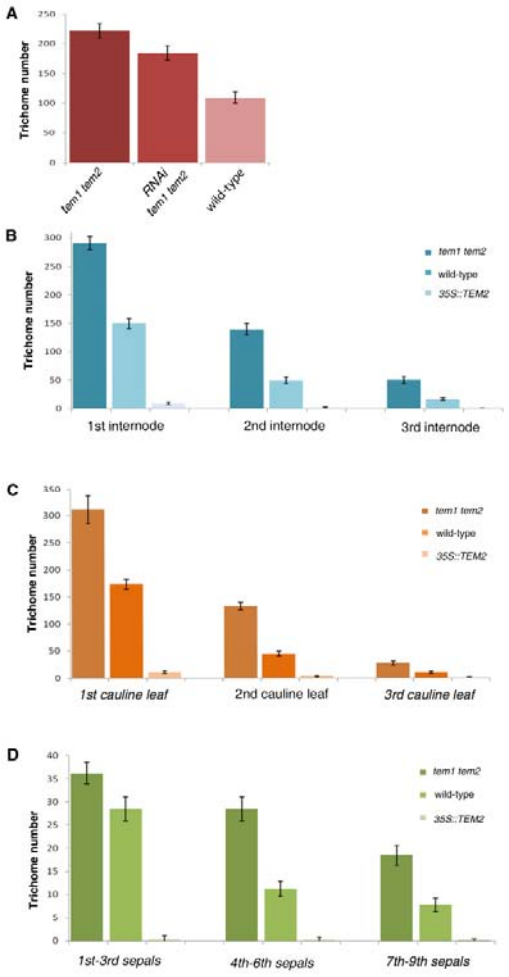

Supplemental Figure S1. Trichome number on different upper inflorescence organs.

(A) Trichome average number in the 5th-6th rosette leaves of twenty one DAG plants of RNAi lines that silence partially *TEM1* and *TEM2* in comparison with *tem1-1 tem2-2* and wild type.

(B) to **(D)** CKs strongly control trichome proliferation in the upper inflorescence organs. Analysis on trichome number was conducted in different upper inflorescence organs including stems **(B)**, cauline leaves **(C)** and sepals **(D)** in *tem1 tem2*, Col-0 and *P35S:TEM2* plant backgrounds. A minimum of 20 plants were used for trichome analysis for each developmental stage and genotype combination. Error bars indicate s.d. of the mean number of trichomes. As described in methodology, trichome average number was measured separately in the first three stem internodes **(B)**, the first three cauline leaves **(C)** and sepals of flowers that have been grouped depending of their developmental stage **(D)**. 1st to 3rd are the flowers that appear first in each inflorescence.

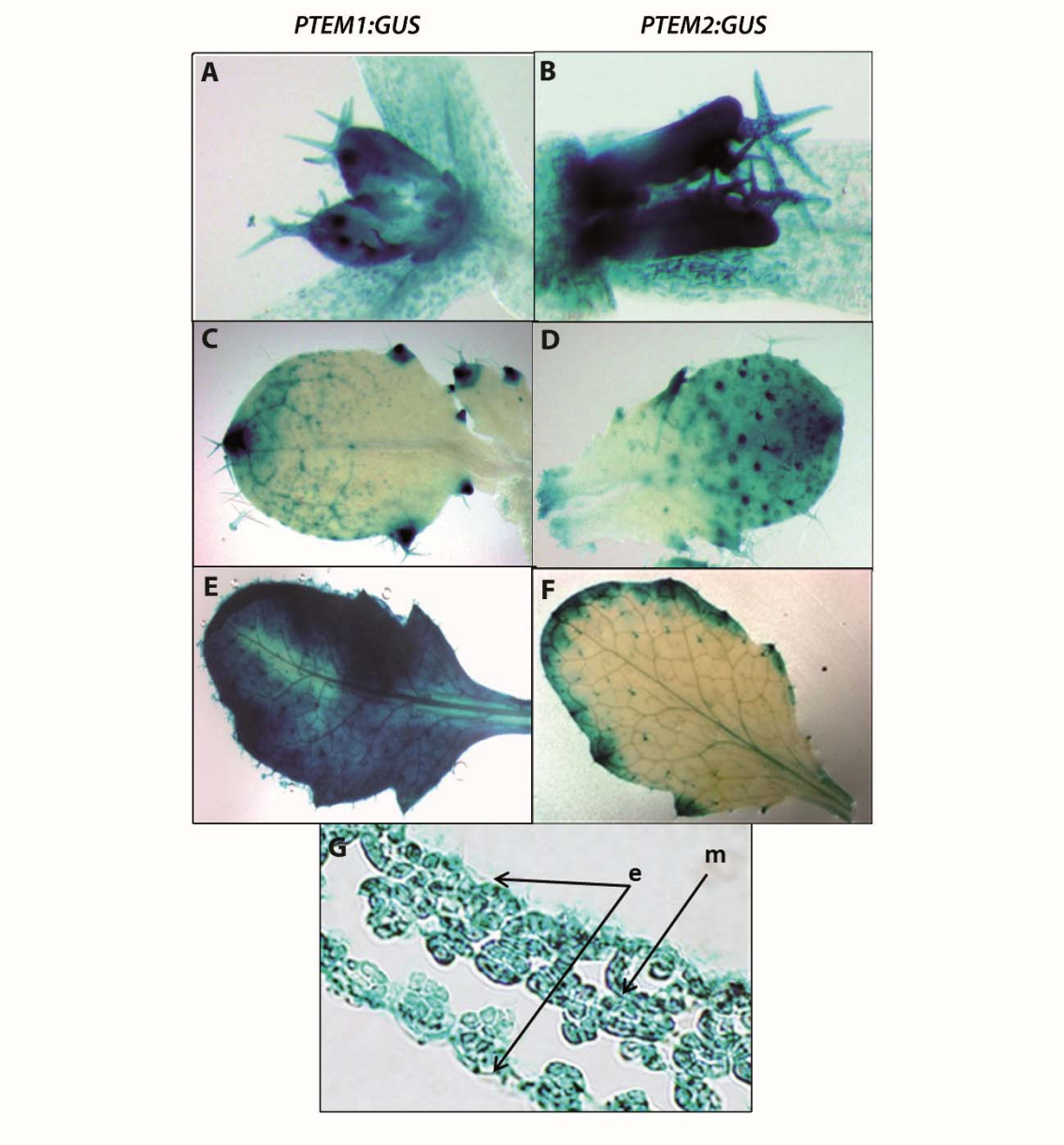

Supplemental Figure S2. *PTEM1:GUS* and *PTEM2:GUS* are highly expressed through trichome development.

(A), **(C)** and **(E)** GUS expression of *PTEM1:GUS* in Col-0 wild type plants show a strong expression in trichomes. *PTEM1:GUS* reporter lines show expression in the trichomes from early stages of rosette leaves development as leaf bud **(A)** to adult leaves **(E)**.

(**B), (D)** and **(F)** *PTEM2:GUS* expression was similarly detected in trichomes trough *Arabidopsis* development. The main difference with *PTEM1:GUS* is that in adult rosette leaves, *PTEM2* expression is only detected on the leaf periphery and restricted to trichomes located at the leaf central part **(F)**. *PTEM2:GUS* expression was detected in both epidermis and mesophyll tissue layers **(G)**.

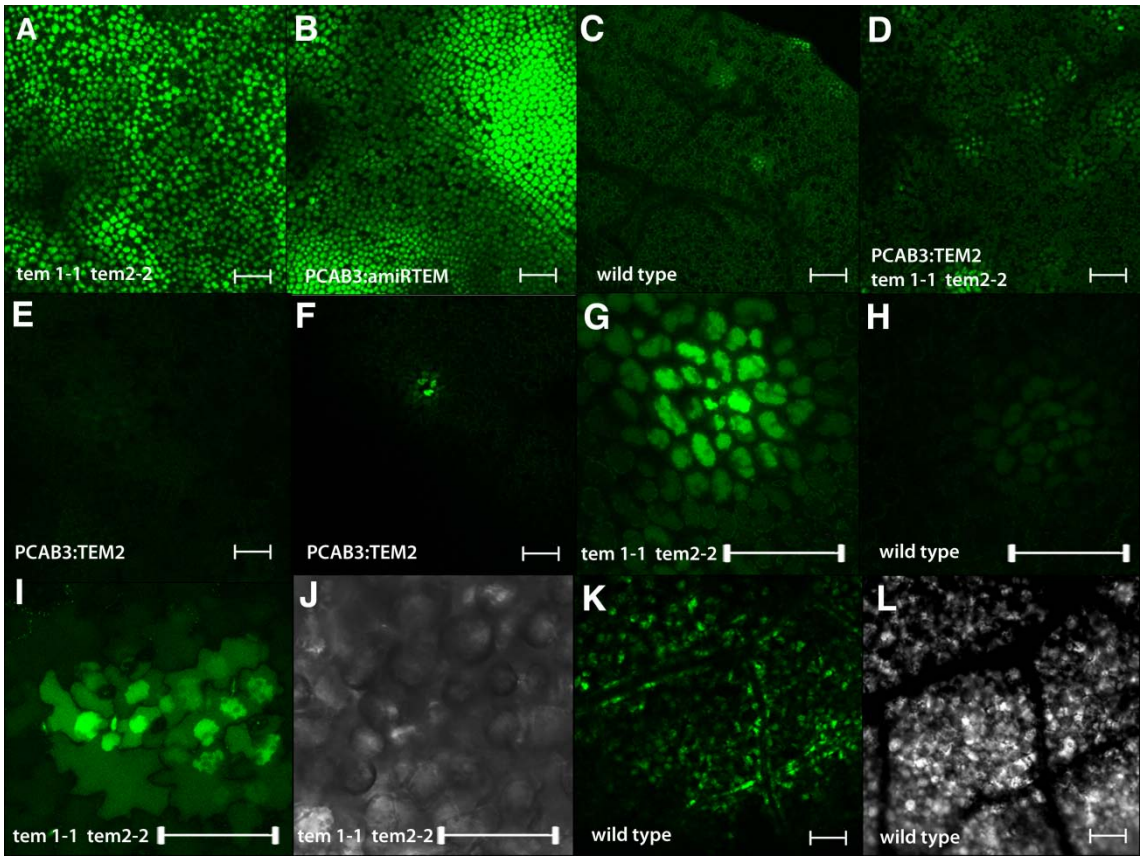

Supplemental Figure S3. Exogenous GA accumulation in the mesophyll is regulated by *TEMPRANILLO* at different stages of development

(A) to **(L)** *Arabidopsis* rosette leaf confocal sections of the first two rosette leaves in thirteen DAG plants.

(A) to **(F)** GA_3-Fl also accumulates exclusively in the mesophyll in thirteen DAG plants. GA_3-Fl accumulates with a higher intensity and it is distributed in a much bigger area in the mesophyll of *tem1-1 tem2-2* **(A)**, and *PCAB3:amiRTEM* **(B)** rosette leaf plants. On the other side, mesophyll fluorescence signal is much lower in wild type **(C)**, *PCAB3:TEM2* in *tem1-1 tem2-2* **(D),** while GA3-Fl accumulation in *PCAB3:TEM2* plants is absent **(E)**. Only two small patches of GA_3-Fl accumulation has been detected among all the plants analyzed (**F**).

(G) and **(H)** GA_3-Fl accumulates not only in bigger quantity but also shows a higher intensity in *tem1-1 tem2-2* **(G)** than in wild type **(H)**.

(I) to **(L)** In rare and exceptional cases epidermal cells were stained, probably due to saturation in areas of the rosette leaf where GA3-Fl was strongly accumulated in the mesophyll **(I)** and **(J)**. A very few examples of accumulation in companion cells of the vascular tissue were also detected **(K)** and **(L). (J)** and **(L)** images taken in bright field.

Scale bars from **(A)** to **(L)** represent 100.

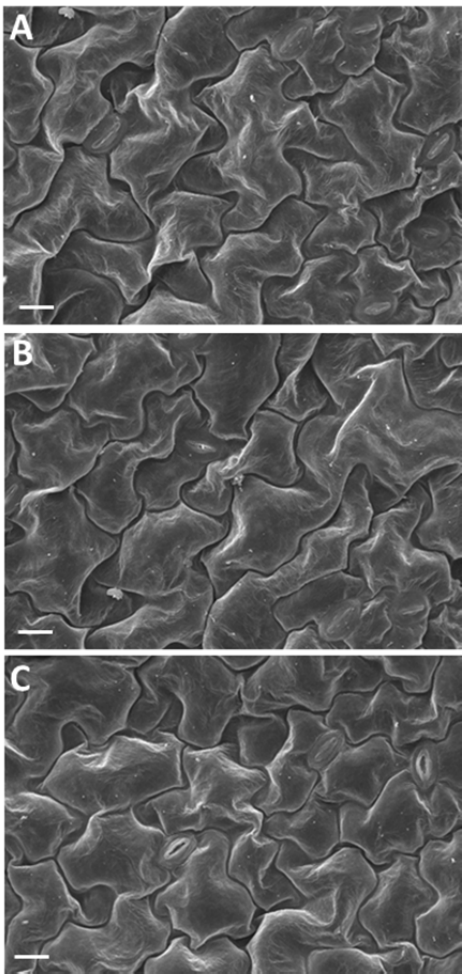

Supplemental Figure S4. SEM of abaxial epidermal cells

Scanning electron micrographs of eleven DAG rosette leaves grown under LD. Images show adaxial epidermal surfaces of the central part of rosette leaves of *PCAB:amiRTEM* **(A)**, wild-type **(B)** and *PCAB·:TEM2* **(C)** plants. As expected, plants that silence and overexpress *TEM* exclusive mesophyll showed normal epidermal cells. Scale bars represent 10μm

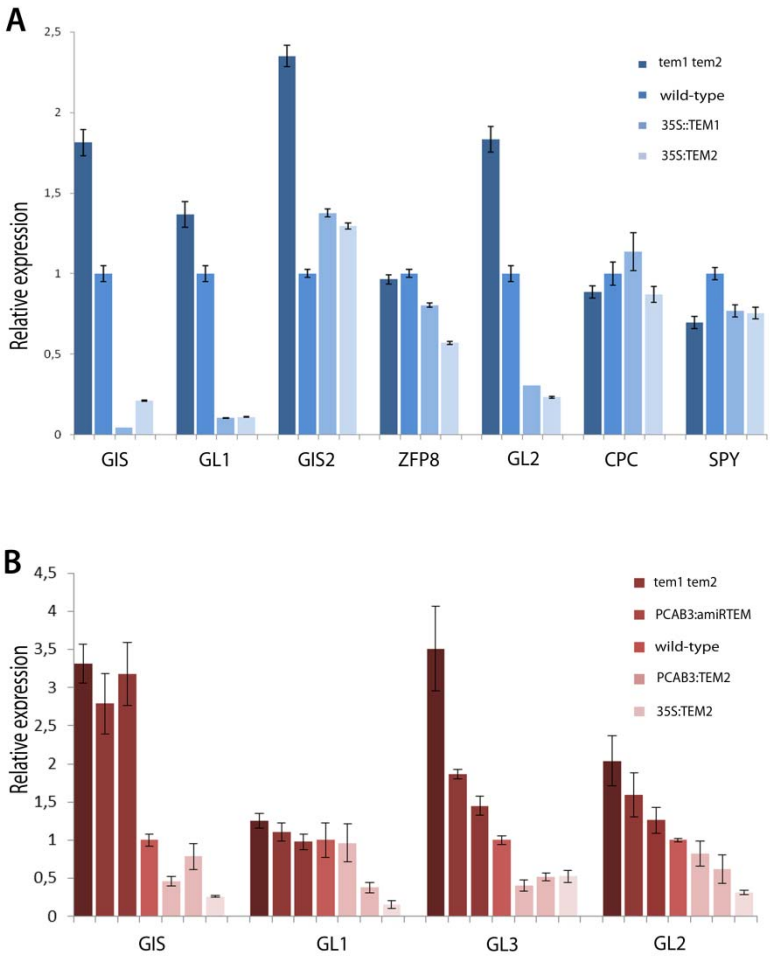

Supplemental Figure S5. Before bolting *TEMPRANILLO* regulates GA- but not CK-dependent trichome gene expression.

(A) Expression analysis of GA- and CK-trichome pathway main genes were done in *tem1 tem2,* wild-type and *P35S:TEM2* seedlings at eleven DAG grown under LD. At eleven DAG, plants have not produced any inflorescence organs. These results are consistent with the fact that CK-dependent pathways are not functional during this stage.

(B) Expression analysis of GA- pathway main genes were done in *tem1 tem2, PCAB:amiRTEM,* wild-type, *PCAB·:TEM2, P35S:TEM1* and *P35S:TEM2* seedlings at eleven DAG grown under LD.

Samples were collected at ZT18. For expression analyses, three biological replicates were performed with similar results. One representative is shown with error bars of three qPCR replicates.

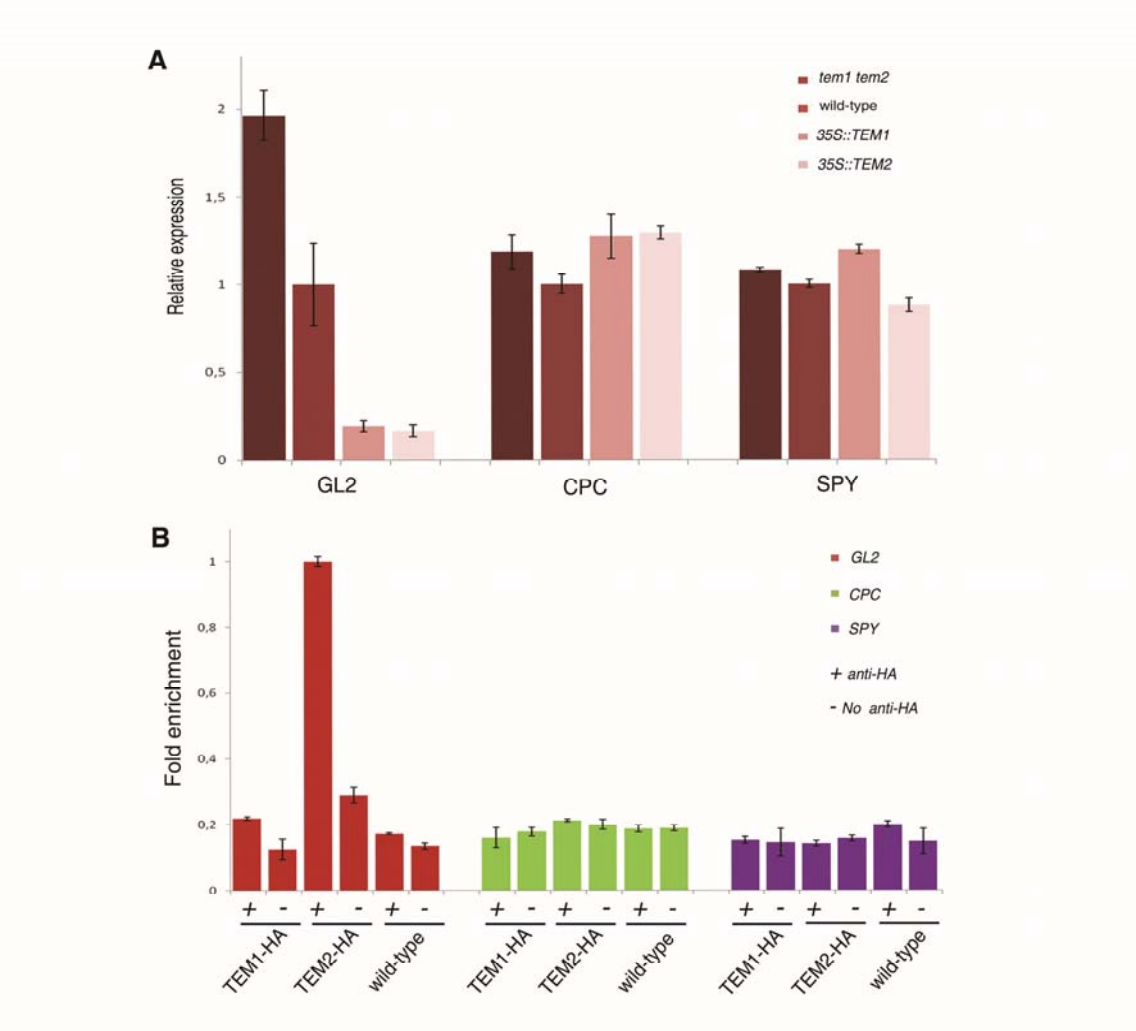

Supplemental Figure S6. Regulation of other trichome genes by *TEMPRANILLO*.

(A) Relative expression levels of *CPC* and *SPY* genes in mutants and overexpressors of *TEM* genes five DAB grown under LD. *CPC* and *SPY* genes seem not to be affected by differential *TEM* expression. *GL2* was used as a positive control. Three biological replicates were performed with similar results, one representative is shown with error bars of three qPCR replicates.

(B) ChIP analysis of TEM1 and TEM2 binding to *GL2*, *CPC*, and *SPY* regulatory regions. Relative enrichment of binding of either TEM1 and/or TEM2 to the regulatory regions of *CPC* and *SPY* was not detected. For expression and ChIP analyses, at least two biological replicates giving similar results were performed. One representative is shown with error bars of three qPCR replicates. TEM binding sites in the regulatory regions are localized 995-1138 bp upstream *GL2* starting codon, 975-847 bp upstream *CPC* starting codon and 1402-1268 bp downstream SPY starting codo

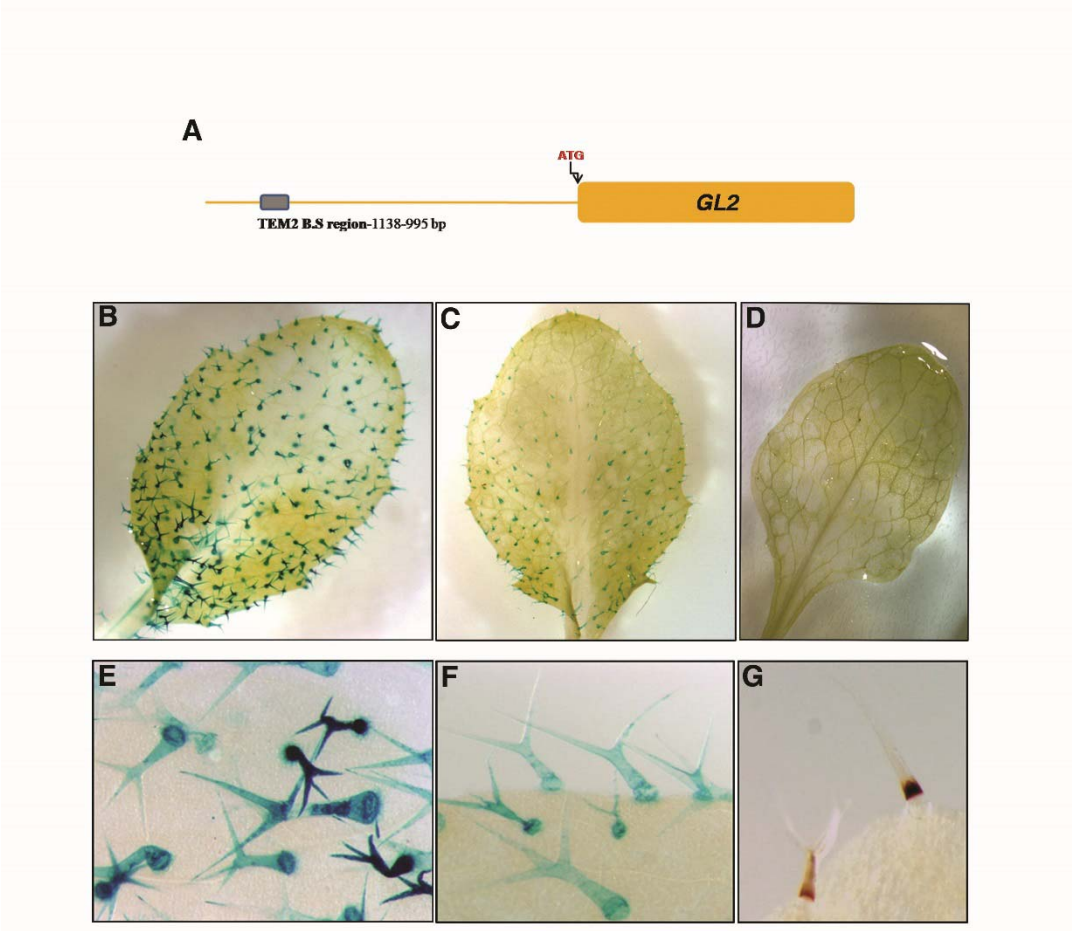

Supplemental Figure S7. *TEM* affects trichome *pGL2:GUS* activity

(A) TEM binding site (B.S.) region is localized 995-1138 bp upstream the *GL2* starting codon.

(**B**) to **(G)** Spatio/temporal *GL2* expression pattern analysis in different *TEM* backgrounds. *PGL2:GUS* include the region where TEM2 is able to bind in vivo to the regulatory region of *GL2*.

(**B**) to **(D)** *PGL2:GUS* expression in fully developed rosette leaves of *tem1*-1 *tem2*-2 (**B**), wild type (**C**) and *P35S:TEM2* (**D**) plants.

(E) to **(G)** close-up of trichomes of *tem1-1 tem2-2* (**E**), wild type (**F**) and *P35S:TEM2* (**G**) leaves.

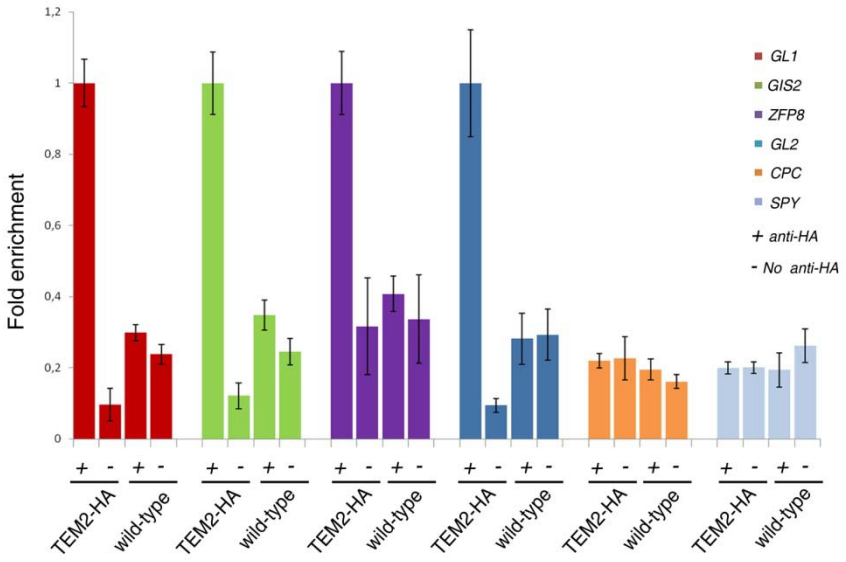

Supplemental Figure S8. *TEM2* binds *in vivo* to the main GA- and CK-dependent trichome genes in plants that have not yet flowered.

Precipitated chromatin was used for ChIP analyses in seedlings eleven DAG grown under LD. Relative enrichment of TEM2 binding to the regulatory regions of *GL1*, *GIS2*, *ZFP8* and *GL2* was similarly detected as in plants five DAB. Despite *GIS2* and *ZFP8* expression seem not to be controlled by TEM at eleven DAG; we observed TEM2 binding to their regulatory regions. On the contrary, relative enrichment of either TEM1 and/or TEM2 binding to the regulatory regions of *CPC* and *SPY* was not detected. For ChIP analyses, at least two biological replicates giving similar results were performed. One representative is shown with error bars of three qPCR replicates.

TEM binding sites in the regulatory regions are localized 2122-1926 bp upstream *GL1* starting codon, 293-372 bp downstream *GIS2* starting codon, 153 upstream and 26 downstream *ZFP8* starting codon, 995-1138 bp upstream *GL2* starting codon, 975-847 bp upstream *CPC* starting codon and 1402-1268 bp downstream SPY starting codon.

Supplemental Table S1. Trichome number and density on different TEM genetic backgrounds.

Fig.1	Trichome Number	Area cm2	Density (trcs/cm2)
tem1 tem2	201,55	0,9690164	208,000149
tem2-2	148,6	0,926794	160,3376802
tem1-1	110	0,81538	134,906424
wild-type	106,6	0,8054632	132,3462077
P35S:TEM1	12,2	0,3212	37,98256538
P35S:TEM2	6,5	0,331032	19,63556393
Fig.2			
tem1 tem2	217	1,121636364	193,4673367
tem2-2	185	1,025090909	180,4717985
tem1-1	118,66	0,952545455	124,5784819
wild-type	117	0,966363636	121,0724365
ga3ox1-3	101,66	0,952909091	106,6908351
ga3ox1 ga3ox2	73,16	0,809818182	90,34949858
P35S:TEM1	10,33	0,354	29,19020716
P35S:TEM2	5,5	0,360909091	15,23929471
Fig.5A			
wild-type	107,8	1,441602487	74,77789541
PCAB3:TEM2.1	80	1,588842025	50,35113543
PCAB3:TEM2.2	25,5	1,583245048	16,10616123
PCAB3:TEM1.1	27,2	1,271313491	21,39519497
PCAB3:TEM1.2	29	1,403051876	20,66922863
P35S:TEM1	16,87	0,519423511	32,48794025
P35S:TEM2	15,66	0,557099166	28,12186341
Fig.5B			
wild-type	122,4	1,032204514	118,5811516
PCAB3:TEM1.4	163,3	1,218993917	133,9629326
PCAB3:TEM1.3	156,3	1,326283807	117,8480799
PCAB3:TEM2.2	132,8	1,36265547	97,45676944
PCAB3:TEM2.4	133	1,13175249	117,516861
tem1 tem2	278,5	1,592378211	174,895636
Fig.5C			
wild-type	136,9	1,400062148	97,78137361
PCAB3:amiRTEM.14.1	196,6	1,509706498	130,2239875
PCAB3:amiRTEM.15.1	193,1	1,333280029	144,8307901
PCAB3:amiRTEM.13.3	223,3	1,315637382	169,7276188
PCAB3:amiRTEM.10.2	226	1,212163613	186,443478
tem1 tem2	257,8	1,498333757	172,0577934

Fig.5D	Trichome Number	Area cm2	Density (trcs/cm2)
P35S:TEM2	7,65	0,335918604	22,773374
cue1-6	33,2	0,290443161	114,3080798
wild-type	150,1	0,703919883	213,2344938
P35S:TEM2	6,75	0,393333055	17,16102911
cab3	42,1	1,261318888	33,3777607
wild-type	105,4	1,217690273	86,55731454
Fig.6A			
wild-type	199,1	1,432499178	138,9878634
wild-type + GA_3	233,7	1,455785305	160,5319131
PCAB3:TEM2	92,6	1,33098127	69,57272959
PCAB3:TEM2 + GA_3	184,4	1,517453302	121,5193902
P35S:TEM2	2,95	0,328778981	8,972593048
P35S:TEM2 + GA_3	9,3	0,4227191	22,00042534
Fig.6B			
wild-type	149,2	1,205142165	123,8028212
PCAB3:TEM2	56,2	1,173875707	47,87559676
PCAB3:TEM2 +GA_3-Fl	123,6	1,1388142	108,5339469
P35S:TEM2	4,35	0,39631499	10,97611776
P35S:TEM2 +GA_3-Fl	13,4	0,402514242	33,29074749

Supplemental Table S2. List of primers used for cloning and ChIP

Name	Sequence
CAB3-BamHI	CGGGATCCGAAACTTTTTGTGTTTTTTTTTTTTTTTG
CAB3-SalI	CGGTCGACAATCAAGAGAAAATGTGATTCTCGG
seq-pCAB3 369 for	CATCCTCTGTGGACCAGGTT
seq-pCAB3 555 for	AATTGCGTTCCAAAGAGTGG
seq-pCAB3 1258 for	GCTGCTTCCAAAAGACTTGC
TEM2::GUS FOR	CACCATCACGCCATGTCCACAATA
TEM2::GUS REV	GATTCTCACCAAACCAAGAAAC
RT-GL2 for	GGACGAGAAGCAAAGACAGC
RT-GL2 rev	TCTCTAGTTCCGCCTTGAGC
ChIP-GL1 for	ATGTCTGCATGTTTCCCTGT
ChIP-GL1ch rev	TCAGTGTCTTGTTGGTGTTGC
ChIP-GIS2ch for	ACCGCCAACAAAACCACATT
ChIP-GIS2ch rev	CGCGTCGTTGATTTGAACAG
ChIP-ZFP8ch for	GCTGCAGGGGTTAAATAGCA
ChIP-ZFP8ch rev	TCTCTTCGTCCGTTGGTTTC
ChIP-pGL2 for	CCGCTGCTGAATTACATTTG
ChIP-pGL2 rev	GGGGTATGTACGTAGCAGTATTAGG
ChIP-CPCch for	GGTCTCGAGATGTGGTTAAAGC
ChIP-CPCch rev	TTGGTCTGATGGTAATGTCGTC
ChIP-SPYch for	CCAATGAATACCAAATGAATTGAC
ChIP-SPYch rev	TGAAGTGGGAAATGGATCAAG
RTNPF2.3 For	CATCTGGAGGCTATGCTCTG
RTNPF2.3 Rev	GCCGGGACTTTGAAATTAGG
RTNPF3.1 For	ATGTGAGCACTTTGCTGGTG
RTNPF3.1 Rev	TCTTGGCGCACCATAGATAA
RTGTR1 For	GAATCGGAGCTGGGTTTACA
RTGTR1 Rev	GCAAGTGTAAGCTGCGGAAT

Supplemental Table S3. Statistical analyses of data from Figures 1, 2, 4, 5, 6 & 7.

ns: not significant. Asterisks indicate statistically significant differences (* $p \leq 0.05$, ** $p \leq 0.01$, *** $p \leq 0.001$).

Fig 1G	**Significance**	***p*-value**
WT vs *tem1 tem2*	***	< 0,0001
WT vs *tem1*	ns	0.965
WT vs *tem2*	***	< 0,0001
WT vs 35S::TEM2	***	< 0,0001
WT vs 35S::TEM2	***	< 0,0001
Fig 2A	**Significance**	***p*-value**
GA9 WT vs *tem1 tem2*	ns	0,2938
GA9 WT vs 35S::TEM2	***	0,0005
GA4 WT vs dm	*	0,0115
GA4 WT vs 35S	ns	0,1583
Fig 2B	**Significance**	***p*-value**
WT vs *tem1 tem2*	***	< 0,0001
WT vs *tem1*	ns	1
WT vs *tem2*	***	< 0,0001
WT vs ga3ox1	ns	0.066
WT vs ga3ox1 ga3ox2	***	< 0,0001
WT vs 35S::TEM2	***	< 0,0001
WT vs 35S::TEM2	***	< 0,0001
Fig 4A	**Significance**	***p*-value**
GA3ox1 WT vs *tem1 tem2*	***	< 0,0001
GA3ox1 WT vs PCAB3::amiRTEM13.3	*	0,0221
GA3ox1 WT vs PCAB3:.amiRTEM10.2	ns	0,8292
GA3ox1 WT vs PCAB3::TEM2.1	*	0,0162
GA3ox1 WT vs PCAB3::TEM2.2	**	0,0032
GA3ox1 WT vs 35S::TEM2	*	0,0126
GA3ox2 WT vs *tem1 tem2*	***	0,0008
GA3ox2 WT vs PCAB3::amiRTEM13.3	***	0,0003
GA3ox2 WT vs PCAB3:.amiRTEM10.2	**	0,0011
GA3ox2 WT vs PCAB3::TEM2.1	ns	0,7668
GA3ox2 WT vs PCAB3::TEM2.2	ns	0,1886
GA3ox2 WT vs 35S::TEM2	*	0,032
Fig 4H	**Significance**	***p*-value**
GTR1 WT vs *tem1 tem2*	***	< 0,0001
GTR1 WT vs 35S::TEM2	***	< 0,0001
NPF3.1 WT vs *tem1 tem2*	***	< 0,0001
NPF3.1 WT vs 35S::TEM2	***	< 0,0001
NPF2.3 WT vs *tem1 tem2*	***	0,0004
NPF2.3 WT vs 35S::TEM2	***	< 0,0001
Fig 5A	**Significance**	***p*-value**

WT vs pCAB3::TEM2.1	***	< 0,0001
WT vs *pCAB3::TEM2.2*	***	< 0,0001
WT vs pCAB3::TEM1.1	***	< 0,0001
WT vs pCAB3::TEM1.2	***	< 0,0001
WT vs 35S::TEM2	***	< 0,0001
WT vs 35S::TEM2	***	< 0,0001
Fig 5B	**Significance**	***p*-value**
tem1 tem2 vs WT	***	< 0,0001
tem1 tem2 vs pCAB3::TEM2.2	***	< 0,0001
tem1 tem2 vs pCAB3::TEM2.4	***	< 0,0001
tem1 tem2 vs pCAB3::TEM1.3	***	< 0,0001
tem1 tem2 vs pCAB3::TEM1.4	***	< 0,0001
Fig 5C	**Significance**	***p*-value**
WT vs pCAB3::amiRTEM.14.1	***	< 0,0001
WT vs pCAB3::amiRTEM.15.1	***	< 0,0001
WT vs pCAB3::amiRTEM.13.3	***	< 0,0001
WT vs pCAB3::amiRTEM.10.2	***	< 0,0001
WT vs tem1 tem2	***	< 0,0001
Fig 5D	**Significance**	***p*-value**
WT vs cue1-6	***	< 0,0001
WT vs 35S::TEM2	***	< 0,0001
WT vs cab3	***	< 0,0001
WT vs 35S::TEM2	***	< 0,0001
Fig 6A	**Significance**	***p*-value**
MOCK WT vs GA WT	***	< 0,0001
MOCK pCAB3::TEM2 vs GA pCAB3::TEM2	***	< 0,0001
MOCK 35S::TEM2 vs GA 35S::TEM2	***	< 0,0001
Fig 6B	**Significance**	***p*-value**
MOCK pCAB3::TEM2 vs GA3-FI pCAB3::TEM2	***	< 0,0001
MOCK 35S::TEM2 vs GA3-FI 35S::TEM2	**	0.005
Fig 6C	**Significance**	***p*-value**
CK WT vs *tem1 tem2*	**	0,0023
CK WT vs 35S::TEM2	*	0,0247
Fig 7A	**Significance**	***p*-value**
GIS WT vs *tem1 tem2*	**	0,0041
GIS WT vs 35S::TEM1	***	< 0,0001
GIS WT vs 35S::TEM2	***	< 0,0001
GL1 WT vs *tem1 tem2*	*	0,0188
GL1 WT vs 35S::TEM1	***	0,0003
GL1 WT vs 35S::TEM2	***	0,0003
GL3 WT vs *tem1 tem2*	ns	0,1361
GL3 WT vs 35S::TEM1	*	0,0103
GL3 WT vs 35S::TEM2	*	0,0157
EGL3 WT vs *tem1 tem2*	*	0,0102

EGL3 WT vs 35S::TEM1	**	0,0031
EGL3 WT vs 35S::TEM2	**	0,0031
TTG1 WT vs *tem1 tem2*	ns	0,5591
TTG1 WT vs 35S::TEM1	**	0,0039
TTG1 WT vs 35S::TEM2	**	0,0039
GIS2 WT vs *tem1 tem2*	***	0,0002
GIS2 WT vs 35S::TEM1	***	0,0008
GIS2 WT vs 35S::TEM2	***	0,0007
ZFP8 WT vs *tem1 tem2*	***	0,0001
ZFP8 WT vs 35S::TEM1	**	0,0037
ZFP8 WT vs 35S::TEM2	***	0,0009
GL2 WT vs *tem1 tem2*	**	0,0036
GL2 WT vs 35S::TEM1	**	0,004
GL2 WT vs 35S::TEM2	**	0,0035

Fig 7B	**Significance**	***p*-value**
GL1 35S:TEM2 No Ab vs 35S:TEM1 anti-HA	ns	0,3039
GL1 35S:TEM2 No Ab vs 35S:TEM1No Ab	ns	0,1086
GL1 35S:TEM2 No Ab vs 35S:TEM2 anti-HA	**	0,002
GL1 35S:TEM2 No Ab vs WT anti-HA	**	0,0026
GL1 35S:TEM2 No Ab vs WT No Ab	**	0,0029
GIS2 35S:TEM2 No Ab vs 35S:TEM1 anti-HA	*	0,0242
GIS2 35S:TEM2 No Ab vs 35S:TEM1No Ab	ns	0,4425
GIS2 35S:TEM2 No Ab vs 35S:TEM2 anti-HA	***	0,0003
GIS2 35S:TEM2 No Ab vs WT anti-HA	***	< 0,0001
GIS2 35S:TEM2 No Ab vs WT No Ab	***	< 0,0001
ZFP8 35S:TEM2 No Ab vs 35S:TEM1 anti-HA	ns	0,135
ZFP8 35S:TEM2 No Ab vs 35S:TEM1No Ab	**	0,0086
ZFP8 35S:TEM2 No Ab vs 35S:TEM2 anti-HA	***	0,0007
ZFP8 35S:TEM2 No Ab vs WT anti-HA	ns	0,9702
ZFP8 35S:TEM2 No Ab vs WT No Ab	ns	0,6214
GL2 35S:TEM2 No Ab vs 35S:TEM1 anti-HA	**	0,0077
GL2 35S:TEM2 No Ab vs 35S:TEM1No Ab	**	0,0018
GL2 35S:TEM2 No Ab vs 35S:TEM2 anti-HA	***	< 0,0001
GL2 35S:TEM2 No Ab vs WT anti-HA	**	0,0011
GL2 35S:TEM2 No Ab vs WT No Ab	***	0,0005

CONCLUSIONES

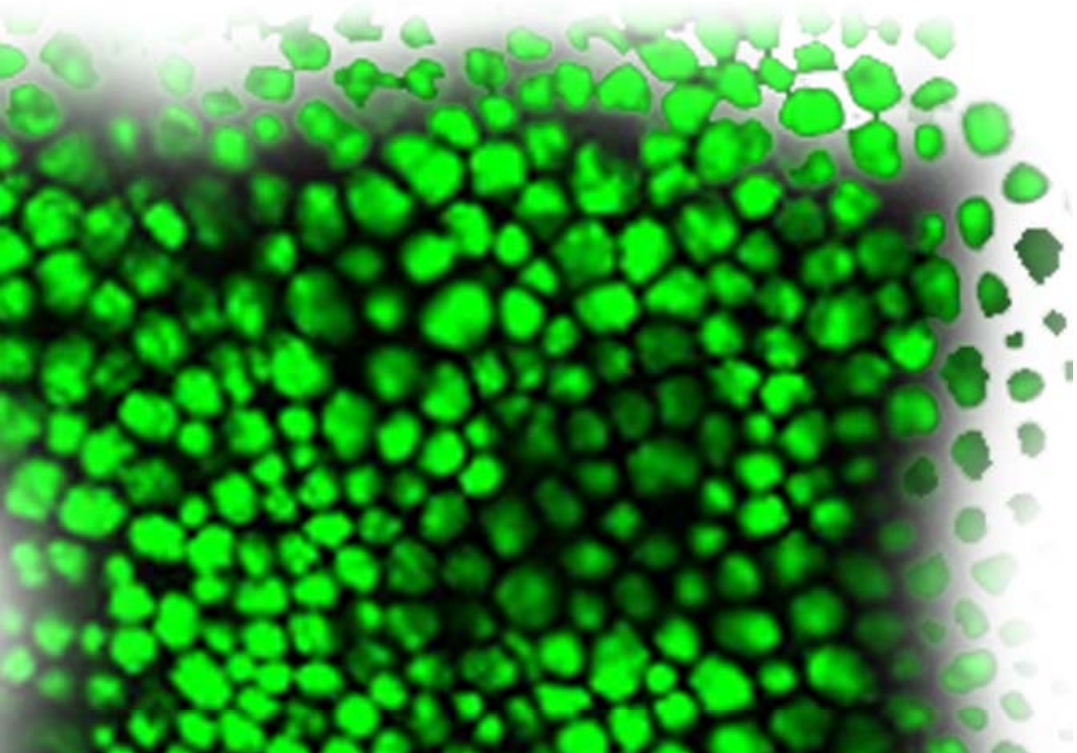

CONCLUSIONES GENERALES

A continuación se describen las conclusiones más relevantes de los tres trabajos realizados.

1. Los genes *TEMPRANILLO* tienen un papel importante en la ruta dependiente de la edad, en la que regulan la transición de la fase juvenil a la adulta y de forma más acusada la floración.

2. TEM1 y TEM2 regulan positivamente, aunque de una manera débil, a miR156, y además TEM1 se une *in vivo* a la cromatina de *MIR156A,* aunque no descartamos una regulación indirecta a través de un *feed-back loop* de los genes diana de miR156.

3. Los genes *TEM* regulan negativamente la expresión de *SPL9* y miR172. Además, se encontró que TEM1 es capaz de unirse *in vivo* a la cromatina de *SPL9* y *MIR172C.*

4. Los TEM además de regular directamente a *SPL9* y miR172, también podrían regularlos de forma indirecta a través miR156.

5. Los TEM regulan la transición de la fase juvenil a la adulta y la floración a través de rutas dependientes e independientes de miR156.

6. Los genes *TEM* desempeñan un papel en la represión floral a temperaturas bajas (16ºC).

7. Las temperaturas bajas provocan un aumento en los niveles de expresión de *TEM*, lo cual se correlaciona con la reducción de los niveles de *FT* y *TSF*, provocando una floración tardía.

8. A 16 ºC *TEM2* reprime directamente la expresión de *FT* y *TSF*.

9. SVP regula directamente a *TEM2*, pero no a *TEM1*, a 16°C. La represión de la floración por SVP está mediada parcialmente por TEM2.

10. Los genes *TEM1* y *TEM2*, por tanto, controlan el tiempo de floración en al menos cuatro rutas genéticas: la del fotoperíodo o longitud del día (Castillejo y Pelaz, 2008), la de las temperaturas bajas (Capítulo II; Marín-González et al., 2015), la de las

GAs (Osnato et al, 2012) y la de la edad (Capítulo I; Aguilar-Jaramillo et al., manuscrito en preparación).

11. Por otro lado, los genes *TEM* controlan negativamente otro proceso biológico, la iniciación de los tricomas, actuando en dos capas celulares de la hoja: la epidermis y el mesófilo.

12. En la epidermis, los TEM reprimen directamente la expresión de varios genes esenciales encargados de la formación de los tricomas, tales como *GL1*, *GL3* y *EGL3*.

13. En el mesófilo, los TEM reprimen la iniciación de los tricomas a través de la represión de la biosíntesis de las GAs y de su distribución, mediante el control de la expresión de los transportadores NPFs.

OTRAS PUBLICACIONES

Journal of Experimental Botany, Vol. 67, No. 5 pp. 1209–1219, 2016
doi:10.1093/jxb/erv534 Advance Access publication 17 December 2015

FLOWERING NEWSLETTER REVIEW

Flowering and trichome development share hormonal and transcription factor regulation

Luis Matías-Hernández[1,2], Andrea E. Aguilar-Jaramillo[1], Riccardo Aiese Cigliano[2], Walter Sanseverino[2] and Soraya Pelaz[1,3,*]

[1] Centre for Research in Agricultural Genomics, CSIC-IRTA-UAB-UB, Campus UAB, Bellaterra (Cerdanyola del Vallès) 08193 Barcelona, Spain
[2] Sequentia Biotech, Parc Científic de Barcelona (PCB), 08028 Barcelona, Spain
[3] ICREA (Institució Catalana de Recerca i EstudisAvançats), Barcelona, Spain

* Correspondence: soraya.pelaz@cragenomica.es

Received 3 August 2015; Accepted 24 November 2015

Editor: Lars Hennig, Swedish University of Agricultural Sciences

Abstract

Gibberellins (GAs) and cytokinins (CKs) are plant hormones that act either synergistically or antagonistically during the regulation of different developmental processes. In *Arabidopsis thaliana*, GAs and CKs overlap in the positive regulation of processes such as the transition from the vegetative to the reproductive phase and the development of epidermal adaxial trichomes. Despite the fact that both developmental processes originate in the rosette leaves, they occur separately in time and space. Here we review how, as genetic and molecular mechanisms are being unraveled, both processes might be closely related. Additionally, this shared genetic network is not only dependent on GA and CK hormone signaling but is also strictly controlled by specific clades of transcription factor families. Some key flowering genes also control other rosette leaf developmental processes such as adaxial trichome formation. Conversely, most of the trichome activator genes, which belong to the MYB, bHLH and C2H2 families, were found to positively control the floral transition. Furthermore, three MADS floral organ identity genes, which are able to convert leaves into floral structures, are also able to induce trichome proliferation in the flower. These data lead us to propose that the spatio-temporal regulation and integration of diverse signals control different developmental processes, such as floral induction and trichome formation, which are intimately connected through similar genetic pathways.

Key words: Cytokinis, Floral induction, Flower organs, Gibberellins, Hormone siganling, Trichome formation.

Introduction

Flowering is one of the most critical developmental steps to ensure species perpetuation. Floral induction must occur at an appropriate time of the year to ensure offspring survival. Early flowering may result in poor flower and seed production as plants do not recruit enough reserves for an energy-consuming process, while late flowering may lead to a robust plant, but perhaps may jeopardize fruit maturation. As the time for floral induction is critical, both late induction and precocious flowering should be avoided. Consequently, plants constantly monitor environmental and endogenous signals to control their growth (Penfield, 2008). When plants are not competent to flower, they are insensitive to inductive environmental factors, while after the juvenile-to-adult transition plants reach the competence to respond to those signals (Bergonzi *et al.*, 2013; Huijser and Schmid, 2011). Indeed, flowering is controlled by a complex network of

interdependent genetic pathways that monitor and respond to both endogenous and environmental signals. Endogenous factors include hormones such as gibberellin (GA) and cytokinin (CK) (Mutasa-Göttgens and Hedden, 2009; Huijser and Schmid, 2011) and the age of the plant (Huijser and Schmid, 2011). Among the major environmental effectors are photoperiod, light intensity/quality and seasonal/daily changes in temperature (Thomas, 2006; Andrés and Coupland, 2012; Song *et al.*, 2012, 2013).

Plant fitness is an essential factor that may directly affect the success of plant reproduction. Not only environmental conditions but also insects can endanger proper plant development, including flower reproductive success. Herbivorous insect attacks can substantially decrease plant survival (Marquis and Alexander, 1992). Due to the fact that plant-insect encounters are not predictable, plants generally do not show high levels of resistance. However, plant plasticity creates the ability to respond rapidly to damage and to divert resistance resources for overcoming that damage (Agrawal, 2000). This plasticity most probably arose because plants are not able to move; consequently they have developed multiple physiological defense responses. Leaf trichomes are among these physiological defenses. Trichomes are epidermal protuberances that protect plants from the attack of herbivorous insects and develop even when plants are growing under optimal conditions (Traw and Bergelson, 2003). Interestingly, plasticity allows plants to respond to insect attacks by increasing the number and density of trichomes in new growing leaves, stems and flowers (Agrawal, 2000; Traw and Bergelson, 2003).

In many plant species trichomes are glandular multicellular structures able to produce, distribute and store toxic substances for protecting the plant against insect attacks (Olsson *et al.*, 2009), however *Arabidopsis thaliana* trichomes are unicellular and non-glandular structures (Hülskamp *et al.*, 2004). Despite not being able to store toxic substances, Arabidopsis trichome morphology, with a big size and three sharp terminations that develop on the adaxial surface of rosette leaves, reduce the access of herbivorous insects to leaf surface (Mauricio, 2005). But trichomes defend the plant not only against insects but also from other external factors such as an excess of UV light or high temperatures (Szymanski *et al.*, 2000; Schellmann *et al.*, 2007).

Adaxial rosette trichome initiation and development processes involve a complex genetic network. These include a multimeric complex, known as trichome activator complex, formed by a R2R3 MYB protein GLABROUS1 (*GL1*), two redundant trichome formation bHLH proteins, GLABRA3 (*GL3*) and ENHANCER OF GLABRA3 (EGL3), and a WD40 repeat containing protein, TRANSPARENT TESTA GLABRA 1 (TTG1) (Fig. 1) (Zhao *et al.*, 2008; Zhou *et al.*, 2011). Mutations in *GL1*, *TTG1*, and both *GL3*/*EGL3* result in Arabidopsis plants with a significant loss of trichomes (Payne *et al.*, 2000; Zhou *et al.*, 2011). In addition to that, this complex has not only a role in trichome initiation but also in later trichome development, as mutations in these genes result in smaller and less branched trichomes (Payne *et al.*, 2000).

It is accepted that the competency to enter the trichome pathway is limited to a few epidermal cells. Once an epidermal precursor is specified to acquire trichome cell fate, a mechanism of lateral inhibition towards the surrounding epidermal cells initiates (Langdale, 1998; Kirik *et al*, 2004*a*) (Fig. 1). This lateral inhibition mechanism involves cell-to-cell communication. Indeed, trichome activation factors such as GL3 and TTG1 also turn on negative regulators of trichome initiation as CAPRICE (CPC) and ENHANCER OF TRIPTYCHON AND CAPRICE 1 (ETC1), which subsequently move into neighboring epidermal pavement cells to prevent trichome formation (Zhao *et al*, 2008; Balkunde *et al*, 2010, 2011) (Fig. 1). In addition, these trichome positive regulators GL3 and TTG1 are also able to move among cells (Bouyer *et al*, 2008; Savage *et al*, 2008). CPC and ETC1 are not the only trichome repressors in Arabidopsis, others have been described to act as trichome inhibitors contributing to an elaborated and well-regulated genetic network that determines which epidermal cell may – or may not –morphogenetically become a trichome (Langdale, 1998; Kirik *et al*, 2004*a*). Interestingly, most of this trichome repressors including CPC, ETC1, ETC2, ETC3, TRICHOMELESS 1 (TCL1), TCL2 and TRIPTYCHON (TRY), belong to the R3-MYB TF family (Wang and Chen, 2014) (Fig. 1). Although TRY is the predominant member controlling trichome clustering on adaxial surface of rosette leaves (Schnittger *et al.*, 1998; Schellmann *et al.*, 2002), CPC, ETC1, ETC2 and ETC3 also regulate trichome development on leaves (Wada *et al.*, 1997, 2002; Esch *et al.*, 2004; Kirik *et al.*, 2004*a*, *b*; Tominaga *et al.*, 2008). However, TCL1 and TCL2 control trichome development mainly on inflorescence stems and pedicels (Wang *et al.*, 2007; Gan *et al.*, 2011). But not all these R3-MYB members are regulated by the trichome activator complex (GL1-TTG1-GL3/EGL3). Only *TRY*, *CPC*, *ETC1* and *ETC3* expressions are controlled by this multimeric complex in the rosette leaf, while *TCL1*, *TCL2* and *TRY* are regulated by an independent trichome pathway mediated by *microRNA156* (*miR156*) and *SQUAMOSA PROMOTER BINDING PROTEIN LIKE* (*SPL*) at least on the inflorescence stems (Yu *et al.*, 2010; Xue *et al.*, 2014). miR156-targeted SPL transcription factors not only play important roles in determining trichome initiation on the abaxial side of the rosette leaf but also on stems (Yu *et al.*, 2010; Xue *et al.*, 2014). Curiously enough, these genes also play a key role in controlling flowering through the age-dependent genetic pathway (Yu *et al.*, 2010; Xue *et al.*, 2014).

In the past decades, strong efforts have been made in the model plant Arabidopsis to unravel the different molecular and genetic mechanisms that regulate diverse cellular differentiation programs. Different results revealed that the network of transcriptional regulators affecting trichome proliferation are themselves affected by two plant hormones, GA and CK (Fig. 1), both of which are able to control and integrate diverse biological processes that occur at different cell levels (Schellmann *et al.*, 2002; Gan *et al.*, 2007; Zhao *et al.*, 2008). GA and CK are phytohormones required throughout plant development that contribute to and overlap in some plant developmental processes but they also have opposite

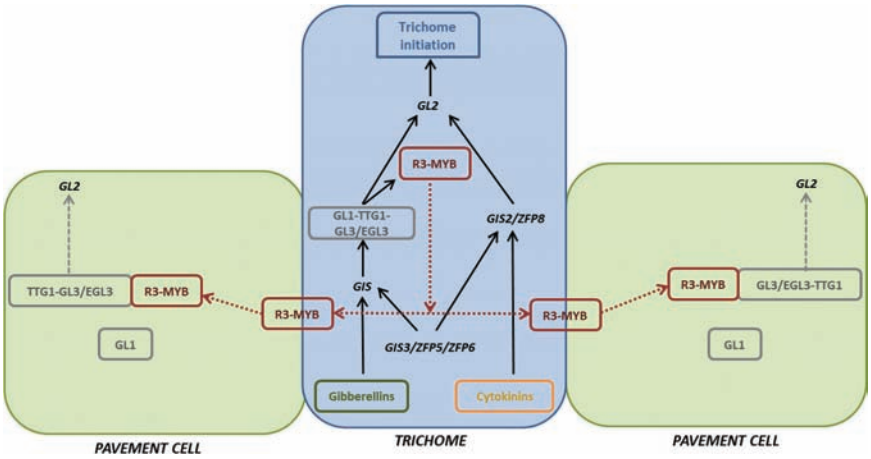

Fig. 1. Model for trichome and pavement cell fate specification in *Arabidopsis thaliana*. Trichome proliferation regulation is affected by gibberellins and cytokinins hormones through transcriptional regulation of the *GIS* clade genes: GIS, GIS2, and ZFP8. GIS2 and ZFP8 activate the trichome activator *GL2*, while GIS positively regulate some of the members of the trichome activation complex – *GL1, TTG1* and *GL3/EGL3* – that in turn activate *GL2* and, at the same time, R3-MYB repressor genes (black arrows). R3-MYB members that include CPC, ETC1, ETC2, ETC3, TCL1, TCL2 and TRY act as repressors of trichome initiation. Some of these R3-MYB move to the neighboring cells (dashed red lines) to prevent trichome formation, where they compete with GL1 for the interaction with GL3 and/or EGL3, thus limiting the activity of the trichome activation complex, and consequently decreasing *GL2* expression (dashed arrow).

roles in others (Zhang *et al.*, 2003). For instance, GA and CK act antagonistically in leaf formation and meristem maintenance and GA counteracts the CK effect in epidermal differentiation (Gan *et al.*, 2007). However, both hormones have synergistic effects on the constitutive induction of epidermal defensive trichomes, floral induction, valve margins and senescence suggesting that genetic interactions may be shared between these two hormonal signaling pathways (Chien and Sussex, 1996; Perazza *et al.*, 1998; Corbesier *et al.*, 2003; Traw and Bergelson, 2003; Gan *et al.*, 2007; D'Aloia *et al.*, 2011; Marsch-Martinez *et al.*, 2012; Pattanaik *et al.*, 2014). The fact that phytohormones play independent and overlapping functions may imply that the spatio-temporal pattern and integration of diverse signals through downstream regulators are of great importance. Two possible strategies have been described so far to explain plant hormone integration. The first one uses a centralized system of upstream hormone signaling integrators, such as the DELLA family, that are able to control plant growth in combination with hormones such as GA, auxin, ethylene and abscisic acid (Silverstone *et al.* 1998; Fu and Harberd, 2003; Achard *et al.*, 2006). The second strategy uses more specialized regulators such as transcription factors that may act downstream controlling the specific gene networks of different developmental processes, but without excluding an upstream regulation (Nemhauser *et al.*, 2006). This review will focus on how a small number of proteins may use one or both strategies for regulating upstream and downstream steps of floral induction and trichome formation by integrating the control of hormone signaling and diverse genetic networks.

Gibberellins and their positive role in flowering and trichome formation

GAs regulate different plant growth and developmental processes that span from seed germination to the control of last processes in the plant life cycle, such as senescence, leaf expansion, hypocotyl and stem elongation (Fig. 2) (Chien and Sussex, 1996; Perazza *et al.*, 1998; Davis, 2009). The GA biosynthetic pathway follows a complex regulatory network that leads to the final production of the GA bioactive form, GA_4 (Mitchum *et al.*, 2006). Most of the genes encoding enzymes of the GA biosynthetic pathway have been well studied (Olszewski *et al.*, 2002). For example, *GA3OXIDASE 1* (*GA3OX1*) and *GA3OX2* encode enzymes that transform GA_9 into the bioactive GA_4, but there are other important enzymes, such as *GA2OXIDASE*, which catabolizes an excess of GA_4 (Mitchum *et al.*, 2006). Therefore, a proper balance between the biosynthetic and catabolic enzymes is of essential importance for keeping a correct amount of GA.

In Arabidopsis, bioactive GAs promote floral induction as well as some other aspects of flower development, such as petal, stamen and viable pollen formation (Koornneef and van der Veen, 1980). GAs are also mobile signals that travel from the leaves to the shoot apical meristem (SAM) to induce the florigen *FLOWERING LOCUS T* (*FT*) and *SUPRESSOR OF OVEREXPRESSION OF CONSTANS1* (*SOC1*) in order to trigger flowering (Fig. 3) (Corbesier *et al.*, 2007; Mathieu *et al.*, 2007). Flowering is induced by GA under both inductive long-days (LD) (16 h light/8 h dark) and non-inductive short-day (SD) (8 h light/16 h dark) conditions, although GAs have a stronger effect controlling floral induction under SD conditions (Wilson *et al.*, 1992; Blázquez *et al.*, 1998; Nilsson *et al.*, 1998). Under SD conditions, GA are able to activate the floral integrator *SOC1* and the floral meristem identity gene *LEAFY* (*LFY*) in the SAM (Blázquez *et al.*, 1998; Moon *et al.*, 2003) (Fig. 3). Trichome proliferation and branching are also among the processes controlled by GA (Smyth *et al.*, 1990; Dill and Sun, 2001). External GA applications increase trichome density in leaves and stems of Arabidopsis (Perazza *et al.*, 1998; Gan *et al.*, 2006).

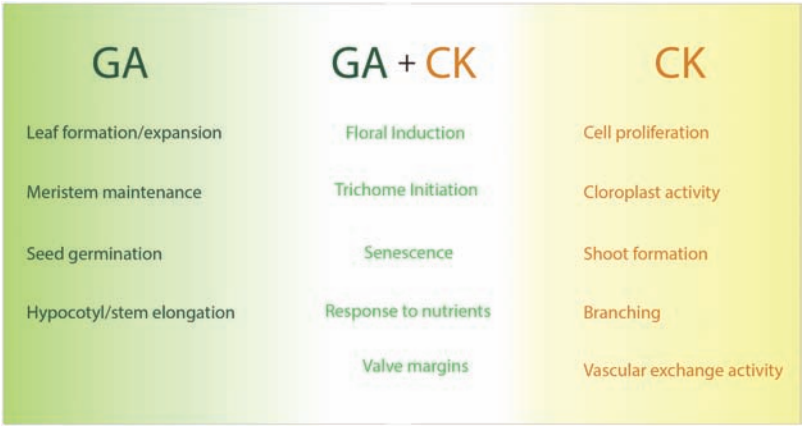

Fig. 2. Diagram showing GA- and CK-dependent overlapping and non-overlapping biological processes. GA and CK phytohormones regulate different plant growth and developmental processes that span from early stages during seed germination to the control of the final processes in the plant life cycle. Despite GA and CK acting antagonistically in several biological processes showed here, both hormones have synergistic effects on floral induction, trichome initiation, valve margins development, senescence and responses to nutrients availability.

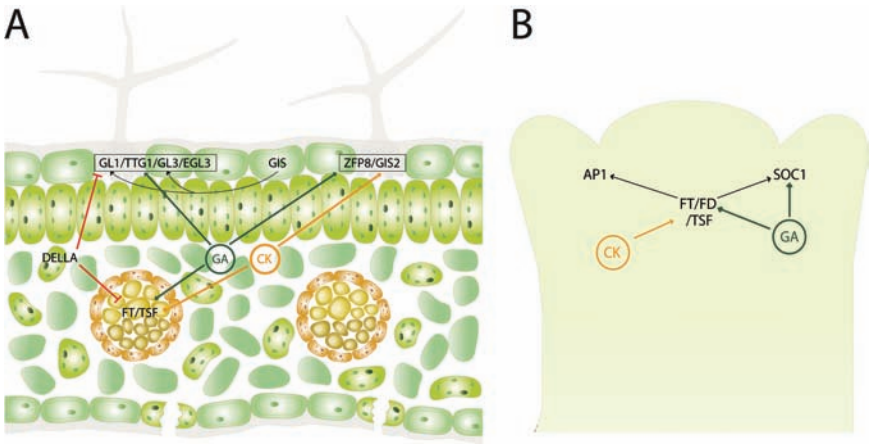

Fig. 3. The transcriptional regulatory network that affects floral and adaxial trichome induction at different organ, tissue and cell levels. (A) In rosette leaves, this complex network is partially controlled by GA and CK hormones that overlap in positively regulating the transcription of diverse trichome- and flowering-genes in either leaf mesophyll or epidermis. (B) Similar transcriptional regulation for the control of floral induction is found in the shoot apical meristem (SAM).

GA3OX1 and *GA3OX2* functions overlap during Arabidopsis development, showing functional redundancy not only in stimulating flowering but also in trichome development (Mitchum, 2006). *ga3ox1 ga3ox2* double mutant plants are semi-dwarf, late flowering and bear a reduced number of trichomes on rosette leaves, stems and flowers (Koornneef and van der Veen, 1980; Chiang *et al.*, 1995; Mitchum *et al.*, 2006). In general, mutant plants in which GA biosynthesis genes have been knocked down and are unable to produce normal GA levels, produce leaves with fewer trichomes (Chien and Sussex, 1996; Traw and Bergelson, 2003). In fact, when GA are exogenously sprayed on an Arabidopsis wild-type plant, rosette leaf adaxial trichome production is significantly increased (Chien and Sussex, 1996), while plants treated with GA biosynthesis inhibitors such as paclobutrazol and uniconazole are not able to produce trichomes (Chien and Sussex, 1996; Perazza *et al.*, 1998).

In Arabidopsis, functional redundancy in GA signalling has been attributed not only to the GA biosynthetic enzymes but also to DELLA proteins (Gallego-Bartolomé *et al.*, 2010). DELLA transcriptional regulators directly or indirectly repress the expression of GA-induced genes. The DELLA family encodes five members: *GIBBERELIC ACID INSENSITIVE* (*GAI*), *REPRESSOR OF gai-3* (*RGA*), and three *RGA-like* genes (*RGL1*, *RGL2* and *RGL3*) (Eckardt, 2002; Wen and Chang, 2002; Achard *et al.*, 2003). DELLA proteins not only repress GA signaling, but they also modulate GA homeostasis by regulating the expression of some GA biosynthetic enzymes such as *GA3OX1* and*GA20OXIDASE2*, and/or GA receptor genes such as *GIBBERELLIN INSENSITIVE DWARF 1a* (*GID1a*) and *GID1b* (Gallego-Bartolomé *et al.*, 2010). DELLA proteins act as repressors of GA-activated processes, consequently controlling floral induction. Among all the five members, *RGA* and *GAI* are the ones with a more important role in the transition to floral initiation (Dill and Sun, 2001; King *et al.*, 2001), while *RGA*, *RGL1* and *RGL2* have a more important role in flower and fruit development (Cheng *et al.*, 2004; Tyler *et al.*, 2004). The role of DELLA repressors in flowering control was determined by measuring the ability of different DELLA mutants

to rescue the strong phenotypes of the *ga1-3* mutant. The *ga1-3* mutant contains a large deletion in *GA REQUIRING 1* (*GA1*) gene, the enzyme that catalyzes the first committed step in GA biosynthesis (Sun and Kamiya, 1994). *rga* and *gai* null alleles are able to interact synergistically in order to rescue the normal vegetative growth and floral initiation in the *ga1*-3 mutant background (Dill and Sun, 2001; King *et al.*, 2001), indicating that *RGA* and *GAI* act as major floral transition repressors. However, some evidence shows that *RGA*, *RGL1*, and *RGL2* are also involved, to a lesser extent, in modulating flowering and floral development (Tyler *et al.*, 2004; Galvão *et al.*, 2012).

In addition, diverse plant species overexpressing DELLA proteins show dwarfism and delayed flowering (Dill *et al.*, 2004; Hamama *et al.*, 2012). It is known that DELLAs also regulate flower development by partly repressing the expression of floral homeotic genes such as *APETALA 3* (*AP3*), *PISTILLATA* (*PI*), and *AGAMOUS* (*AG*) (Yu *et al.*, 2004). Consequently, DELLA proteins are now universally considered as flowering inhibitors. Exogenous GA treatment is enough to restore the wild-type phenotype to *ga1-3* in terms of floral induction and flower development (Wilson *et al.*, 1992). Interestingly, this GA treatment is also able to restore the adaxial trichome number of glabrous *ga1-3* rosette leaves to wild-type levels (Smyth *et al.*, 1990). Later studies also show that DELLAs are directly involved in repressing trichome proliferation. Similar to members that control floral induction, *RGA* and *GAI*, play significant roles in trichome formation (Dill and Sun, 2001). *rga* and *gai* mutants are able to restore adaxial trichome initiation in the glabrous *ga1-3* mutant plants (Dill and Sun, 2001). Furthermore, several trichome activator transcription factor genes, including *GL1* and *GL3*, are induced in these plants, while contrarily *RGA* over-expression represses *GL1* and *GL3* expression (Fig. 3). Indeed, RGA and/or RGL2 proteins are able to interact with GL1, GL3 and EGL3 to repress the transcriptional function of this trichome activator complex (Qi *et al.*, 2014).

Cytokinins overlap with GA in floral induction and trichome formation

Cytokinins are involved in several aspects of plant growth and development. Firstly identified as factors that promote cell proliferation and shoot formation *in vitro*, CKs are found to activate cell-cycle genes in the leaf and interact with genetic regulators of stem cells in the SAM (Fig. 2) (Riou-Khamlichi *et al.*, 1999; Leibfried *et al.*, 2005). Additionally, CKs affect other important processes such as chloroplast or vascular exchange activity, branching and response to different nutrients as well as senescence (Fig. 2) (Yanai *et al.*, 2005; Gordon *et al.*, 2009). Decades ago, exogenous CK application was found to activate the floral transition of relatively old plants (Besnard-Wibaut, 1981; Dennis *et al.*, 1996). Later on, applications of CK in the form of benzylaminopurine (BAP) treatments using a hydroponic system have confirmed that CK are clearly involved in the floral transition (D'Aloia *et al.*, 2011). After BAP treatment, an up-regulation of *APETALA1* (*AP1*) expression, a marker of floral meristems, is detected; and indeed floral meristems are initiated two days later (D'Aloia *et al.*, 2011). CK have been proposed to act transmitting root-to-shoot signals during the floral transition (Kinet *et al.*, 1993; Havelange *et al.*, 2000). In fact, BAP application in the roots strongly promote floral induction in seven-week-old plants grown under SD conditions in the absence of other flowering stimulators such as extra GA, vernalization and/or LD photoperiod (D'Aloia *et al.*, 2011). At the histological level, an increase of CK levels is found in the SAM of Arabidopsis plants at the moment of flowering, suggesting that CKs might be real regulators of floral induction (Corbesier *et al.*, 2003).

CK biosynthetic enzymes have been well elucidated and are encoded by multigene families whose members are functionally redundant (Sakakibara *et al.*, 2006; Hirose *et al.*, 2008); this has always been an obstacle to genetically study in depth the role of CK in flowering. Luckily, physiological information has been obtained using genes that alter endogenous levels of CK, as *ALTERED MERISTEM PROGRAM 1* (*amp1*) overexpression results in early flowering plants (Werner *et al.*, 2006). Contrarily, when enzymes that degrade CK, such as *CYTOKININ OXIDASE/DEHYDROGENASE* (*CKX*), are overexpressed, Arabidopsis plants flower later than wild-type plants (Werner *et al.*, 2006). Genetically, CK applications are not able to activate the main florigen *FT*, but instead are able to promote the expression of its paralogue *TWIN SISTER of FT* (*TSF*) (Fig. 3) (D'Aloia *et al.*, 2011). As FT, TSF protein interacts with *FLOWERING LOCUS D* (*FD*) and is activated by *CONSTANS* (*CO*), therefore *TSF* acts redundantly with *FT* to promote flowering (Michaels *et al.*, 2005; Yamaguchi *et al.*, 2005; Mathieu *et al.*, 2007; Jang *et al.*, 2009). Furthermore, CKs are also able to activate, at least in the SAM, *SOC1* and *FD* (Fig. 3) (D'Aloia *et al.*, 2011). Indeed, it has been shown with BAP treatments on *tsf-1* and *soc1-2* that both genes are necessary for flowering in response to CK. Consequently, a model is proposed in which CKs activate *TSF* in the leaf, TSF moves to the SAM, and through interaction with FD, similarly to the action of FT, TSF induces the transcription of *SOC1* and *AP1* (Fig. 3) (D'Aloia *et al.*, 2011). Moreover, these results provide a clue of how redundant *FT* and *TSF* genes can be differentially regulated by distinct signals (D'Aloia *et al.*, 2011).

CKs are also able to stimulate trichome formation. Plants treated with BAP produce more trichomes on cauline leaves, stems and flowers (Maes *et al.*, 2008). The expression of many genes that act as trichome activators are stimulated by exogenous BAP not only on inflorescence organs but also to a lesser extent on the adaxial surface of rosette leaves (Gan *et al.*, 2007). Furthermore, interesting overlapping roles are found for some enzymes that degrade CK, such as *CKX*, which repress both floral induction and trichome initiation. When *CKX* is overexpressed a reduction in the number of flower trichomes and a late flowering are observed (Werner *et al.*, 2003).

However, phytohormones sometimes play antagonistic functions due to competition. Both GA and CK stimulate trichome formation and floral induction but, for

instance, exogenous GA applications may inhibit the effect of CK treatments as GAs are able to block CK signaling (Greenboim-Wainberg *et al.*, 2005). In contrast, exogenous CK applications increase the expression of genes that negatively regulate GA signaling (Brenner *et al.*, 2005). For example, this exhaustive control has been found to be essential for shoot meristem maintenance (Jasinski *et al.*, 2005; Yanai *et al.*, 2005). In the case of trichome proliferation, GA induction of trichomes is required throughout plant development; while CKs, although slightly affecting trichome formation in rosette leaves, are more specialized in trichome proliferation in upper inflorescences (Gan *et al.*, 2007).

Flowering-time genes affect trichome initiation

Leaves perceive light and other environmental conditions and, as mentioned, different genetic pathways that respond to environmental and endogenous status tightly control floral induction from the leaf. These genetic pathways have been extensively studied in Arabidopsis, and they converge in the activation of the so-called floral pathway integrators *FT* and *SOC1* that induce flowering from the leaf vascular tissue (Takada and Goto, 2003; Fornara *et al.*, 2010; Wellmer and Riechmann, 2010). FT protein, which is part of the florigen (Kardailsky *et al.*, 1999; Kobayashi *et al.*, 1999), travels from the leaf to the SAM, where it triggers flowering after interaction with FD (Fig. 3) (Corbesier *et al.*, 2007, Jaeger and Wigge, 2007; Lin *et al.*, 2007; Mathieu *et al.*, 2007; Tamaki *et al.*, 2007).

Epidermal trichomes are present on both adaxial and abaxial surfaces of rosette leaves in Arabidopsis. The number of trichomes growing on the adaxial surface reaches high numbers from the first true rosette leaf, and keeps increasing in new leaves through development. As mentioned, the main reason for that increase in adaxial trichomes is for protection against predators, excess of UV-light and transpiration, while the presence and utility of abaxial trichomes seems to be rather different. Abaxial trichomes are used as a marker for the juvenile-to-adult phase transition because they only develop in the adult rosette leaves but not in juvenile leaves (Chien and Sussex, 1996; Telfer *et al.*, 1997; Yu *et al.*, 2010). Adaxial trichome analyses have hardly been done in important floral activator mutant backgrounds, but some published results show that the number of abaxial trichomes, but not the time of appearance, of the late flowering *ft-1* and *soc1-2* mutants were clearly and significantly reduced (Willmann and Poethig, 2011). The double mutant *ft-1 soc1-2* produced even fewer trichomes than the single mutants (Willmann and Poethig, 2011), implying that those flowering activators may also have a role in the induction of trichome formation. Moreover, *FLOWERING LOCUS C* (*FLC*), a well-known MADS box gene that delays floral induction by repressing *FT* and *SOC1* (Hepworth *et al.*, 2002; Helliwell *et al.*, 2006; Searle *et al.*, 2006), also inhibit abaxial trichome formation. *flc* mutants show a significant increase in the abaxial trichome numbers independently of its role in flowering (Willmann and Poethig, 2011).

In addition to that, miR156-targeted *SPL* genes known to play key roles in the juvenile-to-adult transition as well as the plant phase transition towards flowering (Wang *et al.*, 2009; Wu *et al.*, 2009) have been found to control trichome initiation on the abaxial side of rosette leaves and stems (Yu *et al.*, 2010). They positively regulate the expression of some R3-MYB trichome repressors as *TCL1*, *TCL2* and *TRY* (Yu *et al.*, 2010; Xue *et al.* 2014). Not only miR156 but also the negative regulator of the GA signaling pathway, DELLAs, interact with SPLs to control flowering (Yu *et al.*, 2012). Therefore, and similarly to other flowering-time genes described in this review, SPLs affect other developmental processes that include trichome proliferation (Yu *et al.*, 2010; Xue *et al.* 2014).

And … all the way around: adaxial trichome activators affect floral transition

As previously described, GA and CK hormones play essential roles in trichome proliferation by positively controlling crucial downstream genes (Schellmann *et al.*, 2002; Gan *et al.*, 2006; Zhao *et al.*, 2008). The GA-dependent trichome pathway acts partially through *GLABROUS INFLORESCENCE STEMS* (*GIS*), which positively regulates the trichome activation complex formed by GL1, GL3, EGL3 and TTG1 (Fig. 1) (Payne *et al.*, 2000; Zhao *et al.*, 2008). On the other hand, the CK-dependent trichome pathway is controlled by *GLABROUS INFLORESCENCE STEMS2* (*GIS2*) and *ZINC FINGER PROTEIN* (*ZFP8*) (Fig. 1) (Gan *et al.*, 2007; Marsch-Martinez *et al*, 2012). Both pathways converge to activate *GLABROUS 2* (*GL2*), the universal trichome activator (Payne *et al.*, 2000) (Fig. 1).

Mutations in *GL1*, *TTG1* and both *GL3*/*EGL3* result in Arabidopsis plants with a significant loss of trichomes (Payne *et al.*, 2000; Zhou *et al.*, 2011). In addition to that, this complex has not only a role in trichome initiation but also in later trichome development, as mutations in these genes result in smaller and less branched trichomes (Payne *et al.*, 2000).

Trichome proliferation regulation affected by both hormones was first found to be activated through transcriptional regulation of the *GIS* clade, a clade that belongs to the extensive C2H2 transcription factor family (Tague and Goodman, 1995; Zhou *et al.*, 2013). GIS, GIS2 and ZFP8 – all members of the GIS clade – are able, collectively and individually, to positively regulate *GL1* (Gan, 2006, 2007; Ishida *et al.*, 2008), but they have diverged in their responses to developmental and hormonal signals, playing different roles in regulating trichome initiation on diverse plant organs (Gan *et al.*, 2006, 2007). Although playing a major role in controlling CK signaling, *GIS2* and *ZFP8* were found to partially integrate GA and CK to control trichome formation in inflorescence organs (Gan *et al.*, 2006, 2007).

Despite the fact that the regulation of trichome initiation has been extensively studied, recent data have identified new transcription factors that belong to the *GIS* clade, which may

play redundant roles in integrating GA and CK signaling, such as *ZINC FINGER PROTEIN 5* and *6* (*ZFP5* and *ZFP6*) and *GLABROUS INFLORESCENCE STEMS3* (*GIS3*) trichome activators (Zhou *et al.*, 2011, 2013; Sun *et al.*, 2015). Similar to the phenotypes of mutants in any of the genes of the trichome activator complex, loss of GIS-clade function leads to a decrease in trichome formation on the adaxial surface of rosette leaves and/or inflorescence organs. In addition, overexpression of any of these proteins generates a high density of trichomes (Tague and Goodman, 1995; Gan *et al.*, 2006, 2007; Zhou *et al.*, 2011, 2013; Sun *et al.*, 2015).

Interestingly, and in comparison with some of the floral activators and floral repressors that show clear trichome phenotypes, an equivalent situation is found in several trichome mutants. Compared with wild-type plants, a significant delay in flowering has been reported in all trichome activation mutants analyzed. *gl1*, *gl3, gis*, *gis2* and *zfp8* show a strong reduction in adaxial trichome production, some of them being almost glabrous, and all flower late (Yan *et al.*, 2012). Among them, the flowering time of the *gl1* mutant is the most delayed, with an average increase of 62.5% in the number of days to flowering relative to control plants (Yan *et al.*, 2012). The single mutants *gis*, *gis2* and *zfp8* show a clear late flowering, with increases of 44.15%, 57.88% and 51.67%, respectively, in the number of days to flowering compared with wild-type *Columbia* (*Col-0*) ecotype plants. The *gl3* mutant in a *Landsberg* erecta (*Ler*) background shows a similar phenotype, with an average of 56.45% more days needed to flower than *Ler* wild-type plants (Yan *et al.*, 2012). In contrast, plants overexpressing *GIS* and *GIS2*, which produce more trichomes, show early flowering in comparison to wild-type plants, with a 28.34% and 36.65% of reduction in the number of days needed to flower (Yan *et al.*, 2012). Additionally, some of the R3-MYBs trichome repressors that control trichome formation in a GL2-independent manner (Wang and Chen, 2014), as *TRY* and ETC3, have been found to play pleiotropic effects such as delaying flowering. Indeed, single *try* and *cpl3* mutants flower earlier with a decrease of 5.31% and 23.13% in the number of days, respectively (Tominaga *et al.*, 2008; Yan *et al.*, 2012).

Consequently, all these observations indicate that different developmental processes separated in time and space, i.e. adaxial trichome proliferation and floral induction, might be closely correlated and inter-connected through the CK and GA hormones (Fig. 3). Indeed, when publicly available high-throughput data was analyzed (www.ebi.ac.uk/arrayexpress) similar results were obtained. Data used included diverse microarrays from Arabidopsis plants treated with GA and CK as well as plants with mutated key-genes for flower transition, trichome initiation, GA-or CK-biosynthesis pathways; specifically mutants in the *FT*, *CO, SPINDLY* (*SPY*), *GA1*, *RESPONSE REGULATOR 1* (*ARR1*), *GL1*, *GL3* and *EGL3* genes. A Venn diagram of the differentially expressed (DE) genes among the different microarrays shows that there is a small but still significant number of genes that overlap at least among three out of the four aspects compared in this review (Fig. 4).

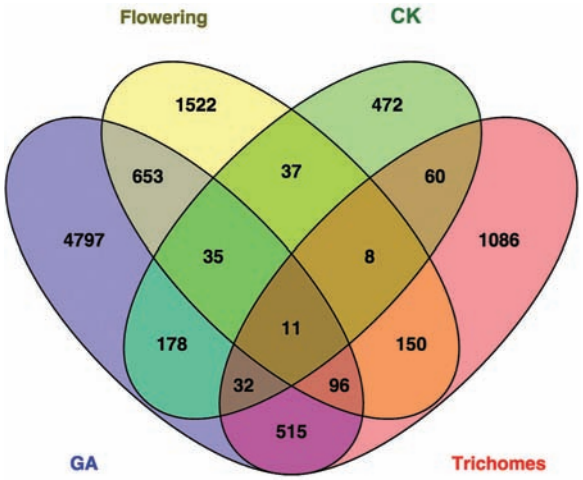

Fig. 4. Venn diagram showing the differentially expressed genes found among the diverse microarrays analyzed. High-throughput data used included microarrays from diverse Arabidopsis backgrounds that affect independently four biological processes: floral induction (yellow), trichome initiation (red), CK- (green) and GA-signaling (blue). A significant number of genes overlap at least among three out of the four aspects compared.

Floral organ identity genes repress inflorescence trichome initiation

This review is focused mainly on developmental processes that originate in the rosette leaves such as trichome initiation and flowering, but Arabidopsis trichomes are also present on inflorescence stems and flowers. In flowering species, floral organs, including sepals, petals, stamens and carpels are specified and controlled by floral organ identity genes (Bowman *et al.*, 1989; Coen and Meyerowitz, 1991; Pelaz *et al.*, 2000, 2001; Theissen, 2002; Ditta *et al.*, 2004). *AG*, a gene involved in stamen and carpel development (Yanofsky *et al.*, 1990; Drews *et al.*, 1991), has recently been found to be involved in repressing trichome proliferation on floral organs (Ó'Maoiléidigh *et al.*, 2013). Computational analyses using microarray data of early stage *ag* mutant flowers revealed that AG represses transcripts that encode proteins with several essential functions in rosette leaf development including trichome formation (Ó'Maoiléidigh *et al.*, 2013). Indeed, inducible artificial miRNA plant lines that silence *AG* (amiRAG) control trichome formation through direct regulation of some important trichome initiation genes, and show increased levels of the trichome initiation activators *GL1* and *ZFP8* (Larkin *et al.*, 1994; Schellmann *et al.*, 2002), while the trichome initiation repressors *CPC* and *TCL1* (Gan *et al.*, 2007; Wang *et al.*, 2007) are repressed (Ó'Maoiléidigh *et al.*, 2013). Phenotypical analyses showed that these amiRAG knockdown lines produce flowers with aberrant-shaped carpels that develop branched trichomes on their valves (Bowman *et al.*, 1989; Ó'Maoiléidigh *et al.*, 2013). The combinatorial function of AG, AP3 and PI proteins is widely known (Riechmann *et al.*, 1996; Honma and Goto, 2001; Theissen, 2002; Wuest *et al.*, 2012). ChIP-seq data analyses from AP3 and PI (Wuest *et al.*, 2012) revealed that both proteins are able to bind *in vivo* to the same trichome regulators targeted by AG, confirming

their combinatorial functions (Ó'Maoiléidigh *et al.*, 2013). Indeed, when all *AG, AP3* and *PI* are simultaneously knocked down, anthers of these mutant flowers develop branched and unbranched trichomes (Wuest *et al.*, 2012; Ó'Maoiléidigh *et al.*, 2013). Interestingly, these aberrant flowers, although slightly weaker, resemble those of plants overexpressing *GL1* trichome activator in the trichome repressor *try* mutant background (Schnittger *et al.*, 1998). *TRY* is able to control trichome initiation not only in rosette leaves but also in flowers (Schnittger *et al.*, 1998; Wellmer *et al.*, 2006). Similar to its GL2-independent function in leaves (Wang and Chen, 2014), TRY suppresses trichome proliferation in the flower independently of AG (Ó'Maoiléidigh *et al.*, 2013).

Conclusions

Using mutant analyses, gene expression studies and overlapping transcriptional regulatory interactions, great effort has been made to unravel the diverse molecular and genetic mechanisms that regulate different cellular differentiation programs in Arabidopsis. Data reveal that a network of transcriptional regulators is able to affect and be affected by GA and CK hormones at different organ, tissue and cell levels.

Indeed, in this review we show that the proper control of cell fate is of central importance and it is well coordinated in apparently distant developmental processes such as floral induction and epidermal trichome development. Both processes happen separately in time and most probably in space, but are interconnected, sharing a small genetic network on GA and CK hormone signaling. Several transcription factors belonging to the MYB, bHLH, C2H2, MADS families as well as DELLA proteins control both separated processes, floral transition and rosette leaf adaxial trichome proliferation, in response to different hormonal and developmental cues. Significant genetic interactions are shared between these two developmental processes. Here, we elucidate on how some important floral key activators and repressors control not only floral transition from the rosette leaf but also other rosette leaf developmental processes such as epidermal trichome formation. However, most of the analyzed trichome activator genes also positively control later developmental processes such as floral induction. In addition to that, as floral organs are essentially modified leaves through the action of different floral organ identity genes, these genes are also able to repress trichome proliferation in the flower. All these described transcription factors regulate floral induction and trichome formation processes by integrating diverse genetic networks and/or the control of hormone signaling. Therefore, while further investigation is necessary in order to dissect this complex regulatory network, these data lead us to suggest that the spatio-temporal regulation pattern and integration of signals of downstream regulators are of great importance; and consequently, different developmental processes separated in time, such as adaxial trichome proliferation and floral induction, might be closely correlated.

Acknowledgements

We thank Paula Suárez-López for critical reading and suggestions to improve the manuscript. Soraya Pelaz's research group has been recognized as a Consolidated Research Group by the Catalan Government (2014 SGR 1406). This work was supported by a MINECO/FEDER grant (BFU2012-33746).

Appendix

Expression information of the genes responding to GA, CK, flowering and trichome formation was obtained by the analysis of the following public microarray studies (http://www.ebi.ac.uk/arrayexpress/): E-GEOD-576,E-GEOD-7353,E-GEOD-8739,E-GEOD-8785,E-GEOD-12522,E-GEOD-12551,E-GEOD-39384,E-GEOD-44919,E-MEXP-344,E-MEXP-2270,E-MEXP-3362. For the datasets E-GEOD-7353, E-GEOD-8739, E-GEOD-8785, E-GEOD-12551 the lists of differentially expressed genes were taken directly from the published papers. E-GEOD-576 dataset was analyzed with the GEO2R tool from the NCBI with the default options. CEL files from E-GEOD-12522 and E-MEXP-2270 were downloaded; data were normalized with RMA using the R grma package (*R package version 2.40.0*). Then normalized data were used for differential expression test with the R package limma (Ritchie *et al.*, 2015). Probe expression values from the dataset E-MEXP-344 were analyzed with a *t*-test to identify the differentially expressed ones. Finally, E-GEOD-44919 and E-MEXP-3362 data were downloaded and limma was used to perform background correction (normexp), within normalization (loess) and between array normalization (quartile).

The differentially expressed genes coming from the four groups of experiments were joined and compared through a Venn diagram. An interactive tool for comparing lists with Venn diagrams was used (http://bioinfogp.cnb.csic.es/tools/venny/index.html).

References

Achard P, Cheng H, De Grauwe L, Decat J, Schoutteten H, Moritz T, Van Der Straeten D, Peng J, Harberd NP. 2006. Integration of plant responses to environmentally activated phytohormonal signals. Science **311,** 91–94.

Achard P, Vriezen WH, Van Der Straeten D, Harberd NP. 2003. Ethylene regulates arabidopsis development via the modulation of DELLA protein growth repressor function. Plant Cell **15,** 2816–2825.

Agrawal AA. 2000. Communication between plants: this time it's real. Trends in Ecology & Evolution **15,** 444–446.

Andres F, Coupland G. 2012. The genetic basis of flowering responses to seasonal cues. Nature Review Genetics **13,** 627–639.

Balkunde R, Bouyer D, Hulskamp M. 2011. Nuclear trapping by GL3 controls. Development **138,** 5039–5048.

Balkunde R, Pesch M, Hulskamp M. 2010. Trichome patterning in *Arabidopsis thaliana* from genetic to molecular models. Current Topics in Developmental Biology **91,** 299–321.

Bergonzi S, Albani MC, Ver Loren van Themaat E, Nordstrom KJ, Wang R, Schneeberger K, Moerland PD, Coupland G. 2013. Mechanisms of age-dependent response to winter temperature in perennial flowering of *Arabis alpina*. Science **340,** 1094–1097.

Besnard-Wibaut C. 1981. Effectiveness of gibberellins and 6-benzyladenine on flowering of *Arabidopsis thaliana*. Physiologia Plantarum **53,** 205–212.

Blázquez MA, Green R, Nilsson O, Sussman MR, Weigel D. 1998. Gibberellins promote flowering of arabidopsis by activating the LEAFY promoter. Plant Cell **10,** 791–800.

Bowman JL, Smyth DR, Meyerowitz EM. 1989. Genes directing flower development in Arabidopsis. Plant Cell **1,** 37–52.

Bouyer D, Geier F, Kragler F, Schnittger A, Pesch M, Wester K, Balkunde R, Timmer J, Fleck C, Hulskamp M. 2008. Two-dimensional patterning by a trapping/depletion mechanism: the role of TTG1 and GL3 in Arabidopsis trichome formation. PLoS Biology **6,** e141.

Brenner WG, Romanov GA, Kollmer I, Burkle L, Schmulling T. 2005. Immediate-early and delayed cytokinin response genes of *Arabidopsis thaliana* identified by genome-wide expression profiling reveal novel cytokinin-sensitive processes and suggest cytokinin action through transcriptional cascades. Plant Journal **44,** 314–333.

Coen ES, Meyerowitz EM. 1991. The war of the whorls: genetic interactions controlling flower development. Nature **353,** 31–37.

Corbesier L, Prinsen E, Jacqmard A, Lejeune P, Van Onckelen H, Perilleux C, Bernier G. 2003. Cytokinin levels in leaves, leaf exudate and shoot apical meristem of *Arabidopsis thaliana* during floral transition. Journal of Experimental Botany **54,** 2511–2517.

Corbesier L, Vincent C, Jang S, *et al*.2007. FT protein movement contributes to long-distance signaling in floral induction of Arabidopsis. Science **316,** 1030–1033.

Cheng H, Qin L, Lee S, Fu X, Richards DE, Cao D, Luo D, Harberd NP, Peng J. 2004. Gibberellin regulates Arabidopsis floral development via suppression of DELLA protein function. Development **131,** 1055–1064.

Chiang HH, Hwang I, Goodman HM. 1995. Isolation of the Arabidopsis GA4 locus. Plant Cell **7,** 195–201.

Chien JC, Sussex IM. 1996. Differential regulation of trichome formation on the adaxial and abaxial leaf surfaces by gibberellins and photoperiod in *Arabidopsis thaliana* (L.) Heynh. Plant Physiology **111,** 1321–1328.

D'Aloia M, Bonhomme D, Bouche F, Tamseddak K, Ormenese S, Torti S, Coupland G, Perilleux C. 2011. Cytokinin promotes flowering of Arabidopsis via transcriptional activation of the FT paralogue TSF. Plant Journal **65,** 972–979.

Davis SJ. 2009. Integrating hormones into the floral-transition pathway of *Arabidopsis thaliana*. Plant, Cell & Environment **32,** 1201–1210.

Dennis ES, Finnegan EJ, Bilodeau P, Chaudhury A, Genger R, Helliwell CA, Sheldon CC, Bagnall DJ, Peacock WJ. 1996. Vernalization and the initiation of flowering. Seminars in Cell and Developmental Biology **7,** 441–448.

Dill A, Sun T. 2001. Synergistic derepression of gibberellin signaling by removing RGA and GAI function in *Arabidopsis thaliana*. Genetics **159,** 777–785.

Dill A, Thomas SG, Hu J, Steber CM, Sun TP. 2004. The Arabidopsis F-box protein SLEEPY1 targets gibberellin signaling repressors for gibberellin-induced degradation. Plant Cell **16,** 1392–1405.

Ditta G, Pinyopich A, Robles P, Pelaz S, Yanofsky MF. 2004. The SEP4 gene of Arabidopsis thaliana functions in floral organ and meristem identity. Current Biology **14,** 1935–1940.

Drews GN, Bowman JL, Meyerowitz EM. 1991. Negative regulation of the Arabidopsis homeotic gene AGAMOUS by the APETALA2 product. Cell **65,** 991–1002.

Eckardt NA. 2002. Foolish seedlings and DELLA regulators: the functions of rice SLR1 and Arabidopsis RGL1 in GA signal transduction. Plant Cell **14,** 1–5.

Esch JJ, Chen MA, Hillestad M, Marks MD. 2004. Comparison of *TRY* and the closely related *At1g01380* gene in controlling Arabidopsis trichome patterning. Plant Journal **40,** 860–869.

Fornara F, de Montaigu A, Coupland G. 2010. SnapShot: control of flowering in Arabidopsis. Cell **141,** 550–552.

Fu X, Harberd NP. 2003. Auxin promotes Arabidopsis root growth by modulating gibberellin response. Nature **421,** 740–743.

Gallego-Bartolome J, Minguet EG, Marin JA, Prat S, Blázquez MA, Alabadi D. 2010. Transcriptional diversification and functional conservation between DELLA proteins in Arabidopsis. Molecular Biology and Evolution **27,** 1247–1256.

Galväo VC, Horrer D, Kuttner F, Schmid M. 2012. Spatial control of flowering by DELLA proteins in *Arabidopsis thaliana*. Development **139,** 4072–4082.

Gan L, Xia K, Chen JG, Wang S. 2011. Functional characterization of TRICHOMELESS2, a new single repeat R3MYB transcription factor in the regulation of trichome patterning in Arabidopsis. BMC Plant Biology **11,** 176–187.

Gan Y, Kumimoto R, Liu C, Ratcliffe O, Yu H, Broun P. 2006. GLABROUS INFLORESCENCE STEMS modulates the regulation by gibberellins of epidermal differentiation and shoot maturation in Arabidopsis. Plant Cell **18,** 1383–1395.

Gan Y, Liu C, Yu H, Broun P. 2007. Integration of cytokinin and gibberellin signalling by Arabidopsis transcription factors GIS, ZFP8 and GIS2 in the regulation of epidermal cell fate. Development **134,** 2073–2081.

Gordon SP, Chickarmane VS, Ohno C, Meyerowitz EM. 2009. Multiple feedback loops through cytokinin signaling control stem cell number within the Arabidopsis shoot meristem. Proceedings of the National Academy of Sciences, USA **106,** 16529–16534.

Greenboim-Wainberg Y, Maymon I, Borochov R, Alvarez J, Olszewski N, Ori N, Eshed Y, Weiss D. 2005. Cross talk between gibberellin and cytokinin: the Arabidopsis GA response inhibitor SPINDLY plays a positive role in cytokinin signaling. Plant Cell **17,** 92–102.

Hamama L, Naouar A, Gala R, *et al*. 2012. Overexpression of RoDELLA impacts the height, branching, and flowering behaviour of *Pelargonium* × *domesticum* transgenic plants. Plant Cell Reports **31,** 2015–2029.

Havelange A, Lejeune P, Bernier G. 2000. Sucrose/cytokinin interaction in *Sinapis alba* at floral induction: a shoot-to-root-to-shoot physiological loop. Physiologia Plantarum **109,** 343–350.

Helliwell CA, Wood CC, Robertson M, James Peacock W, Dennis ES. 2006. The Arabidopsis FLC protein interacts directly in vivo with SOC1 and FT chromatin and is part of a high-molecular-weight protein complex. Plant Journal **46,** 183–192.

Hepworth SR, Valverde F, Ravenscroft D, Mouradov A, Coupland G. 2002. Antagonistic regulation of flowering-time gene *SOC1* by CONSTANS and FLC via separate promoter motifs. EMBO Journal **21,** 4327–4337.

Hirose N, Takei K, Kuroha T, Kamada-Nobusada T, Hayashi H, Sakakibara H. 2008. Regulation of cytokinin biosynthesis, compartmentalization and translocation. Journal of Experimental Botany **59,** 75–83.

Honma T, Goto K. 2001. Complexes of MADS-box proteins are sufficient to convert leaves into floral organs. Nature **409,** 525–529.

Huijser P, Schmid M. 2011. The control of developmental phase transitions in plants. Development **138,** 4117–4129.

Hulskamp M. 2004. Plant trichomes: a model for cell differentiation. Nature Reviews Molecular Cell Biology **5,** 471–480.

Ishida T, Kurata T, Okada K, Wada T. 2008. A genetic regulatory network in the development of trichomes and root hairs. Annual Review of Plant Biology **59,** 365–386.

Jaeger KE, Wigge PA. 2007. FT protein acts as a long-range signal in Arabidopsis. Current Biology **17,** 1050–1054.

Jang S, Torti S, Coupland G. 2009. Genetic and spatial interactions between FT, TSF and SVP during the early stages of floral induction in Arabidopsis. Plant Journal **60,** 614–625.

Jasinski S, Piazza P, Craft J, Hay A, Woolley L, Rieu I, Phillips A, Hedden P, Tsiantis M. 2005. KNOX action in Arabidopsis is mediated by coordinate regulation of cytokinin and gibberellin activities. Current Biology **15,** 1560–1565.

Kardailsky I, Shukla VK, Ahn JH, Dagenais N, Christensen SK, Nguyen JT, Chory J, Harrison MJ, Weigel D. 1999. Activation tagging of the floral inducer FT. Science **286,** 1962–1965.

Kinet JM, Lejeune P, Bernier G. 1993. Shoot-root interactions during floral transition: a possible role for cytokinins. Enviromental and Experimental Botany **33,** 459–469.

King KE, Moritz T, Harberd NP. 2001. Gibberellins are not required for normal stem growth in Arabidopsis thaliana in the absence of GAI and RGA. Genetics **159,** 767–776.

Kirik V, Simon M, Hülskamp M, Schiefelbein J. 2004*a*. The *ENHANCER OF TRY AND CPC1* gene acts redundantly with *TRIPTYCHON* and *CAPRICE* in trichome and root hair cell patterning in Arabidopsis. Developmental Biology **268,** 506–513.

Kirik V, Simon M, Wester K, Schiefelbein J, Hülskamp M. 2004*b*. *ENHANCER* of *TRY* and *CPC 2* (*ETC2*) reveals redundancy in the region-specific control of trichome development of Arabidopsis. Plant Molecular Biology **55,** 389–398.

Kobayashi Y, Kaya H, Goto K, Iwabuchi M, Araki T. 1999. A pair of related genes with antagonistic roles in mediating flowering signals. Science **286,** 1960–1962.

Koornneef M, van der Veen JH. 1980. Induction and analysis of gibberellin sensitive mutants in *Arabidopsis thaliana* (L.) heynh. Theoretical and Applied Genetics **58,** 257–263.

Langdale JA. 1998. Cellular differentiation in the leaf. Current Opinion in Cell Biology **10,** 734–738.

Larkin JC, Oppenheimer DG, Lloyd AM, Paparozzi ET, Marks MD. 1994. Roles of the GLABROUS1 and TRANSPARENT TESTA GLABRA genes in arabidopsis trichome development. Plant Cell **6,** 1065–1076.

Leibfried A, To JP, Busch W, Stehling S, Kehle A, Demar M, Kieber JJ, Lohmann JU. 2005. WUSCHEL controls meristem function by direct regulation of cytokinin-inducible response regulators. Nature **438,** 1172–1175.

Lin MK, Belanger H, Lee YJ, *et al*. 2007. FLOWERING LOCUS T protein may act as the long-distance florigenic signal in the cucurbits. Plant Cell **19,** 1488–1506.

Maes L, Inze D, Goossens A. 2008. Functional specialization of the TRANSPARENT TESTA GLABRA1 network allows differential hormonal control of laminal and marginal trichome initiation in Arabidopsis rosette leaves. Plant Physiology **148,** 1453–1464.

Marquis RJ, Alexander HM. 1992. Evolution of resistance and virulence in plant-herbivore and plant-pathogen interactions. Trends in Ecology & Evolution **7,** 126–129.

Marsch-Martinez N, Reyes-Olalde JI, Ramos-Cruz D, Lozano-Sotomayor P, Zuniga-Mayo VM, de Folter S. 2012. Hormones talking: does hormonal cross-talk shape the Arabidopsis gynoecium? Plant Signal Behaviour **7,** 1698–1701.

Mathieu J, Warthmann N, Kuttner F, Schmid M. 2007. Export of FT protein from phloem companion cells is sufficient for floral induction in Arabidopsis. Current Biology **17,** 1055–1060.

Mauricio R. 2005. Ontogenetics of QTL: the genetic architecture of trichome density over time in *Arabidopsis thaliana*. Genetica **123,** 75–85.

Michaels SD, Himelblau E, Kim SY, Schomburg FM, Amasino RM. 2005. Integration of flowering signals in winter-annual Arabidopsis. Plant Physiology **137,** 149–156.

Mitchum MG, Yamaguchi S, Hanada A, Kuwahara A, Yoshioka Y, Kato T, Tabata S, Kamiya Y, Sun TP. 2006. Distinct and overlapping roles of two gibberellin 3-oxidases in Arabidopsis development. Plant Journal **45,** 804–818.

Moon J, Suh SS, Lee H, Choi KR, Hong CB, Paek NC, Kim SG, Lee I. 2003. The SOC1 MADS-box gene integrates vernalization and gibberellin signals for flowering in Arabidopsis. Plant Journal **35,** 613–623.

Mutasa-Göttgens E, Hedden P. 2009. Gibberellin as a factor in floral regulatory networks. Journal of Experimental Botany **60,** 1979–1989.

Nemhauser JL, Hong F, Chory J. 2006. Different plant hormones regulate similar processes through largely nonoverlapping transcriptional responses. Cell **126,** 467–475.

Nilsson O, Lee I, Blázquez MA, Weigel D. 1998. Flowering-time genes modulate the response to LEAFY activity. Genetics **150,** 403–410.

Olsson ME, Olofsson LM, Lindahl AL, Lundgren A, Brodelius M, Brodelius PE. 2009. Localization of enzymes of artemisinin biosynthesis to the apical cells of glandular secretory trichomes of *Artemisia annua* L. Phytochemistry **70,** 1123–1128.

Olszewski N, Sun TP, Gubler F. 2002. Gibberellin signaling: biosynthesis, catabolism, and response pathways. Plant Cell **14,** 61–80.

Ó'Maoiléidigh DS, Wuest SE, Rae L, *et al*. 2013. Control of reproductive floral organ identity specification in Arabidopsis by the C function regulator AGAMOUS. Plant Cell **25,** 2482–2503.

Pattanaik S, Patra B, Singh SK, Yuan L. 2014. An overview of the gene regulatory network controlling trichome development in the model plant, Arabidopsis. Frontiers in Plant Science **5,** 259.

Payne CT, Zhang F, Lloyd AM. 2000. GL3 encodes a bHLH protein that regulates trichome development in arabidopsis through interaction with GL1 and TTG1. Genetics **156,** 1349–1362.

Pelaz S, Ditta GS, Baumann E, Wisman E, Yanofsky MF. 2000. B and C floral organ identity functions require SEPALLATA MADS-box genes. Nature **405,** 200–203.

Pelaz S, Tapia-Lopez R, Alvarez-Buylla ER, Yanofsky MF. 2001. Conversion of leaves into petals in Arabidopsis. Current Biology **11,** 182–184.

Penfield S. 2008. Temperature perception and signal transduction in plants. New Phytologist **179,** 615–628.

Perazza D, Vachon G, Herzog M. 1998. Gibberellins promote trichome formation by Up-regulating GLABROUS1 in Arabidopsis. Plant Physiology **117,** 375–383.

Qi T, Huang H, Wu D, Yan J, Qi Y, Song S, Xie D. 2014. Arabidopsis DELLA and JAZ proteins bind the WD-repeat/bHLH/MYB complex to modulate gibberellin and jasmonate signaling synergy. Plant Cell **26,** 1118–1133.

Riechmann J, Krizek B, Meyerowitz E. 1996. Dimerization specificity of Arabidopsis MADS domain homeotic proteins APETALA1, APETALA3, PISTILLATA, and AGAMOUS. Proceedings of the National Academy of Sciences, USA **93,** 4793–4798.

Riou-Khamlichi C, Huntley R, Jacqmard A, Murray JA. 1999. Cytokinin activation of Arabidopsis cell division through a D-type cyclin. Science **283,** 1541–1544.

Sakakibara H, Takei K, Hirose N. 2006. Interactions between nitrogen and cytokinin in the regulation of metabolism and development. Trends in Plant Science **11,** 440–448.

Savage NS, Walker T, Wieckowski Y, Schiefelbein J, Dolan L, Monk NA. 2008. A mutual support mechanism through intercellular movement of CAPRICE and GLABRA3 can pattern the Arabidopsis root epidermis. PLoS Biology **6,** e235.

Schellmann S, Schnittger A, Kirik V, Wada T, Okada K, Beermann A, Thumfahrt J, Jurgens G, Hulskamp M. 2002. TRIPTYCHON and CAPRICE mediate lateral inhibition during trichome and root hair patterning in Arabidopsis. EMBO Journal **21,** 5036–5046.

Schellmann S, Hulskamp M, Uhrig J. 2007. Epidermal pattern formation in the root and shoot of Arabidopsis. Biochemical Society Transactions **35,** 146–148.

Schnittger A, Jürgens G, Hülskamp M. 1998. Tissue layer and organ specificity of trichome formation are regulated by GLABRA1 and TRIPTYCHON in Arabidopsis. Development **125,** 2283–2289.

Searle I, He Y, Turck F, Vincent C, Fornara F, Krober S, Amasino RA, Coupland G. 2006. The transcription factor FLC confers a flowering response to vernalization by repressing meristem competence and systemic signaling in Arabidopsis. Genes & Development **20,** 898–912.

Silverstone AL, Ciampaglio CN, Sun T. 1998. The Arabidopsis RGA gene encodes a transcriptional regulator repressing the gibberellin signal transduction pathway. Plant Cell **10,** 155–169.

Smyth DR, Bowman JL, Meyerowitz EM. 1990. Early flower development in Arabidopsis. Plant Cell **2,** 755–767.

Song YH, Ito S, Imaizumi T. 2013. Flowering time regulation: photoperiod- and temperature-sensing in leaves. Trends in Plant Science **18,** 575–583.

Song YH, Lee I, Lee SY, Imaizumi T, Hong JC. 2012. CONSTANS and ASYMMETRIC LEAVES 1 complex is involved in the induction of FLOWERING LOCUS T in photoperiodic flowering in Arabidopsis. Plant Journal **69,** 332–342.

Sun L, Zhang A, Zhou Z, Zhao Y, Yan A, Bao S, Yu H, Gan Y. 2015. GLABROUS INFLORESCENCE STEMS3 (GIS3) regulates trichome initiation and development in Arabidopsis. New Phytologist **206,** 220–230.

Sun TP, Kamiya Y. 1994. The Arabidopsis GA1 locus encodes the cyclase ent-kaurene synthetase A of gibberellin biosynthesis. Plant Cell **6,** 1509–1518.

Szymanski DB, Lloyd AM, Marks MD. 2000. Progress in the molecular genetic analysis of trichome initiation and morphogenesis in Arabidopsis. Trends in Plant Science **5,** 214–219.

Tague BW, Goodman HM. 1995. Characterization of a family of Arabidopsis zinc finger protein cDNAs. Plant Molecular Biology **28,** 267–279.

Takada S, Goto K. 2003. Terminal flower2, an Arabidopsis homolog of heterochromatin protein1, counteracts the activation of flowering locus T by constans in the vascular tissues of leaves to regulate flowering time. Plant Cell **15,** 2856–2865.

Tamaki S, Matsuo S, Wong HL, Yokoi S, Shimamoto K. 2007. Hd3a protein is a mobile flowering signal in rice. Science **316,** 1033–1036.

Telfer A, Bollman KM, Poethig RS. 1997. Phase change and the regulation of trichome distribution in Arabidopsis thaliana. Development **124,** 645–654.

Theissen G. 2002. Secret life of genes. Nature **415,** 741.

Thomas B. 2006. Light signals and flowering. Journal of Experimental Botany **57,** 3387–3393.

Tominaga R, Iwata M, Sano R, Inoue K, Okada K, Wada T. 2008. Arabidopsis CAPRICE-LIKE MYB 3 (CPL3) controls endoreduplication and flowering development in addition to trichome and root hair formation. Development **135,** 1335–1345.

Traw MB, Bergelson J. 2003. Interactive effects of jasmonic acid, salicylic acid, and gibberellin on induction of trichomes in Arabidopsis. Plant Physiology **133,** 1367–1375.

Tyler L, Thomas SG, Hu J, Dill A, Alonso JM, Ecker JR, Sun TP. 2004. Della proteins and gibberellin-regulated seed germination and floral development in Arabidopsis. Plant Physiology **135,** 1008–1019.

Wada T, Kurata T, Tominaga R, Koshino-Kimura Y, Tachibana T, Goto K. 2002. Role of a positive regulator of root hair development, *CAPRICE*, in Arabidopsis root epidermal cell differentiation. Development **129,** 5409–5419.

Wada T, Tachibana T, Shimura Y, Okada K. 1997. Epidermal cell differentiation in Arabidopsis determined by a Myb homolog, CPC. Science **277,** 1113–1116.

Wang JW, Czech B, Weigel D. 2009. miR156-regulated SPL transcription factors define an endogenous flowering pathway in *Arabidopsis thaliana*. Cell **138,** 738–749.

Wang S, Kwak SH, Zeng Q, Ellis BE, Chen XY, Schiefelbein J, Chen JG. 2007. TRICHOMELESS1 regulates trichome patterning by suppressing GLABRA1 in Arabidopsis. Development **134,** 3873–3882.

Wang S, Chen JG. 2014. Regulation of cell fate determination by single-repeat R3 MYB transcription factors in Arabidopsis. Frontiers in Plant Science **8,** 133–138.

Wellmer F, Alves-Ferreira M, Dubois A, Riechmann JL, Meyerowitz EM. 2006. Genome-wide analysis of gene expression during early Arabidopsis flower development. PLoS Genetics **2,** e117.

Wellmer F, Riechmann JL. 2010. Gene networks controlling the initiation of flower development. Trends in Genetics **26,** 519–527.

Wen CK, Chang C. 2002. Arabidopsis RGL1 encodes a negative regulator of gibberellin responses. Plant Cell **14,** 87–100.

Werner T, Hanus J, Holub J, Schmulling T, Van Onckelen H, Strnad M. 2003. New cytokinin metabolites in IPT transgenic *Arabidopsis thaliana* plants. Physiologia Plantarum **118,** 127–137.

Werner T, Kollmer I, Bartrina I, Holst K, Schmulling T. 2006. New insights into the biology of cytokinin degradation. Plant Biology **8,** 371–381.

Willmann MR, Poethig RS. 2011. The effect of the floral repressor FLC on the timing and progression of vegetative phase change in Arabidopsis. Development **138,** 677–685.

Wilson RN, Heckman JW, Somerville CR. 1992. Gibberellin is required for flowering in *Arabidopsis thaliana* under short days. Plant Physiology **100,** 403–408.

Wu G, Park MY, Conway SR, Wang JW, Weigel D, Poethig RS. 2009. The sequential action of miR156 and miR172 regulates developmental timing in Arabidopsis. Cell **138,** 750–759.

Wuest SE, Ó'Maoiléidigh DS, Rae L, Kwasniewska K, Raganelli A, Hanczaryk K, Lohan AJ, Loftus B, Graciet E, Wellmer F. 2012. Molecular basis for the specification of floral organs by APETALA3 and PISTILLATA. Proceedings of the National Academy of Sciences, USA **109,** 13452–13457.

Xue XY, Zhao B, Chao LM, Chen DY, Cui WR, Mao YB, Wang LJ, Chen XY. 2014. Interaction between two timing microRNAs controls trichome distribution in Arabidopsis. PLoS Genetics **10,** e1004266.

Yamaguchi A, Kobayashi Y, Goto K, Abe M, Araki T. 2005. TWIN SISTER OF FT (TSF) acts as a floral pathway integrator redundantly with FT. Plant and Cell Physiology **46,** 1175–1189.

Yan A, Pan J, An L, Gan Y, Feng H. 2012. The responses of trichome mutants to enhanced ultraviolet-B radiation in *Arabidopsis thaliana*. Journal of Photochemistry and Photobiology B **113,** 29–35.

Yanai O, Shani E, Dolezal K, Tarkowski P, Sablowski R, Sandberg G, Samach A, Ori N. 2005. Arabidopsis KNOXI proteins activate cytokinin biosynthesis. Current Biology **15,** 1566–1571.

Yanofsky MF, Ma H, Bowman JL, Drews GN, Feldmann KA, Meyerowitz EM. 1990. The protein encoded by the Arabidopsis homeotic gene agamous resembles transcription factors. Nature **346,** 35–39.

Yu H, Ito T, Zhao Y, Peng J, Kumar P, Meyerowitz EM. 2004. Floral homeotic genes are targets of gibberellin signaling in flower development. Proceedings of the National Academy of Sciences, USA **101,** 7827–7832.

Yu N, Cai WJ, Wang S, Shan CM, Wang LJ, Chen XY. 2010. Temporal control of trichome distribution by microRNA156-targeted SPL genes in *Arabidopsis thaliana*. Plant Cell **22,** 2322–2335.

Yu S, Galvão VC, Zhang YC, Horrer D, Zhang TQ, Hao YH, Feng YQ, Wang S, Schmid M, Wang JW. 2012. Gibberellin regulates the Arabidopsis floral transition through miR156-targeted SQUAMOSA promoter binding-like transcription factors. Plant Cell **24,** 3320–3332.

Zhang F, Gonzalez A, Zhao M, Payne CT, Lloyd A. 2003. A network of redundant bHLH proteins functions in all TTG1-dependent pathways of Arabidopsis. Development **130,** 4859–4869.

Zhao M, Morohashi K, Hatlestad G, Grotewold E, Lloyd A. 2008. The TTG1-bHLH-MYB complex controls trichome cell fate and patterning through direct targeting of regulatory loci. Development **135,** 1991–1999.

Zhou Z, An L, Sun L, Zhu S, Xi W, Broun P, Yu H, Gan Y. 2011. Zinc finger protein5 is required for the control of trichome initiation by acting upstream of zinc finger protein8 in Arabidopsis. Plant Physiology **157,** 673–682.

Zhou Z, Sun L, Zhao Y, An L, Yan A, Meng X, Gan Y. 2013. Zinc Finger Protein 6 (ZFP6) regulates trichome initiation by integrating gibberellin and cytokinin signaling in Arabidopsis thaliana. New Phytologist **198,** 699–708.

Zhou Z, Sun L, Zhao Y, An L, Yan A, Meng X, Gan Y. 2013. Zinc Finger Protein 6 (ZFP6) regulates trichome initiation by integrating gibberellin and cytokinin signaling in Arabidopsis thaliana. New Phytologist **198,** 699–708.

Annals of Botany **114**: 1459–1470, 2014
doi:10.1093/aob/mcu069, available online at www.aob.oxfordjournals.org

ANNALS OF BOTANY
Founded 1887

REVIEW: PART OF A SPECIAL ISSUE ON FLOWER DEVELOPMENT

RAV genes: regulation of floral induction and beyond

Luis Matías-Hernández[1], Andrea E. Aguilar-Jaramillo[1], Esther Marín-González[1], Paula Suárez-López[1,*] and Soraya Pelaz[1,2,*]

[1]*Centre for Research in Agricultural Genomics, CSIC-IRTA-UAB-UB, Campus UAB, 08193 Bellaterra, Spain and* [2]*ICREA (Institució Catalana de Recerca i Estudis Avançats), Barcelona, Spain*
** For correspondence. E-mail paula.suarez@cragenomica.es or soraya.pelaz@cragenomica.es*

Received: 14 December 2013 Returned for revision: 30 January 2014 Accepted: 12 March 2014 Published electronically: 8 May 2014

• **Background** Transcription factors of the RAV (RELATED TO ABI3 AND VP1) family are plant-specific and possess two DNA-binding domains. In *Arabidopsis thaliana*, the family comprises six members, including TEMPRANILLO 1 (TEM1) and TEM2. Arabidopsis RAV1 and TEM1 have been shown to bind bipartite DNA sequences, with the consensus motif C(A/C/G)ACA$(N)_{2-8}$(C/A/T)ACCTG. Through direct binding to DNA, RAV proteins act as transcriptional repressors, probably in complexes with other co-repressors.
• **Scope and Conclusions** In this review, a summary is given of current knowledge of the regulation and function of *RAV* genes in diverse plant species, paying particular attention to their roles in the control of flowering in arabidopsis. TEM1 and TEM2 delay flowering by repressing the production of two florigenic molecules, FLOWERING LOCUS T (FT) and gibberellins. In this way, TEM1 and TEM2 prevent precocious flowering and postpone floral induction until the plant has accumulated enough reserves or has reached a growth stage that ensures survival of the progeny. Recent results indicate that TEM1 and TEM2 are regulated by genes acting in several flowering pathways, suggesting that TEMs may integrate information from diverse pathways. However, flowering is not the only process controlled by RAV proteins. Family members are involved in other aspects of plant development, such as bud outgrowth in trees and leaf senescence, and possibly in general growth regulation. In addition, they respond to pathogen infections and abiotic stresses, including cold, dehydration, high salinity and osmotic stress.

Key words: RAV family, *TEMPRANILLO* genes, flowering, arabidopsis development, transcription factors, biotic/abiotic stress, photoperiod, gibberellins, flower development.

INTRODUCTION

Flowering must occur at an appropriate time of the year to ensure offspring survival and species perpetuation. A delay in floral induction may lead to a robust plant, but be late for seed maturation. By contrast, a precocious flowering will result in a plant without enough energy for the development of fruits. Therefore, the time for floral induction is critical, and consequently both late induction and precocious flowering should be avoided. Plants respond to seasonal changes in daylength and temperature. In both inductive and non-inductive conditions flowering must be postponed until the plant obtains enough reserves for flower formation, and in unfavourable conditions it must be delayed to reach the appropriate time for seed-set. *Arabidopsis thaliana* is a good model to study this process. It is a facultative long day (LD) plant, i.e. it flowers rapidly when days are long, such as in spring, but it also eventually flowers in short days (SD). Several genetic pathways control flowering time in response to environmental or endogenous conditions. The major environmental effectors are daylength or photoperiod, seasonal and daily changes in temperature, and light intensity and quality (Thomas, 2006; Andrés and Coupland, 2012; Song *et al*., 2012, 2013). Among the endogenous factors are hormones such as gibberellins (GAs) and the age of the plant (Mutasa-Göttgens and Hedden, 2009; Huijser and Schmid, 2011). These pathways have been studied extensively in arabidopsis. The information provided by these genetic pathways is integrated in the activation of the expression of the so-called floral pathway integrators, *FLOWERING LOCUS* T (*FT*) and *SUPRESSOR OF OVEREXPRESSION OF CONSTANS 1* (*SOC1*), which trigger flowering (Fornara *et al*., 2010; Wellmer and Riechmann, 2010). A major inducer of flowering in response to long days is CONSTANS (CO). *CO* transcript levels are high at the end of the light period under LD and its protein is stabilized only under light. If the expression coincides with the dark period, as in SD, the protein is immediately degraded. Therefore, CO is only active under LD (Suárez-López *et al*., 2001; Valverde *et al*., 2004; Jang *et al*., 2008; Liu *et al*., 2008).

Leaves perceive light and other environmental conditions, and CO is expressed in their vascular tissue, where it activates *FT* transcription (Takada and Goto, 2003; An *et al*., 2004). FT protein, identified as part of the florigen, travels to the shoot apical meristem (SAM), where flowers will be produced, to induce flowering (Corbesier *et al*., 2007; Jaeger and Wigge, 2007; Lin *et al*., 2007; Mathieu *et al*., 2007; Tamaki *et al*., 2007). In addition to FT, GAs are also mobile signals that travel from the leaves to the SAM to induce *FT* and *SOC1* in order to trigger flowering (Eriksson *et al*., 2006). Different enzymatic activities give rise to the bioactive GA form GA_4 (Mutasa-Göttgens and Hedden, 2009). As mentioned, these mobile inductive signals should be repressed for the correct timing of flowering. Several proteins have been identified as repressors and together prevent precocious flowering (Jarillo and Piñeiro, 2011). Two of these proteins are

TEMPRANILLO1 (TEM1) and TEM2 (Castillejo and Pelaz, 2008; Osnato *et al*., 2012), which belong to the RAV (Related to ABI3/VP1) family of transcription factors.

Here we review the role of *RAV* genes in different species and show that they are involved in several plant processes such as flowering, bud outgrowth, leaf senescence, responses to hormones, stress and other environmental signals.

RAV FAMILY OF TRANSCRIPTION FACTORS

In arabidopsis there are six members of the RAV family of transcription factors: RAV1, RAV1-like, RAV2, RAV2-like, RAV3 and RAV3-like (Fig. 1A) (Riechmann *et al*., 2000). The first four have also been named ETHYLENE RESPONSE DNA BINDING FACTORS (EDF1–EDF4) (Alonso *et al*., 2003). Based on their function in flowering, *RAV2-like* and *RAV2* were renamed *TEM1* and *TEM2*, respectively (Castillejo and Pelaz, 2008). The main characteristic of RAV members is the presence of two different DNA-binding domains, a B3 and an AP2 domain (Fig. 1B). RAV family members have thus been classified as members of either the B3 super-family or the AP2/EREBP (APETALA2) family of transcription factors.

The B3 domain was initially identified in the VIVIPAROUS1 (VP1) protein from *Zea mays*, and in the ABSCISIC ACID INSENSITIVE3 (ABI3), the VP1 orthologue from arabidopsis (Giraudat *et al*., 1992; Suzuki *et al*., 1997). B3 domains, consisting of a seven-stranded β-sheet arranged in an open barrel and two short α helices, generally share a common structural framework for DNA recognition (Yamasaki *et al*., 2004; Waltner *et al*., 2005). As mentioned, the RAV proteins are characterized by the presence of not only a C-terminal B3 domain that recognizes the consensus CACCTG sequence, but also an N-terminal AP2 domain that recognizes the consensus CAACA sequence (Kagaya *et al*., 1999). The AP2 domain is about 60 amino acids (aa) long (Okamuro *et al*., 1997; Riechmann and Meyerowitz, 1998; Riechmann *et al*., 2000; Sakuma *et al*., 2002; Magnani *et al*., 2004). This makes the RAV transcription factors unique, with two different DNA binding domains (Fig. 1B).

The contribution of transcriptional repressors may be of crucial importance in various plant biological processes. Around 10 % of arabidopsis transcription factors might be transcriptional repressors (Ikeda and Ohme-Takagi, 2009). Among the B3 super-family, it was found that many members had a repressive activity due to the existence of a 15-aa peptide (GNSKTLRLFGVNMEC), which has been named the B3 repression domain (BRD). Although replacement experiments pointed to the first leucine and/or the methionine residue (in bold) of the BRD (GNSKT**L**RLFGVN**M**EC) as crucial to maintain repressive activity, other amino acids of this domain are not always conserved. Deletion of the BRD of some B3 proteins revealed that only a short peptide of five amino acids, R/KLFGV, is essential as a repression domain. Four members of the RAV family, TEM1, TEM2, RAV1 and RAV1-like, share the core of the BRD (Ikeda and Ohme-Takagi, 2009). A quite similar sequence, MLFGV, is present in RAV3 and RAV3-like (Causier *et al*., 2012). The R/KLFGV sequence is also conserved in other RAV homologues from various plants such as rice (Ikeda and Ohme-Takagi, 2009). These results suggest strongly that RAV genes encoding RLFGV motifs could play roles as transcriptional repressors (Fig. 1B).

TEM GENES REPRESS FLOWERING IN TWO DIFFERENT PATHWAYS

As mentioned, *FT* plays a central role during the floral induction event (Turck *et al*., 2008) and is activated in response to CO (Kardailsky *et al*., 1999; Kobayashi *et al*., 1999; Samach *et al*., 2000). However, CO is already expressed in the phloem early in development (Takada and Goto, 2003), and changes in *CO* expression levels do not seem to account for the increase in *FT* accumulation for inducing flowering (Castillejo and Pelaz, 2008). Consequently, something else that accounts for this late FT accumulation must exist.

TEM *genes affect the photoperiod pathway*

Regulation of flowering initiation in response to photoperiod is mediated by the interaction between external light signals and the circadian clock (Suárez-López *et al*., 2001; Yanovsky and Kay, 2002). In the photoperiod pathway, FT promotes flowering in response to LD. *TEM1* and *TEM2* were identified as repressors of flowering in the photoperiod pathway (Castillejo and Pelaz, 2008). Single loss-of-function alleles of *TEM1*, *tem1–1*, and *TEM2*, *tem2–2*, cause a slight early flowering phenotype in LD, and a double *tem1–1 tem2–2* mutant shows enhanced early flowering compared with the single mutants under LD conditions. In this photoperiod, *tem1–1 tem2–2* flowers as early as CO overexpressors (*35S::CO*). Supporting these results, it was found that both *35S::TEM1* and 35S::*TEM2* plants show the opposite phenotype and flower extremely late under LD conditions (Castillejo and Pelaz, 2008; Osnato *et al*., 2012). Consequently, TEMs seem to play a pivotal role as repressors in floral induction (Fig. 2).

TEM1 transcript levels follow a diurnal oscillation, such that *TEM1* abundance is low during the daytime and peaks at dusk. Similar developmental and circadian regulations were observed for *TEM1* and *TEM2*, supporting the proposed redundant role of both genes (Castillejo and Pelaz, 2008; Osnato *et al*., 2012). Moreover, *TEM1* mRNA abundance is very high during early stages of seedling development but a pronounced decline takes place just before floral transition. *CO* expression remains almost unaltered throughout development, although a subtle increase occurs during the transition to flowering (Castillejo and Pelaz, 2008).

In addition in wild-type plants, *FT* mRNA remains at basal levels until the transition to flowering, at days 10–12, when there is a pronounced increase in *FT* accumulation. However, *FT* expression increases from day 6 in the *tem1–1 tem2–2* double mutant, when plants had only formed the first two true leaves (Osnato *et al*., 2012). The significant increase of FT expression responsible for floral induction is abolished in the *35S::TEM1* seedlings (Castillejo and Pelaz, 2008). Therefore, TEM1 represses *FT* expression at early developmental stages.

The identical precocious flowering phenotypes of *35S::CO* and *tem1 tem2* plants suggested strongly that only when *TEM* levels drop drastically can CO activate *FT* to reach the threshold level necessary to trigger the floral transition under inductive photoperiods (Castillejo and Pelaz, 2008). When both *CO* and *TEM* levels are elevated, in 35S::*CO 35S::TEM1* plants, the balance between the activator and the repressor is restored and consequently these plants flower after producing a wild-type

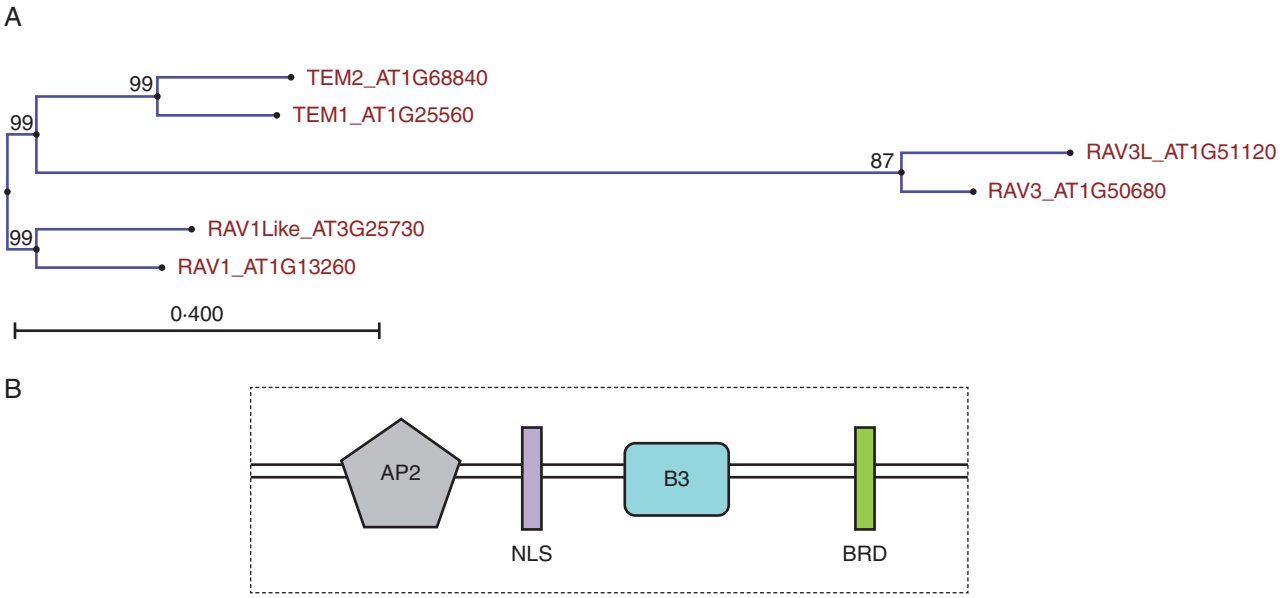


```
TEM1_AT1G25560    ---MEY-SCVDD-SSTTSESLSISTTPKPTTTTEKKLSSPPATSMR--LYRMGSGGSSVV
TEM2_AT1G68840    ---MDS-SCIDEISSSTSESFS--------ATTAKKLSPPPAAALR--LYRMGSGGSSVV
RAV1_AT1G13260    ---MES-SSVDE-STTSTGSIC-----------ETPAITPAKKSSVGNLYRMGSG-SSVV
RAV1Like_AT3G25730 ---MDAMSSVDE-SSTTTDSIP-----------ARKSSSPAS-----LLYRMGSG-TSVV

TEM1_AT1G25560    LDSENG----VETESRKLPSSKYKGVVPQPNGRWGAQIYEKHQRVWLGTFNEEEEAASSY
TEM2_AT1G68840    LDSENG----LETESRKLPSSKYKGVVPQPNGRWGAQIYEKHQRVWLGTFNEQEEAARSY
RAV1_AT1G13260    LDSENG----VEAESRKLPSSKYKGVVPQPNGRWGAQIYEKHQRVWLGTFNEEDEAARAY
RAV1Like_AT3G25730 LDSENGVEVEVEAESRKLPSSRFKGVVPQPNGRWGAQIYEKHQRVWLGTFNEEDEAARAY

TEM1_AT1G25560    DIAVRRFRGRDAVTNFKSQVDGN-DAESAFLDAHSKAEIVDMLRKHTYADEFEQSRRK--
TEM2_AT1G68840    DIAACRFRGRDAVVNFKNVLE---DGDLAFLEAHSKAEIVDMLRKHTYADELEQNNKRQL
RAV1_AT1G13260    DVAVHRFRRRDAVTNFKDVKMD--EDEVDFLNSHSKSEIVDMLRKHTYNEELEQSKRR--
RAV1Like_AT3G25730 DVAAHRFRGRDAVTNFKDTTF---EEEVEFLNAHSKSEIVDMLRKHTYKEELDQRKRN--

TEM1_AT1G25560    --FVNGDGKRSGLETATYG-----NDAVLRAREVLFEKTVTPSDVGKLNRLVIPKQHAEK
TEM2_AT1G68840    FLSVDANGKRNG--SSTTQ-----NDKVLKTREVLFEKAVTPSDVGKLNRLVIPKQHAEK
RAV1_AT1G13260    ---RNGNGNMTRTLLTSGLSNDGVSTTGFRSAEALFEKAVTPSDVGKLNRLVIPKHHAEK
RAV1Like_AT3G25730 ---RDGNGKETTAFALASM----VVMTGFKTAELLFEKTVTPSDVGKLNRLVIPKHQAEK

TEM1_AT1G25560    HFPLPAMTTA---MGMNPSPTKGVLINLEDRTGKVWRFRYSYWNSSQSYVLTKGWSRFVK
TEM2_AT1G68840    HFPLPSPS---------PAVTKGVLINFEDVNGKVWRFRYSYWNSSQSYVLTKGWSRFVK
RAV1_AT1G13260    HFPLPS----------SNVSVKGVLLNFEDVNGKVWRFRYSYWNSSQSYVLTKGWSRFVK
RAV1Like_AT3G25730 HFPLPLGN--------NNVSVKGMLLNFEDVNGKVWRFRYSYWNSSQSYVLTKGWSRFVK

TEM1_AT1G25560    EKNLRAGDVVCFERSTGPD--------RQLYIHWKVRS----SPVQTVVRLFGVNIFNVS
TEM2_AT1G68840    EKNLRAGDVVCFERSTGLE--------RQLYIDWKVRSGPRENPVQVVVRLFGVDIFNVT
RAV1_AT1G13260    EKNLRAGDVVCFERSNGQD--------QQLYIGWKSRSGS-DLDAGRVLRLFGVNISPES
RAV1Like_AT3G25730 EKNLCAGDLISFKRSNDQD--------QKFFIGWKSKSGL-DLETGRVMRLFGVDIS---

TEM1_AT1G25560    NEKPNDVAVECVGKKRSREDDLFSLGCSKKQAIINIL
TEM2_AT1G68840    TVKPNDVVAVCGGKRSRDVDDMFALRCSKKQAIINAL
RAV1_AT1G13260    S--RNDVVGN----KRVNDTEMLSLVCSKKQRIFHAS
RAV1Like_AT3G25730 ---LNAVVVV----KETTEVLMSSLRC-KKQRVL---
```

FIG. 1. (A) Phylogenetic unrooted tree of the RAV family in *Arabidopsis thaliana.* Analysis was done using the CLC Genomics Workbench v6.5 program; bootstrap values are indicated. (B) Amino acid sequence of four RAV members, TEM1, TEM2, RAV1 and RAV1L, with the exact location of these domains. Analysis was done using Clustal v2.1 multiple amino acid alignment; substitution rate model = WAG. Main characteristic protein domains of RAV transcription factor family include: *AP2* (grey) and *B3* (blue) DNA-binding domains; nuclear localization signal (*NLS*) in purple; and B3 repression domain (*BRD*) in green.

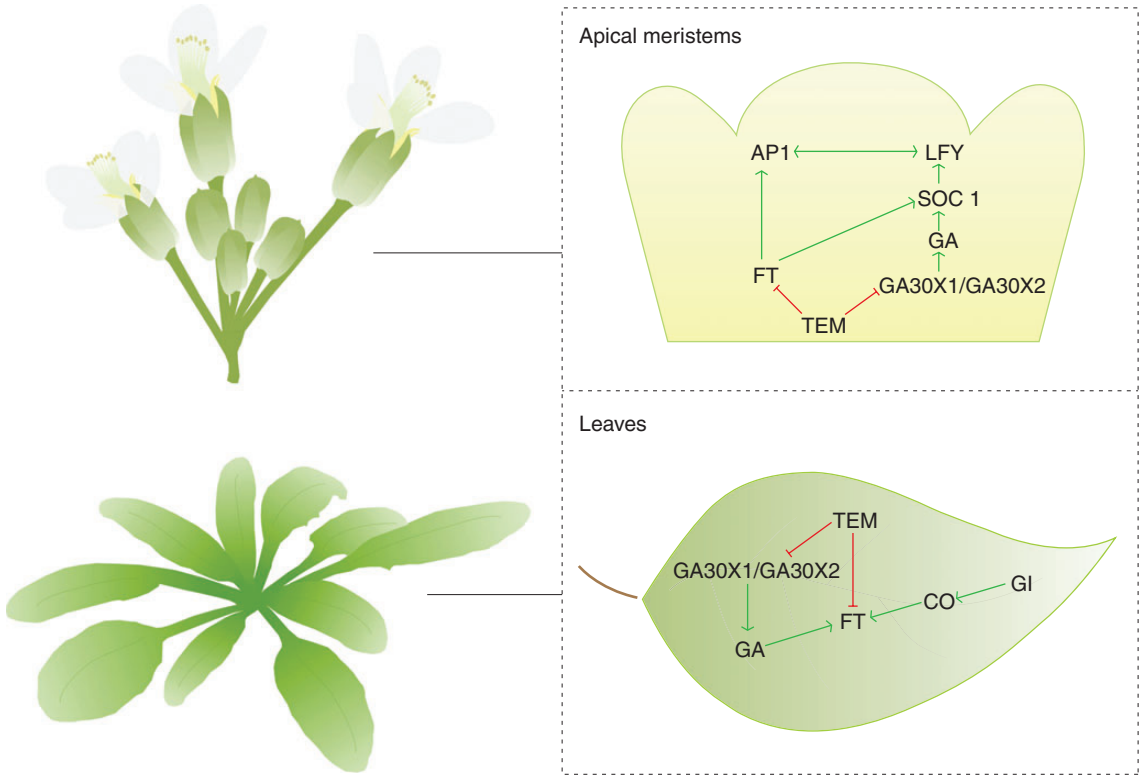

FIG. 2. Floral transition model in *Arabidopsis thaliana*. *TEM1* and *TEM2* genes play a central role in regulating the flowering process by repressing at least the photoperiod and gibberellin pathways under inductive and non-inductive daylengths, in leaves and apical meristems.

number of leaves. The late-flowering phenotype of *35S::*TEM1 plants is completely suppressed by the constitutive expression of *FT*, which is consistent with FT acting downstream of *TEM1*. The combination of *tem1–1* and *ft* mutants confirmed the epistatic relationship between both genes, as the double mutant *tem1–1 ft-101* flowers at the same time as *ft-101* alone (Castillejo and Pelaz, 2008). These results also suggest that *FT* is the primary downstream target of TEM1 to repress flowering.

TEM1 expression is detected in all vegetative tissues (Castillejo and Pelaz, 2008). It has been proposed that TEM could act in the vascular bundles of leaves, together with CO, to tightly control FT accumulation; however, *TEM1* is expressed throughout the leaf as well as in the SAM and the hypocotyl. An artificial micro RNA (amiRNA) targeted against *TEM1* and *TEM2* genes was expressed under control of the *KNAT1* promoter to drive their silencing only in the SAM and hypocotyls. An early flowering phenotype of *pKNAT1::amiR-TEM* lines was associated with an up-regulation of *FT* expression. All this indicated that TEM has a role in controlling flowering, at least in the SAM (Osnato *et al*., 2012).

RAV binding motifs (Kagaya *et al*., 1999) were found in the 5′ untranslated region (UTR) of the *FT* gene. *In vitro* and *in vivo* interactions of TEM1 protein with the *FT* 5′UTR were confirmed by gel-shift and chromatin immunoprecipitation (ChIP) assays, respectively. Interestingly, the RAV binding site in *FT* is located just next to the CO binding site found 43 bp upstream of the ATG (Wenkel *et al*., 2006; Castillejo and Pelaz, 2008). Therefore, precise control of flowering time could be explained if the CO and TEM proteins compete for their respective binding sites to directly regulate *FT* accumulation. Consequently, *FT* levels are the result of a quantitative balance between the respective promoter and repressive activities of CO and TEM (Castillejo and Pelaz, 2008).

GIGANTEA (GI), a circadian clock regulator, plays a role in floral induction through regulation of the timing and amplitude of *CO* expression (Fowler *et al*., 1999; Park *et al*., 1999; Mizoguchi *et al*., 2005; Sawa *et al*., 2007). GI and FLAVIN-BINDING, KELCH REPEAT, F BOX protein 1 (FKF1) form a protein complex that mediates the degradation of CYCLING DOF FACTOR 1 (CDF1), a key *CO* repressor. Under LDs, GI and FKF1 expression peak at the same time, at the end of the day, leading to the optimal formation of the GI–FKF1 complex. However, under SDs, the expression of GI peaks a few hours before the peak of FKF1 expression, resulting in low levels of the GI–FKF1 complex and maintenance of the repressor CDF1 (Sawa and Kay, 2011).

CO and *FT* are mainly expressed in vascular tissue, whereas (and similarly to *TEM* genes) *GI* is expressed in various tissues including vascular bundles, mesophyll, SAM and root (Takada and Goto, 2003; An *et al*., 2004; Winter *et al*., 2007). In fact, *GI* expression in either mesophyll and/or vascular tissue rescues the late-flowering phenotype of the gi-2 mutant under both SD and LD conditions (Sawa and Kay, 2011). It was observed that the GI N-terminal region was able to interact with TEM1 and TEM2 through yeast-two-hybrid (Y2H) assays. Moreover, the *in vivo* physical interactions of these proteins were found to take place in the nucleus but not in the cytosol (Sawa and Kay, 2011). These authors also showed that

GI activates *FT* expression independently of CO through direct binding to *FT* promoter regions (alone or in a complex with another protein). A possible explanation is that GI could neutralize the TEM1 and TEM2 repressors by interfering with their access to the *FT* promoter or their activity and/or stability.

TEM *genes also regulate the GA pathway*

By contrast, under SD conditions, in which CO is inactive, flowering is induced in the SAM by GAs through activation of the floral integrator *SOC1*, and the floral meristem identity gene *LEAFY* (*LFY*) (Blazquez and Weigel, 2000; Moon *et al*., 2003; Mutasa-Göttgens and Hedden, 2009). Under SDs, *tem1–1 tem2–2* double mutants still flower much earlier than wild-type plants. When expression levels of *SOC1* and *LFY* are analysed in wild-type and *tem1–1 tem2–2* mutant plants under SDs, a significant enhancement of *SOC1* and *LFY* expression is observed in *tem1–1 tem2–2*, indicating an additional role of TEM in flowering-time regulation under SD conditions (Osnato *et al*., 2012). By contrast, *35S::TEM1* plants flower extremely late under SDs, most of them remaining at the vegetative phase and producing leaves indefinitely. In this photoperiod, *TEM* mRNA levels are low during the light period, start to increase at dusk and peak early in the night in wild-type plants. *TEM1* and *TEM2* expression patterns are similar, except for an extra *TEM2* peak late at night (Osnato *et al*., 2012).

pKNAT1::amiR-TEM plants have elongated hypocotyls both in LD and in SD conditions, while *35S::TEM1* plants show, apart from the extremely late flowering, a dwarf phenotype, loss of apical dominance and shorter hypocotyls (Osnato *et al*., 2012). These are phenotypes typical of GA-deficient mutants, such as *ga3ox1–3* and the double mutant *ga3ox1 ga3ox2* (Eriksson *et al*., 2006; Mitchum *et al*., 2006). When GA is sprayed onto the *35S::TEM1* plants the apical dominance and flowering phenotypes are rescued (Osnato *et al*., 2012), suggesting that *TEM* genes play a major role in the GA pathway.

Furthermore, a significant down-regulation of *GA20OX2*, *GA3OX1* and *GA3OX2* expression is found in *35S::TEM1*, whereas an up-regulation of *GA3OX1* and *GA3OX2* is observed in *tem1–1* and *tem1–1 tem2–2* in comparison with the wild type (Osnato *et al*., 2012). *35S::TEM1* produces a down-regulation of GUS expression in plants carrying a *GA3OX1::*GUS reporter construct (Mitchum *et al*., 2006), specifically in the SAM of young plants and in leaves of older plants (Osnato *et al*., 2012). These results indicate a clear effect of TEM on the enzymes that catalyse the last step of GA_4 biosynthesis. In addition, ChIP assays show that TEM1 is a direct *in vivo* regulator of the GA_4 biosynthetic genes *GA3OX1* and *GA3OX2* by binding an RAV binding site positioned in the first exon in both cases (Osnato *et al*., 2012). These data therefore corroborate that TEM directly represses *GA3OX* genes, which may result in a reduction of bioactive GA_4. *tem1 tem2 ga3ox1* triple mutant plants flower later than *tem1 tem2* plants but still earlier than the wild type and *ga3ox1* single mutant, indicating that the early flowering phenotype of *tem1 tem2* double mutants in LD is due at least partially to the *GA3OX1* up-regulation (Osnato *et al*., 2012), which also indicates that GAs act both in LD and in SD.

In conclusion, *TEM* genes link the photoperiod- and GA-dependent flowering pathways, controlling the floral transition under inductive and non-inductive daylengths (Fig. 2).

OTHER RAV FAMILY MEMBERS MAY AFFECT FLOWERING

Results with RAV1 antisense lines suggest that RAV1 may be a flowering repressor in arabidopsis (Hu *et al*., 2004). However, it has not been shown whether the full-length antisense construct used to generate these antisense lines is specific for RAV1. Levels of other *RAV* family transcripts should be checked in these plants to discard the possibility that the early flowering is due to off-target effects on *TEM1* and/or *TEM2*. It is also possible that RAV1 antisense plants flower a few days earlier than wild-type plants as a result of differences in the rate of leaf production (Hu *et al*., 2004).

When GmRAV, a soybean (*Glycine max*) TEM/RAV homologue, is overexpressed in tobacco (*Nicotiana tabacum*) it delays flowering. This suggests that GmRAV, similar to TEM1 and TEM2, can act as a flowering repressor. Although soybean flowering is promoted by SD, *GmRAV* shows higher expression under SD than under LD (Zhao *et al*., 2008). They proposed that the repression of flowering by GmRAV in tobacco may indirectly result from negative effects on photosynthesis and other aspects of plant physiology. Further research should determine whether GmRAV is a regulator of flowering.

RAV GENES ARE REGULATED BY DIFFERENT FLOWERING PATHWAYS

Age-dependent flowering pathway

Genes involved in several flowering pathways regulate *TEM*/*RAV* genes. Several *AP2* family genes are targets of the miRNA miR172 and encode floral repressors that act in the photoperiod- and the age-dependent flowering pathways. In arabidopsis these repressors include AP2 itself, TARGET OF EAT1 (TOE1), TOE2, TOE3, SCHLAFMÜTZE (SMZ) and SCHNARCHZAPFEN (SNZ) (Zhu and Helliwell, 2011). AP2 and SMZ bind *TEM1* chromatin in ChIP-chip experiments (Mathieu *et al*., 2009; Yant *et al*., 2010), suggesting that they may induce *TEM1* expression. However, *TEM1* mRNA levels are not altered in the leaves and the shoot meristem of an activation-tagged *smz-D* mutant, which flowers later than the wild type (Mathieu *et al*., 2009). By contrast, *TEM2* is upregulated in *smz-D*, despite not being bound by SMZ in ChIP-chip experiments (Mathieu *et al*., 2009). These observations suggest that TEM1 and TEM2 may mediate at least part of the effects of AP2 and SMZ on flowering, although additional experiments are required to demonstrate this.

TOPLESS (TPL) and TPL-related (TPR) proteins constitute a family of five members that interact with diverse transcription factors and act as transcriptional co-repressors in arabidopsis (Long *et al*., 2006; Szemenyei *et al*., 2008). TOE1, TOE2 and AP2 are among these TPL/TPR-interacting transcription factors (Arabidopsis Interactome Mapping Consortium, 2011; Causier *et al*., 2012; Krogan *et al*., 2012). Overexpression of TOE1 delays flowering and TPL is required for this phenotype, suggesting that TPL, and perhaps also TPRs, acts as a co-repressor of flowering (Causier *et al*., 2012). Interestingly, all members of the RAV family, with the exception of RAV1L, also interact with TPL/TPR proteins. The RLFGV or MLFGV domains present in all RAV proteins (see above) are required for the interaction of at least RAV1 and RAV3L with TPL (Causier *et al*., 2012). Therefore, RAV proteins probably act in complexes

with TPL/TPR to repress transcription of floral regulators. The action of TPL and its homologues in mammals and yeast involves histone deacetylation and chromatin condensation (Long *et al.*, 2006; Krogan *et al.*, 2012; Turki-Judeh and Courey, 2012; Wang *et al.*, 2013). It will be interesting to determine whether the mechanism of transcriptional repression by RAV proteins also implies chromatin remodelling through the recruitment of TPL/TPR.

Ambient temperature pathway

Changes in ambient temperature affect flowering and low temperatures delay the floral transition in arabidopsis (Blazquez *et al.*, 2003). EARLY FLOWERING 3 (ELF3) is a repressor of flowering involved in this response (Strasser *et al.*, 2009). *elf3* mutants flower earlier and are less sensitive to temperature than wild-type plants, such that the delay caused by low temperature is smaller in *elf3* than in the wild type. *TEM2* is downregulated in *elf3* both at 16 and at 23 °C (Strasser *et al.*, 2009), which correlates with the early flowering phenotype at both temperatures. In addition, the downregulation of *TEM2* in *elf3* is more dramatic at 16 than at 23 °C (Strasser *et al.*, 2009), consistent with a bigger difference in flowering time between *elf3* and the wild type at 16 than at 23 °C. This suggests that the repression of flowering by ELF3 may be mediated at least in part by an increase in *TEM2* expression. *RAV1* shows lower transcript levels in *elf3* than in the wild type at 16 °C, but higher expression at 23 °C, indicating that *RAV1* expression is also regulated by ELF3.

Two MADS-box transcription factors, FLOWERING LOCUS C (FLC) and SHORT VEGETATIVE PHASE (SVP), form a complex that represses flowering during vegetative growth (Li *et al.*, 2008). FLC and SVP have both overlapping and distinct functions (Balasubramanian *et al.*, 2006; Lee *et al.*, 2007*b*; Li *et al.*, 2008). Both are involved in responses to ambient temperature. SVP is important for the repression of flowering at low ambient temperature, while FLC suppresses the induction of flowering by high temperatures (Balasubramanian *et al.*, 2006; Lee *et al.*, 2007*b*). FLC also plays an important role in vernalization, a response to long periods of cold that induces flowering after winter has passed (Song *et al.*, 2012). In addition, FLC acts in the autonomous flowering pathway (Simpson, 2004). ChIP-seq experiments revealed that FLC binds to the promoter of *TEM1*, although *TEM1* mRNA levels were not altered in an *flc* mutant (Deng *et al.*, 2011). *TEM1* and *TEM2* chromatin is also bound by SVP, which up-regulates expression of these two genes (Tao *et al.*, 2012). Therefore, the FLC–SVP complex may positively regulate at least *TEM1* through direct binding to the *TEM1* promoter. It would be interesting to test whether TEM1 and/or TEM2 affect the response of flowering to ambient temperature and/or vernalization. Although SVP and FLC had initially been described as transcriptional repressors (Hepworth *et al.*, 2002; Gregis *et al.*, 2006), they also seem capable of inducing transcription, including that of other flowering repressors in addition to *TEM1* and *TEM2* (Deng *et al.*, 2011; Tao *et al.*, 2012). The mechanism of this positive regulation remains unknown, but probably contributes to reinforce the repression of flowering under unfavourable conditions.

Another MADS-box protein with an important role in flowering-time control, SOC1, regulates *TEM1* and *TEM2* expression, but in the opposite way to the regulation by SVP. Regulatory regions of the *TEM1* and *RAV1* genes are bound by SOC1, indicating that the effect of SOC1 on at least *TEM1* is probably direct (Tao *et al.*, 2012). The repression of *TEM1* and *TEM2* by SOC1 is consistent with the induction of flowering by SOC1.

Brassinosteroids

Brassinosteroids (BRs) are a class of steroid hormones that regulate many developmental processes throughout plant life, such as vascular development, senescence and flowering. Mutants with altered content in endogenous BRs, such as *deetiolated2* or *dwarf4*, flower late, indicating that components of the BR pathway also affect flowering time (reviewed by Li *et al.*, 2010). Treatment with BR reduces *RAV1* and *GmRAV* transcript levels in arabidopsis and in soybean, respectively (Hu *et al.*, 2004; Zhao *et al.*, 2008), indicating that BR down-regulates these genes. In arabidopsis, the effect of BR on *RAV1* seems independent of the BR receptor BRI1 (Hu *et al.*, 2004), suggesting that other BR receptors may be involved. The effect of BR on flowering might therefore be mediated by RAV family members. Given that BR affects many aspects of plant development and growth, additional research is required to determine in which aspect *TEM*/*RAV* genes may be involved.

Although the rice *SVP* group of genes seems not to be involved in flowering, they do affect BR responses (Duan *et al.*, 2006; Lee *et al.*, 2008). This, together with the regulation of *TEM1* and *TEM2* by SVP, the regulation of *FLC* expression by BR and the binding of FLC to *TEM1* DNA (Domagalska *et al.*, 2007; Deng *et al.*, 2011; Tao *et al.*, 2012), establishes another possible link between BR and *RAV* genes.

Light intensity and quality

In addition to photoperiod, light intensity and quality affect floral induction, as well as many other aspects of plant development and growth (Chen *et al.*, 2004; Thomas, 2006). Several results indicate that *RAV* genes may be involved in light responses.

ELONGATED HYPOCOTYL 5 (HY5) is a transcription factor that promotes photomorphogenesis downstream of several photoreceptors (Oyama *et al.*, 1997). In addition, HY5 represses flowering, as shown by the early flowering of *hy5* mutants (Goto *et al.*, 1991; Holm *et al.*, 2002). *TEM2* expression is positively regulated by HY5, which binds to *TEM1*, *TEM2* and *RAV1* chromatin, suggesting that the regulation of *TEM2* is direct (Lee *et al.*, 2007*a*). Therefore, TEM2 is a good candidate to link HY5 with the regulation of flowering in response to light signals.

EFFECT OF RAV FAMILY MEMBERS ON OTHER ASPECTS OF PLANT DEVELOPMENT

RAV *genes regulate hypocotyl elongation*

Transcriptomic analyses of arabidopsis seedlings grown in continuous white light and in the dark have shown that *TEM2* is up-regulated in the hypocotyl and root in response to light, whereas *RAV1* is down-regulated in cotyledons of light-grown seedlings (Ma *et al.*, 2005). *TEM1*, *RAV1* and *RAV1L* are rapidly repressed upon exposure of dark-grown seedlings to

red light (Monte *et al*., 2004; Leivar *et al*., 2009; Shin *et al*., 2009). Moreover, *TEM2* expression is induced by a short exposure to far-red light (Tepperman *et al*., 2004). These data indicate that *RAV* genes show specificity in their response to different light conditions in different organs.

PHYTOCHROME INTERACTING FACTORS (PIFs) play important roles in the regulation of light responses by the photoreceptors phytochrome A (PHYA) and PHYB (Leivar and Quail, 2011). The repression of *RAV1* and *RAV1L* by red light requires the function of at least PIF3 (Monte *et al*., 2004), and other PIFs are involved in transcriptional regulation of *TEM1* and *TEM2* (Leivar *et al*., 2009). ChIP-seq experiments have identified *TEM2* as a gene bound by PIF5 in plants subjected to low red/far-red light ratio, a condition that simulates shade (Hornitschek *et al*., 2012). Although the relevance of this binding for *TEM2* expression is not yet clear, it suggests that PIF5 might be involved in the regulation of *TEM2* by shade. A quadruple mutant lacking PIF1, PIF3, PIF4 and PIF5 (*pifq*) shows shorter hypocotyls and, under certain conditions, higher *TEM1* and *TEM2* transcript levels than wild-type plants (Leivar *et al*., 2008, 2009). Consistent with this, *tem* mutants and plants overexpressing *TEM1* have longer and shorter hypocotyls than wild-type plants, respectively, under SD (Osnato *et al*., 2012). It remains to be shown whether PIFs affect *TEM2* and/or *TEM1* under this photoperiod, but the fact that PIFs promote hypocotyl growth under SD (Nozue *et al*., 2007) makes this hypothesis plausible. Therefore, TEM1 and TEM2 might play a role in light-regulated growth downstream of PIFs.

RAV *genes might inhibit plant growth*

Overexpression of *TEM1* or *TEM2* in arabidopsis causes dwarfism (Osnato *et al*., 2012). Tobacco plants overexpressing GmRAV (GmRAV-OX) also exhibit smaller leaves and roots and shorter internodes than wild-type plants. Soybean growth is reduced under SD compared with LD, inversely correlated with higher GmRAV levels under SD than LD (Zhao *et al*., 2008). Also, GmRAV causes a reduction in chlorophyll content and photosynthetic rate when overexpressed in tobacco (Zhao *et al*., 2008), which may explain the reduced growth of these plants. These findings suggest that TEM1, TEM2 and GmRAV might repress plant growth. This is consistent with the fact that BR treatment down-regulates GmRAV (Zhao *et al*., 2008). A detailed analysis of plant growth in loss-of-function *tem* mutants and *GmRAV*-silenced lines would be useful to demonstrate whether these genes play a role as growth regulators.

GmRAV might also be involved in root development, as tobacco GmRAV-OX plants develop fewer roots than wild-type plants (Zhao *et al*., 2008). Again, silencing of GmRAV in soybean would help to determine its biological function. Although overexpression of *RAV1* causes a reduction in the number of lateral roots and probably in the rate of leaf production, suggesting that RAV1 may be a negative regulator of plant growth, down-regulation of *RAV1* by an antisense construct does not have a significant effect on these processes (Hu *et al*., 2004).

RAV1 *might regulate leaf senescence*

Leaf senescence, a physiological mechanism affected by many internal and external factors (Lim *et al*., 2007), is strongly regulated by several genes to provide optimal plant fitness. This maximum plant fitness is obtained by remobilizing nutrients from senescent leaves (Woo *et al*., 2010). *In silico* technology has allowed identification of a subset of genes named as the *SENESCENCE-ASSOCIATED GENES* (SAGs). Among these SAGs, *RAV1* was isolated due to the fact that not only *RAV1* but also other *RAV* genes have been associated with leaf maturation and senescence. *RAV1* expression is triggered at a mature stage, reaching maximum expression at an early senescence stage and decreasing at later stages. A similar expression pattern is found for *TEM1*, while for *RAV1L* the expression remains at high level until late senescence (Woo *et al*., 2010). These similar expression patterns during leaf development and senescence suggest a possible redundant role among this family in this aspect. However, neither single loss-of-function mutants of these genes nor the *rav1 tem1* and *rav1 rav1l* double mutants show any significant alteration of the senescence process. By contrast, arabidopsis plants overexpressing *RAV1* under a constitutive promoter show an early age-dependent leaf senescence phenotype as well as one induced by artificial dark (Woo *et al*., 2010). The main senescence-associated physiological markers, such as the degree of leaf yellowing, chlorophyll content and photochemical efficiency, are altered. Moreover, the expression of two senescence marker genes (*SEN4* and *SAG12*) is upregulated in plants overexpressing *RAV1*, whereas *RAV1* expression is induced by senescence-accelerating hormones such as jasmonic acid (JA) and ethylene. Similar results are found in transgenic plants that express *RAV1* under an inducible promoter.

Consequently, these data suggest that at least *RAV1* might play a role during leaf senescence initiation by the activation and/or repression of genes involved in the successful execution of the leaf senescence process (Woo *et al*., 2010). This control could be done by integrating the age-dependent aspects of leaf senescence with senescence-accelerating hormones and environmental influences. Moreover, tobacco *GmRAV*-OX plants show accelerated senescence in response to abscisic acid (ABA) and dark treatments (Zhao *et al*., 2008). Because the analyses of single and double mutants do not demonstrate a role of *RAV* genes in senescence, additional work is required to test whether other family members may control this process in a redundant manner with *RAV1* or *GmRAV*.

The three outer whorls of the flowers in arabidopsis, sepals, petals and stamens, are also organs that senesce and shed after pollination (Chen *et al*., 2011). The time of senescence and organ abscission is controlled by diverse hormones; one of the most important is ethylene, which accelerates this process (Roberts *et al*., 2002). It is known that *FOREVER YOUNG FLOWER* (*FYF*), a MADS transcription factor, acts as a repressor of the ethylene response controlling floral senescence and abscission (Chen *et al*., 2011). Recently, it was found that *TEM1* and *TEM2*, which were previously characterized as downstream genes in the ethylene signalling pathway (Alonso *et al*., 2003), are significantly down-regulated in *35S::FYF* plants. Interestingly, the *FYF* expression pattern is opposite to that of *TEM1* and *TEM2* during flower development. Therefore, these results suggest that FYF controls senescence and organ abscission by inactivating downstream genes in the ethylene response such as *TEM1* and *TEM2* (Chen *et al*., 2011).

RAV *genes control bud outgrowth in trees*

RAV homologous genes have also been identified in trees. A *RAV* gene from chestnut (*Castanea sativa*), *CsRAV1*, has recently been characterized. The closest relatives to *CsRAV1* are two poplar (*Populus thricocarpa*) *RAVs*, *PtRAV1* and *PtRAV2*, and all group with the arabidopsis *TEM1* and *TEM2* genes (Moreno-Cortés *et al*., 2012). Trees are known to have a long juvenile phase when they are still not able to flower. Trees usually form lateral buds that undergo dormancy in the winter period and these buds will grow out the following spring after the cold period. In poplar, sylleptic branching, i.e. outgrowth of branches in the same season in which the buds were formed, is produced and is mainly associated with juvenility (Ceulemans *et al*., 1990; Cooke *et al*., 2005). Tree breeders have long desired to shorten the juvenile phase to speed up breeding and to increase sylleptic branching to obtain a higher woody biomass (Novaes *et al*., 2009; Rae *et al*., 2009). The possibility that *TEM* genes might be involved in the age-dependent pathway in arabidopsis and that this could be conserved across species is of great interest for biomass production in trees. Moreover, the CO/FT module is conserved in *Populus* and, in addition to flowering, regulates bud-set and growth cessation (Böhlenius *et al*., 2006; Hsu *et al*., 2011). This suggests that poplar *TEM* orthologues could be involved in those processes. Although there is still no information on the function of poplar *RAV* genes, the chestnut *CsRAV1* is induced during winter dormancy and in response to low temperatures, which might suggest a role in bud-set and growth cessation; however, more experiments are needed to confirm this. In addition, when *CsRAV1* is overexpressed in hybrid poplar it induces extensive sylleptic branching that it is not observed in control trees (Moreno-Cortés *et al*., 2012). This extra branching greatly increases the biomass of these transgenic trees, which is consequently of agronomic and commercial interest.

RAV GENES AS INTERACTORS OF RESPONSES TO BIOTIC AND ABIOTIC STRESS

Plants, using a complex system, defend themselves against both biotic and abiotic stresses. Plants are able to adapt and survive under several types of biotic and abiotic stresses, such as drought, high salinity, high/low temperatures or pathogen attacks. Worldwide crop productivity and quality are threatened by this wide variety of stresses, and therefore a better understanding of the complex and interconnected systems of plant defence and adaptation to these stresses is crucial. It is known that plants respond to such stresses by inducing morphological, physiological and biochemical changes through crosstalk among different genetic pathways (Zhuang *et al*., 2011). The activation of plant defence responses is first initiated by the recognition/identification of primary pathogen-derived elicitors by plant cell receptors (Yang *et al*., 1997; Kim and Martin, 2004). This triggers signal transduction pathways regulated by the hormones ethylene, salicylic acid (SA) and JA (Glazebrook, 1999; Lee *et al*., 2005), which induce the expression of plant defensive genes that produce defensive compounds, such as pathogen-related (PR) proteins, chitinase and/or enzymes involved in the biosynthesis of protective secondary metabolites (Gu *et al*., 2002; Koo *et al*., 2007).

In recent years, it has been discovered that *RAV* family members from different plant species not only are induced by ethylene but also play essential roles in biotic and abiotic environmental stresses (Alonso *et al*., 2003; Feng *et al*., 2005; Kim *et al*., 2005; Sohn *et al*., 2006; Zhuang *et al*., 2011). For instance, *RAV1* and *TEM2* expression in arabidopsis is upregulated by touch-related stimuli such as touch, wind and water spray, suggesting that these genes may function for developmental adaptation in response to different environmental stimuli (Kagaya and Hattori, 2009). In fact, it was found that expression of both genes is induced in arabidopsis after treatment with biotic and abiotic stresses such as bacterial pathogens, SA, mannitol, high salinity and wounding (Feng *et al*., 2005; Sohn *et al*., 2006). In addition, *RAV1* is rapidly induced by cold and this response is regulated by the circadian clock (Fowler & Thomashow, 2002; Fowler *et al*., 2005). *Galegae orientalis* is a nitrogen-fixing legume used for forage production and soil improvement in scandinavian agriculture (Varis, 1986). Similarly to other plant species, *GoRAV* expression is induced by cold, exogenous ABA, high salinity and drought (Chen *et al*., 2009). Moreover, *BnaRAV-1-HY15*,

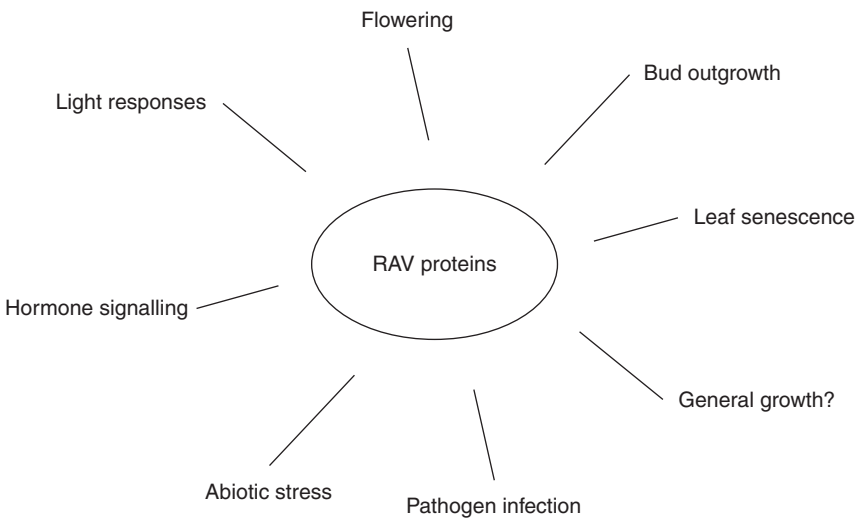

FIG. 3. Summary of the processes regulated by RAV proteins in different plant species.

a *RAV* orthologue in *Brassica napus*, an important agricultural-oil crop, is also induced by cold, NaCl and polyethylene glycol treatments (Zhuang *et al*., 2011).

A *RAV* orthologue (*CaRAV1*) from chili pepper (*Capsicum annuum*) is strongly induced during pathogen infection with *Xanthomonas campestris*, environmental stresses and abiotic elicitors (Sohn *et al*., 2006). Overexpression of *CaRAV1* in arabidopsis induces several PR genes and enhances resistance not only against other pathogens such as *Pseudomonas syringae*, but also against osmotic stresses by high dehydration and salinity (Sohn *et al*., 2006). *Solanum lycopersicum*, tomato, is the second most consumed vegetable in the world. *Ralstonia solanacearum* causes the bacterial wilt disease, probably the most important bacterial vascular disease in tomato (Hai *et al*., 2008). Ectopic expression of *SlRAV2* increases bacterial wilt tolerance in tomato plants by inducing the expression of PR genes such as *SlERF5* and *PR5* (Li *et al*., 2011).

Endogenous small RNA pathways and RNA silencing are major components of the plant response to different biotic and abiotic stresses. RNA silencing is a sequence-specific RNA degradation mechanism activated during viral infection that serves to protect plants against viruses (Ding and Voinnet, 2007). On the other side, plant viruses try to block the plant RNA silencing defence using different proteins (Diaz-Pendon and Ding, 2008). *TEM2* is essential for suppression of RNA silencing by at least two unrelated plant viral proteins, potyviral HC-Pro and carmoviral P38, two potent viral suppressors of silencing that block primary and transitive RNA silencing (Endres *et al*., 2010). In tobacco, both viral repressors require *NtRAV2* to block exclusively the activity of primary small interfering RNAs. *NtRAV2* interacts physically with HC-Pro proteins and is required for HC-Pro suppression of virus-induced gene silencing (VIGS). Moreover, *TEM2* induces the expression of *FRY1* and *CML38*, two genes that act as endogenous suppressors of silencing in arabidopsis (Anandalakshmi *et al*., 2000). Consequently, *TEM2* seems to be an essential control point in viral suppression of silencing. However, neither of the related arabidopsis genes *RAV1* or *TEM1* seems to have a redundant role in this specific aspect as they are not able to compensate for the loss of *TEM2* to divert host defences toward responses that interfere with antiviral silencing (Endres *et al*., 2010). *TEM2* may repress directly or indirectly the transcription of genes that encode proteins of the plant silencing machinery (Endres *et al*., 2010). Therefore, *RAV* orthologues from different plant species could function as key modulators of biotic and abiotic stress responses by integrating the regulation of diverse plant defence signalling pathways.

CONCLUSIONS

Despite *RAV* genes not being completely characterized, promising results obtained in recent years suggest strongly that RAV family members play important roles in many different physiological and developmental pathways in several plant species (Fig. 3). *RAV* genes act as repressors in the regulation of gene expression in various plant biological processes that may be of crucial importance for plant survival and crop production. Among these processes, floral transition is the best studied and *TEM1* and *TEM2* control at least the photoperiod- and GA-dependent flowering pathways. Moreover, *RAV* genes in different species may play important roles in other developmental processes and may also modulate some of the complex systems of response to diverse abiotic and biotic stresses. In conclusion, the RAV family, a unique family of transcription factors in plants, seems to integrate and control different physiological mechanisms that are affected by many internal and external factors. These essential controls should contribute to improve plant fitness, with the final outcome being optimal plant development and adaptation to environmental threats.

ACKNOWLEDGEMENTS

We thank Pablo Leivar for comments on the manuscript. Our work on floral development is supported by a grant from the Spanish MINECO (BFU2012–33746) and S.P.'s research group has been recognized as a Consolidated Research Group by the Catalonia Government (2009 SGR 697). A.E.A-J. is a predoctoral fellow of the investigator formation programme (FI) from the Catalonia Government.

LITERATURE CITED

Alonso JM, Stepanova AN, Leisse TJ, *et al*. 2003. Genome-wide insertional mutagenesis of *Arabidopsis thaliana*. *Science* **301**: 653–657.

An H, Roussot C, Suárez-López P, *et al*. 2004. CONSTANS acts in the phloem to regulate a systemic signal that induces photoperiodic flowering of *Arabidopsis*. *Development* **131**: 3615–3626.

Anandalakshmi R, Marathe R, Ge X, *et al*. 2000. A calmodulin-related protein that suppresses posttranscriptional gene silencing in plants. *Science* **290**: 142–144.

Andrés F, Coupland G. 2012. The genetic basis of flowering responses to seasonal cues. *Nature Reviews Genetics* **13**: 627–639.

Arabidopsis Interactome Mapping Consortium. 2011. Evidence for network evolution in an *Arabidopsis* interactome map. *Science* **333**: 601–607.

Balasubramanian S, Sureshkumar S, Lempe J, Weigel D. 2006. Potent induction of *Arabidopsis thaliana* flowering by elevated growth temperature. *PLoS Genetics* **2**: 980–989.

Blazquez MA, Weigel D. 2000. Integration of floral inductive signals in Arabidopsis. *Nature* **404**: 889–892.

Blazquez MA, Ahn JH, Weigel D. 2003. A thermosensory pathway controlling flowering time in *Arabidopsis thaliana*. *Nature Genetics* **33**: 168–71.

Böhlenius H, Huang T, Charbonnel-Campaa L, *et al*. 2006. CO/FT regulatory module controls timing of flowering and seasonal growth cessation in trees. *Science* **312**: 1040–1043.

Castillejo C, Pelaz S. 2008. The balance between CONSTANS and TEMPRANILLO activities determines FT expression to trigger flowering. *Current Biology* **18**: 1338–1343.

Causier B, Ashworth M, Guo W, Davies B. 2012. The TOPLESS Interactome: a framework for gene repression in Arabidopsis. *Plant Physiology* **158**: 423–438.

Ceulemans R, Stettler RF, Hinckley TM, Isebrands JG, Heilman PE. 1990. Crown architecture of *Populus* clones as determined by branch orientation and branch characteristics. *Tree Physiology* **7**: 157–167.

Cooke JE, Martin TA, Davis JM. 2005. Short-term physiological and developmental responses to nitrogen availability in hybrid poplar. *New Phytologist* **167**: 41–52.

Corbesier L, Vincent C, Jang S, *et al*. 2007. FT protein movement contributes to long-distance signaling in floral induction of Arabidopsis. *Science* **316**: 1030–1033.

Chen M, Chory J, Fankhauser C. 2004. Light signal transduction in higher plants. *Annual Review of Genetics* **38**: 87–117.

Chen MK, Hsu WH, Lee PF, Thiruvengadam M, Chen HI, Yang CH. 2011. The MADS box gene, FOREVER YOUNG FLOWER, acts as a repressor controlling floral organ senescence and abscission in Arabidopsis. *Plant Journal* **68**: 168–185.

Chen X, Wang Z, Wang X, Dong J, Ren J, Gao H. 2009. Isolation and characterization of *GoRAV*, a novel gene encoding a RAV-type protein in *Galegae orientalis*. *Genes and Genetic Systems* **84**: 101–109.

Deng W, Ying H, Helliwell CA, Taylor JM, Peacock WJ, Dennis ES. 2011. FLOWERING LOCUS C (FLC) regulates development pathways throughout the life cycle of Arabidopsis. *Proceedings of the National Academy of Sciences of the United States of America* **108**: 6680–6685.

Diaz-Pendon JA, Ding SW. 2008. Direct and indirect roles of viral suppressors of RNA silencing in pathogenesis. *Annual Review of Phytopathology* **46**: 303–326.

Ding SW, Voinnet O. 2007. Antiviral immunity directed by small RNAs. *Cell* **130**: 413–426.

Domagalska MA, Schomburg FM, Amasino RM, Vierstra RD, Nagy F, Davis SJ. 2007. Attenuation of brassinosteroid signaling enhances FLC expression and delays flowering. *Development* **134**: 2841–2850.

Duan K, Li L, Hu P, Xu SP, Xu ZH, Xue HW. 2006. A brassinolide-suppressed rice MADS-box transcription factor, OsMDP1, has a negative regulatory role in BR signaling. *Plant Journal* **47**: 519–31.

Endres MW, Gregory BD, Gao Z, *et al*. 2010. Two plant viral suppressors of silencing require the ethylene-inducible host transcription factor RAV2 to block RNA silencing. *PLoS Pathogens* **6**: e1000729.

Eriksson S, Bohlenius H, Moritz T, Nilsson O. 2006. GA4 is the active gibberellin in the regulation of LEAFY transcription and Arabidopsis floral initiation. *The Plant Cell* **18**: 2172–2181.

Feng J-X, Liu D, Pan Y, *et al*. 2005. An annotation update via cDNA sequence analysis and comprehensive profiling of developmental, hormonal or environmental responsiveness of the *Arabidopsis* AP2/EREBP transcription factor gene family. *Plant Molecular Biology* **59**: 853–868.

Fornara F, de Montaigu A, Coupland G. 2010. SnapShot: control of flowering in Arabidopsis. *Cell* **141**: 550, 550 e1–2.

Fowler S, Thomashow MF. 2002. Arabidopsis transcriptome profiling indicates that multiple regulatory pathways are activated during cold acclimation in addition to the CBF cold response pathway. *The Plant Cell* **14**, 1675–1690.

Fowler S, Lee K, Onouchi H, *et al*. 1999. *GIGANTEA*: a circadian clock-controlled gene that regulates photoperiodic flowering in *Arabidopsis* and encodes a protein with several possible membrane-spanning domains. *The EMBO Journal* **18**: 4679–4688.

Fowler SG, Cook D, Thomashow MF. 2005. Low temperature induction of Arabidopsis CBF1, 2, and 3 is gated by the circadian clock. *Plant Physiology* **137**: 961–968.

Giraudat J, Hauge BM, Valon C, Smalle J, Parcy F, Goodman HM. 1992. Isolation of the Arabidopsis ABI3 gene by positional cloning. *The Plant Cell* **4**: 1251–1261.

Glazebrook J. 1999. Genes controlling expression of defense responses in Arabidopsis. *Current Opinion in Plant Biology* **2**: 280–286.

Goto N, Kumagai T, Koornneef M. 1991. Flowering responses to light-breaks in photomorphogenic mutants of *Arabidopsis thaliana*, a long-day plant. *Physiologia Plantarum* **83**: 209–215.

Gregis V, Sessa A, Colombo L, Kater MM. 2006. AGL24, SHORT VEGETATIVE PHASE, and APETALA1 redundantly control AGAMOUS during early stages of flower development in Arabidopsis. *The Plant Cell* **18**: 1373–1382.

Gu YQ, Wildermuth MC, Chakravarthy S, *et al*. 2002. Tomato transcription factors pti4, pti5, and pti6 activate defense responses when expressed in Arabidopsis. *The Plant Cell* **14**: 817–831.

Hai TTH, Esch E, Wang JF. 2008. Resistance to Taiwanese race 1 strains of *Ralstonia solanacearum* in wild tomato germplasm. *European Journal of Plant Pathology* **122**: 471–479.

Hepworth SR, Valverde F, Ravenscroft D, Mouradov A, Coupland G. 2002. Antagonistic regulation of flowering-time gene *SOC1* by CONSTANS and FLC via separate promoter motifs. *The EMBO Journal* **21**: 4327–4337.

Holm M, Ma L-G, Qu L-J, Deng X-W. 2002. Two interacting bZIP proteins are direct targets of COP1-mediated control of light-dependent gene expression in Arabidopsis. *Genes & Development* **16**: 1247–1259.

Hornitschek P, Kohnen MV, Lorrain S, *et al*. 2012. Phytochrome interacting factors 4 and 5 control seedling growth in changing light conditions by directly controlling auxin signaling. *The Plant Journal* **71**: 699–711.

Hsu CY, Adams JP, Kim H, *et al*. 2011. FLOWERING LOCUS T duplication coordinates reproductive and vegetative growth in perennial poplar. *Proceedings of the National Academy of Sciences USA* 108: 10756–10761.

Hu YX, Wang YH, Liu XF, Li JY. 2004. Arabidopsis RAV1 is down-regulated by brassinosteroid and may act as a negative regulator during plant development. *Cell Research* **14**: 8–15.

Huijser P, Schmid M. 2011. The control of developmental phase transitions in plants. *Development* **138**: 4117–4129.

Ikeda M, Ohme-Takagi M. 2009. A novel group of transcriptional repressors in Arabidopsis. *Plant and Cell Physiology* **50**: 970–975.

Jaeger KE, Wigge PA. 2007. FT protein acts as a long-range signal in *Arabidopsis*. *Current Biology* **17**: 1050–1054.

Jang S, Marchal V, Panigrahi KCS, *et al*. 2008. Arabidopsis COP1 shapes the temporal pattern of CO accumulation conferring a photoperiodic flowering response. *The EMBO Journal* **27**: 1277–1288.

Jarillo JA, Piñeiro M. 2011. Timing is everything in plant development. The central role of floral repressors. *Plant Science* **181**: 364–378.

Kagaya Y, Hattori T. 2009. *Arabidopsis* transcription factors, RAV1 and RAV2, are regulated by touch-related stimuli in a dose-dependent and biphasic manner. *Genes & Genetic Systems* **84**: 95–99.

Kagaya Y, Ohmiya K, Hattori T. 1999. RAV1, a novel DNA-binding protein, binds to bipartite recognition sequence through two distinct DNA-binding domains uniquely found in higher plants. *Nucleic Acids Research* **27**: 470–478.

Kardailsky I, Shukla VK, Ahn JH, *et al*. 1999. Activation tagging of the floral inducer *FT*. *Science* **286**: 1962–1965.

Kim S-Y, Kim Y-C, Lee J-H, *et al*. 2005. Identification of a CaRAV1 possessing an AP2/ERF and B3 DNA-binding domain from pepper leaves infected with *Xanthomonas axonopodis* pv. *glycines* 8ra by differential display. *Biochimica et Biophysica Acta (BBA) – Gene Structure and Expression* **1729**: 141–146.

Kim YJ, Martin GB. 2004. Molecular mechanisms involved in bacterial speck disease resistance of tomato. *Plant Pathology Journal* **20**: 7–12.

Kobayashi Y, Kaya H, Goto K, Iwabuchi M, Araki T. 1999. A pair of related genes with antagonistic roles in mediating flowering signals. *Science* **286**: 1960–1962.

Koo YJ, Kim MA, Kim EH, *et al*. 2007. Overexpression of salicylic acid carboxyl methyltransferase reduces salicylic acid-mediated pathogen resistance in *Arabidopsis thaliana*. *Plant Molecular Biology* **64**: 1–15.

Krogan NT, Hogan K, Long JA. 2012. APETALA2 negatively regulates multiple floral organ identity genes in *Arabidopsis* by recruiting the co-repressor TOPLESS and the histone deacetylase HDA19. *Development* **139**: 4180–4190.

Lee JH, Kim SH, Jung YH, *et al*. 2005. Molecular cloning and functional analysis of rice (*Oryza sativa* L.) OsNDR1 on defense signaling pathway. *Plant Pathology Journal* **21**: 149–157.

Lee JH, He K, Stolc V, *et al*. 2007*a*. Analysis of transcription factor HY5 genomic binding sites revealed its hierarchical role in light regulation of development. *The Plant Cell* **19**: 731–749.

Lee JH, Yoo SJ, Park SH, Hwang I, Lee JS, Ahn JH. 2007*b*. Role of SVP in the control of flowering time by ambient temperature in Arabidopsis. *Genes and Development* **21**: 397–402.

Lee S, Choi SC, An G. 2008. Rice SVP-group MADS-box proteins, OsMADS22 and OsMADS55, are negative regulators of brassinosteroid responses. *The Plant Journal* **54**: 93–105.

Leivar P, Quail PH. 2011. PIFs: pivotal components in a cellular signaling hub. *Trends in Plant Science* **16**: 19–28.

Leivar P, Monte E, Oka Y, *et al*. 2008. Multiple phytochrome-interacting bHLH transcription factors repress premature seedling photomorphogenesis in darkness. *Current Biology* **18**: 1815–1823.

Leivar P, Tepperman JM, Monte E, Calderon RH, Liu TL, Quail PH. 2009. Definition of early transcriptional circuitry involved in light-induced reversal of PIF-imposed repression of photomorphogenesis in young Arabidopsis seedlings. *The Plant Cell* **21**: 3535–3553.

Li CW, Su RC, Cheng CP, *et al*. 2011. Tomato RAV transcription factor is a pivotal modulator involved in the AP2/EREBP-mediated defense pathway. *Plant Physiology* **156**: 213–227.

Li D, Liu C, Shen L, *et al*. 2008. A repressor complex governs the integration of flowering signals in Arabidopsis. *Developmental Cell* **15**: 110–120.

Li J, Li Y, Chen S, An L. 2010. Involvement of brassinosteroid signals in the floral-induction network of Arabidopsis. *Journal of Experimental Botany* **61**: 4221–4230.

Lim PO, Kim HJ, Gil Nam H. 2007. Leaf senescence. *Annual Review of Plant Biology* **58**: 115–136.

Lin M-K, Belanger H, Lee YJ, *et al*. 2007. FLOWERING LOCUS T protein may act as the long-distance florigenic signal in the cucurbits. *The Plant Cell* **19**: 1488–1506.

Liu LJ, Zhang YC, Li QH, *et al*.. 2008. COP1-mediated ubiquitination of CONSTANS is implicated in cryptochrome regulation of flowering in Arabidopsis. *The Plant Cell* **20**, 292–306.

Long JA, Ohno C, Smith ZR, Meyerowitz EM. 2006. TOPLESS regulates apical embryonic fate in Arabidopsis. *Science* **312**: 1520–1523.

Ma L, Sun N, Liu X, Jiao Y, Zhao H, Deng XW. 2005. Organ-specific expression of Arabidopsis genome during development. *Plant Physiology* **138**: 80–91.

Magnani E, Sjolander K, Hake S. 2004. From endonucleases to transcription factors: evolution of the AP2 DNA binding domain in plants. *Plant Cell* **16**: 2265–2277.

Mathieu J, Warthmann N, Küttner F, Schmid M. 2007. Export of FT protein from phloem companion cells is sufficient for floral induction in *Arabidopsis*. *Current Biology* **17**: 1055–1060.

Mathieu J, Yant LJ, Mürdter F, Küttner F, Schmid M. 2009. Repression of flowering by the miR172 target SMZ. *PLoS Biology* **7**: e1000148.

Mitchum MG, Yamaguchi S, Hanada A, *et al*. 2006. Distinct and overlapping roles of two gibberellin 3-oxidases in Arabidopsis development. *The Plant Journal* **45**: 804–818.

Mizoguchi T, Wright L, Fujiwara S, *et al*. 2005. Distinct roles of GIGANTEA in promoting flowering and regulating circadian rhythms in Arabidopsis. *The Plant Cell* **17**: 2255–2270.

Monte E, Tepperman JM, Al-Sady B, *et al*. 2004. The phytochrome-interacting transcription factor, PIF3, acts early, selectively, and positively in light-induced chloroplast development. *Proceedings of the National Academy of Sciences of the United States of America* 101: 16091–16098.

Moon J, Suh S-S, Lee H, Choi K-R, Hong CB, Paek N-C, Kim S-G, Lee I. 2003. The *SOC1* MADS-box gene integrates vernalization and gibberellin signals for flowering in *Arabidopsis*. *The Plant Journal* **35**: 613–623.

Moreno-Cortés A, Hernández-Verdeja T, Sánchez-Jiménez P, González-Melendi P, Aragoncillo C, Allona I. 2012. CsRAV1 induces sylleptic branching in hybrid poplar. *New Phytologist* **194**: 98–90.

Mutasa-Göttgens E, Hedden P. 2009. Gibberellin as a factor in floral regulatory networks. *Journal of Experimental Botany* **60**: 1979–1989.

Novaes E, Osorio L, Drost DR, *et al*. 2009. Quantitative genetic analysis of biomass and wood chemistry of Populus under different nitrogen levels. *New Phytologist* **182**: 878–90.

Nozue K, Covington MF, Duek PD, *et al*. 2007. Rhythmic growth explained by coincidence between internal and external cues. *Nature* **448**: 358–361.

Okamuro JK, Caster B, Villarroel R, Van Montagu M, Jofuku KD. 1997. The AP2 domain of APETALA2 defines a large new family of DNA binding proteins in Arabidopsis. *Proceeding of the National Academy of Sciences USA* **94**: 7076–81.

Osnato M, Castillejo C, Matías-Hernández L, Pelaz S. 2012. *TEMPRANILLO* genes link photoperiod and gibberellin pathways to control flowering in *Arabidopsis*. *Nature Communications* 3: 808.

Oyama T, Shimura Y, Okada K. 1997. The Arabidopsis HY5 gene encodes a bZIP protein that regulates stimulus-induced development of root and hypocotyl. *Genes & Development* **11**: 2983–2995.

Park DH, Somers DE, Kim YS, *et al*. 1999. Control of circadian rhythms and photoperiodic flowering by the *Arabidopsis GIGANTEA* gene. *Science* **285**: 1579–1582.

Rae AM, Street NR, Robinson KM, Harris N, Taylor G. 2009. Five QTL hotspots for yield in short rotation coppice bioenergy poplar: the Poplar Biomass Loci. *BMC Plant Biology* **9**: 23.

Riechmann JL, Meyerowitz EM. 1998. The AP2/EREBP family of plant transcription factors. *Biological Chemistry* **379**: 633–646.

Riechmann JL, Heard J, Martin G, *et al*. 2000. Arabidopsis transcription factors: genome-wide comparative analysis among eukaryotes. *Science* **290**: 2105–2110.

Roberts JA, Hussain A, Taylor IB, Black CR. 2002. Use of mutants to study long-distance signalling in response to compacted soil. *Journal of Experimental Botany* **53**: 45–50.

Sakuma Y, Liu Q, Dubouzet JG, Abe H, Shinozaki K, Yamaguchi-Shinozaki K. 2002. DNA-binding specificity of the ERF/AP2 domain of Arabidopsis DREBs, transcription factors involved in dehydration- and cold-inducible gene expression. *Biochemistry Biophysics Research Communications* **290**: 998–1009.

Samach A, Onouchi H, Gold SE, *et al*. 2000. Distinct roles of CONSTANS target genes in reproductive development of *Arabidopsis*. *Science* **288**: 1613–1616.

Sawa M, Kay SA. 2011. GIGANTEA directly activates Flowering Locus T in *Arabidopsis thaliana*. *Proceedings of the National Academy of Sciences of the United States of America* 108: 11698–11703.

Sawa M, Nusinow DA, Kay SA, Imaizumi T. 2007. FKF1 and GIGANTEA complex formation is required for day-length measurement in Arabidopsis. *Science* **318**: 261–265.

Shin J, Kim K, Kang H, *et al*. 2009. Phytochromes promote seedling light responses by inhibiting four negatively-acting phytochrome-interacting factors. *Proceedings of the National Academy of Sciences of the United States of America* 106: 7660–7665.

Simpson GG. 2004. The autonomous pathway: epigenetic and post-transcriptional gene regulation in the control of Arabidopsis flowering time. *Current Opinion in Plant Biology* **7**: 570–574.

Sohn K, Lee S, Jung H, Hong J, Hwang B. 2006. Expression and functional roles of the pepper pathogen-induced transcription factor RAV1 in bacterial disease resistance, and drought and salt stress tolerance. *Plant Molecular Biology* **61**: 897–915.

Song J, Angel A, Howard M, Dean C. 2012. Vernalization – a cold-induced epigenetic switch. *Journal of Cell Science* **125**: 3723–3731.

Song YH, Ito S, Imaizumi T. 2013. Flowering time regulation: photoperiod- and temperature-sensing in leaves. *Trends in Plant Science* **18**: 575–583.

Strasser B, Alvarez MJ, Califano A, Cerdán PD. 2009. A complementary role for ELF3 and TFL1 in the regulation of flowering time by ambient temperature. *The Plant Journal* **58**: 629–640.

Suárez-López P, Wheatley K, Robson F, Onouchi H, Valverde F, Coupland G. 2001. *CONSTANS* mediates between the circadian clock and the control of flowering in *Arabidopsis*. *Nature* 410: 1116–1120.

Suzuki M, Kao CY, McCarty DR. 1997. The conserved B3 domain of VIVIPAROUS1 has a cooperative DNA binding activity. *The Plant Cell* **9**: 799–807.

Szemenyei H, Hannon M, Long JA. 2008. TOPLESS mediates auxin-dependent transcriptional repression during Arabidopsis embryogenesis. *Science* **319**: 1384–1386.

Takada S, Goto K. 2003. TERMINAL FLOWER2, an Arabidopsis homolog of HETEROCHROMATIN PROTEIN1, counteracts the activation of *FLOWERING LOCUS T* by CONSTANS in the vascular tissues of leaves to regulate flowering time. *The Plant Cell* **15**: 2856–2865.

Tamaki S, Matsuo S, Wong HL, Yokoi S, Shimamoto K. 2007. Hd3a protein is a mobile flowering signal in rice. *Science* **316**: 1033–1036.

Tao Z, Shen L, Liu C, Liu L, Yan Y, Yu H. 2012. Genome-wide identification of SOC1 and SVP targets during the floral transition in *Arabidopsis*. *The Plant Journal* **70**: 549–561.

Tepperman JM, Hudson ME, Khanna R, *et al*. 2004. Expression profiling of phyB mutant demonstrates substantial contribution of other phytochromes to red-light-regulated gene expression during seedling de-etiolation. *The Plant Journal* **38**: 725–739.

Thomas B. 2006. Light signals and flowering. *Journal of Experimental Botany* **57**: 3387–3393.

Turck F, Fornara F, Coupland G. 2008. Regulation and identity of florigen: FLOWERING LOCUS T moves center stage. *Annual Review of Plant Biology* **59**: 573–594.

Turki-Judeh W, Courey AJ. 2012. Groucho: a corepressor with instructive roles in development. In: Plaza S, Payre F, eds. *Current topics in developmental biology*. New York: Academic Press, 65–96.

Valverde F, Mouradov A, Soppe W, Ravenscroft D, Samach A, Coupland G. 2004. Photoreceptor regulation of CONSTANS protein in photoperiodic flowering. *Science* **303**: 1003–1006.

Varis E. 1986. Goat's rue (*Galega orientalis* L.) a potential pasture legume for temperate conditions. *Journal of Agricultural Science Finland* **58**: 83–101.

Waltner JK, Peterson FC, Lytle BL, Volkman BF. 2005. Structure of the B3 domain from *Arabidopsis thaliana* protein At1g16640. *Protein Science* **14**: 2478–2483.

Wang L, Kim J, Somers DE. 2013. Transcriptional corepressor TOPLESS complexes with pseudoresponse regulator proteins and histone deacetylases to regulate circadian transcription. *Proceedings of the National Academy of Sciences USA* 110: 761–766.

Wellmer F, Riechmann JL. 2010. Gene networks controlling the initiation of flower development. *Trends in Genetics* **26**: 519–527.

Wenkel S, Turck F, Singer K, *et al*. 2006. CONSTANS and the CCAAT box binding complex share a functionally important domain and interact to regulate flowering of Arabidopsis. *The Plant Cell* **18**: 2971–84.

Winter D, Vinegar B, Nahal H, Ammar R, Wilson GV, Provart NJ. 2007. An "electronic fluorescent pictograph" browser for exploring and analyzing large-scale biological data sets. *PLoS ONE* **2**: e718.

Woo HR, Kim JH, Kim J, *et al*. 2010. The RAV1 transcription factor positively regulates leaf senescence in *Arabidopsis*. *Journal of Experimental Botany* **61**: 3947–3957.

Yamasaki K, Kigawa T, Inoue M, *et al*. 2004. Solution structure of the B3 DNA binding domain of the Arabidopsis cold-responsive transcription factor RAV1. *The Plant Cell* **16**: 3448–3459.

Yang Y, Shah J, Klessig DF. 1997. Signal perception and transduction in plant defense responses. *Genes & Development* **11**: 1621–1639.

Yanovsky MJ, Kay SA. 2002. Molecular basis of seasonal time measurement in *Arabidopsis*. *Nature* **419**: 308–312.

Yant L, Mathieu J, Dinh TT, *et al*. 2010. Orchestration of the floral transition and floral development in *Arabidopsis* by the bifunctional transcription factor APETALA2. *The Plant Cell* **22**: 2156–2170.

Zhao L, Luo Q, Yang C, Han Y, Li W. 2008. A RAV-like transcription factor controls photosynthesis and senescence in soybean. *Planta* **227**: 1389–1399.

Zhu Q-H, Helliwell CA. 2011. Regulation of flowering time and floral patterning by miR172. *Journal of Experimental Botany* **62**: 487–495.

Zhuang J, Sun CC, Zhou XR, Xiong AS, Zhang J. 2011. Isolation and characterization of an AP2/ERF-RAV transcription factor BnaRAV-1-HY15 in *Brassica napus* L. HuYou15. *Molecular Biology Reports* **38**: 3921–3928.